Lysosomal nutrients and the mTORC1 pathway

by

Gregory A. Wyant

B.S., Biochemistry
Northeastern University

SUBMITTED TO THE DEPARTMENT OF BIOLOGY IN PARTIAL FULFILLMENT OF THE REQUIREMENTS FOR THE DEGREE OF

DOCTOR OF PHILOSOPHY
AT THE
MASSACHUSETTS INSTITUTE OF TECHNOLOGY

February 2019

© Gregory A. Wyant. All rights reserved.

The author hereby grants to MIT permission to reproduce and to distribute publicly paper and electronic copies of this thesis in whole or in part in any medium now known or hereafter created.

Signature of Author:

Gregory A. Wyant
Department of Biology
October 12th, 2018

Certified by:

David M. Sabatini
Professor of Biology
Member, Whitehead Institute

Certified by:

Amy Keating
Professor of Biology
Chair, Biology Graduate Committee

Abstract

The lysosome is the major catabolic organelle, is the site of activation of the master growth regulator mTORC1 (mechanistic target of rapamycin (mTOR) complex 1), and is often deregulated in common diseases, such as cancer. Given the critical role of lysosomes in maintaining cellular homeostasis, a better understanding of lysosomal function and metabolism and its relation to the mTOR pathway is necessary.

Most components of the nutrient-sensing machinery upstream of mTORC1 localize to the lysosomal surface, and amino acids generated by lysosomes regulate mTORC1 by promoting its translocation there, a key step in its activation. Activation of mTORC1 by the amino acid arginine requires SLC38A9, a poorly understood lysosomal membrane protein with homology to amino acid transporters. To study SLC38A9 function at the lysosome, we developed a novel method for the rapid isolation of intact mammalian lysosomes suitable for metabolite profiling. First, we validate that SLC38A9 is an arginine sensor for the mTORC1 pathway, and we uncover a central role for SLC38A9 in amino acid homeostasis. SLC38A9 mediates the transport, in an arginine-regulated fashion, of many essential amino acids out of lysosomes to be used in growth-promoting processes. Pancreatic cancer cells, which use lysosomal protein degradation as a nutrient source, require SLC38A9 to form tumors. Thus, through SLC38A9, arginine acts a lysosomal messenger to connect mTORC1 activation and the release of the essential amino acids to drive cell growth.

Finally, by performing quantitative proteomic analyses of rapidly isolated lysosomes, we find that ribosome degradation provides the lysosomal arginine that promotes SLC38A9 activation. Lysosome degradation of ribosomes is mediated by NUFIP1 (nuclear fragile X mental retardation–interacting protein 1). The starvation-induced degradation of ribosomes via autophagy (ribophagy) depends on the capacity of NUFIP1 to bind LC3B and promotes cell survival. Thus, the NUFIP1-mediated degradation of ribosomes provides both the necessary substrate to activate SLC38A9 and the nutrients needed to promote cell survival under starvation. Altogether, this work provides insight into the regulation of lysosomal nutrients and their role in cellular growth and survival.

Thesis supervisor: David M. Sabatini

Title: Member, Whitehead Institute; Professor of Biology, MIT

Acknowledgments

My decision to join the lab of David Sabatini I can confidently say was one of the important decisions of my life and also one of the best. It is funny because it almost didn't happen as after I told him I would be interested in joining, I did not respond to his email (for reasons I can't exactly remember) for almost two weeks leading him to believe I had changed my mind. There was a slight moment of terror when I thought he no longer had space. He has taught me the importance of just "doing," this is an experimental work that even failed ideas is progress toward something, and that science is incredibly random and a moment of clarity could arrive at any time and it just requires you to be present. I feel incredibly fortunate to have spent the last five years under his mentorship.

David says he follows the "choose people, not projects" philosophy and with that, he has cultivated an environment of the most intelligent and passionate individuals I have ever met. There are few people that have had the biggest impact on me and wouldn't want to imagine what it would have been like without them. First, I am extremely thankful to Alejo Efeyan and Bill Comb, who trained me during my rotation. I would like to especially speak on the impact Bill has made on me during my PhD. Bill was someone who pushed me to always focus on the big problems and to take advantage of the opportunity I had in front of me. Second, I have been very fortunate to work very closely with Monther Abu Remaileh. We have shared every moment of success and failure together, and as he likes to say "brothers." I will miss this collaboration very much, but I am sure it is not the end. Lastly, I met Rachel Wolfson essentially on day one of my PhD. Her passion for science makes me remember why I decided to do any of this in the first place and her passion for everything she does outside of science has taught me it is possible to not to let a life in science consume who I am and that it is possible to relax. She is someone who impresses me everyday and I am fortunate to call her my best friend.

I would also like to thank various members of the lab, who I believe have shaped me into the scientist I am today, including Bob Saxton, Jose Orozco, Hank Adelmann, Kendall Condon, Shuyu Wang, Xin Gu, Zhi Tsun, Lynne Chantranupong, Kuang Shen, Jason Cantor, and Tim Wang. I have also had the pleasure of working very closely with a group of the lab's newest students- Jordan Ray, Justin Roberts, and Jibril Kedir- and I am excited to see their success in the future. The lab would also not be so successful without the organization of Kathleen Ottina, Edie Valeri, and Danica Rili.

Throughout my graduate career, my thesis committee has remained a constant source of support. I am extremely grateful to Bob Sauer and Monty Krieger for what they've done to shape me as a young scientist. I would also like to thank Tobias Walther for serving on my committee for my thesis defense.

Also, without the support of my best friends Dave Patel, Kathy Ching, Jon Neal, Alexandra Cote, Greg Franzblau, and Merrie Weintraub, I cannot imagine where I'd be. Despite our group being spread across the country, we have always found time to see each other. The amount of times Dave has said he'd "quiz" me for my defense, despite having very little knowledge of what I actually do has been ridiculous.

Finally, I am incredibly lucky to be supported so strongly by my family through every decision I've made. My sister, despite being across the country, has always been an ear for anything I've wanted to talk about and her independence has always been an example that I've tried to emulate. My father has always been a source of inspiration and I have always pushed to be a man that would make him proud. And finally, my mother. She is loving and supportive, and also expects perfection and holds me to the highest standards. I would not be who I am today without what she's done for me.

Table of Contents

CHAPTER 1:

I. Introduction

Cell growth is defined by the accumulation of mass. This is a process that all eukaryotic cells, both unicellular and multicellular alike, require in order to proliferate, and as such, the ability to grow is a highly resource-intensive process. Therefore, it is unsurprising that cells have evolved sophisticated systems that detect when conditions are favorable for growth, and conversely, halt growth promoting processes when growth factors, nutrient stores, or energy levels deplete. Across eukaryotic organisms, the mechanistic target of rapamycin complex 1 (mTORC1) pathway has emerged as the major regulator of cell growth (*1*). mTORC1 integrates a diverse set of signals, such as growth factor availability, nutrients, energy status, and stress to regulate both anabolic processes, such as protein, nucleotide, and lipid synthesis, as well as catabolic ones, such as autophagy. Given mTORC1's central role in cellular homeostasis, it is unsurprising that is often deregulated in a multitude of human diseases, such as cancer and aging.

II. The mTOR Pathway

Rapamycin and the Discovery of mTOR

It is impossible to discuss the mTORC1 pathway without a discussion of rapamycin. In the early 1970's, with the goal of identifying novel antimicrobial agents, Surendra Sehgal isolated rapamycin from *Streptomyces Hygroscopicus* in a soil sample from Easter Island, also known as Rapa Nui from which rapamycin

derives its name (*1*). Although lacking antibacterial activity, rapamycin was soon found to have potent growth-inhibitory affects on yeast and these effects were soon found to extend to human cells suggesting that the growth-inhibitory effects of rapamycin were conserved from yeast to human (*2*). Subsequently, it was found that rapamycin acts as a potent immunosuppressant in humans leading to its FDA approval for the prevention of organ transplant rejection, and several pharmaceutical companies further developed derivatives of rapamycin, known as rapalogues (*1*). These derivatives are currently are in use as anti-restenosis agents along with as chemotherapeutic agents in cancer.

Given its potent anti-fungal effects, many sought to identify its mechanism of action. While many drugs bind and inhibit their target directly, rapamycin acts in part by forming a gain of function complex with the peptidyl-prolyl-isomerase FK506 binding protein 12 (FKBP12) (*3, 4*). Utilizing genetic screens in yeast, two groups identified mutant alleles in three genes that are required to mediate the affects of rapamycin: recessive mutations in FKBP12, and dominant mutations in the TOR1 and TOR2 genes. FKBP12 loss did not recapitulate the growth arrest seen with rapamycin treatment, however duel loss of TOR1/TOR2 phenocopied the growth-inhibitory properties of rapamycin suggesting the gene products of TOR1/TOR2 are the molecular target of rapamycin (*5*). The full mechanism of action of rapamycin remained elusive until 1994, when biochemical studies identified the mechanistic (formally “mammalian”) target of rapamycin (mTOR) as the direct target of the rapamycin-FKBP12 complex in mammals, revealing it to be the homolog of the yeast TOR genes that were previously identified in genetic

screens (*6*-*8*). The discovery of mTOR lead to what has become a sprawling field with connections to almost every aspect of human physiology and disease.

mTORC1 and mTORC2

mTOR is a serine-threonine kinase and work in both fungal and mammalian systems it nucleates two distinct protein complexes, mTOR Complex I and mTOR Complex II (mTORC1 and mTORC2, respectively). Each complex is comprised of a unique set of proteins and as such, each complex has distinct substrates and modes of regulation. For instance, in response to growth factors and nutrient availability, mTORC1 regulates key cell growth processes, such as protein, lipid, and nucleotide synthesis, as well as autophagy. Conversely, mTORC2 is less well understood but is considered part of the PI3K-AKT pathway and responds to growth factor signaling. While I will discuss briefly mTORC2, the focus on this thesis will be on mTORC1.

mTORC2

Yeast TOR2, unlike TOR1, was found to have rapamycin-insensitive downstream processes. While initially this remained a mystery, it was clarified with the discovery of two distinct complexes containing the TOR protein. In yeast, the TOR1 or TOR2 gene products can associate with the rapamycin-sensitive TOR complex 1 (TORC1), which consists of KOG1 (homologous to the human raptor) and LST8 (homologous to the human GBL/mLST8). Conversely, only the TOR2 gene product is found in the TOR complex 2 (TORC2) protein complex, comprised of AVO1 (homologous to human SIN1), AVO2, and AVO3 (homologous to the

human Rictor). In humans, there is only one mTOR protein and it is found in both mTORC1 and mTORC2 protein complexes.

The function of the mTORC2 pathway has not been fully clarified however, loss of TORC2 components in yeast or mTORC2 components in mammalian systems leads to cytoskeletal defects. Intense interest in mTORC2 began when it was found to be the elusive kinase for AKT activation. The PI3K/AKT pathway mediates insulin signaling and is the most commonly mutated pathway in cancer. AKT is a serine-threonine kinase that promotes cell growth, cell cycle progression, glucose metabolism, and cellular survival, and for years it was known it required phosphorylation of two distinct sites for full kinase activity, T308 and S473. It is now clear that PDK1 mediates T308 phosphorylation while mTORC2 phosphorylates S473. The identification of mTORC2 as the S473 kinase established mTORC2 as key growth-regulatory kinase and immediately connected the mTOR pathway to insulin signaling (*9*). How PI3K signaling activates mTORC2 remains unclear, however recent work has suggested that the production of phosphatidylinositol-3,4,5 trisphosphate (PIP3), the product of PI3K activation, binds mSIN1 leading to its displacement and reliving its inhibition on mTORC2(*10*). While the understanding of the mTORC2 pathway is incomplete, the regulation and output of the mTORC1 pathway is far better understood and is the focus of this thesis.

mTORC1

mTORC1 is composed of mTOR, as well as Raptor, Gbl/mLST8, and two inhibitory subunits PRAS40 (Proline Rich AKT substrate of 40 Kd) and DEPTOR(*11-14*). Interestingly, while the RAPTOR subunit is the defining component of the mTORC1 complex it is not require for mTOR kinase activity in vitro but is likely required for substrate recruitment. The mTORC1 pathway is the primary regulator of mass accumulation through the regulation of many anabolic and catabolic processes, such as protein, lipid, and nucleotide synthesis, as well as energy metabolism, organelle biogenesis, and autophagy and proteasome activity. The diverse mechanisms by which mTORC1 regulates these processes are described in detail below.

Functions and Substrates of mTORC1

To have the ability to grow and divide, a cell must increase the production of proteins, lipids, and nucleotides as well as suppress catabolic processes such as autophagy and proteasome activity(*15*). mTORC1 plays a central role in regulating all these processes by phosphorylating distinct substrates in order to control the balance between anabolism and catabolism. Here I will review the critical mTORC1

substrates that contribute to cellular growth (Figure 1).

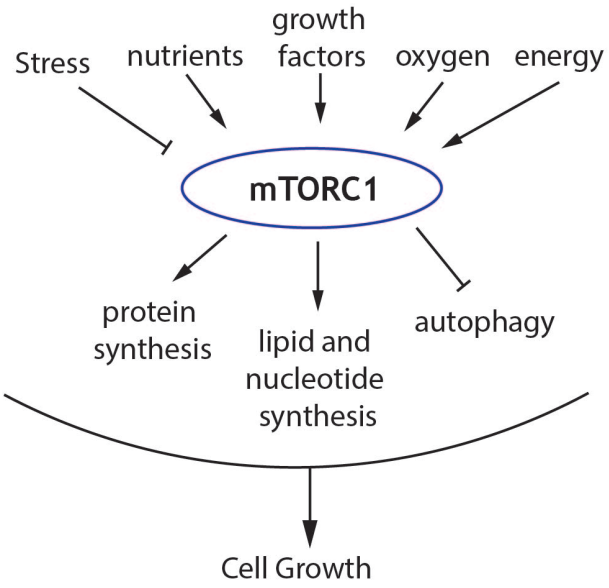

Figure 1: the mTORC1 pathway senses numerous nutritional and environmental cues to increase growth-promoting processes, such as protein synthesis, lipid and nucleotide synthesis, and inhibiting catabolic ones, such as autophagy.

Protein Synthesis

Active mTORC1 drives protein synthesis primarily through two processes: increasing the production of the protein synthesis machinery (ribosomes) and increasing the efficiency of the rate-limiting step of translation (translation initiation).

First, with the development of ATP-competitive inhibitors of mTOR, it became clear that mTOR inhibition strongly reduces translation initiation as it suppresses incorporation of 35S-Cys/Met into protein by 65% and dramatically shifts ribosomes away from polysomes to monosomes(*16*). Translation initiation inhibition occurs largely through mTORC1's phosphorylation of two substrates, the S6Ks and 4EBPs. Before the identification of mTOR, these key substrates were known to be rapamycin-sensitive, however recent work has shown that certain

4EBP1 phosphorylation sites are insensitive to rapamycin (*17-19*). mTORC1 directly phosphorylates S6K1 on its hydrophobic motif site, Thr389, which enables subsequent phosphorylation and activation by PDK1. S6K1 activation leads to the subsequent phosphorylation and activation several substrates that promote mRNA translation initiation, such as eIF4B, a positive regulator of the 5'cap binding eIF4F complex(*15*). S6K1 activation also leads to the degradation of PDCD4, an inhibitor or eIF4B, leading to the enhanced translation efficiency of spliced mRNAs as well as phosphorylation of S6, a subunit of the 40S ribosome, which permits its association with the pre-initiation complex promoting translation(*20*). Loss of S6K1 causes a 20% size reduction relative to wild-type mice(*21*). The mTORC1 substrate 4EBP1 inhibits translation by binding and sequestering eIF4E leading to the prevention of eIF4F complex assembly (*22, 23*). 4EBP1 contains multiple mTORC1 phosphorylation sites that affect its dissociation from eIF4F allowing 5'cap-dependent mRNA translation to occur (*23*).

mTORC1 promotes the production of ribosomes by regulation rRNA synthesis through positively regulating RNA Polymerase I and RNA Polymerase III via the recruitment of transcription factors required for polymerase activity (*24, 25*). Similarly, mTORC1 regulates a subset of mRNAs that all share 5' terminal oligopyrimidine (TOP) motifs, or a series of cytosine and uracil bases. These 5' TOP motifs occur frequently in the 5' UTR of many genes encoding ribosomal proteins consistent with mTOR activity increasing ribosome abundance. The regulation of these mRNAs primarily occurs at the level of 4EBP as 4EBP loss blocks the affects of mTOR inhibition on the translation of these 5' TOP mRNAs (*16*).

Lipid Biosynthesis

Apart from an increase in protein abundance, in order for a cell to grow it must have adequate lipids for membrane expansion and formation(*15*). mTORC1 increases lipid biosynthesis by promoting the processing of the transcription factor sterol-regulatory-element-binding protein 1/2 (SREBP1/2), which is responsible for increasing the expression of enzymes involved in lipid synthesis. SREBP1/2 resides on the ER membrane in an inactive form, and when sterol levels drop SREBP1/2 moves to the golgi and is proteolytically cleaved into an active form that acts as a transcription factor to stimulate transcription of genes necessary for lipid synthesis(*26-28*). SREBP is canonically activated in response to low sterols; it also can be activated independently through an S6K-dependnet mechanism as well as through an additional mTORC1 substrate Lipin1, which inhibits SREBP in the absence of mTORC1 activity (*29*).

Nucleotide Metabolism

Recent work has shown that mTORC1 also promotes the synthesis of nucleotides required for DNA replication. mTORC1 stimulates ATF4-dependent expression of MTHFD2, a key component of the mitochondrial tetrahydrofolate cycle that provides one-carbon units for purine synthesis. SREBP activation by mTORC1 also increases a number of genes in the pentose phosphate pathway (PPP) leading to the biosynthesis of both purines and pyrimidines. Additionally, mTORC1 directly phosphorylates the enzyme carbamoyl-phosphate synthetase 2 (CAD2), which is involved in the production of pyrimidines (*30-32*).

Protein Turnover

The processes described above focuses on the role of mTORC1 in anabolism, or building of cellular mass. Conversely, mTORC1 promotes cell growth by also inhibiting protein catabolism, such as autophagy and proteasome activity, which will be described below.

Autophagy

Autophagy is a key process in which cytoplasmic components, including organelles, are captured by the autophagosome and delivered to the lysosome for degradation and recycling of macromolecules that can be used for growth(*33*). mTORC1 activity directly inhibits autophagy through phosphorylation of ULK1, a kinase that is important in the early step of autophagy initiation. ULK1 forms a complex with ATG13, FIP200, and ATG101 that promotes autophagosome formation (*34, 35*). In essence, under conditions in which nutrients and growth factors are present, mTORC1 is active and inhibits the recycling of cellular components. Conversely, when nutrients are low, mTORC1 is inhibited and stimulates autophagy. Autophagy induction leads to the degradation and recycling of cellular materials that over time can provide the necessary nutrients to stimulate mTORC1 activity as well as survive nutrient starvation. Autophagy will be discussed in depth later in this introduction.

Ubiquitin-Proteasome System

Apart from autophagy, the Ubiquitin-Proteasome system (UPS) is the second major pathway responsible for protein turnover. Proteins are targeted for degradation by the 20S proteasome following covalent modification with ubiquitin. Recently, it has been shown that acute mTORC1 inhibition rapidly increases proteasome-dependent proteolysis either through a general increases in protein ubiquitylation, or an increase in proteasome chaperone abundance(*36*). Interestingly, another study has shown that genetic hyper activation of mTORC1 via TSC1/2 loss also increases proteasome activity through an elevation of proteasome subunit expression (*36*). Despite the discrepancy, the UPS is responsible for a majority of cellular protein degradation; therefore, understanding its regulation by mTORC1 will be an area of intense interest in the future.

Regulation of mTORC1

A shift toward a growth-promoting program must only occur when there are sufficient pro-growth signals as well as the necessary energy and chemical building blocks needed for macromolecule synthesis. In mammals, these signals are largely dependent on diet, wherein mTORC1 activity is promoted upon feeding and inhibited upon fasting. Here will discuss the various upstream signals and how they promote mTORC1 activation (Figure 2).

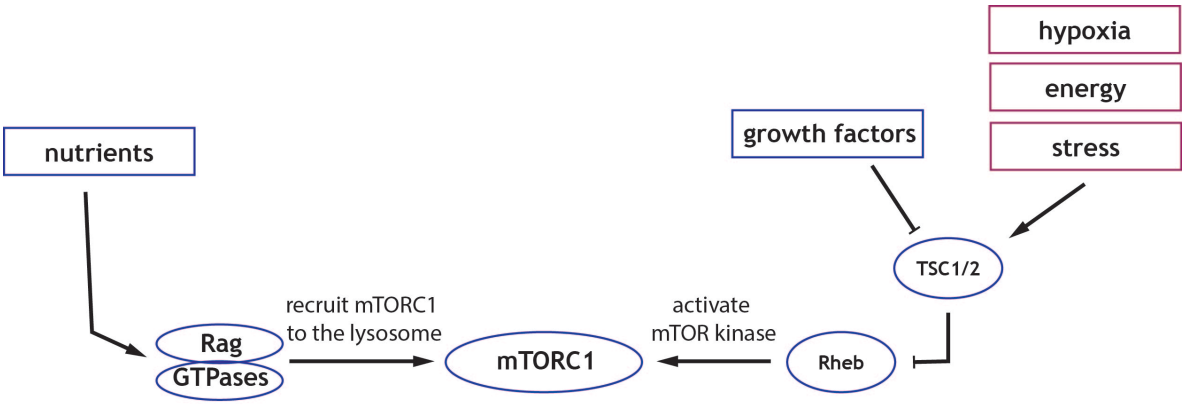

Figure 2: Growth factors activate mTORC1 through a signaling pathway that involves the TSC complex and RHEB GTPase. Nutrients, such as amino acids and glucose, activate the mTORC1 through a pathway that impinges on the Rag GTPases. When nutrients are present, the Rag GTPases recruit mTORC1 to the lysosomal surface where it can interact with its kinase activator Rheb. In the presence of sufficient growth factors, Rheb can then activate mTORC1 kinase activity.

Growth Factors, Energy, Oxygen, and DNA Damage

While there are a variety of environmental signals that impinge on mTORC1 to coordinate its activity, most of these, such growth factors, energy, oxygen, and DNA damage, input through the tuberous sclerosis complex (TSC), which is composed of TSC1, TSC2, and TBC1D7. The TSC complex acts as a GTPase activating protein (GAP) for the small GTPase Ras homologoue enriched in brain (Rheb), which is an essential activator of mTORC1 kinase activity. Interestingly, how exactly Rheb activates mTORC1 is still unclear (*37-41*).

Growth factor pathways converge on the TSC complex, including the insulin/insulin-like growth factor-1 (IGF-1) pathway, leading to the AKT-dependent multi-site phosphorylation of TSC2(*42*). First, growth factors, such as insulin, bind their cognate receptors on the plasma membrane. This binding leads to the recruitment of insulin receptor substrate 1 (IRS1), which activates PI3K, a heterotrimeric lipid kinase, to the plasma membrane where it comes in contact with its substrate phosphatidylinositol-4,5 bisphosphate (PI-4,5-bisphosphate). PI3K

then catalyzes the phosphorylation of its substrate to form phospohatidylinositol-3,4,5-triphosphate (PIP3) (*9*). An important negative regulator of this pathway, phosphatase and tensin homolog deleted on chromosome 10 (PTEN), reverses this reaction and resets PI3K signaling. The creation of PIP3 on the inside of the plasma membrane leads to the recruitment of AKT to this site through binding its pleckstrin homology domain (PH)(*9*). As discussed previously, AKT is activated by two independent phosphorylation events and both events are required for full activation of AKT. The phosphorylation of threonine 308 is catalyzed by PDK1, while the phosphorylation of serine 473 is catalyzed by mTORC2(*9, 13, 43*). How PI3K regulates mTORC1 is still unclear. Activation of AKT stimulates its kinase activity leading to the phosphorylation of TSC2, a core member of the TSC complex(*42*). This phosphorylation leads to its inhibition and dissociation from the lysosomal surface(*41*). As the TSC complex acts as the GAP for Rheb, this regulation is critical as when the TSC complex no longer resides at the lysosomal surface, Rheb, which also resides at the lysosomal surface, become GTP-loaded and is therefore capable of activating mTORC1, as long as it is properly localized to the lysosomal surface. Similarly, receptor tyrosine kinase-dependent Ras signaling activates mTORC1 via the MAP Kinase Erk and its effector p90RSK, both of which phosphorylate TSC2; however, it has not been shown whether these inputs control the localization of TSC or simply inhibit its GAP activity. Additional growth factor pathways, such as Wnt and cytokine TNFalpha, activate mTORC1 via inhibition of TSC1 as well(*44*). Precisely how the TSC complex integrates these diverse growth-factor signaling pathways is still unclear.

Apart from growth factor availability, mTORC1 also responds to stresses that are incompatible with growth promotion, such as low ATP levels, hypoxia, or DNA damage. A reduction in cellular energy, typically modeled using glucose deprivation, activates the 5'AMP-activated protein kinase (AMPK), which inhibits mTORC1 indirectly, through the phosphorylation of TSC2, as well as directly, through the phosphorylation of Raptor(*45*). Interestingly, mTORC1 also responds to low glucose in a manner independent of AMPK, through the inhibition of the Rag GTPases, how exactly is still an open question(*46*). Other cellular stresses, such as low oxygen or DNA damage, are thought to inhibit the pathway similarly, via the TSC complex. For instance, hypoxia inhibits mTORC1 in part through AMPK activation, but also through the induction of REDD1 (Regulated in DNA damage and development), which activates TSC(*47*). The DNA-damage response pathway inhibits mTORC1 through the induction of p53 target genes, such as AMPK regulatory subunit (*AMPKb*), *PTEN*, and *TSC2* itself, all of which lead to increased TSC activity(*48*). It is clear the TSC complex is a critical node in the sensing of many growth signals; however, whether they all affect TSC localization or strictly TSC GAP activity is still unclear.

Amino Acids

While many environmental signals input into mTORC1 via the TSC complex and Rheb activation, Rheb is only able to activate mTORC1 if it is properly localized to the lysosomal surface. This localization is controlled by the availability of nutrients through the Ras-related GTPases (Rags)(*49*).

The identification of the Rag GTPases was breakthrough in the understanding of how nutrients were sensed by mTORC1. The Rags are obligate heterodimers of RagA or B (A/B) bound to RagC or D (C/D) tethered to the lysosomal surface by the Ragulator complex comprised of p18, p14, MP1, HBXIP, and C7ORF59. In the presence of sufficient amino acids, the Rags convert to their active nucleotide state, RagA/B in a GTP-loaded conformation while RagC/D is GDP-loaded, which then binds the Raptor subunit of mTORC1, leading to the recruitment of mTORC1 to the lysosomal surface where it can then interact with its essential kinase activator Rheb(*49-51*). Therefore, the mTORC1 pathway is constructed as an "AND-gate," where mTORC1 is only active when both the Rag and Rheb GTPases are active; this leads to a simple understanding of why both amino acids and growth factors are required for mTORC1 activity (Figure 3).

How amino acids control mTORC1 activity upstream of the Rag GTPases has been an area of intense research over the past decade. Our lab and others have identified a number of regulators of the Rag GTPases and it is now clear that mTORC1 senses both cytosolic and lysosomal amino acids. Amino acids inside the lysosomal lumen signal to mTORC1 via a mechanism that is dependent on the lysosomal v-ATPase, which interacts with the Rag-Ragulator complex(*52*). Recently, we have identified the lysosomal amino acid transporter SLC38A9 as a Rag-Ragulator interacting protein that is required for arginine to activate mTORC1(*53*). Its function as a putative arginine sensor as well as the importance of lysosomal nutrient sensing will be a focus of this thesis and will be discussed later.

Cytosolic leucine and arginine signal to mTORC1 through a distinct pathway comprised of the GATOR1 and GATOR2 complexes. GATOR1, consisting of DEPDC5, Nprl2, and Nprl3, is a negative regulator of the mTORC1 pathway and acts as a GAP for RagA/B. The KICStor complex, comprised of KPTN, ITFG2, C12orf66, and SZT2, tethers GATOR1 to the lysosomal surface and similarly acts as a negative regulator to the mTORC1 pathway. The GATOR2 complex is a pentameric complex of unknown function, comprised of Mios, WDR24, WDR59, Seh1L, and Sec13, and acts as a positive regulator of the mTORC1 pathway(*54, 55*). In the past three years, our lab has made an enormous progress into the mechanism of cytosolic leucine and arginine sensing. First, the identification of Sestrin2 as a GATOR2 interacting protein that inhibits mTORC1 signaling under amino acid deprivation led to subsequent biochemical and structural analyses that established Sestrin2 as a direct leucine sensor upstream of mTORC1. Sestrin2 binds leucine and its affinity for leucine determines the sensitivity of mTORC1 signaling to leucine in cultured cells(*56-60*) (Figure 3). While it has remained to be established whether tissues leucine concentrations fluctuate within the relevant range to be sensed by Sestrin2 in vivo, this will an active area of research for years to come. Interestingly, *Sestrin2* has shown to be transcriptionally activated upon long time amino acid deprivation via ATF4, suggesting a model that Sestrin2 functions both as an acute leucine sensor as well as an indirect sensor of long-term amino acid deprivation. Similarly, cytosolic arginine signals to mTORC1 via the CASTOR1 protein in a mechanism analogous to Sestrin2. Much like Sestrin2, CASTOR1 binds and inhibits GATOR2 in the absence of arginine and dissociates upon arginine binding leading to mTORC1 activation(*61, 62*). The fact that two

amino acid sensors to the mTORC1 pathway are centered on the inhibition of the GATOR2 complex has established GATOR2 as a central node of amino acid sensing; however its molecular function and how Sestrin2 and CASTOR1 inhibit GATOR2 remain unknown (Figure 3).

Recently, our lab has also identified that methionine is sensed upstream of mTORC1 via the surrogate metabolite S-adenosylmethionine (SAM). Utilizing published IP-MS databases, C7orf60 was found to interact with the GATOR1 and KICSTOR complexes and biochemical validation showed its function as a SAM binding protein that signals methionine availability to mTORC1(*63*). This suggests that many other sensors may exist, not only for amino acids but for other key nutrients as well. Similarly, it is clear there are several other mechanisms by which amino acids regulate mTORC1. For instance, the Folliculin/FNIP12 complex acts as the GAP for RagC but its upstream regulation is still unknown(*64*) (Figure 3). Also, studies have reported that the amino acid glutamine activates mTORC1 independent of the Rag GTPases through the related Arf family GTPases(*65*).

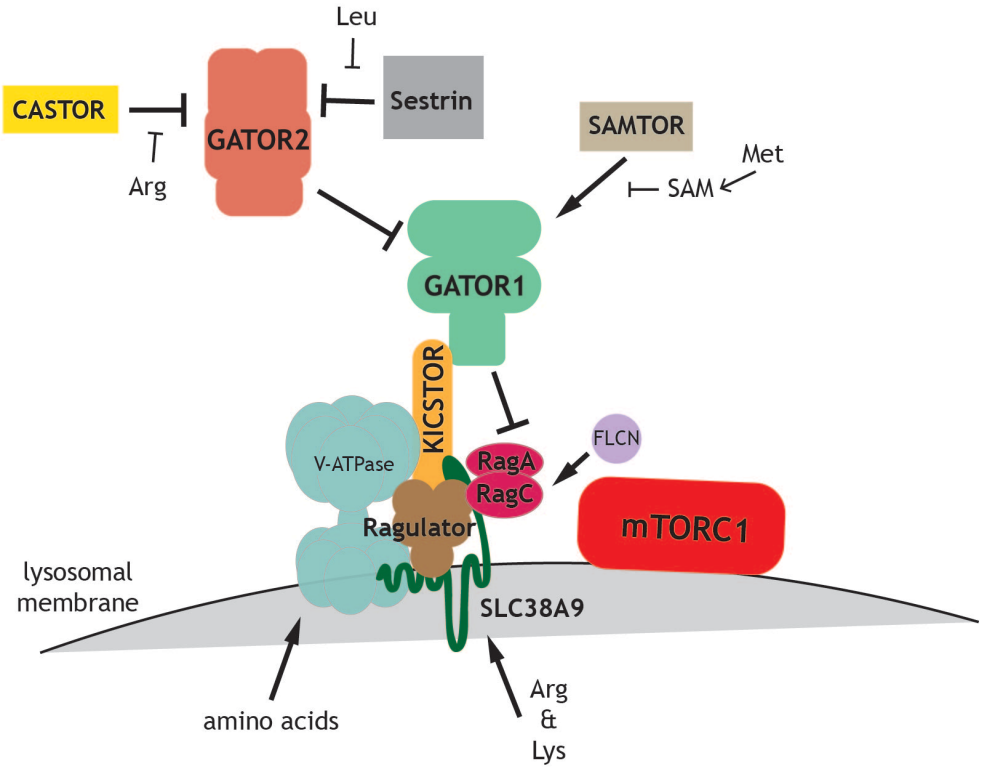

Figure 3: A model for the activation of mTORC1 by amino acids. The cytosolic branch is comprised of the GATOR1, GATOR2, and KICSTOR complexes. Cytosolic leucine and arginine signal to mTORC1 via the Sestrin and Castor family of proteins in a GATOR2-dependent mechanism. Amino acids within the lysosome signal to mTORC1 in an V-ATPase dependent mechanism. Lysosomal arginine (and lysine) signal to mTORC1 via SLC38A9. SLC38A9, in an arginine-dependent mechanism, effluxes the non-polar essential amino acids out of the lysosome for use in growth promoting processes. Ragulator acts as a scaffold for the Rag GTPases at the lysosome and has nucleotide exchange activity on the Rag GTPases.

mTORC1 pathway and cancer

Many mTORC1 pathway regulators are mutated in both sporadic cancers and familial cancer syndromes. For instance, regulators of the growth factor sensing branch, such as PI3Kinase or AKT, are two of the most commonly mutated genes in a variety of cancer malignancies. Similarly, PTEN, a critical negative regulator of the PI3Kinsae signaling pathway is a tumor suppressor that is frequently mutated or lost in sporadic cancers (reviewed in (*9*). Germline mutations

in *AKT*, *PI3K*, and *PTEN* are associated with familial overgrowth syndrome and recent clinical work has shown the efficacy of PI3K/mTOR inhibitors in the treatment of these diseases(*66*).

Downstream of the growth factor signaling pathway, TSC1/2 has been commonly recognized as tumor suppressor genes due to their association with familial tumor syndrome tuberous sclerosis. These cancers are inherited in an autosomal dominant fashion in which patients inherited one mutated allele of *TSC1* or *TSC2*. Frequently, these cancers are associated with loss of heterozygosity, and then inactivating mutations are found in the wild-type allele of the disease-causing gene(*67*).

Apart from the growth factor/insulin signaling side of the mTORC1 pathway, recently recurrent, sporadic mutations in *MTOR* have been found in a subset of cancers, which have been biochemically characterized to activate mTORC1 signaling in cell culture(*68-70*). Similarly, *GATOR1* loss has been found in a low percentage of sporadic ovarian cancers and gliobastomas. Biochemical follow-up has shown that these cancers have constitutive mTORC1 signaling in absence of nutrients, however, it is unclear if GATOR1 loss is critical to these cancers(*55*). Recurrent mTORC1-activating *RRAGC* mutations were recently found in follicular lymphoma, and biochemical follow-up found these RagC variants increased raptor binding while rendering mTORC1 signaling resistant to amino acid deprivation. Interestingly, more than half of the *RRAGC* mutations preferentially co-occurred with mutations in *ATP6V1B2* and *ATP6AP1,* which encode components of the vacuolar H+-ATPase (V-ATPase) known to be necessary for amino acid-induced

activation of mTORC1. The functional outcome of these V-ATPase mutations still require biochemical follow-up(*71*).

mTOR inhibitors as cancer therapy

As it is clear that mTORC1 signaling plays a major role in tumorigenesis, the development of specific mTOR inhibitors has been an area of intense interest and has gathered promising pre-clinical data to support mTOR inhibition's anti-tumor effects. It is quite surprising though that rapamycin and its derivatives (rapalogues) have currently shown limited use in cancer therapy. The best indication of the efficacy of mTOR inhibition has been shown in blocking angiomyolipoma growth in tuberous sclerosis patients, where hyperactive mTORC1 signaling is the basis of the disease(*72*). Similarly, in a Phase III clinical trial, treatment with a rapamycin derivative, everolimus, showed a 42% response rate in reducing angiomyolipoma size (*73*). So far, this has been the best-case scenario of the use of mTOR inhibitors in cancer.

Why rapalogues have currently proven less effective has been a topic of intense debate. The simplest hypothesis would be that the outcome of mTOR inhibition, the inhibition of its downstream effectors, is just insufficient to kill cancer cells despite these processes being necessary for growth, exerting a cytostatic effect rather than cytotoxic. There is also evidence that mTORC1 inhibition might even enable more aggressive tumor growth rather than inhibit it. As mentioned previously, mTORC1 activity negatively regulates AKT signaling, and rapalogue treatment has been shown to activate AKT in colorectal carcinomas (*74*). Also, we now appreciate that rapamycin and other rapalogues are only partial mTORC1

inhibitors and potentially catalytic mTOR inhibitors may have higher efficacy(*75*). Also, it is clear that long-term rapamycin treatment, as would be seen in the clinic, also inhibits mTORC2 via disruption of mTORC2 assembly and it is possible the response of cancer cells to rapamycin may be due to its affects on mTORC2 inhibition(*76*). Currently, there are no known mTORC2 selective inhibitors and ATP-competitive inhibitors are currently not FDA-approved.

III. Lysosome

Lysosomes are membrane-bound organelles that are classically known to be the degradation center of the cell. They are also critically important in signal transduction, specifically in nutrient-sensing by the mTORC1 pathway. They have been most widely studied in their role in a class of rare metabolic diseases known as lysosomal storage diseases and deregulated in common diseases, such as cancer (as reviewed in (*77*)). The lysosome is a major location for producing and sensing many metabolites, but our knowledge about lysosomal metabolism and how it affects cellular homeostasis and signaling pathways is far less understood. Here, I will review our basic understanding of lysosome physiology (Figure 4).

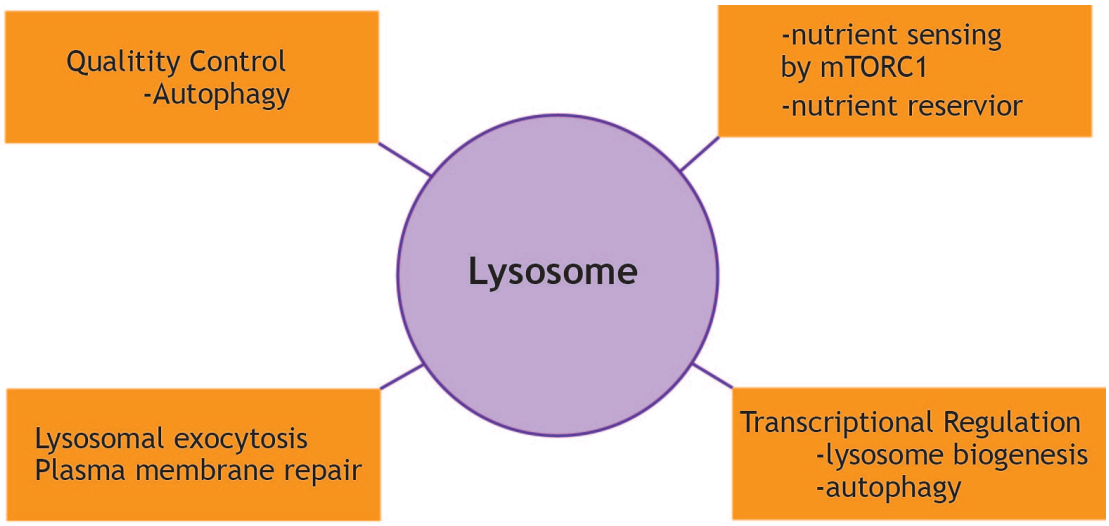

Figure 4: Lysosomal Function

Structure

Lysosomes are organelles found in all eukaryotic cells that are critical to maintain cellular health. They are well known as degradation centers and were discovered in 1955 by the Christian de Duve. While studying the mechanism of action of insulin, de Duve detected a biochemical fraction enriched in hydrolytic activities toward proteins and lipids. With the advent of electron microscopy and follow-up biochemical experiments, the lysosome was identified as a membrane-bound compartment that specializes in the breakdown and recycling of cellular components. The lysosome is defined by its acidic internal pH (~4.5-5.5) that is established by the vacuolar H+ATPase (v-ATPase) and is aided by the counter transport of other ions, such as Cl-, Na+, and K+. The hydrolases located within the lysosomal lumen function optimally at low pH and thus facilitates the compartmentalization of the degradation of vast variety of macromolecules leading to the production of free amino acids, sugars, and free fatty acids which can then be utilized by the cell (as reviewed in (*77-79*)). Furthermore, the lysosome is the

end point of the main degradative process in the cell, autophagy, where cytoplasmic macromolecules, damaged proteins, or even entire organelles are captured and shuttled to the lysosome for degradation (*33*). Hence, it is unsurprising the lysosome can be considered the quality control center of the cell and is required for maintaining cellular homeostasis.

The shape, size, number, and function of lysosome vary across cell types and species. For instance, metazoans cells contain hundreds of lysosomes that range in size from 100 nm to 1 uM, while yeast and plants contain only one or few lysosome-like structures, referred to as vacuoles, which range up to several microns in diameter (as reviewed in (*77*)). Specialized cell types, such as melanosomes in melanocytes or lytic granules in lymphocytes, share features with lysosomes but differ in function and likely protein content. The lysosome is composed of a single phospholipid bilayer decorated with transmembrane proteins; the most abundant lysosome protein is the lysosome-assoicated membrane proteins (LAMP) 1 and 2, which constitute nearly 80% of lysosomal membrane proteins. Interestingly, the function of the LAMP proteins is still unclear. Residing in the lysosomal lumen are ~60 resident acidic hydrolases that digest all classes of macromolecules, such as proteins, lipids, nucleic acids, and sugars (*80*).

The cataloging and identification of all resident lysosomal transmembrane and luminal proteins as well as lysosomal associated proteins is far from complete. With the development of differential centrifugation based techniques the isolation specific organelle compartments has allowed the study of purified lysosomal fractions; however, these techniques are dampened by their lack of specificity. In

order to further understand function and regulation, development of rapid methods for organelle isolation is required and will be discussed later in this thesis.

Lysosomes and Disease

The major feature of lysosomes is the production and release of simple metabolites from inside the lysosomal lumen to the cytoplasm or other compartments. Failure to degrade cargo or release lysosomal catabolites is the underlying mechanism of the rare class of metabolite diseases called lysosomal storage diseases (LSDs), whose cumulative incidence is 1 in 5,000. These disorders display a wide variety of symptoms; most common are developmental delays, neurological defects, and metabolic imbalances that lead to early death. Currently, 60 different lysosomal storage diseases have been identified, and the specific hydrolase or putative transporter that is defective dictates the nature of the accumulated substance in the lysosomal lumen. The treatment of LSDs mainly focuses on the restoration of lysosomal function and current efforts are focused on gene therapy or enzyme replacement therapy(*81*).

A common outcome of lysosomal dysfunction is progressive neurodegeneration, suggesting that neurons are highly susceptible to impaired lysosomal activity. A clear instance of this is found in Niemann-Pick type C (NPC) disease, caused by loss of cholesterol export via NPC1 or NPC2 and leading to massive accumulation of un-esterified cholesterol within lysosomes(*82*). NPC patients show progressive neuropathological features typically seen in Alzheimer's patients, including accumulation of neurofibrillary tangles and amyloid B-peptide in absence of mutations in known alzheimer's disease-related genes. Similarly, Gaucher's disease is the most common LSD, which results from homozygous loss-

of-function mutations in the lysosomal enzyme B-glucocerebrosidase (GBA) leading to the accumulation of glucosylceramide. Patients develop severe neurodegeneration and have a five-fold increased risk in developing Parkinson's disease and an eight-fold risk in developing Lewy body dementia(*83*). Because of this, heterozygous mutations in GBA are the most common risk factors for Parkinson's disease identified currently(*84*). Consistent with this, the autophagy-lysosomal axis has been shown to have a protective role in the brain, as mice harboring neuron-specific deletion of *ATG5* leads to progressive neurodegeneration in absence of any other disease-associated mutations(*85*). However, whether mutations in lysosomal-related genes can be used as risk factors for the development of neurodegenerative disorders is unclear, as well as why neuronal populations are highly susceptible to lysosome dysfunction.

Apart from inherited diseases that disrupt lysosome function, it is clear the lysosomal axis is deregulated in cancer progression. Because rapidly proliferating cells have an enormous demand for the synthesis of new proteins, lipids, DNA, and RNA, the ability to recycle and reuse intracellular stores of these necessary metabolites becomes critically important for cancer cell survival. This becomes important within the tumor microenvironment where nutrients and oxygen are low and nutrient scavenging pathways, such as autophagy or endocytosis, converge on the lysosome to generate the needed metabolites for survival and proliferation. Cancers that harbor oncogenic KRAS mutations have been shown to highly increase macropinocytosis, the process of bulk uptake of extracellular proteins and subsequent lysosomal degradation of sequestered material, and utilize this pathway as an important nutrient delivery source to fuel metabolism and

biosynthetic reactions important for survival and proliferation(*86, 87*). Similarly, studies in lung and pancreatic tumor models have shown that these tumors are highly reliant on autophagy and the lysosome for growth. Moreover, recent work has shown that increased autophagy is coordinated with increased lysosomal biogenesis and is critical in pancreatic cancers (*88*). Specifically, the master transcription factor for lysosomal biogenesis, MiT/TFE family of proteins are increased in pancreatic cancer and their expression is necessary for the maintenance of intracellular amino acids levels and likely to fuel metabolism and biosynthetic pathways needed for growth in these cancers. The transcriptional control of lysosomal function will be discussed in depth in the next section. The reliance on the lysosomal-autophagy axis in certain cancers supports the need for therapeutic interventions that target this pathway or to block the utilization of lysosomal-derived nutrients; however, no known selective inhibitors exist and this will be discussed further in this thesis.

The Lysosome as a regulatory hub for nutrient sensing

The lysosome is the epicenter for nutrient sensing through its physical and functional association with the mTORC1 pathway. As discussed previously, mTORC1 integrates both positive and negative signals from nutrient, growth factors, and energy sources to initiate a growth program. A critical advance in the mTORC1 field was the identification of the lysosome as the site of activation of the mTORC1 pathway. As such, many of the nutrient and growth factor sensing components are localized to the lysosomal surface and nutrient signals from within the lysosomal lumen signal to mTORC1.

The association of a growth-promoting pathway with a major degradative organelle seems surprising at first; however, if one considers the lysosome as a nutrient storage and recycling center, it suggests that the cell has organized its ability to promote strategies that lead to cell growth with physically locating its main growth regulator with a source of the substrates needed for growth. If considered in evolutionary terms, the relation of the lysosome to the yeast vacuole provides clear evidence why this is the case. Despite morphological differences, lysosomes and vacuoles share many of the same components, such as hydrolases, transporters, and the vacuolar proton pump. It has been appreciated that the vacuole represents a large internal reservoir for ions such as phosphate, calcium, zinc, as well as nutrients, such as amino acids, that are fundamental to fungi survival. During starvation, the vacuole increases its nutrient pool via autophagy-mediated protein degradation, which then is exported out of the vacuole via a number of vacuolar permeases to be used in growth-promoting processes. As yeast typically live in an external nutrient and osmotic environment that fluctuates heavily, the presence of a large internal nutrient storage pool allows for sustained survival independent of external nutrient inputs and ensures rapid recovery from non-proliferative states caused by long-term nutrient starvation (as reviewed in (*89*)). In yeast, the TOR kinase is also associated with the vacuolar surface(*90*). Thus, this provides an elegant feedback mechanism by which upon localizing to the surface of the lysosome or vacuole allows the mTOR pathway to directly integrate information from inside the lysosome as well as from the surrounding cytoplasm to regulate anabolic and catabolic processes. Likely, with the emergence of multicellular organisms and systemic growth factors, the mTOR pathway has maintained its

connection with the lysosome as it provides a critical nutrient resource to maintain whole body homeostasis during periods of fasting.

Transcriptional Regulation of the Lysosome

The lysosome has been classically viewed as a static structure strictly to function in a degradative dead-end. This view has been radically altered with the discovery that entire classes of lysosome genes, including those encoding hydrolases, membrane transporters, lysosome-associated proteins, and autophagy-related factors, are under coordinated transcriptional control. Utilizing bioinformatics analysis, shared E box-related consensus elements were identified in promoter regions of many lysosomal genes, aptly named the CLEAR (coordinated lysosomal expression and regulation) element. A family of basic helix-loop-helix transcription factors known as the MiT/TFE proteins, whose members include TFEB, TFEC, TFE3, and MITF bind the CLEAR element motif (*91*). Previously, MITF had been associated with the biogenesis of melanosomes, a lysosome-related organelle, and is frequently amplified in melanoma, while the function of TFEB/TFEC/TFE3 were less understood. Utilizing chromatin immunoprecipitation (ChIP), TFEB, as well as MITF and TFE3, directly binds CLEAR elements and overexpression is sufficient to induce a dramatic expansion of the lysosomal compartment(*92*).

Interestingly, TFEB activation also drives the expression of many proteins involved in multiple steps of autophagy as well as expanding the lysosome compartment. These include genes involved in autophagosome initiation (*BECN1*, *NRBF2*) or elongation (*GABARAP*), selective autophapgy (*SQSTM1*), and

autophagosome-lysosome fusion (*UVRAG*)(*91*). TFEB therefore acts as the master transcriptional regulator of catabolism and coordinates the cells ability to capture substrates for autophagic degradation and then degrade them in the lysosome. Subsequent work in vivo indicates that TFEB in the liver strongly promotes lipid catabolism via activation of PGC1-alpha and downstream fatty acid oxidation and mitochondrial biogenesis; similarly, *TFEB*-deletion in the mouse liver leads to weight gain and deregulation of fat metabolism, while TFEB overexpression led to resistance to lipid accumulation in an autophagy-dependent manner(*93*).

Initial studies detected TFEB in both the cytoplasm and nucleus, and nutrient withdrawal promotes TFEB strictly in the nucleus. A key discovery found that the mTOR pathway had a major role in controlling the nuclear-cytoplasmic shuttling of TFEB. Utilizing either acute mTOR inhibition with either nutrient starvation of catalytic mTOR inhibitors (Torin1), TFEB rapidly concentrated in the nucleus leading to the activation of target lysosomal-autophagy genes. Under full nutrient conditions in which mTOR is activated, mTORC1 directly phosphorylates TFEB on Serine 142 and Serine 211 leading to its retention in the cytoplasm at the lysosomal surface(*94*). Collectively, these studies connect the nutrient sensing arm of the master growth regulator of mTORC1 to the cell's ability to regulate its catabolic compartment.

IV. Autophagy

The term autophagy is derived from the Greek "auto", oneself, and "phagy", to eat. To summarize, it functions as the major intracellular degradation pathway by which cytoplasmic materials are delivered to and degraded to their basic

macromolecules in the lysosome for reuse in cellular processes. Autophagy is an evolutionary conserved degradation pathway that is essential for survival, differentiation, development, and cellular homeostasis (Figure 5). Given its central role in maintaining cellular homeostasis, it is unsurprising it plays a role in diverse disease pathologies such as infection, cancer, neurodegeneration, and aging (*33*).

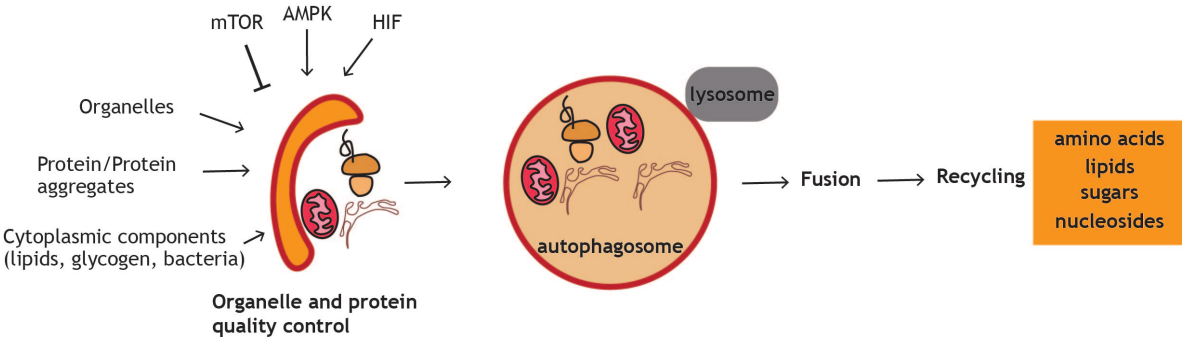

Figure 5: Autophagy as a nutrient resource and qualitity control mechanism. Various critical signaling pathways regulate autophagy induction, with mTORC1 being the most critical. Autophagy mediates the degradation of damaged organelles, protein aggregates, cytoplasmic bacteria, and other cytoplasmic components. This can be thought of as both a mechanism of clearing damaged compartments but also as a recycling system. The formed autophagosome fuses with the lysosome (autophagolysosome) leading to the degradation of its internalized contents to their basic consituents (amino acids, lipids, sugars, and nucleosides) that can then be utilized in growth processes.

History

Apart from his central role in the identification and characterization of lysosomes as discussed previously, Christian de Duve utilized newly developed cell fractionation techniques to identify acid phosphatase-positive vesicles containing degrading mitochondria, endoplasmic reticulum membranes, ribosomes, and other cytoplasmic contents. de Duve proposed the term “autophagy” in order to denote this function of lysosomes in the process of self-eating. Through the use of electron microscopy, autophagosome-like structures (double-membrane vesicles) were found to enriched in the developing kidney and during insect metamorphosis. By the early 1960’s it was clear that autophagosome number

increased upon periods of starvation in rat liver, and by the mid-1970's, the presence of nutrients and growth factors were found to suppress autophagosome number (as reviewed in (*95*)). With these key early findings, the existence of autophagy in mammals was established while its functionality remained merely phenomenological.

By the early 1990's, genetic studies in yeast propelled the existence autophagosomes from just a morphological finding to a critical survival mechanism. Utilizing protease-deficient yeast mutants, Ohsumi and colleagues described "autophagic bodies" enriched in the vacuole when deprived of nutrients, which he then used as a screening method to isolate mutants in what is now referred to as autophagy-related (*ATG*) genes. Several laboratories took similar efforts, first to isolate yeast deficient in protein uptake for degradation in the vacuole (*aut* mutants) as well as mutants deficient in the delivery of a resident hydrolase from the cytoplasm to the vacuole (*cvt* mutants). Taken together, the various laboratories working in yeast identified genes encoding components that function at each stage of autophagy, including initiation, phagophore expansion, and maturation. It is now clear that autophagy-deficient mutants show decreased viability during nitrogen starvation, and these findings ushered in the genetic era of mammalian autophagy research, which has further been extended across all eukaryotic organisms (as reviewed in (*33*)). These early studies followed up by additional genetic and biochemical analyses in various model organisms have shown very clearly that the autophagy machinery is crucial across almost all aspects of cellular physiology, from differentiation and development, nutrient and

energy homeostasis, stress adaptation, tumor suppression, immunity, protection against disease, neurodegeneration, and aging.

Autophagy as an adaptive metabolic response

The primary physiological role of autophagy is likely to maintain cellular homeostasis when nutrient or other metabolic supplies fall below a threshold. Autophagy-deficient mutants are more sensitive to nutrient deprivation than wild-type cells, and genetic loss of the essential components of the autophagy pathway lead to death shortly after birth due to the inability to mobilize sufficient nutrient reserves to survive the period of starvation that occurs when the placental supply of nutrients is lost (*96*). Autophagy can be thought of as generally non-selective, where random portions of the cytoplasm are engulfed in the autophagosome for delivery to the lysosome, but recent evidence suggests specific cellular compartments can be targeted in a regulated fashion. Selective autophagy will be discussed further in the next section. Autophagy is key for not only an adaptive response to starvation but also general cellular housekeeping via the removal of damaged organelles, protein aggregates, or intracellular bacteria.

Typically, autophagy is induced by limitations in ATP availability or amino acid deprivation and many mechanisms exist that promote autophagy under these conditions. The energy charge of the cell, a function of intracellular ATP, ADP, and AMP concentrations, is a potent inducer of autophagy. When ATP is not actively made through glycolysis or oxidative phosphorylation, the energy charge decreases with a concurrent increase in AMP leading to the stimulation of autophagy via AMPK activation. Interestingly, these conditions occur both in cells

that rely heavily on glycolysis or similarly via inhibition of the mitochondrial respiratory chain. Similarly, nutrient deprivation leads to accumulation of NAD, an essential substrate for multiple metabolic reactions, promoting autophagy upon activation of the Sirtuin family of histone deacetylases(*97*). Also, amino acid starvation leads to a significant decrease in cytosolic acetyl-CoA which can potently stimulate autophagy as it is the sole donor of acetyl groups for acetyl transferases, some of which regulate a variety of components of the autophagy machinery at the post-translational level(*98*). Amino acid deprivation also directly results in autophagy induction due to an accumulation of uncharged tRNA species, which is sensed by the stress kinase eukaryotic translation initiation factor 2alpha kinase 4 (EIF2AK4, also known as GCN2), leading to protein synthesis inhibition and autophagy via activating transcription factor 4 (ATF4)(*99*). As described earlier, amino acid deprivation is immediately sensed by mTORC1, which directly regulates autophagy by ULK1 phosphorylation, the initial step in autophagosome formation (*35, 100*).

Apart from amino acid deprivation, autophagy can also be stimulated by the accumulation of specific metabolites, such as fatty acids or ammonia or iron deprivation. Iron is an essential co-factor for many enzymes that catalyze intracellular redox reactions. Drops in free intracellular iron stores leads to the immediate immobilization and degradation of ferritin oligomers in the lysosome by an autophagic response, coordinated by nuclear receptor coactivator 4 (NCOA4), termed “ferritinophagy” (*101*). Ammonia can potently induce autophagy; however, the mechanism is unclear, as it appears to not rely on ULK1/ULK2 activation or mTORC1 inhibition but rather by promoting ER stress(*102*). Finally, both saturated

and unsaturated fatty acids can stimulate autophagy through distinct mechanisms. Palmitate-induced, but not oleate-induced autophagy, requires EIF2AK2 and mitrogen-activated protein kinase 8 (MAPK8). Stearoyl-CoA desaturase, which converts saturated lipids to their monounsaturated forms is required for starvation-induced autophagy; however it is likely that this is due to their need in the formation of autophagosome membranes rather than a nutrient need(*103*). Conversely, dietary lipids stored in triglyceride-containing droplets can be mobilized by autophagy to replenish lipid stores under starvation, but the mechanism is unclear (*104*).

Cargo Recognition and degradation by selective autophagy

While the autophagic response is generally considered to result in bulk degradation of cytosolic material, recent evidence has suggested that autophagy is more selective than previously appreciated. For instance, types of stresses other than nutrient deprivation, such as damaged organelles or aggregated proteins, require selective sequestration of the specific cargo into the autophagosome. The earliest described instance of selective autophagy was found in methylotrophic yeast, which responds to a methanol substrate by increased synthesis of peroxisomal enzymes leading to enlarged peroxisomes. When switched to glucose rather than methanol as a carbon source, this yeast undergo a rapid loss of peroxisomes with increased sequestration of peroxisomes in the vacuole for degradation suggesting peroxisome loss during glucose supplementation is due to a selective degradation of peroxisomes by autophagy.

Selective autophagy is achieved via a defined autophagy receptor that can couple cargo sequestration with association with the autophagosome membrane, typically through an LC3-interacting region (LIR) but this is not a universal characteristic. These LIR motifs generally interact with the ATG8- family proteins LC3/GABARAP and allow the direct connection of the autophagy receptor to the autophagosome membrane. In general, in order to be selective, three main criteria must be met: the cargo must be specifically recognized, the cargo must be effectively tethered to the nascent autophagosome, and non-cargo material has to be excluded from the autophagosome(*105*).

In yeast, the cytoplasm to vacuole pathway (Cvt) has been used as the defining example of selective autophagy. Specifically, the hydrolase aminopeptidase I, prApe1, is synthesized in the cytoplasm as a zymogen with an N-terminal propeptide; prApe1 monomers assemble in the cytoplasm into higher order dodecamers that further assemble into higher order particles in a propeptide-dependent manner. The Cvt pathway sequesters the prApe1 into a pre-formed phagophore and delivers it into the vacuole where it is then activated. While the Cvt pathway is an example of selective transport into the vacuole, currently selective autophagy is considered a process for how to specifically degrade unwanted material in the complex environment of the cytoplasm (*106*). Several targets and receptors of selective autophagy have been identified thus far, such as for aggregate proteins (aggrephagy), mitochondria (mitophagy), peroxisomes (pexophagy), ribosomes (ribophagy), endoplasmic reticulum (reticulophagy), glycogen, intracellular free iron (ferritinophagy), and pathogens (xenophagy) (*95, 101, 104, 107-118*). While the upstream signals to induce the formation of the

autophagosome are quite clear and were discussed previously, the regulation of the degradation of selective targets is still unknown and will be the goal of future work.

Autophagy *in vivo*

The clearest example of the importance of autophagy in mammalian physiology comes from genetic data that systematic deletion of *ATG3*, *ATG5*, or *ATG7* in mice leads to death immediately after birth during the neonatal starvation period. Thus, the enhanced degradation of intracellular components by autophagy is critical to survival during starvation periods. These results have been further pursued using tissue-specific gene targeting and have revealed that autophagy is critical to maintaining several differentiation lineages, such as adipocytes, erythrocytes, T cells, and B-1a cells, as well as maintaining tissue homeostasis and renovation(*96, 119*).

Regardless of nutritional status, the autophagy pathway monitors cytoplasmic components to prevent accumulation of misfolded proteins and non-functional organelles. This has been explored across various tissues in the body. First, *ATG7*-loss in mouse hepatocytes causes accumulation of swollen and deformed mitochondria as well as increased number of peroxisomes and lipid droplets; accordingly, these mice exhibit severe hepatomegaly and hepatocytic hypertrophy leading to hepatitis. Also, constitutive loss of autophagy in the pancreas leads to reduction in beta cell mass, hypoinsulinemia, and an accumulation of ubiquitinated proteins and organelles(*119*). Podocyte-specific deletion of *ATG5* leads to glomeruolsclerosis and an increased susceptibility to

proteinuric renal diseases(*120*). Mice lacking autophagy in the central nervous system exhibit neurological defects with significant losses of pyramidal neurons in the cerebral cortex and of Purkinje cells in the cerebellar cortex. Furthermore, autophagy loss specific in the Purkinje cells leads to progressive axonal dystrophy and degeneration of axon terminals followed by cell death(*85*). Autophagy appears critical for maintaining size both skeletal and cardiac muscle, as autophagy deficiency leads to sarcomere disruption and dysfunction, along with age-dependent muscle atrophy (*121, 122*). Crohn's disease is one of the most common inflammatory diseases and several studies have identified an association between Crohn and a SNP of *ATG16L1,* potentially suggesting the importance of autophagy in intestinal biology. Similarly, the autophagy pathway is critical in maintaining normal function of intestinal Paneth cells (*123*).

In contrast to genetic loss of the autophagy pathway across different tissues, the induction of autophagy varies widely across the body. For instance, even under prolonged fasting conditions, the brain does not strongly induce autophagosome number in nerve cells likely due to the supply of nutrients to the brain from peripheral organs(*124*). However, recent studies have shown that Purkinje cells and hypothalamic neurons are autophagy responsive during fasting, and autophagy induction in the hypothalamus induces lipophagy and increases food intake via upregulation of agouti-related peptide (AgRP) expression. Utilizing transgenic models for measuring autophagic flux, the podocytes in the kidney display high levels of basal autophagy implying its importance for their general homeostasis. Similarly, the acinar cells of the pancreas appear to not require autophagy for normal physiology. The skeletal muscle is composed of multiple fiber

types, which interestingly range in their ability to induce autophagy upon fasting. While the glycolytic fast twitch muscle fibers rapidly induce autophagy upon fasting, the oxidative slow twitch muscle fibers appear strongly resistant (*124*). The mechanistic details behind these differences are not understood.

Autophagy and disease

Autophagy has been studied quite heavily in cancer as work has supported both a tumor-suppressive role along with being a survival mechanism. Mild inhibition of the autophagy pathway has been shown to lead to spontaneous benign tumorigenesis in multiple contexts. For instance, systematic mosaic deletion of *ATG5* in the liver leads to increased tumor formation (*125*). Similarly, heterozygous disruption of *ATG6* leads to increased cancer incidence, including hepatocellular carcinoma, and increased incidence of liver tumors after infection with hepatitis B virus (*126-128*). In contrast, apart from its apparent tumor-suppressive function, autophagy appears critical as a pathway to supply cancer cells with metabolic substrates needed for rapid proliferation. As cancer cells have an increased metabolic demand, especially within a nutrient depleted microenvironment, the role of autophagy to supply necessary substrates for growth and proliferation becomes critical. One clear instance of this is the increased need of lysosomal degradation in *Ras*-mutant pancreatic cancers. These cancers have increased dependence on lysosomal lineage transcription factors for survival as well as upregulate the process of macropinocytosis(*86, 129*). Because of this, autophagy suppression has been proposed to be a viable cancer therapy, but no

known therapies exist that specifically inhibits autophagy induction. This idea will be explored further in this thesis.

While cancer suppression is a major focus of the autophagy field, across multiple model organisms, it is clear that autophagy is critical in the aging process. As autophagy is a major pathway regulating cellular renovation, suppression of autophagy leads to age-dependent dysfunction in various organs. Genetic studies in *C. elegans* have shown that autophagy-related genes are required for life-span extension induced by inhibition of insulin/IGF-like signaling, caloric restriction, and TOR inhibition, suggesting that autophagy is a common downstream mechanism in various pro-life span-signaling pathways (*130, 131*). While it is not clear how autophagy can mediate prolonged life span, the obvious hypothesis is the reduction of toxic protein accumulation or clearance of damaged organelles. Additionally, autophagy induction may have a non-cell autonomous role by reducing inflammatory cytokine production.

V. Preface for work presented in this thesis

The mTORC1 pathway is the master regulator of cellular growth and integrates a diverse set of environmental signals to stimulate growth only in the appropriate context. Through a decade of work, it is clear that the mTORC1 pathway integrates these signals at the lysosome surface, its site of activation. In the presence of sufficient nutrients, mTORC1 is recruited to the lysosomal surface via the Rag GTPase where mTORC1 is physically capable of interacting with its kinase activator Rheb. The Rheb GTPase can then stimulate mTORC1 kinase activity as long as there are sufficient growth factors present. Thus, regulation of

mTORC1 kinase activity is comprised a lysosome-centric coincidence detector that controls its kinase activity as well as its subcellular localization.

Lysosomal Amino Acid Sensing

While the upstream regulators of Rheb have been extensively characterized, how nutrients activate the mTORC1 pathway is an active area of research. It is now clear there are two separate branches (cytosolic and lysosomal) of amino acid sensing that both impinge on the Rag GTPases to regulate mTORC1 activity. On the cytosolic side, the Sestrin and Castor family of proteins signal the presence of cytosolic leucine and arginine, respectively, to mTORC1 in a GATOR2-dependence manner, as discussed previously(*56, 57, 61, 62*). On the other hand, how lysosomal amino acids are transmitted to mTORC1 is a major focus of this thesis. Previous work has shown that amino acids can signal to mTORC1 via the lysosome in an inside-out mechanism dependent on the V-ATPase(*52*). In addition, we have previously identified a novel lysosomal transmembrane protein SLC38A9, which has homology to amino acid transporters that interacts with the core lysosomal nutrient-sensing components of the mTORC1 pathway(*53*). Based on follow-up biochemical characterization, we hypothesized that SLC38A9 acts as a lysosomal arginine sensor upstream of mTORC1.

Our current work shows that SLC38A9 is far more interesting than initially anticipated. Specifically, SLC38A9 transports, in an arginine-regulated fashion, the essential amino acids out of the lysosome for their use in growth-promoting processes. In essence, SLC38A9 couples the signaling of arginine to mTORC1 to the release of essential nutrients out of the lysosome. SLC38A9 is required to

reactivate mTORC1 after autophagy-dependent degradation of proteins, cementing it as a critical link between autophagic-acquisition of amino acid and mTORC1. Pancreatic cancers that rely heavily on the lysosome as a nutrient source require SLC38A9 to form tumors. Thus, SLC38A9 forms a critical link between lysosomal nutrients and growth control.

Emerging roles of Lysosomes in signal transduction and metabolism

Lysosomes are increasingly appreciated as a hub for signal transduction, mainly for the mTORC1 pathway, due to their ability to produce and sense many metabolites. It remains critical to understand its internal metabolite content and its regulation under diverse conditions. Our work on SLC38A9 required the ability to profile the internal contents of mammalian lysosomes in order for us to study how SLC38A9 function impacts its physiological environment. Therefore, we developed a simple method for the rapid purification of intact lysosomes for further analysis.

As many biochemical processes are compartmentalized within the cell, organelle isolation has been of great interest in cell biology as it allows for the specific study of the function of specific cellular compartments, whose functions may be masked when measured at a whole cell level. Previous work has utilized differential centrifugation based techniques, which are unsuitable for our purposes as their lengthy time frames are unable to maintain what is likely a labile organelle metabolite pool and utilize buffers that are incompatible with mass spectrometry based metabolite profiling. Therefore, we developed an immunoprecipitation-based isolation technique that allows for the rapid isolation of intact lysosomes in conditions that are suitable for current metabolite profiling methods and we have

made many interesting discoveries. For example, the concentration of metabolites in lysosomes is very different than in whole cells, and while inhibition of the V-ATPase, a key lysosomal protein complex necessary for maintaining the proton gradient across the lysosomal membrane, increases the levels of most lysosomal metabolites, the non-polar-essential amino acids are unaffected. Instead, nutrient starvation regulates the concentration of these amino acids, an effect we traced to regulation by the mTORC1 pathway. Acute inhibition of mTORC1 strongly increased lysosomal concentrations of these amino acids in an autophagy-independent fashion revealing that the V-ATPase and mTORC1 regulate a distinct set of lysosomal amino acids. With the development of this technique, we are now able to globally profile the contents of mammalian lysosomes and understand its metabolite pool under diverse conditions.

What is the source of lysosomal nutrients that are sensed by SLC38A9?

A major point that emerged from our work on SLC38A9 is that lysosomal arginine acted is a messenger to coordinate the activation of mTORC1 with essential amino acid efflux. What the source of lysosomal arginine that SLC38A9 sensed, however, was unclear. Given that ribosomal proteins are highly enriched in arginine, we hypothesized that ribosome degradation supplies the lysosomal arginine that is sensed by SLC38A9. By preforming quantitative proteomic analyses of lysosomes rapidly isolated using the LysoIP method, we found that nutrient levels and mTOR activity dynamically modulate the lysosomal proteome, and I have focused on NUFIP1, a protein that had previously been associated with ribosome which, upon mTORC1 inhibition, redistributes from the nucleus to

autophagosomes and lysosomes. Under these conditions, NUFIP1 interacts with ribosomes and delivers them to autophagosomes by directly binding to LC3B. The starvation-induced degradation of ribosomes via autophagy (ribophagy) depends on the capacity of NUFIP1 to bind LC3B and promotes cell survival. Accordingly, NUFIP1 is required for the reactivation of mTORC1 upon long-term starvation. Thus, we conclude that NUFIP1 is a receptor for the selective autophagy of ribosomes and provides the needed source that link lysosomal amino acid sensing to mTORC1 and growth control.

References

1. R. T. Abraham, G. J. Wiederrecht, Immunopharmacology of rapamycin. *Annual review of immunology* **14**, 483-510 (1996)10.1146/annurev.immunol.14.1.483).
2. C. P. Eng, S. N. Sehgal, C. Vezina, Activity of rapamycin (AY-22,989) against transplanted tumors. *The Journal of antibiotics* **37**, 1231-1237 (1984); published online EpubOct (
3. J. Heitman, N. R. Movva, M. N. Hall, Targets for cell cycle arrest by the immunosuppressant rapamycin in yeast. *Science* **253**, 905-909 (1991); published online EpubAug 23 (
4. Y. Koltin, L. Faucette, D. J. Bergsma, M. A. Levy, R. Cafferkey, P. L. Koser, R. K. Johnson, G. P. Livi, Rapamycin sensitivity in Saccharomyces cerevisiae is mediated by a peptidyl-prolyl cis-trans isomerase related to human FK506-binding protein. *Molecular and cellular biology* **11**, 1718-1723 (1991); published online EpubMar (
5. S. B. Helliwell, P. Wagner, J. Kunz, M. Deuter-Reinhard, R. Henriquez, M. N. Hall, TOR1 and TOR2 are structurally and functionally similar but not identical phosphatidylinositol kinase homologues in yeast. *Molecular biology of the cell* **5**, 105-118 (1994); published online EpubJan (
6. D. M. Sabatini, H. Erdjument-Bromage, M. Lui, P. Tempst, S. H. Snyder, RAFT1: a mammalian protein that binds to FKBP12 in a rapamycin-dependent fashion and is homologous to yeast TORs. *Cell* **78**, 35-43 (1994); published online EpubJul 15 (
7. E. J. Brown, M. W. Albers, T. B. Shin, K. Ichikawa, C. T. Keith, W. S. Lane, S. L. Schreiber, A mammalian protein targeted by G1-arresting rapamycin-receptor complex. *Nature* **369**, 756-758 (1994); published online EpubJun 30 (10.1038/369756a0).
8. C. J. Sabers, M. M. Martin, G. J. Brunn, J. M. Williams, F. J. Dumont, G. Wiederrecht, R. T. Abraham, Isolation of a protein target of the FKBP12-rapamycin complex in mammalian cells. *The Journal of biological chemistry* **270**, 815-822 (1995); published online EpubJan 13 (
9. Y. Sancak, C. C. Thoreen, T. R. Peterson, R. A. Lindquist, S. A. Kang, E. Spooner, S. A. Carr, D. M. Sabatini, PRAS40 is an insulin-regulated inhibitor of the mTORC1

protein kinase. *Molecular cell* **25**, 903-915 (2007); published online EpubMar 23 (10.1016/j.molcel.2007.03.003).
10. D. H. Kim, D. D. Sarbassov, S. M. Ali, J. E. King, R. R. Latek, H. Erdjument-Bromage, P. Tempst, D. M. Sabatini, mTOR interacts with raptor to form a nutrient-sensitive complex that signals to the cell growth machinery. *Cell* **110**, 163-175 (2002); published online EpubJul 26 (
11. D. A. Guertin, D. M. Stevens, C. C. Thoreen, A. A. Burds, N. Y. Kalaany, J. Moffat, M. Brown, K. J. Fitzgerald, D. M. Sabatini, Ablation in mice of the mTORC components raptor, rictor, or mLST8 reveals that mTORC2 is required for signaling to Akt-FOXO and PKCalpha, but not S6K1. *Developmental cell* **11**, 859-871 (2006); published online EpubDec (10.1016/j.devcel.2006.10.007).
12. T. R. Peterson, M. Laplante, C. C. Thoreen, Y. Sancak, S. A. Kang, W. M. Kuehl, N. S. Gray, D. M. Sabatini, DEPTOR is an mTOR inhibitor frequently overexpressed in multiple myeloma cells and required for their survival. *Cell* **137**, 873-886 (2009); published online EpubMay 29 (10.1016/j.cell.2009.03.046).
13. R. A. Saxton, D. M. Sabatini, mTOR Signaling in Growth, Metabolism, and Disease. *Cell* **168**, 960-976 (2017); published online EpubMar 09 (10.1016/j.cell.2017.02.004).
14. C. C. Thoreen, L. Chantranupong, H. R. Keys, T. Wang, N. S. Gray, D. M. Sabatini, A unifying model for mTORC1-mediated regulation of mRNA translation. *Nature* **485**, 109-113 (2012); published online EpubMay 2 (10.1038/nature11083).
15. C. J. Kuo, J. Chung, D. F. Fiorentino, W. M. Flanagan, J. Blenis, G. R. Crabtree, Rapamycin selectively inhibits interleukin-2 activation of p70 S6 kinase. *Nature* **358**, 70-73 (1992); published online EpubJul 2 (10.1038/358070a0).
16. J. Chung, C. J. Kuo, G. R. Crabtree, J. Blenis, Rapamycin-FKBP specifically blocks growth-dependent activation of and signaling by the 70 kd S6 protein kinases. *Cell* **69**, 1227-1236 (1992); published online EpubJun 26 (
17. L. Beretta, A. C. Gingras, Y. V. Svitkin, M. N. Hall, N. Sonenberg, Rapamycin blocks the phosphorylation of 4E-BP1 and inhibits cap-dependent initiation of translation. *The EMBO journal* **15**, 658-664 (1996); published online EpubFeb 1 (
18. B. Magnuson, B. Ekim, D. C. Fingar, Regulation and function of ribosomal protein S6 kinase (S6K) within mTOR signalling networks. *The Biochemical journal* **441**, 1-21 (2012); published online EpubJan 1 (10.1042/BJ20110892).
19. M. Pende, S. H. Um, V. Mieulet, M. Sticker, V. L. Goss, J. Mestan, M. Mueller, S. Fumagalli, S. C. Kozma, G. Thomas, S6K1(-/-)/S6K2(-/-) mice exhibit perinatal lethality and rapamycin-sensitive 5'-terminal oligopyrimidine mRNA translation and reveal a mitogen-activated protein kinase-dependent S6 kinase pathway. *Molecular and cellular biology* **24**, 3112-3124 (2004); published online EpubApr (
20. M. K. Holz, B. A. Ballif, S. P. Gygi, J. Blenis, mTOR and S6K1 mediate assembly of the translation preinitiation complex through dynamic protein interchange and ordered phosphorylation events. *Cell* **123**, 569-580 (2005); published online EpubNov 18 (10.1016/j.cell.2005.10.024).
21. X. M. Ma, J. Blenis, Molecular mechanisms of mTOR-mediated translational control. *Nat Rev Mol Cell Biol* **10**, 307-318 (2009); published online EpubMay (10.1038/nrm2672).
22. C. Mayer, J. Zhao, X. Yuan, I. Grummt, mTOR-dependent activation of the transcription factor TIF-IA links rRNA synthesis to nutrient availability. *Genes & development* **18**, 423-434 (2004); published online EpubFeb 15 (10.1101/gad.285504).

23. B. Shor, J. Wu, Q. Shakey, L. Toral-Barza, C. Shi, M. Follettie, K. Yu, Requirement of the mTOR kinase for the regulation of Maf1 phosphorylation and control of RNA polymerase III-dependent transcription in cancer cells. *The Journal of biological chemistry* **285**, 15380-15392 (2010); published online EpubMay 14 (10.1074/jbc.M109.071639).
24. K. Duvel, J. L. Yecies, S. Menon, P. Raman, A. I. Lipovsky, A. L. Souza, E. Triantafellow, Q. Ma, R. Gorski, S. Cleaver, M. G. Vander Heiden, J. P. MacKeigan, P. M. Finan, C. B. Clish, L. O. Murphy, B. D. Manning, Activation of a metabolic gene regulatory network downstream of mTOR complex 1. *Molecular cell* **39**, 171-183 (2010); published online EpubJul 30 (10.1016/j.molcel.2010.06.022).
25. S. Li, M. S. Brown, J. L. Goldstein, Bifurcation of insulin signaling pathway in rat liver: mTORC1 required for stimulation of lipogenesis, but not inhibition of gluconeogenesis. *Proceedings of the National Academy of Sciences of the United States of America* **107**, 3441-3446 (2010); published online EpubFeb 23 (10.1073/pnas.0914798107).
26. T. Porstmann, C. R. Santos, B. Griffiths, M. Cully, M. Wu, S. Leevers, J. R. Griffiths, Y. L. Chung, A. Schulze, SREBP activity is regulated by mTORC1 and contributes to Akt-dependent cell growth. *Cell metabolism* **8**, 224-236 (2008); published online EpubSep (10.1016/j.cmet.2008.07.007).
27. T. R. Peterson, S. S. Sengupta, T. E. Harris, A. E. Carmack, S. A. Kang, E. Balderas, D. A. Guertin, K. L. Madden, A. E. Carpenter, B. N. Finck, D. M. Sabatini, mTOR complex 1 regulates lipin 1 localization to control the SREBP pathway. *Cell* **146**, 408-420 (2011); published online EpubAug 5 (10.1016/j.cell.2011.06.034).
28. I. Ben-Sahra, G. Hoxhaj, S. J. H. Ricoult, J. M. Asara, B. D. Manning, mTORC1 induces purine synthesis through control of the mitochondrial tetrahydrofolate cycle. *Science* **351**, 728-733 (2016); published online EpubFeb 12 (10.1126/science.aad0489).
29. S. J. Ricoult, J. L. Yecies, I. Ben-Sahra, B. D. Manning, Oncogenic PI3K and K-Ras stimulate de novo lipid synthesis through mTORC1 and SREBP. *Oncogene* **35**, 1250-1260 (2016); published online EpubMar 10 (10.1038/onc.2015.179).
30. A. M. Robitaille, S. Christen, M. Shimobayashi, M. Cornu, L. L. Fava, S. Moes, C. Prescianotto-Baschong, U. Sauer, P. Jenoe, M. N. Hall, Quantitative phosphoproteomics reveal mTORC1 activates de novo pyrimidine synthesis. *Science* **339**, 1320-1323 (2013); published online EpubMar 15 (10.1126/science.1228771).
31. N. Mizushima, M. Komatsu, Autophagy: renovation of cells and tissues. *Cell* **147**, 728-741 (2011); published online EpubNov 11 (10.1016/j.cell.2011.10.026).
32. I. G. Ganley, H. Lam du, J. Wang, X. Ding, S. Chen, X. Jiang, ULK1.ATG13.FIP200 complex mediates mTOR signaling and is essential for autophagy. *J Biol Chem* **284**, 12297-12305 (2009); published online EpubMay 01 (10.1074/jbc.M900573200).
33. C. H. Jung, C. B. Jun, S. H. Ro, Y. M. Kim, N. M. Otto, J. Cao, M. Kundu, D. H. Kim, ULK-Atg13-FIP200 complexes mediate mTOR signaling to the autophagy machinery. *Molecular biology of the cell* **20**, 1992-2003 (2009); published online EpubApr (10.1091/mbc.E08-12-1249).
34. J. Zhao, A. L. Goldberg, Coordinate regulation of autophagy and the ubiquitin proteasome system by MTOR. *Autophagy* **12**, 1967-1970 (2016); published online EpubOct 02 (10.1080/15548627.2016.1205770).
35. A. A. Alfaiz, L. Micale, B. Mandriani, B. Augello, M. T. Pellico, J. Chrast, I. Xenarios, L. Zelante, G. Merla, A. Reymond, TBC1D7 mutations are associated

with intellectual disability, macrocrania, patellar dislocation, and celiac disease. *Human mutation* **35**, 447-451 (2014); published online EpubApr (10.1002/humu.22529).
36. S. M. Goorden, M. Hoogeveen-Westerveld, C. Cheng, G. M. van Woerden, M. Mozaffari, L. Post, H. J. Duckers, M. Nellist, Y. Elgersma, Rheb is essential for murine development. *Molecular and cellular biology* **31**, 1672-1678 (2011); published online EpubApr (10.1128/MCB.00985-10).
37. K. Inoki, Y. Li, T. Xu, K. L. Guan, Rheb GTPase is a direct target of TSC2 GAP activity and regulates mTOR signaling. *Genes & development* **17**, 1829-1834 (2003); published online EpubAug 1 (10.1101/gad.1110003).
38. K. Inoki, T. Zhu, K. L. Guan, TSC2 mediates cellular energy response to control cell growth and survival. *Cell* **115**, 577-590 (2003); published online EpubNov 26 (
39. S. Menon, C. C. Dibble, G. Talbott, G. Hoxhaj, A. J. Valvezan, H. Takahashi, L. C. Cantley, B. D. Manning, Spatial control of the TSC complex integrates insulin and nutrient regulation of mTORC1 at the lysosome. *Cell* **156**, 771-785 (2014); published online EpubFeb 13 (10.1016/j.cell.2013.11.049).
40. K. Inoki, Y. Li, T. Zhu, J. Wu, K. L. Guan, TSC2 is phosphorylated and inhibited by Akt and suppresses mTOR signalling. *Nature cell biology* **4**, 648-657 (2002); published online EpubSep (10.1038/ncb839).
41. S. Sengupta, T. R. Peterson, D. M. Sabatini, Regulation of the mTOR complex 1 pathway by nutrients, growth factors, and stress. *Molecular cell* **40**, 310-322 (2010); published online EpubOct 22 (10.1016/j.molcel.2010.09.026).
42. D. D. Sarbassov, D. A. Guertin, S. M. Ali, D. M. Sabatini, Phosphorylation and regulation of Akt/PKB by the rictor-mTOR complex. *Science* **307**, 1098-1101 (2005); published online EpubFeb 18 (10.1126/science.1106148).
43. R. J. Shaw, L. C. Cantley, Ras, PI(3)K and mTOR signalling controls tumour cell growth. *Nature* **441**, 424-430 (2006); published online EpubMay 25 (10.1038/nature04869).
44. D. M. Gwinn, D. B. Shackelford, D. F. Egan, M. M. Mihaylova, A. Mery, D. S. Vasquez, B. E. Turk, R. J. Shaw, AMPK phosphorylation of raptor mediates a metabolic checkpoint. *Molecular cell* **30**, 214-226 (2008); published online EpubApr 25 (10.1016/j.molcel.2008.03.003).
45. A. Efeyan, R. Zoncu, S. Chang, I. Gumper, H. Snitkin, R. L. Wolfson, O. Kirak, D. D. Sabatini, D. M. Sabatini, Regulation of mTORC1 by the Rag GTPases is necessary for neonatal autophagy and survival. *Nature* **493**, 679-683 (2013); published online EpubJan 31 (10.1038/nature11745).
46. J. Brugarolas, K. Lei, R. L. Hurley, B. D. Manning, J. H. Reiling, E. Hafen, L. A. Witters, L. W. Ellisen, W. G. Kaelin, Jr., Regulation of mTOR function in response to hypoxia by REDD1 and the TSC1/TSC2 tumor suppressor complex. *Genes & development* **18**, 2893-2904 (2004); published online EpubDec 1 (10.1101/gad.1256804).
47. C. H. Lee, K. Inoki, M. Karbowniczek, E. Petroulakis, N. Sonenberg, E. P. Henske, K. L. Guan, Constitutive mTOR activation in TSC mutants sensitizes cells to energy starvation and genomic damage via p53. *The EMBO journal* **26**, 4812-4823 (2007); published online EpubNov 28 (10.1038/sj.emboj.7601900).
48. Y. Sancak, T. R. Peterson, Y. D. Shaul, R. A. Lindquist, C. C. Thoreen, L. Bar-Peled, D. M. Sabatini, The Rag GTPases bind raptor and mediate amino acid signaling to mTORC1. *Science* **320**, 1496-1501 (2008); published online EpubJun 13 (10.1126/science.1157535).

49. L. Bar-Peled, L. D. Schweitzer, R. Zoncu, D. M. Sabatini, Ragulator is a GEF for the rag GTPases that signal amino acid levels to mTORC1. *Cell* **150**, 1196-1208 (2012); published online EpubSep 14 (10.1016/j.cell.2012.07.032).
50. Y. Sancak, L. Bar-Peled, R. Zoncu, A. L. Markhard, S. Nada, D. M. Sabatini, Ragulator-Rag complex targets mTORC1 to the lysosomal surface and is necessary for its activation by amino acids. *Cell* **141**, 290-303 (2010); published online EpubApr 16 (10.1016/j.cell.2010.02.024).
51. R. Zoncu, L. Bar-Peled, A. Efeyan, S. Wang, Y. Sancak, D. M. Sabatini, mTORC1 senses lysosomal amino acids through an inside-out mechanism that requires the vacuolar H(+)-ATPase. *Science* **334**, 678-683 (2011); published online EpubNov 04 (10.1126/science.1207056).
52. S. Wang, Z. Y. Tsun, R. L. Wolfson, K. Shen, G. A. Wyant, M. E. Plovanich, E. D. Yuan, T. D. Jones, L. Chantranupong, W. Comb, T. Wang, L. Bar-Peled, R. Zoncu, C. Straub, C. Kim, J. Park, B. L. Sabatini, D. M. Sabatini, Metabolism. Lysosomal amino acid transporter SLC38A9 signals arginine sufficiency to mTORC1. *Science* **347**, 188-194 (2015); published online EpubJan 09 (10.1126/science.1257132).
53. R. L. Wolfson, L. Chantranupong, G. A. Wyant, X. Gu, J. M. Orozco, K. Shen, K. J. Condon, S. Petri, J. Kedir, S. M. Scaria, M. Abu-Remaileh, W. N. Frankel, D. M. Sabatini, KICSTOR recruits GATOR1 to the lysosome and is necessary for nutrients to regulate mTORC1. *Nature* **543**, 438-442 (2017); published online EpubMar 16 (10.1038/nature21423).
54. L. Bar-Peled, L. Chantranupong, A. D. Cherniack, W. W. Chen, K. A. Ottina, B. C. Grabiner, E. D. Spear, S. L. Carter, M. Meyerson, D. M. Sabatini, A Tumor suppressor complex with GAP activity for the Rag GTPases that signal amino acid sufficiency to mTORC1. *Science* **340**, 1100-1106 (2013); published online EpubMay 31 (10.1126/science.1232044).
55. R. L. Wolfson, L. Chantranupong, R. A. Saxton, K. Shen, S. M. Scaria, J. R. Cantor, D. M. Sabatini, Sestrin2 is a leucine sensor for the mTORC1 pathway. *Science* **351**, 43-48 (2016); published online EpubJan 01 (10.1126/science.aab2674).
56. R. A. Saxton, K. E. Knockenhauer, R. L. Wolfson, L. Chantranupong, M. E. Pacold, T. Wang, T. U. Schwartz, D. M. Sabatini, Structural basis for leucine sensing by the Sestrin2-mTORC1 pathway. *Science* **351**, 53-58 (2016); published online EpubJan 01 (10.1126/science.aad2087).
57. J. S. Kim, S. H. Ro, M. Kim, H. W. Park, I. A. Semple, H. Park, U. S. Cho, W. Wang, K. L. Guan, M. Karin, J. H. Lee, Sestrin2 inhibits mTORC1 through modulation of GATOR complexes. *Scientific reports* **5**, 9502 (2015); published online EpubMar 30 (10.1038/srep09502).
58. A. Parmigiani, A. Nourbakhsh, B. Ding, W. Wang, Y. C. Kim, K. Akopiants, K. L. Guan, M. Karin, A. V. Budanov, Sestrins inhibit mTORC1 kinase activation through the GATOR complex. *Cell reports* **9**, 1281-1291 (2014); published online EpubNov 20 (10.1016/j.celrep.2014.10.019).
59. L. Chantranupong, R. L. Wolfson, J. M. Orozco, R. A. Saxton, S. M. Scaria, L. Bar-Peled, E. Spooner, M. Isasa, S. P. Gygi, D. M. Sabatini, The Sestrins interact with GATOR2 to negatively regulate the amino-acid-sensing pathway upstream of mTORC1. *Cell reports* **9**, 1-8 (2014); published online EpubOct 09 (10.1016/j.celrep.2014.09.014).
60. L. Chantranupong, S. M. Scaria, R. A. Saxton, M. P. Gygi, K. Shen, G. A. Wyant, T. Wang, J. W. Harper, S. P. Gygi, D. M. Sabatini, The CASTOR Proteins Are Arginine Sensors for the mTORC1 Pathway. *Cell* **165**, 153-164 (2016); published online EpubMar 24 (10.1016/j.cell.2016.02.035).

61. R. A. Saxton, L. Chantranupong, K. E. Knockenhauer, T. U. Schwartz, D. M. Sabatini, Mechanism of arginine sensing by CASTOR1 upstream of mTORC1. *Nature* **536**, 229-233 (2016); published online EpubAug 11 (10.1038/nature19079).
62. X. Gu, J. M. Orozco, R. A. Saxton, K. J. Condon, G. Y. Liu, P. A. Krawczyk, S. M. Scaria, J. W. Harper, S. P. Gygi, D. M. Sabatini, SAMTOR is an S-adenosylmethionine sensor for the mTORC1 pathway. *Science* **358**, 813-818 (2017); published online EpubNov 10 (10.1126/science.aao3265).
63. Z. Y. Tsun, L. Bar-Peled, L. Chantranupong, R. Zoncu, T. Wang, C. Kim, E. Spooner, D. M. Sabatini, The folliculin tumor suppressor is a GAP for the RagC/D GTPases that signal amino acid levels to mTORC1. *Molecular cell* **52**, 495-505 (2013); published online EpubNov 21 (10.1016/j.molcel.2013.09.016).
64. J. L. Jewell, Y. C. Kim, R. C. Russell, F. X. Yu, H. W. Park, S. W. Plouffe, V. S. Tagliabracci, K. L. Guan, Metabolism. Differential regulation of mTORC1 by leucine and glutamine. *Science* **347**, 194-198 (2015); published online EpubJan 9 (10.1126/science.1259472).
65. Q. Venot, T. Blanc, S. H. Rabia, L. Berteloot, S. Ladraa, J. P. Duong, E. Blanc, S. C. Johnson, C. Hoguin, O. Boccara, S. Sarnacki, N. Boddaert, S. Pannier, F. Martinez, S. Magassa, J. Yamaguchi, B. Knebelmann, P. Merville, N. Grenier, D. Joly, V. Cormier-Daire, C. Michot, C. Bole-Feysot, A. Picard, V. Soupre, S. Lyonnet, J. Sadoine, L. Slimani, C. Chaussain, C. Laroche-Raynaud, L. Guibaud, C. Broissand, J. Amiel, C. Legendre, F. Terzi, G. Canaud, Targeted therapy in patients with PIK3CA-related overgrowth syndrome. *Nature* **558**, 540-546 (2018); published online EpubJun (10.1038/s41586-018-0217-9).
66. D. J. Kwiatkowski, B. D. Manning, Molecular basis of giant cells in tuberous sclerosis complex. *The New England journal of medicine* **371**, 778-780 (2014); published online EpubAug 21 (10.1056/NEJMcibr1406613).
67. N. Wagle, B. C. Grabiner, E. M. Van Allen, E. Hodis, S. Jacobus, J. G. Supko, M. Stewart, T. K. Choueiri, L. Gandhi, J. M. Cleary, A. A. Elfiky, M. E. Taplin, E. C. Stack, S. Signoretti, M. Loda, G. I. Shapiro, D. M. Sabatini, E. S. Lander, S. B. Gabriel, P. W. Kantoff, L. A. Garraway, J. E. Rosenberg, Activating mTOR mutations in a patient with an extraordinary response on a phase I trial of everolimus and pazopanib. *Cancer discovery* **4**, 546-553 (2014); published online EpubMay (10.1158/2159-8290.CD-13-0353).
68. B. C. Grabiner, V. Nardi, K. Birsoy, R. Possemato, K. Shen, S. Sinha, A. Jordan, A. H. Beck, D. M. Sabatini, A diverse array of cancer-associated MTOR mutations are hyperactivating and can predict rapamycin sensitivity. *Cancer discovery* **4**, 554-563 (2014); published online EpubMay (10.1158/2159-8290.CD-13-0929).
69. N. Wagle, B. C. Grabiner, E. M. Van Allen, A. Amin-Mansour, A. Taylor-Weiner, M. Rosenberg, N. Gray, J. A. Barletta, Y. Guo, S. J. Swanson, D. T. Ruan, G. J. Hanna, R. I. Haddad, G. Getz, D. J. Kwiatkowski, S. L. Carter, D. M. Sabatini, P. A. Janne, L. A. Garraway, J. H. Lorch, Response and acquired resistance to everolimus in anaplastic thyroid cancer. *The New England journal of medicine* **371**, 1426-1433 (2014); published online EpubOct 9 (10.1056/NEJMoa1403352).
70. J. Okosun, R. L. Wolfson, J. Wang, S. Araf, L. Wilkins, B. M. Castellano, L. Escudero-Ibarz, A. F. Al Seraihi, J. Richter, S. H. Bernhart, A. Efeyan, S. Iqbal, J. Matthews, A. Clear, J. A. Guerra-Assuncao, C. Bodor, H. Quentmeier, C. Mansbridge, P. Johnson, A. Davies, J. C. Strefford, G. Packham, S. Barrans, A. Jack, M. Q. Du, M. Calaminici, T. A. Lister, R. Auer, S. Montoto, J. G. Gribben, R. Siebert, C. Chelala, R. Zoncu, D. M. Sabatini, J. Fitzgibbon, Recurrent mTORC1-

activating RRAGC mutations in follicular lymphoma. *Nature genetics* **48**, 183-188 (2016); published online EpubFeb (10.1038/ng.3473).
71. P. B. Crino, K. L. Nathanson, E. P. Henske, The tuberous sclerosis complex. *The New England journal of medicine* **355**, 1345-1356 (2006); published online EpubSep 28 (10.1056/NEJMra055323).
72. J. J. Bissler, J. C. Kingswood, E. Radzikowska, B. A. Zonnenberg, M. Frost, E. Belousova, M. Sauter, N. Nonomura, S. Brakemeier, P. J. de Vries, V. H. Whittemore, D. Chen, T. Sahmoud, G. Shah, J. Lincy, D. Lebwohl, K. Budde, Everolimus for angiomyolipoma associated with tuberous sclerosis complex or sporadic lymphangioleiomyomatosis (EXIST-2): a multicentre, randomised, double-blind, placebo-controlled trial. *Lancet* **381**, 817-824 (2013); published online EpubMar 9 (10.1016/S0140-6736(12)61767-X).
73. K. E. O'Reilly, F. Rojo, Q. B. She, D. Solit, G. B. Mills, D. Smith, H. Lane, F. Hofmann, D. J. Hicklin, D. L. Ludwig, J. Baselga, N. Rosen, mTOR inhibition induces upstream receptor tyrosine kinase signaling and activates Akt. *Cancer research* **66**, 1500-1508 (2006); published online EpubFeb 1 (10.1158/0008-5472.CAN-05-2925).
74. C. C. Thoreen, S. A. Kang, J. W. Chang, Q. Liu, J. Zhang, Y. Gao, L. J. Reichling, T. Sim, D. M. Sabatini, N. S. Gray, An ATP-competitive mammalian target of rapamycin inhibitor reveals rapamycin-resistant functions of mTORC1. *The Journal of biological chemistry* **284**, 8023-8032 (2009); published online EpubMar 20 (10.1074/jbc.M900301200).
75. D. W. Lamming, L. Ye, P. Katajisto, M. D. Goncalves, M. Saitoh, D. M. Stevens, J. G. Davis, A. B. Salmon, A. Richardson, R. S. Ahima, D. A. Guertin, D. M. Sabatini, J. A. Baur, Rapamycin-induced insulin resistance is mediated by mTORC2 loss and uncoupled from longevity. *Science* **335**, 1638-1643 (2012); published online EpubMar 30 (10.1126/science.1215135).
76. R. M. Perera, R. Zoncu, The Lysosome as a Regulatory Hub. *Annual review of cell and developmental biology* **32**, 223-253 (2016); published online EpubOct 6 (10.1146/annurev-cellbio-111315-125125).
77. C. De Duve, R. Wattiaux, Functions of lysosomes. *Annual review of physiology* **28**, 435-492 (1966)10.1146/annurev.ph.28.030166.002251).
78. J. A. Mindell, Lysosomal acidification mechanisms. *Annual review of physiology* **74**, 69-86 (2012)10.1146/annurev-physiol-012110-142317).
79. P. Saftig, J. Klumperman, Lysosome biogenesis and lysosomal membrane proteins: trafficking meets function. *Nature reviews. Molecular cell biology* **10**, 623-635 (2009); published online EpubSep (10.1038/nrm2745).
80. F. M. Platt, B. Boland, A. C. van der Spoel, The cell biology of disease: lysosomal storage disorders: the cellular impact of lysosomal dysfunction. *The Journal of cell biology* **199**, 723-734 (2012); published online EpubNov 26 (10.1083/jcb.201208152).
81. E. D. Carstea, J. A. Morris, K. G. Coleman, S. K. Loftus, D. Zhang, C. Cummings, J. Gu, M. A. Rosenfeld, W. J. Pavan, D. B. Krizman, J. Nagle, M. H. Polymeropoulos, S. L. Sturley, Y. A. Ioannou, M. E. Higgins, M. Comly, A. Cooney, A. Brown, C. R. Kaneski, E. J. Blanchette-Mackie, N. K. Dwyer, E. B. Neufeld, T. Y. Chang, L. Liscum, J. F. Strauss, 3rd, K. Ohno, M. Zeigler, R. Carmi, J. Sokol, D. Markie, R. R. O'Neill, O. P. van Diggelen, M. Elleder, M. C. Patterson, R. O. Brady, M. T. Vanier, P. G. Pentchev, D. A. Tagle, Niemann-Pick C1 disease gene: homology to mediators of cholesterol homeostasis. *Science* **277**, 228-231 (1997); published online EpubJul 11 (

82. G. Bultron, K. Kacena, D. Pearson, M. Boxer, R. Yang, S. Sathe, G. Pastores, P. K. Mistry, The risk of Parkinson's disease in type 1 Gaucher disease. *Journal of inherited metabolic disease* **33**, 167-173 (2010); published online EpubApr (10.1007/s10545-010-9055-0).
83. J. Aharon-Peretz, H. Rosenbaum, R. Gershoni-Baruch, Mutations in the glucocerebrosidase gene and Parkinson's disease in Ashkenazi Jews. *The New England journal of medicine* **351**, 1972-1977 (2004); published online EpubNov 4 (10.1056/NEJMoa033277).
84. T. Hara, K. Nakamura, M. Matsui, A. Yamamoto, Y. Nakahara, R. Suzuki-Migishima, M. Yokoyama, K. Mishima, I. Saito, H. Okano, N. Mizushima, Suppression of basal autophagy in neural cells causes neurodegenerative disease in mice. *Nature* **441**, 885-889 (2006); published online EpubJun 15 (10.1038/nature04724).
85. C. Commisso, S. M. Davidson, R. G. Soydaner-Azeloglu, S. J. Parker, J. J. Kamphorst, S. Hackett, E. Grabocka, M. Nofal, J. A. Drebin, C. B. Thompson, J. D. Rabinowitz, C. M. Metallo, M. G. Vander Heiden, D. Bar-Sagi, Macropinocytosis of protein is an amino acid supply route in Ras-transformed cells. *Nature* **497**, 633-637 (2013); published online EpubMay 30 (10.1038/nature12138).
86. N. N. Pavlova, C. B. Thompson, The Emerging Hallmarks of Cancer Metabolism. *Cell metabolism* **23**, 27-47 (2016); published online EpubJan 12 (10.1016/j.cmet.2015.12.006).
87. R. M. Perera, S. Stoykova, B. N. Nicolay, K. N. Ross, J. Fitamant, M. Boukhali, J. Lengrand, V. Deshpande, M. K. Selig, C. R. Ferrone, J. Settleman, G. Stephanopoulos, N. J. Dyson, R. Zoncu, S. Ramaswamy, W. Haas, N. Bardeesy, Transcriptional control of autophagy-lysosome function drives pancreatic cancer metabolism. *Nature* **524**, 361-365 (2015); published online EpubAug 20 (10.1038/nature14587).
88. L. Chantranupong, R. L. Wolfson, D. M. Sabatini, Nutrient-sensing mechanisms across evolution. *Cell* **161**, 67-83 (2015); published online EpubMar 26 (10.1016/j.cell.2015.02.041).
89. F. Dubouloz, O. Deloche, V. Wanke, E. Cameroni, C. De Virgilio, The TOR and EGO protein complexes orchestrate microautophagy in yeast. *Molecular cell* **19**, 15-26 (2005); published online EpubJul 1 (10.1016/j.molcel.2005.05.020).
90. C. Settembre, C. Di Malta, V. A. Polito, M. Garcia Arencibia, F. Vetrini, S. Erdin, S. U. Erdin, T. Huynh, D. Medina, P. Colella, M. Sardiello, D. C. Rubinsztein, A. Ballabio, TFEB links autophagy to lysosomal biogenesis. *Science* **332**, 1429-1433 (2011); published online EpubJun 17 (10.1126/science.1204592).
91. C. Settembre, A. Fraldi, D. L. Medina, A. Ballabio, Signals from the lysosome: a control centre for cellular clearance and energy metabolism. *Nature reviews. Molecular cell biology* **14**, 283-296 (2013); published online EpubMay (10.1038/nrm3565).
92. C. Settembre, R. De Cegli, G. Mansueto, P. K. Saha, F. Vetrini, O. Visvikis, T. Huynh, A. Carissimo, D. Palmer, T. J. Klisch, A. C. Wollenberg, D. Di Bernardo, L. Chan, J. E. Irazoqui, A. Ballabio, TFEB controls cellular lipid metabolism through a starvation-induced autoregulatory loop. *Nature cell biology* **15**, 647-658 (2013); published online EpubJun (10.1038/ncb2718).
93. C. Settembre, R. Zoncu, D. L. Medina, F. Vetrini, S. Erdin, S. Erdin, T. Huynh, M. Ferron, G. Karsenty, M. C. Vellard, V. Facchinetti, D. M. Sabatini, A. Ballabio, A lysosome-to-nucleus signalling mechanism senses and regulates the lysosome via

mTOR and TFEB. *The EMBO journal* **31**, 1095-1108 (2012); published online EpubMar 07 (10.1038/emboj.2012.32).
94. N. N. Noda, Y. Ohsumi, F. Inagaki, Atg8-family interacting motif crucial for selective autophagy. *FEBS letters* **584**, 1379-1385 (2010); published online EpubApr 02 (10.1016/j.febslet.2010.01.018).
95. A. Kuma, M. Hatano, M. Matsui, A. Yamamoto, H. Nakaya, T. Yoshimori, Y. Ohsumi, T. Tokuhisa, N. Mizushima, The role of autophagy during the early neonatal starvation period. *Nature* **432**, 1032-1036 (2004); published online EpubDec 23 (10.1038/nature03029).
96. D. G. Hardie, F. A. Ross, S. A. Hawley, AMPK: a nutrient and energy sensor that maintains energy homeostasis. *Nature reviews. Molecular cell biology* **13**, 251-262 (2012); published online EpubMar 22 (10.1038/nrm3311).
97. G. Marino, F. Pietrocola, T. Eisenberg, Y. Kong, S. A. Malik, A. Andryushkova, S. Schroeder, T. Pendl, A. Harger, M. Niso-Santano, N. Zamzami, M. Scoazec, S. Durand, D. P. Enot, A. F. Fernandez, I. Martins, O. Kepp, L. Senovilla, C. Bauvy, E. Morselli, E. Vacchelli, M. Bennetzen, C. Magnes, F. Sinner, T. Pieber, C. Lopez-Otin, M. C. Maiuri, P. Codogno, J. S. Andersen, J. A. Hill, F. Madeo, G. Kroemer, Regulation of autophagy by cytosolic acetyl-coenzyme A. *Molecular cell* **53**, 710-725 (2014); published online EpubMar 6 (10.1016/j.molcel.2014.01.016).
98. J. Ye, M. Kumanova, L. S. Hart, K. Sloane, H. Zhang, D. N. De Panis, E. Bobrovnikova-Marjon, J. A. Diehl, D. Ron, C. Koumenis, The GCN2-ATF4 pathway is critical for tumour cell survival and proliferation in response to nutrient deprivation. *The EMBO journal* **29**, 2082-2096 (2010); published online EpubJun 16 (10.1038/emboj.2010.81).
99. N. Hosokawa, T. Hara, T. Kaizuka, C. Kishi, A. Takamura, Y. Miura, S. Iemura, T. Natsume, K. Takehana, N. Yamada, J. L. Guan, N. Oshiro, N. Mizushima, Nutrient-dependent mTORC1 association with the ULK1-Atg13-FIP200 complex required for autophagy. *Molecular biology of the cell* **20**, 1981-1991 (2009); published online EpubApr (10.1091/mbc.E08-12-1248).
100. J. D. Mancias, X. Wang, S. P. Gygi, J. W. Harper, A. C. Kimmelman, Quantitative proteomics identifies NCOA4 as the cargo receptor mediating ferritinophagy. *Nature* **509**, 105-109 (2014); published online EpubMay 01 (10.1038/nature13148).
101. L. M. Harder, J. Bunkenborg, J. S. Andersen, Inducing autophagy: a comparative phosphoproteomic study of the cellular response to ammonia and rapamycin. *Autophagy* **10**, 339-355 (2014); published online EpubFeb (10.4161/auto.26863).
102. Y. Ogasawara, E. Itakura, N. Kono, N. Mizushima, H. Arai, A. Nara, T. Mizukami, A. Yamamoto, Stearoyl-CoA desaturase 1 activity is required for autophagosome formation. *The Journal of biological chemistry* **289**, 23938-23950 (2014); published online EpubAug 22 (10.1074/jbc.M114.591065).
103. S. A. Khaldoun, M. A. Emond-Boisjoly, D. Chateau, V. Carriere, M. Lacasa, M. Rousset, S. Demignot, E. Morel, Autophagosomes contribute to intracellular lipid distribution in enterocytes. *Molecular biology of the cell* **25**, 118-132 (2014); published online EpubJan (10.1091/mbc.E13-06-0324).
104. A. B. Birgisdottir, T. Lamark, T. Johansen, The LIR motif - crucial for selective autophagy. *Journal of cell science* **126**, 3237-3247 (2013); published online EpubAug 01 (10.1242/jcs.126128).
105. D. J. Klionsky, R. Cueva, D. S. Yaver, Aminopeptidase I of Saccharomyces cerevisiae is localized to the vacuole independent of the secretory pathway. *The Journal of cell biology* **119**, 287-299 (1992); published online EpubOct (

106. P. Verlhac, I. P. Gregoire, O. Azocar, D. S. Petkova, J. Baguet, C. Viret, M. Faure, Autophagy receptor NDP52 regulates pathogen-containing autophagosome maturation. *Cell host & microbe* **17**, 515-525 (2015); published online EpubApr 08 (10.1016/j.chom.2015.02.008).
107. D. A. Tumbarello, P. T. Manna, M. Allen, M. Bycroft, S. D. Arden, J. Kendrick-Jones, F. Buss, The Autophagy Receptor TAX1BP1 and the Molecular Motor Myosin VI Are Required for Clearance of Salmonella Typhimurium by Autophagy. *PLoS pathogens* **11**, e1005174 (2015); published online EpubOct (10.1371/journal.ppat.1005174).
108. H. Huang, T. Kawamata, T. Horie, H. Tsugawa, Y. Nakayama, Y. Ohsumi, E. Fukusaki, Bulk RNA degradation by nitrogen starvation-induced autophagy in yeast. *The EMBO journal* **34**, 154-168 (2015); published online EpubJan 13 (10.15252/embj.201489083).
109. C. Kraft, A. Deplazes, M. Sohrmann, M. Peter, Mature ribosomes are selectively degraded upon starvation by an autophagy pathway requiring the Ubp3p/Bre5p ubiquitin protease. *Nature cell biology* **10**, 602-610 (2008); published online EpubMay (10.1038/ncb1723).
110. A. D. Mathis, B. C. Naylor, R. H. Carson, E. Evans, J. Harwell, J. Knecht, E. Hexem, F. F. Peelor, 3rd, B. F. Miller, K. L. Hamilton, M. K. Transtrum, B. T. Bikman, J. C. Price, Mechanisms of In Vivo Ribosome Maintenance Change in Response to Nutrient Signals. *Molecular & cellular proteomics : MCP* **16**, 243-254 (2017); published online EpubFeb (10.1074/mcp.M116.063255).
111. G. Zaffagnini, S. Martens, Mechanisms of Selective Autophagy. *Journal of molecular biology* **428**, 1714-1724 (2016); published online EpubMay 08 (10.1016/j.jmb.2016.02.004).
112. E. Deosaran, K. B. Larsen, R. Hua, G. Sargent, Y. Wang, S. Kim, T. Lamark, M. Jauregui, K. Law, J. Lippincott-Schwartz, A. Brech, T. Johansen, P. K. Kim, NBR1 acts as an autophagy receptor for peroxisomes. *Journal of cell science* **126**, 939-952 (2013); published online EpubFeb 15 (10.1242/jcs.114819).
113. G. A. Wyant, M. Abu-Remaileh, E. M. Frenkel, N. N. Laqtom, V. Dharamdasani, C. A. Lewis, S. H. Chan, I. Heinze, A. Ori, D. M. Sabatini, NUFIP1 is a ribosome receptor for starvation-induced ribophagy. *Science* **360**, 751-758 (2018); published online EpubMay 18 (10.1126/science.aar2663).
114. A. R. Kristensen, S. Schandorff, M. Hoyer-Hansen, M. O. Nielsen, M. Jaattela, J. Dengjel, J. S. Andersen, Ordered organelle degradation during starvation-induced autophagy. *Molecular & cellular proteomics : MCP* **7**, 2419-2428 (2008); published online EpubDec (10.1074/mcp.M800184-MCP200).
115. Y. Wei, W. C. Chiang, R. Sumpter, Jr., P. Mishra, B. Levine, Prohibitin 2 Is an Inner Mitochondrial Membrane Mitophagy Receptor. *Cell* **168**, 224-238 e210 (2017); published online EpubJan 12 (10.1016/j.cell.2016.11.042).
116. A. Khaminets, T. Heinrich, M. Mari, P. Grumati, A. K. Huebner, M. Akutsu, L. Liebmann, A. Stolz, S. Nietzsche, N. Koch, M. Mauthe, I. Katona, B. Qualmann, J. Weis, F. Reggiori, I. Kurth, C. A. Hubner, I. Dikic, Regulation of endoplasmic reticulum turnover by selective autophagy. *Nature* **522**, 354-358 (2015); published online EpubJun 18 (10.1038/nature14498).
117. T. L. Thurston, G. Ryzhakov, S. Bloor, N. von Muhlinen, F. Randow, The TBK1 adaptor and autophagy receptor NDP52 restricts the proliferation of ubiquitin-coated bacteria. *Nature immunology* **10**, 1215-1221 (2009); published online EpubNov (10.1038/ni.1800).

118. M. Komatsu, S. Waguri, T. Ueno, J. Iwata, S. Murata, I. Tanida, J. Ezaki, N. Mizushima, Y. Ohsumi, Y. Uchiyama, E. Kominami, K. Tanaka, T. Chiba, Impairment of starvation-induced and constitutive autophagy in Atg7-deficient mice. *The Journal of cell biology* **169**, 425-434 (2005); published online EpubMay 09 (10.1083/jcb.200412022).
119. B. Hartleben, M. Godel, C. Meyer-Schwesinger, S. Liu, T. Ulrich, S. Kobler, T. Wiech, F. Grahammer, S. J. Arnold, M. T. Lindenmeyer, C. D. Cohen, H. Pavenstadt, D. Kerjaschki, N. Mizushima, A. S. Shaw, G. Walz, T. B. Huber, Autophagy influences glomerular disease susceptibility and maintains podocyte homeostasis in aging mice. *The Journal of clinical investigation* **120**, 1084-1096 (2010); published online EpubApr (10.1172/JCI39492).
120. E. Masiero, L. Agatea, C. Mammucari, B. Blaauw, E. Loro, M. Komatsu, D. Metzger, C. Reggiani, S. Schiaffino, M. Sandri, Autophagy is required to maintain muscle mass. *Cell metabolism* **10**, 507-515 (2009); published online EpubDec (10.1016/j.cmet.2009.10.008).
121. M. Taneike, O. Yamaguchi, A. Nakai, S. Hikoso, T. Takeda, I. Mizote, T. Oka, T. Tamai, J. Oyabu, T. Murakawa, K. Nishida, T. Shimizu, M. Hori, I. Komuro, T. S. Takuji Shirasawa, N. Mizushima, K. Otsu, Inhibition of autophagy in the heart induces age-related cardiomyopathy. *Autophagy* **6**, 600-606 (2010); published online EpubJul (10.4161/auto.6.5.11947).
122. J. Hampe, A. Franke, P. Rosenstiel, A. Till, M. Teuber, K. Huse, M. Albrecht, G. Mayr, F. M. De La Vega, J. Briggs, S. Gunther, N. J. Prescott, C. M. Onnie, R. Hasler, B. Sipos, U. R. Folsch, T. Lengauer, M. Platzer, C. G. Mathew, M. Krawczak, S. Schreiber, A genome-wide association scan of nonsynonymous SNPs identifies a susceptibility variant for Crohn disease in ATG16L1. *Nature genetics* **39**, 207-211 (2007); published online EpubFeb (10.1038/ng1954).
123. N. Mizushima, A. Yamamoto, M. Matsui, T. Yoshimori, Y. Ohsumi, In vivo analysis of autophagy in response to nutrient starvation using transgenic mice expressing a fluorescent autophagosome marker. *Molecular biology of the cell* **15**, 1101-1111 (2004); published online EpubMar (10.1091/mbc.e03-09-0704).
124. A. Takamura, M. Komatsu, T. Hara, A. Sakamoto, C. Kishi, S. Waguri, Y. Eishi, O. Hino, K. Tanaka, N. Mizushima, Autophagy-deficient mice develop multiple liver tumors. *Genes & development* **25**, 795-800 (2011); published online EpubApr 15 (10.1101/gad.2016211).
125. K. Degenhardt, R. Mathew, B. Beaudoin, K. Bray, D. Anderson, G. Chen, C. Mukherjee, Y. Shi, C. Gelinas, Y. Fan, D. A. Nelson, S. Jin, E. White, Autophagy promotes tumor cell survival and restricts necrosis, inflammation, and tumorigenesis. *Cancer cell* **10**, 51-64 (2006); published online EpubJul (10.1016/j.ccr.2006.06.001).
126. X. H. Liang, S. Jackson, M. Seaman, K. Brown, B. Kempkes, H. Hibshoosh, B. Levine, Induction of autophagy and inhibition of tumorigenesis by beclin 1. *Nature* **402**, 672-676 (1999); published online EpubDec 9 (10.1038/45257).
127. X. Qu, J. Yu, G. Bhagat, N. Furuya, H. Hibshoosh, A. Troxel, J. Rosen, E. L. Eskelinen, N. Mizushima, Y. Ohsumi, G. Cattoretti, B. Levine, Promotion of tumorigenesis by heterozygous disruption of the beclin 1 autophagy gene. *The Journal of clinical investigation* **112**, 1809-1820 (2003); published online EpubDec (10.1172/JCI20039).
128. J. Y. Guo, X. Teng, S. V. Laddha, S. Ma, S. C. Van Nostrand, Y. Yang, S. Khor, C. S. Chan, J. D. Rabinowitz, E. White, Autophagy provides metabolic substrates to maintain energy charge and nucleotide pools in Ras-driven lung cancer cells.

Genes & development **30**, 1704-1717 (2016); published online EpubAug 1 (10.1101/gad.283416.116).
129. C. T. Murphy, S. A. McCarroll, C. I. Bargmann, A. Fraser, R. S. Kamath, J. Ahringer, H. Li, C. Kenyon, Genes that act downstream of DAF-16 to influence the lifespan of Caenorhabditis elegans. *Nature* **424**, 277-283 (2003); published online EpubJul 17 (10.1038/nature01789).
130. T. Vellai, K. Takacs-Vellai, Y. Zhang, A. L. Kovacs, L. Orosz, F. Muller, Genetics: influence of TOR kinase on lifespan in C. elegans. *Nature* **426**, 620 (2003); published online EpubDec 11 (10.1038/426620a).
131. A. Ballabio, V. Gieselmann, Lysosomal disorders: from storage to cellular damage. *Biochimica et biophysica acta* **1793**, 684-696 (2009); published online EpubApr (10.1016/j.bbamcr.2008.12.001).
132. S. M. Davidson, M. G. Vander Heiden, Critical Functions of the Lysosome in Cancer Biology. *Annual review of pharmacology and toxicology* **57**, 481-507 (2017); published online EpubJan 06 (10.1146/annurev-pharmtox-010715-103101).
133. W. W. Chen, E. Freinkman, T. Wang, K. Birsoy, D. M. Sabatini, Absolute Quantification of Matrix Metabolites Reveals the Dynamics of Mitochondrial Metabolism. *Cell* **166**, 1324-1337 e1311 (2016); published online EpubAug 25 (10.1016/j.cell.2016.07.040).
134. B. Schroder, C. Wrocklage, A. Hasilik, P. Saftig, Molecular characterisation of 'transmembrane protein 192' (TMEM192), a novel protein of the lysosomal membrane. *Biological chemistry* **391**, 695-704 (2010); published online EpubJun (10.1515/BC.2010.062).
135. G. M. Mancini, C. E. Beerens, P. P. Aula, F. W. Verheijen, Sialic acid storage diseases. A multiple lysosomal transport defect for acidic monosaccharides. *The Journal of clinical investigation* **87**, 1329-1335 (1991); published online EpubApr (10.1172/JCI115136).
136. J. D. Schulman, K. H. Bradley, J. E. Seegmiller, Cystine: compartmentalization within lysosomes in cystinotic leukocytes. *Science* **166**, 1152-1154 (1969); published online EpubNov 28 (
137. E. J. Bowman, A. Siebers, K. Altendorf, Bafilomycins: a class of inhibitors of membrane ATPases from microorganisms, animal cells, and plant cells. *Proceedings of the National Academy of Sciences of the United States of America* **85**, 7972-7976 (1988); published online EpubNov (
138. M. Huss, G. Ingenhorst, S. Konig, M. Gassel, S. Drose, A. Zeeck, K. Altendorf, H. Wieczorek, Concanamycin A, the specific inhibitor of V-ATPases, binds to the V(o) subunit c. *The Journal of biological chemistry* **277**, 40544-40548 (2002); published online EpubOct 25 (10.1074/jbc.M207345200).
139. R. L. Pisoni, T. L. Acker, K. M. Lisowski, R. M. Lemons, J. G. Thoene, A cysteine-specific lysosomal transport system provides a major route for the delivery of thiol to human fibroblast lysosomes: possible role in supporting lysosomal proteolysis. *The Journal of cell biology* **110**, 327-335 (1990); published online EpubFeb (
140. C. Sagne, C. Agulhon, P. Ravassard, M. Darmon, M. Hamon, S. El Mestikawy, B. Gasnier, B. Giros, Identification and characterization of a lysosomal transporter for small neutral amino acids. *Proceedings of the National Academy of Sciences of the United States of America* **98**, 7206-7211 (2001); published online EpubJun 19 (10.1073/pnas.121183498).
141. K. Hara, K. Yonezawa, Q. P. Weng, M. T. Kozlowski, C. Belham, J. Avruch, Amino acid sufficiency and mTOR regulate p70 S6 kinase and eIF-4E BP1 through a

common effector mechanism. *The Journal of biological chemistry* **273**, 14484-14494 (1998); published online EpubJun 5 (
142. S. Udenfriend, J. R. Cooper, The enzymatic conversion of phenylalanine to tyrosine. *The Journal of biological chemistry* **194**, 503-511 (1952); published online EpubFeb (
143. C. M. Chresta, B. R. Davies, I. Hickson, T. Harding, S. Cosulich, S. E. Critchlow, J. P. Vincent, R. Ellston, D. Jones, P. Sini, D. James, Z. Howard, P. Dudley, G. Hughes, L. Smith, S. Maguire, M. Hummersone, K. Malagu, K. Menear, R. Jenkins, M. Jacobsen, G. C. Smith, S. Guichard, M. Pass, AZD8055 is a potent, selective, and orally bioavailable ATP-competitive mammalian target of rapamycin kinase inhibitor with in vitro and in vivo antitumor activity. *Cancer research* **70**, 288-298 (2010); published online EpubJan 01 (10.1158/0008-5472.CAN-09-1751).
144. K. Yu, C. Shi, L. Toral-Barza, J. Lucas, B. Shor, J. E. Kim, W. G. Zhang, R. Mahoney, C. Gaydos, L. Tardio, S. K. Kim, R. Conant, K. Curran, J. Kaplan, J. Verheijen, S. Ayral-Kaloustian, T. S. Mansour, R. T. Abraham, A. Zask, J. J. Gibbons, Beyond rapalog therapy: preclinical pharmacology and antitumor activity of WYE-125132, an ATP-competitive and specific inhibitor of mTORC1 and mTORC2. *Cancer research* **70**, 621-631 (2010); published online EpubJan 15 (10.1158/0008-5472.CAN-09-2340).
145. J. Kim, M. Kundu, B. Viollet, K. L. Guan, AMPK and mTOR regulate autophagy through direct phosphorylation of Ulk1. *Nature cell biology* **13**, 132-141 (2011); published online EpubFeb (10.1038/ncb2152).
146. R. Amaravadi, A. C. Kimmelman, E. White, Recent insights into the function of autophagy in cancer. *Genes & development* **30**, 1913-1930 (2016); published online EpubSep 01 (10.1101/gad.287524.116).
147. J. Zhao, B. Zhai, S. P. Gygi, A. L. Goldberg, mTOR inhibition activates overall protein degradation by the ubiquitin proteasome system as well as by autophagy. *Proceedings of the National Academy of Sciences of the United States of America* **112**, 15790-15797 (2015); published online EpubDec 29 (10.1073/pnas.1521919112).
148. J. Adams, V. J. Palombella, E. A. Sausville, J. Johnson, A. Destree, D. D. Lazarus, J. Maas, C. S. Pien, S. Prakash, P. J. Elliott, Proteasome inhibitors: a novel class of potent and effective antitumor agents. *Cancer research* **59**, 2615-2622 (1999); published online EpubJun 01 (
149. L. Yu, C. K. McPhee, L. Zheng, G. A. Mardones, Y. Rong, J. Peng, N. Mi, Y. Zhao, Z. Liu, F. Wan, D. W. Hailey, V. Oorschot, J. Klumperman, E. H. Baehrecke, M. J. Lenardo, Termination of autophagy and reformation of lysosomes regulated by mTOR. *Nature* **465**, 942-946 (2010); published online EpubJun 17 (10.1038/nature09076).
150. S. A. Kang, M. E. Pacold, C. L. Cervantes, D. Lim, H. J. Lou, K. Ottina, N. S. Gray, B. E. Turk, M. B. Yaffe, D. M. Sabatini, mTORC1 phosphorylation sites encode their sensitivity to starvation and rapamycin. *Science* **341**, 1236566 (2013); published online EpubJul 26 (10.1126/science.1236566).
151. A. Y. Choo, S. O. Yoon, S. G. Kim, P. P. Roux, J. Blenis, Rapamycin differentially inhibits S6Ks and 4E-BP1 to mediate cell-type-specific repression of mRNA translation. *Proceedings of the National Academy of Sciences of the United States of America* **105**, 17414-17419 (2008); published online EpubNov 11 (10.1073/pnas.0809136105).
152. M. E. Feldman, B. Apsel, A. Uotila, R. Loewith, Z. A. Knight, D. Ruggero, K. M. Shokat, Active-site inhibitors of mTOR target rapamycin-resistant outputs of

mTORC1 and mTORC2. *PLoS biology* **7**, e38 (2009); published online EpubFeb 10 (10.1371/journal.pbio.1000038).
153. J. Jung, H. M. Genau, C. Behrends, Amino Acid-Dependent mTORC1 Regulation by the Lysosomal Membrane Protein SLC38A9. *Molecular and cellular biology* **35**, 2479-2494 (2015); published online EpubJul (10.1128/MCB.00125-15).
154. M. Rebsamen, L. Pochini, T. Stasyk, M. E. de Araujo, M. Galluccio, R. K. Kandasamy, B. Snijder, A. Fauster, E. L. Rudashevskaya, M. Bruckner, S. Scorzoni, P. A. Filipek, K. V. Huber, J. W. Bigenzahn, L. X. Heinz, C. Kraft, K. L. Bennett, C. Indiveri, L. A. Huber, G. Superti-Furga, SLC38A9 is a component of the lysosomal amino acid sensing machinery that controls mTORC1. *Nature* **519**, 477-481 (2015); published online EpubMar 26 (10.1038/nature14107).
155. T. Sekiguchi, E. Hirose, N. Nakashima, M. Ii, T. Nishimoto, Novel G proteins, Rag C and Rag D, interact with GTP-binding proteins, Rag A and Rag B. *The Journal of biological chemistry* **276**, 7246-7257 (2001); published online EpubMar 09 (10.1074/jbc.M004389200).
156. E. Kim, P. Goraksha-Hicks, L. Li, T. P. Neufeld, K. L. Guan, Regulation of TORC1 by Rag GTPases in nutrient response. *Nature cell biology* **10**, 935-945 (2008); published online EpubAug (10.1038/ncb1753).
157. C. S. Petit, A. Roczniak-Ferguson, S. M. Ferguson, Recruitment of folliculin to lysosomes supports the amino acid-dependent activation of Rag GTPases. *The Journal of cell biology* **202**, 1107-1122 (2013); published online EpubSep 30 (10.1083/jcb.201307084).
158. D. L. Jack, I. T. Paulsen, M. H. Saier, The amino acid/polyamine/organocation (APC) superfamily of transporters specific for amino acids, polyamines and organocations. *Microbiology* **146 (Pt 8)**, 1797-1814 (2000); published online EpubAug (10.1099/00221287-146-8-1797).
159. X. Gao, F. Lu, L. Zhou, S. Dang, L. Sun, X. Li, J. Wang, Y. Shi, Structure and mechanism of an amino acid antiporter. *Science* **324**, 1565-1568 (2009); published online EpubJun 19 (10.1126/science.1173654).
160. H. S. Hundal, P. M. Taylor, Amino acid transceptors: gate keepers of nutrient exchange and regulators of nutrient signaling. *American journal of physiology. Endocrinology and metabolism* **296**, E603-613 (2009); published online EpubApr (10.1152/ajpendo.91002.2008).
161. Y. Popova, P. Thayumanavan, E. Lonati, M. Agrochao, J. M. Thevelein, Transport and signaling through the phosphate-binding site of the yeast Pho84 phosphate transceptor. *Proceedings of the National Academy of Sciences of the United States of America* **107**, 2890-2895 (2010); published online EpubFeb 16 (10.1073/pnas.0906546107).
162. G. Van Zeebroeck, B. M. Bonini, M. Versele, J. M. Thevelein, Transport and signaling via the amino acid binding site of the yeast Gap1 amino acid transceptor. *Nature chemical biology* **5**, 45-52 (2009); published online EpubJan (10.1038/nchembio.132).
163. G. Van Zeebroeck, M. Rubio-Texeira, J. Schothorst, J. M. Thevelein, Specific analogues uncouple transport, signalling, oligo-ubiquitination and endocytosis in the yeast Gap1 amino acid transceptor. *Molecular microbiology* **93**, 213-233 (2014); published online EpubJul (10.1111/mmi.12654).
164. B. Liu, H. Du, R. Rutkowski, A. Gartner, X. Wang, LAAT-1 is the lysosomal lysine/arginine transporter that maintains amino acid homeostasis. *Science* **337**, 351-354 (2012); published online EpubJul 20 (10.1126/science.1220281).

165. R. Milkereit, A. Persaud, L. Vanoaica, A. Guetg, F. Verrey, D. Rotin, LAPTM4b recruits the LAT1-4F2hc Leu transporter to lysosomes and promotes mTORC1 activation. *Nature communications* **6**, 7250 (2015); published online EpubMay 22 (10.1038/ncomms8250).
166. P. M. Taylor, Role of amino acid transporters in amino acid sensing. *The American journal of clinical nutrition* **99**, 223S-230S (2014); published online EpubJan (10.3945/ajcn.113.070086).
167. Q. Verdon, M. Boonen, C. Ribes, M. Jadot, B. Gasnier, C. Sagne, SNAT7 is the primary lysosomal glutamine exporter required for extracellular protein-dependent growth of cancer cells. *Proceedings of the National Academy of Sciences of the United States of America* **114**, E3602-E3611 (2017); published online EpubMay 02 (10.1073/pnas.1617066114).
168. R. L. Pisoni, J. G. Thoene, H. N. Christensen, Detection and characterization of carrier-mediated cationic amino acid transport in lysosomes of normal and cystinotic human fibroblasts. Role in therapeutic cystine removal? *The Journal of biological chemistry* **260**, 4791-4798 (1985); published online EpubApr 25 (
169. R. L. Pisoni, J. G. Thoene, R. M. Lemons, H. N. Christensen, Important differences in cationic amino acid transport by lysosomal system c and system y+ of the human fibroblast. *The Journal of biological chemistry* **262**, 15011-15018 (1987); published online EpubNov 05 (
170. W. Palm, Y. Park, K. Wright, N. N. Pavlova, D. A. Tuveson, C. B. Thompson, The Utilization of Extracellular Proteins as Nutrients Is Suppressed by mTORC1. *Cell* **162**, 259-270 (2015); published online EpubJul 16 (10.1016/j.cell.2015.06.017).
171. S. Yoshida, R. Pacitto, Y. Yao, K. Inoki, J. A. Swanson, Growth factor signaling to mTORC1 by amino acid-laden macropinosomes. *The Journal of cell biology* **211**, 159-172 (2015); published online EpubOct 12 (10.1083/jcb.201504097).
172. J. T. Wang, R. D. Teasdale, D. Liebl, Macropinosome quantitation assay. *MethodsX* **1**, 36-41 (2014)10.1016/j.mex.2014.05.002).
173. D. Bar-Sagi, J. R. Feramisco, Induction of membrane ruffling and fluid-phase pinocytosis in quiescent fibroblasts by ras proteins. *Science* **233**, 1061-1068 (1986); published online EpubSep 05 (
174. S. M. Davidson, O. Jonas, M. A. Keibler, H. W. Hou, A. Luengo, J. R. Mayers, J. Wyckoff, A. M. Del Rosario, M. Whitman, C. R. Chin, K. J. Condon, A. Lammers, K. A. Kellersberger, B. K. Stall, G. Stephanopoulos, D. Bar-Sagi, J. Han, J. D. Rabinowitz, M. J. Cima, R. Langer, M. G. Vander Heiden, Direct evidence for cancer-cell-autonomous extracellular protein catabolism in pancreatic tumors. *Nature medicine* **23**, 235-241 (2017); published online EpubFeb (10.1038/nm.4256).
175. B. M. Castellano, A. M. Thelen, O. Moldavski, M. Feltes, R. E. van der Welle, L. Mydock-McGrane, X. Jiang, R. J. van Eijkeren, O. B. Davis, S. M. Louie, R. M. Perera, D. F. Covey, D. K. Nomura, D. S. Ory, R. Zoncu, Lysosomal cholesterol activates mTORC1 via an SLC38A9-Niemann-Pick C1 signaling complex. *Science* **355**, 1306-1311 (2017); published online EpubMar 24 (10.1126/science.aag1417).
176. K. Takeshige, M. Baba, S. Tsuboi, T. Noda, Y. Ohsumi, Autophagy in yeast demonstrated with proteinase-deficient mutants and conditions for its induction. *The Journal of cell biology* **119**, 301-311 (1992); published online EpubOct (
177. T. P. Ashford, K. R. Porter, Cytoplasmic components in hepatic cell lysosomes. *The Journal of cell biology* **12**, 198-202 (1962); published online EpubJan (
178. P. Cohn, Properties of ribosomal proteins from two mammalian sources. *The Biochemical journal* **102**, 735-741 (1967); published online EpubMar (

179. S. K. Singh, A. Yamashita, E. Gouaux, Antidepressant binding site in a bacterial homologue of neurotransmitter transporters. *Nature* **448**, 952-956 (2007); published online EpubAug 23 (10.1038/nature06038).
180. L. Shi, M. Quick, Y. Zhao, H. Weinstein, J. A. Javitch, The mechanism of a neurotransmitter:sodium symporter--inward release of Na+ and substrate is triggered by substrate in a second binding site. *Molecular cell* **30**, 667-677 (2008); published online EpubJun 20 (10.1016/j.molcel.2008.05.008).
181. H. A. Neubauer, C. G. Hansen, O. Wiborg, Dissection of an allosteric mechanism on the serotonin transporter: a cross-species study. *Molecular pharmacology* **69**, 1242-1250 (2006); published online EpubApr (10.1124/mol.105.018507).
182. M. Quick, L. Shi, B. Zehnpfennig, H. Weinstein, J. A. Javitch, Experimental conditions can obscure the second high-affinity site in LeuT. *Nature structural & molecular biology* **19**, 207-211 (2012); published online EpubJan 15 (10.1038/nsmb.2197).
183. Z. Li, A. S. Lee, S. Bracher, H. Jung, A. Paz, J. P. Kumar, J. Abramson, M. Quick, L. Shi, Identification of a second substrate-binding site in solute-sodium symporters. *The Journal of biological chemistry* **290**, 127-141 (2015); published online EpubJan 02 (10.1074/jbc.M114.584383).
184. Z. Zhou, J. Zhen, N. K. Karpowich, R. M. Goetz, C. J. Law, M. E. Reith, D. N. Wang, LeuT-desipramine structure reveals how antidepressants block neurotransmitter reuptake. *Science* **317**, 1390-1393 (2007); published online EpubSep 07 (10.1126/science.1147614).
185. C. L. Piscitelli, H. Krishnamurthy, E. Gouaux, Neurotransmitter/sodium symporter orthologue LeuT has a single high-affinity substrate site. *Nature* **468**, 1129-1132 (2010); published online EpubDec 23 (10.1038/nature09581).
186. O. Boussif, F. Lezoualc'h, M. A. Zanta, M. D. Mergny, D. Scherman, B. Demeneix, J. P. Behr, A versatile vector for gene and oligonucleotide transfer into cells in culture and in vivo: polyethylenimine. *Proceedings of the National Academy of Sciences of the United States of America* **92**, 7297-7301 (1995); published online EpubAug 01 (
187. O. H. Yilmaz, P. Katajisto, D. W. Lamming, Y. Gultekin, K. E. Bauer-Rowe, S. Sengupta, K. Birsoy, A. Dursun, V. O. Yilmaz, M. Selig, G. P. Nielsen, M. Mino-Kenudson, L. R. Zukerberg, A. K. Bhan, V. Deshpande, D. M. Sabatini, mTORC1 in the Paneth cell niche couples intestinal stem-cell function to calorie intake. *Nature* **486**, 490-495 (2012); published online EpubJun 28 (10.1038/nature11163).
188. L. Groth-Pedersen, M. Jaattela, Combating apoptosis and multidrug resistant cancers by targeting lysosomes. *Cancer letters* **332**, 265-274 (2013); published online EpubMay 28 (10.1016/j.canlet.2010.05.021).
189. M. Abu-Remaileh, G. A. Wyant, C. Kim, N. N. Laqtom, M. Abbasi, S. H. Chan, E. Freinkman, D. M. Sabatini, Lysosomal metabolomics reveals V-ATPase- and mTOR-dependent regulation of amino acid efflux from lysosomes. *Science* **358**, 807-813 (2017); published online EpubNov 10 (10.1126/science.aan6298).
190. A. Roczniak-Ferguson, C. S. Petit, F. Froehlich, S. Qian, J. Ky, B. Angarola, T. C. Walther, S. M. Ferguson, The transcription factor TFEB links mTORC1 signaling to transcriptional control of lysosome homeostasis. *Science signaling* **5**, ra42 (2012); published online EpubJun 12 (10.1126/scisignal.2002790).
191. J. A. Martina, H. I. Diab, L. Lishu, A. L. Jeong, S. Patange, N. Raben, R. Puertollano, The nutrient-responsive transcription factor TFE3 promotes autophagy, lysosomal biogenesis, and clearance of cellular debris. *Science signaling* **7**, ra9 (2014); published online EpubJan 21 (10.1126/scisignal.2004754).

192. R. P. Murmu, E. Martin, A. Rastetter, T. Esteves, M. P. Muriel, K. H. El Hachimi, P. S. Denora, A. Dauphin, J. C. Fernandez, C. Duyckaerts, A. Brice, F. Darios, G. Stevanin, Cellular distribution and subcellular localization of spatacsin and spastizin, two proteins involved in hereditary spastic paraplegia. *Molecular and cellular neurosciences* **47**, 191-202 (2011); published online EpubJul (10.1016/j.mcn.2011.04.004).
193. J. Hirst, G. H. Borner, J. Edgar, M. Y. Hein, M. Mann, F. Buchholz, R. Antrobus, M. S. Robinson, Interaction between AP-5 and the hereditary spastic paraplegia proteins SPG11 and SPG15. *Molecular biology of the cell* **24**, 2558-2569 (2013); published online EpubAug (10.1091/mbc.E13-03-0170).
194. B. Bardoni, R. Willemsen, I. J. Weiler, A. Schenck, L. A. Severijnen, C. Hindelang, E. Lalli, J. L. Mandel, NUFIP1 (nuclear FMRP interacting protein 1) is a nucleocytoplasmic shuttling protein associated with active synaptoneurosomes. *Experimental cell research* **289**, 95-107 (2003); published online EpubSep 10 (
195. M. Quinternet, M. E. Chagot, B. Rothe, D. Tiotiu, B. Charpentier, X. Manival, Structural Features of the Box C/D snoRNP Pre-assembly Process Are Conserved through Species. *Structure* **24**, 1693-1706 (2016); published online EpubOct 04 (10.1016/j.str.2016.07.016).
196. B. Rothe, J. M. Saliou, M. Quinternet, R. Back, D. Tiotiu, C. Jacquemin, C. Loegler, F. Schlotter, V. Pena, K. Eckert, S. Morera, A. V. Dorsselaer, C. Branlant, S. Massenet, S. Sanglier-Cianferani, X. Manival, B. Charpentier, Protein Hit1, a novel box C/D snoRNP assembly factor, controls cellular concentration of the scaffolding protein Rsa1 by direct interaction. *Nucleic acids research* **42**, 10731-10747 (2014)10.1093/nar/gku612).
197. S. Boulon, N. Marmier-Gourrier, B. Pradet-Balade, L. Wurth, C. Verheggen, B. E. Jady, B. Rothe, C. Pescia, M. C. Robert, T. Kiss, B. Bardoni, A. Krol, C. Branlant, C. Allmang, E. Bertrand, B. Charpentier, The Hsp90 chaperone controls the biogenesis of L7Ae RNPs through conserved machinery. *The Journal of cell biology* **180**, 579-595 (2008); published online EpubFeb 11 (10.1083/jcb.200708110).
198. K. S. McKeegan, C. M. Debieux, S. Boulon, E. Bertrand, N. J. Watkins, A dynamic scaffold of pre-snoRNP factors facilitates human box C/D snoRNP assembly. *Molecular and cellular biology* **27**, 6782-6793 (2007); published online EpubOct (10.1128/MCB.01097-07).
199. M. Quinternet, B. Rothe, M. Barbier, C. Bobo, J. M. Saliou, C. Jacquemin, R. Back, M. E. Chagot, S. Cianferani, P. Meyer, C. Branlant, B. Charpentier, X. Manival, Structure/Function Analysis of Protein-Protein Interactions Developed by the Yeast Pih1 Platform Protein and Its Partners in Box C/D snoRNP Assembly. *Journal of molecular biology* **427**, 2816-2839 (2015); published online EpubAug 28 (10.1016/j.jmb.2015.07.012).
200. M. K. Sung, T. R. Porras-Yakushi, J. M. Reitsma, F. M. Huber, M. J. Sweredoski, A. Hoelz, S. Hess, R. J. Deshaies, A conserved quality-control pathway that mediates degradation of unassembled ribosomal proteins. *eLife* **5**, (2016); published online EpubAug 23 (10.7554/eLife.19105).
201. M. K. Sung, J. M. Reitsma, M. J. Sweredoski, S. Hess, R. J. Deshaies, Ribosomal proteins produced in excess are degraded by the ubiquitin-proteasome system. *Molecular biology of the cell* **27**, 2642-2652 (2016); published online EpubSep 01 (10.1091/mbc.E16-05-0290).

202. J. R. Warner, In the absence of ribosomal RNA synthesis, the ribosomal proteins of HeLa cells are synthesized normally and degraded rapidly. *Journal of molecular biology* **115**, 315-333 (1977); published online EpubSep 25 (
203. J. R. Warner, The economics of ribosome biosynthesis in yeast. *Trends in biochemical sciences* **24**, 437-440 (1999); published online EpubNov (
204. D. E. Weinberg, P. Shah, S. W. Eichhorn, J. A. Hussmann, J. B. Plotkin, D. P. Bartel, Improved Ribosome-Footprint and mRNA Measurements Provide Insights into Dynamics and Regulation of Yeast Translation. *Cell reports* **14**, 1787-1799 (2016); published online EpubFeb 23 (10.1016/j.celrep.2016.01.043).
205. J. E. Darnell, Jr., Ribonucleic acids from animal cells. *Bacteriological reviews* **32**, 262-290 (1968); published online EpubSep (
206. E. R. Lindley, R. L. Pisoni, Demonstration of adenosine deaminase activity in human fibroblast lysosomes. *The Biochemical journal* **290 (Pt 2)**, 457-462 (1993); published online EpubMar 1 (
207. G. A. Wyant, M. Abu-Remaileh, R. L. Wolfson, W. W. Chen, E. Freinkman, L. V. Danai, M. G. Vander Heiden, D. M. Sabatini, mTORC1 Activator SLC38A9 Is Required to Efflux Essential Amino Acids from Lysosomes and Use Protein as a Nutrient. *Cell* **171**, 642-654 e612 (2017); published online EpubOct 19 (10.1016/j.cell.2017.09.046).
208. S. Klinge, F. Voigts-Hoffmann, M. Leibundgut, N. Ban, Atomic structures of the eukaryotic ribosome. *Trends in biochemical sciences* **37**, 189-198 (2012); published online EpubMay (10.1016/j.tibs.2012.02.007).
209. Y. C. Wong, E. L. Holzbaur, Optineurin is an autophagy receptor for damaged mitochondria in parkin-mediated mitophagy that is disrupted by an ALS-linked mutation. *Proceedings of the National Academy of Sciences of the United States of America* **111**, E4439-4448 (2014); published online EpubOct 21 (10.1073/pnas.1405752111).
210. H. An, J. W. Harper, Systematic analysis of ribophagy in human cells reveals bystander flux during selective autophagy. *Nature cell biology*, (2017); published online EpubDec 11 (10.1038/s41556-017-0007-x).
211. R. Bruderer, O. M. Bernhardt, T. Gandhi, S. M. Miladinovic, L. Y. Cheng, S. Messner, T. Ehrenberger, V. Zanotelli, Y. Butscheid, C. Escher, O. Vitek, O. Rinner, L. Reiter, Extending the limits of quantitative proteome profiling with data-independent acquisition and application to acetaminophen-treated three-dimensional liver microtissues. *Molecular & cellular proteomics : MCP* **14**, 1400-1410 (2015); published online EpubMay (10.1074/mcp.M114.044305).
212. G. Rosenberger, I. Bludau, U. Schmitt, M. Heusel, C. L. Hunter, Y. Liu, M. J. MacCoss, B. X. MacLean, A. I. Nesvizhskii, P. G. A. Pedrioli, L. Reiter, H. L. Rost, S. Tate, Y. S. Ting, B. C. Collins, R. Aebersold, Statistical control of peptide and protein error rates in large-scale targeted data-independent acquisition analyses. *Nature methods* **14**, 921-927 (2017); published online EpubSep (10.1038/nmeth.4398).
213. J. D. Storey, A direct approach to false discovery rates. *J Roy Stat Soc B* **64**, 479-498 (2002)Unsp 1369-7412/02/64479
Doi 10.1111/1467-9868.00346).

CHAPTER 2

Reprinted from Science:

Lysosomal metabolomics reveals V-ATPase and mTOR-dependent regulation of amino acid efflux from lysosomes

Monther Abu-Remaileh[1,2,3,4,*], Gregory A. Wyant[1,2,3,4,*], Choah Kim[1,2,3,4], Nouf N. Laqtom[1,2,3,4], Maria Abbasi[1,2,3,4], Sze Ham Chan[1], Elizaveta Freinkman[1,5] & David M. Sabatini[1,2,3,4,†]

[1] Whitehead Institute for Biomedical Research and Massachusetts Institute of Technology, Department of Biology, 9 Cambridge Center, Cambridge, MA 02142, USA.

[2] Howard Hughes Medical Institute, Department of Biology, Massachusetts Institute of Technology, Cambridge, MA 02139, USA.

[3] Koch Institute for Integrative Cancer Research, 77 Massachusetts Avenue, Cambridge, MA 02139, USA.

[4] Broad Institute of Harvard and Massachusetts Institute of Technology, 7 Cambridge Center, Cambridge, MA 02142, USA.
[5] Current address: Metabolon, Inc., Research Triangle Park, NC 27709, USA.

† Corresponding author. E-mail: sabatini@wi.mit.edu
Tel: 617-258-6407; Fax: 617-452-3566;
* These authors contributed equally to this work.

Experiments in Figure 1 were performed by MAR and GAW with technical assistance from SHC, and EF
Experiments in Figure 2 were performed by MAR and GAW with technical assistance from SHC, and EF
Experiments in Figure 3 were performed by MAR and GAW
Experiments in Figure 4 were performed by MAR and GAW
Experiments in Figure S1 were performed by MAR and GAW with technical assistance from SHC, and EF
Experiments in Figure S2-S4 were performed by MAR
Manuscript was written by MAR and DMS with input from GAW

Abstract

The lysosome degrades and recycles macromolecules, signals to the cytosol and nucleus, and is implicated in many diseases. Here we describe a method for the rapid isolation of mammalian lysosomes and use it to quantitatively profile lysosomal metabolites under various cell states. Under nutrient replete conditions, many lysosomal amino acids are in rapid exchange with those in the cytosol. Loss of lysosomal acidification through inhibition of the vacuolar H+ATPase (V-ATPase) increased the luminal concentrations of most metabolites, but had no effect on those of the majority of essential amino acids. Instead, nutrient starvation regulates the lysosomal concentrations of these amino acids, an effect we traced to regulation of the mTOR pathway. Inhibition of mTOR strongly reduced the lysosomal efflux of most essential amino acids, converting the lysosome into a cellular depot for them. These results reveal the dynamic nature of lysosomal metabolites and that V-ATPase- and mTOR-dependent mechanisms exist for controlling lysosomal amino acid efflux.

Lysosomes are membrane-bound organelles best known for their capacity to degrade macromolecules and recycle their constituent metabolites, and for their dysfunction in a group of rare metabolic disorders known as lysosomal storage diseases (*81, 132*). Lysosomes also participate in signal transduction (*92*), particularly in nutrient sensing by the mechanistic target of rapamycin complex 1 (mTORC1) pathway (*51, 52*), and are often deregulated in common diseases, such as cancer (*133*). Given the critical roles of lysosomes in producing and sensing many metabolites, a better understanding of lysosomal function requires uncovering its metabolite content, and its regulation in diverse cell states.

Traditional techniques for purifying lysosomes, such as density-based centrifugation, are too slow to preserve what is likely a labile lysosomal metabolome ("lysobolome"). To overcome this issue, we used insights from a recently reported method for the rapid isolation of mitochondria (*134*) to develop an analogous approach for lysosomes. Our "LysoIP" method uses anti-human Influenza virus hemagglutinin (HA) magnetic beads to immunopurify lysosomes from human embryonic kidney (HEK-293T) cells expressing transmembrane Protein 192 (TMEM192) fused to three tandem HA-epitopes (HA-Lyso cells) (Fig. 1A and B). TMEM192 is a transmembrane protein (*135*) that we find retains its lysosomal localization upon overexpression better than other such proteins, like lysosomal-associated membrane protein 1 (LAMP1). Starting with live cells, it takes ~10 minutes to isolate lysosomes that are highly pure and intact, as judged by the absence of markers for other cellular compartments (Fig. 1C), retention of Cathepsin D activity (Fig. 1D), and capacity to take up radiolabeled arginine in vitro (Fig. 1E). Moreover, tracking of either a lysosomal membrane protein (LAMP2), a

luminal protein (Cathepsin D), or a small molecule (LysoTracker Red), yielded the same value for the fraction of total cellular lysosomes purified (Fig. 1F), indicating that the lysosomes do not leak soluble contents during the purification. Importantly, the LysoIP method uses buffers compatible with subsequent analyses of the lysosomal metabolome by liquid chromatography and mass spectrometry (LC/MS).

Because the metabolite content of human lysosomes is not established, we used LC/MS to determine the relative abundances of ~150 polar small molecules in lysosomes versus control anti-HA immunoprecipitates from cells stably expressing Flag-tagged TMEM192 (Control-Lyso cells) (Fig. S1A and Supplementary Table 1). Of these, 57 were twice as abundant in the isolated lysosomes and thus deemed lysosomal metabolites (Fig. S1A and Supplementary table 1). The lysosomes did not contain metabolites characteristic of other compartments, such as the cytosolic glycolytic intermediates fructose 1,6-bisphosphate and lactate or the mitochondrially-enriched Coenzyme A (*134*) (Fig. S1B).

We quantified the concentrations of the 57 metabolites in lysosomal and whole-cell samples using standard curves for each and the volumes of lysosomes and intact cells (see methods). Lysosomal metabolite concentrations correlated highly across biological replicates (r^2 = 0.95; Fig. 1G) and even with those obtained using the less preferable LAMP1-RFP-3xHA as the lysosomal antigen tag (r^2 = 0.95; Fig. S1C), mitigating concerns that expression of TMEM192, whose function is unknown, might have effects on the lysosomal metabolome. In the proliferating cells used in these experiments, the concentrations of metabolites tended to be, with a few exceptions, lower in lysosomes than in whole cells (Fig. 1H,I and Supplementary table 2). Two molecules previously predicted to be stored in

lysosomes, cystine (the oxidized dimeric form of cysteine) and glucuronic acid (*136, 137*), were indeed enriched in lysosomes, with concentrations 28- and 5.5-fold greater than those of whole cells, respectively (Fig. 1H,I and Supplementary table 2). All nucleosides (guanosine, adenine, cytidine, uridine, and inosine) were lysosomally enriched (9 to 25 fold), consistent with the lysosome also being a depot for these metabolites, at least in HEK-293T cells (Fig. 1H,I). The lysosomal concentrations of proteinogenic amino acids varied widely and did not correlate well with those in whole cells (Fig. 1I), suggesting that while some lysosomal amino acids are in equilibrium with the rest of the cell, others are either sequestered in a different compartment or undergo preferred transport out of the lysosome, and thus show higher concentrations in the whole-cell samples. Lysosomes also contained metabolites that are not thought to result from the degradation of macromolecules, and thus are likely transported into lysosomes (Fig. 1I). These include non-proteinogenic amino acids, like beta-alanine (20 uM), taurine (11 uM), and hypotaurine (12 uM); cofactors and vitamins, like choline (7 uM) and phosphocholine (94 uM); creatine (274 uM) and phosphocreatine (111 uM); and multiple species of carnitines (Fig. 1I). The metabolomic landscape of the human lysosome is consistent with its role as a recycling center, but also indicates that the transport of metabolites into lysosomes may influence lysosomal biology more than is widely appreciated.

The multicomponent vacuolar H^+-ATPase (V-ATPase) maintains the lysosomal lumen at a pH of ~4.5 (*79*), which is thought to be required for the optimal activity of lysosomal hydrolases and to set up a proton gradient with the cytosol that provides energy for transporters to move metabolites across the

lysosomal membrane. To directly ask how loss of the acidic pH impacts lysosomal metabolites, we profiled lysosomes from cells acutely treated with the V-ATPase inhibitors Bafilomycin A1 (BafA1) or Concanamycin A (ConA) (*138, 139*), at concentrations that do not inhibit mTORC1 signaling (*52*) (Fig. S2A). Although neither had a major impact on the whole-cell metabolome, both caused large changes in the metabolome of the lysosome (Fig. 2A and Fig. S2B). This emphasizes the value of LysoIP for studying an organelle that in HEK-293T cells occupies only 2 to 3% of the total cell volume. V-ATPase inhibition caused the accumulation of many metabolites in lysosomes (Fig. 2B and Supplementary table 3), and only the concentration of cystine dropped significantly ($P \leq 0.01$ in either treatment, two-tailed *t* test) (Fig. S2C), consistent with in vitro work showing that the lysosomal entry of cysteine requires the pH gradient (*140*). Although all the non-essential amino acids accumulated in lysosomes upon V-ATPase inhibition (Fig. 2C), with proline, alanine, and glycine being the most affected (Fig. 2C), 7 of the 9 essential amino acids did not, with histidine and threonine being the exceptions (Fig. 2D). Given that lysosomes harbor several well-characterized proton-dependent amino acid transporters, such as lysosomal amino acid transporter 1 (LYAAT-1) (*141*), lysosomal accumulation of the non-essential amino acids caused by V-ATPase inhibition may result from their decreased efflux. We therefore undertook pulse-chase experiments using ^{15}N-labeled alanine, a representative pH-dependent amino acid, and isoleucine, a non-pH-dependent one (Fig. 2C-F). In live cells both entered lysosomes, with isoleucine doing so more rapidly than alanine (Fig. 2E). ConA treatment slowed the efflux of alanine, but not that of isoleucine, from lysosomes (Fig. 2F), consistent with proton-dependent

transporters mediating the efflux of this and other non-essential amino acids from lysosomes. Furthermore, the failure of V-ATPase inhibition to impact the lysosomal levels of most essential amino acids, particularly the non-polar ones, raises the question of what, if anything, regulates their abundance.

To investigate this, we examined other conditions that might affect lysosomal metabolites, including nutrient starvation. We starved cells of all amino acids for 60 minutes and measured the concentrations of amino acids in lysosomes and in whole cells. Concentrations of most non-essential amino acids did not drop in either sample, consistent with the capacity of cells to synthesize them. In contrast, the concentrations of most essential amino acids, including those that were insensitive to V-ATPase inhibition, diminished in the whole-cell samples, but most showed little if any change, in lysosomes (Fig. 3A and supplementary table 4). Thus, amino acid starvation appears to inhibit the lysosomal egress of many essential amino acids.

Given that a major consequence of amino acid starvation is inhibition of mTORC1 (Fig. 3B) (*12, 142*), we asked if mTORC1 regulates the abundance of amino acids in lysosomes. Consistent with this possibility, in cells that lack functional GATOR1 (DEPDC5 KO cells) and thus have amino acid-insensitive mTORC1 signaling (*55*), amino acid starvation did decrease the concentrations of lysosomal amino acids (Fig. 3A and 3B). Moreover, inhibition of the kinase activity of mTOR with Torin1 (*75*) increased the lysosomal concentrations of 6 of the 7 V-ATPase-insensitive amino acids (leucine, phenylalanine, isoleucine, tryptophan, methionine and valine) and of tyrosine, while having small effects on most other amino acids, including histidine and serine, as well as many additional metabolites

(Fig. 3C, 3D, Fig. S3A and supplementary table 5). Torin1 also increased the lysosomal concentrations of nucleosides, although in this case the effect was also seen in whole cells (Fig. 3E). Of the 7 amino acids most strongly affected by Torin1, all are non-polar and essential, with the exception of tyrosine, which is generated from the essential amino acid phenylalanine (*143*). Importantly, other chemically distinct ATP-competitive inhibitors of mTOR, including AZD8055 and WYE-132 (*144, 145*), also increased the concentration of these 7 amino acids (Fig. S3B) and mTOR inhibition had similar effects across multiple cell lines (Fig. S3C). Although Torin1, AZD8055, and WYE-132, inhibit both mTORC1 and mTOR Complex 2 (mTORC2), inhibition of only mTORC1 with the allosteric inhibitor rapamycin or with lower concentrations of Torin1 also increased the concentration of these amino acids, albeit to smaller extents (Fig. S3B, Fig. S3D). mTORC1 is essential for cell survival but it is possible to generate cells lacking rictor, a critical mTORC2-specific component needed for phosphorylation of the protein kinase Akt (*43*). Loss of rictor did not increase lysosomal amino acid concentrations, and, importantly, Torin1 increased the abundance of the 7 amino acids in lysosomes even more in cells lacking rictor than in wild-type cells (Fig. S3E). Thus, mTORC1 appears to mediate the effects of mTOR inhibition on lysosomal amino acids.

Because mTORC1 inhibits autophagy (*34, 35, 100, 146, 147*), a potential explanation for the effects of Torin1 is that it activates autophagic flux to such a degree that the production of metabolites by lysosomal macromolecular degradation exceeds the capacity of lysosomes to export them. We tested this possibility in cells lacking *ATG7* (Fig. S3F), which encodes a key component of the autophagy machinery (*119*). For most metabolites, loss of autophagy almost

completely eliminated the Torin1-induced increases in their lysosomal concentrations, but it had only minor effects on those of the 7 strongly affected amino acids (leucine, tyrosine, phenylalanine, isoleucine, tryptophan, methionine, and valine) (Fig. 3D, 3E, Fig. S3G and supplementary table 5). mTOR inhibition also activates the proteasome (*148*), but Bortezomib, a proteasomal inhibitor (*149*), had no effect on the capacity of Torin1 to increase abundance of lysosomal amino acids (Fig. 3F and Fig. S3H). Lastly, mTORC1 inhibition suppresses mRNA translation (*23*), but the protein synthesis inhibitor cycloheximide did not mimic the effects of the mTOR inhibitors on lysosomal amino acid levels, although it did mildly increase whole-cell and lysosomal pools of the mTOR-regulated amino acids (Fig. S3L). Thus, mTORC1 regulates the lysosomal concentrations of a largely distinct set of amino acids from those affected by the V-ATPase (Fig. 3G) through a mechanism that does not involve autophagy, the proteasome, or protein synthesis (Fig. 3G).

Given that mTORC1 does not impact the 7 amino acids through established downstream processes, we considered the possibility that it controls their flux across the lysosomal membrane. We used ^{15}N-labeled amino acids to monitor the transport of four of the mTOR-regulated amino acids (leucine, tyrosine, phenylalanine, and isoleucine) and a control amino acid (serine) into lysosomes in live cells. When added to the culture media the labeled amino acids rapidly exchanged with the ^{14}N-containing amino acids already in lysosomes (Fig. 2E and Fig. 4A). In cells treated with or without cycloheximide, Torin1 caused lysosomal accumulation of ^{15}N-labeled leucine, tyrosine, phenylalanine, and isoleucine, but not serine (Fig. S4A, S4B and Fig. 4B), demonstrating that mTOR regulates the

movement of free amino acids across the lysosomal membrane independently of their incorporation into protein. Pulse-chase experiments revealed that mTOR inhibition slows the efflux of leucine, tyrosine, phenylalanine, and isoleucine, but not that of serine, from lysosomes but not from whole cells (Fig. 4C and Fig. S4C).

We recently identified the multi-pass protein SLC38A9 as a lysosomal effluxer of many essential non-polar amino acids (Wyant GA, Cell, in press). Its loss led to the accumulation in lysosomes of the 7 amino acids most impacted by mTOR inhibition and greatly reduced their efflux from lysosomes (Fig. 4D and Fig. S4D). In cells lacking SLC38A9, Torin1 did not boost the already high lysosomal concentrations of the 7 amino acids (Fig. 4D). Thus, mTOR inhibition and loss of SLC38A9 do not have additive effects on lysosomal amino acids, suggesting that mTORC1 regulates the lysosomal abundance of amino acids through a mechanism that involves SLC38A9. Loss of SLC38A9 greatly impaired the capacity of cells to survive amino acid starvation, and of the GCN2 pathway, which senses uncharged tRNAs, to return to baseline activity levels upon prolonged starvation (Fig. 4E and Fig 4F). Thus, the efflux of the mTORC1-regulated essential amino acids from lysosomes is important for the cellular response to starvation.

Our data show that mTORC1 has a previously unknown role in promoting the efflux of essential amino acids from the lysosome into the cytosol (Fig. 4G). mTORC1 inhibition leads to the sequestration of these amino acids in the lysosome by slowing their movement across the lysosomal membrane, in effect converting it into a storage compartment for them. We speculate that this function of mTORC1 is important for preventing the inappropriate use of essential amino

acids during amino acid starvation, a state in which lysosomal and proteasomal protein degradation are thought to be a major source of amino acids (*36, 148, 150*). One can imagine the following scenario: early in a starvation period mTORC1 becomes profoundly inhibited, which, by suppressing SLC38A9 and perhaps other transporters, prevents the exit from lysosomes of essential amino acids. Over time, as proteolysis partially restores amino acid levels, mTORC1 becomes sufficiently reactivated so that essential amino acids are released into the cytosol at a faster rate to be used to execute the ongoing gene expression program that cells induce to adapt to starvation (*92, 150*). In this regard, it is interesting that Torin1, which completely inhibits mTORC1, causes a greater accumulation of amino acids in lysosomes than rapamycin, which only partially inhibits it (*75, 151-153*). This pattern is also true for several other processes downstream of mTORC1, such as autophagy and protein synthesis (*75, 151-153*), and may indicate that the mechanisms through which mTORC1 regulates lysosomal amino acid efflux, such as through SLC38A9, are also sensitive to the exact amount of mTORC1 activity, allowing for distinct outcomes at different levels. How mTORC1 impacts SLC38A9 function is unknown and it may do so indirectly or directly. Activated mTORC1 resides on the lysosomal surface (*49, 51*), so it has the correct localization to control SLC38A9 or its regulators. The fact that SLC38A9 also signals arginine levels to mTORC1 (*53, 154, 155*) suggests that SLC38A9 is part of sophisticated system for coordinating mTORC1 activity and lysosomal amino acid efflux with the concentrations of cytosolic and lysosomal amino acids. Our findings provide an example of the utility of LysoIP for uncovering a new function for lysosomes—the sequestering of essential amino acids upon mTORC1 inhibition.

The method we described may be useful for studying the emerging roles of lysosomes and for probing the metabolic state of the lysosome in the various diseases in which it is implicated.

References and Notes

1. A. Ballabio, V. Gieselmann, Lysosomal disorders: from storage to cellular damage. *Biochimica et biophysica acta* **1793**, 684 (Apr, 2009).
2. F. M. Platt, B. Boland, A. C. van der Spoel, The cell biology of disease: lysosomal storage disorders: the cellular impact of lysosomal dysfunction. *The Journal of cell biology* **199**, 723 (Nov 26, 2012).
3. C. Settembre, A. Fraldi, D. L. Medina, A. Ballabio, Signals from the lysosome: a control centre for cellular clearance and energy metabolism. *Nature reviews. Molecular cell biology* **14**, 283 (May, 2013).
4. R. Zoncu *et al.*, mTORC1 senses lysosomal amino acids through an inside-out mechanism that requires the vacuolar H(+)-ATPase. *Science* **334**, 678 (Nov 04, 2011).
5. Y. Sancak *et al.*, Ragulator-Rag complex targets mTORC1 to the lysosomal surface and is necessary for its activation by amino acids. *Cell* **141**, 290 (Apr 16, 2010).
6. S. M. Davidson, M. G. Vander Heiden, Critical Functions of the Lysosome in Cancer Biology. *Annual review of pharmacology and toxicology* **57**, 481 (Jan 06, 2017).
7. W. W. Chen, E. Freinkman, T. Wang, K. Birsoy, D. M. Sabatini, Absolute Quantification of Matrix Metabolites Reveals the Dynamics of Mitochondrial Metabolism. *Cell* **166**, 1324 (Aug 25, 2016).

8. B. Schroder, C. Wrocklage, A. Hasilik, P. Saftig, Molecular characterisation of 'transmembrane protein 192' (TMEM192), a novel protein of the lysosomal membrane. *Biological chemistry* **391**, 695 (Jun, 2010).

9. G. M. Mancini, C. E. Beerens, P. P. Aula, F. W. Verheijen, Sialic acid storage diseases. A multiple lysosomal transport defect for acidic monosaccharides. *The Journal of clinical investigation* **87**, 1329 (Apr, 1991).

10. J. D. Schulman, K. H. Bradley, J. E. Seegmiller, Cystine: compartmentalization within lysosomes in cystinotic leukocytes. *Science* **166**, 1152 (Nov 28, 1969).

11. J. A. Mindell, Lysosomal acidification mechanisms. *Annual review of physiology* **74**, 69 (2012).

12. E. J. Bowman, A. Siebers, K. Altendorf, Bafilomycins: a class of inhibitors of membrane ATPases from microorganisms, animal cells, and plant cells. *Proceedings of the National Academy of Sciences of the United States of America* **85**, 7972 (Nov, 1988).

13. M. Huss *et al.*, Concanamycin A, the specific inhibitor of V-ATPases, binds to the V(o) subunit c. *The Journal of biological chemistry* **277**, 40544 (Oct 25, 2002).

14. R. L. Pisoni, T. L. Acker, K. M. Lisowski, R. M. Lemons, J. G. Thoene, A cysteine-specific lysosomal transport system provides a major route for the delivery of thiol to human fibroblast lysosomes: possible role in supporting lysosomal proteolysis. *The Journal of cell biology* **110**, 327 (Feb, 1990).

15. C. Sagne *et al.*, Identification and characterization of a lysosomal transporter for small neutral amino acids. *Proceedings of the National*

Academy of Sciences of the United States of America **98**, 7206 (Jun 19, 2001).

16. K. Hara *et al.*, Amino acid sufficiency and mTOR regulate p70 S6 kinase and eIF-4E BP1 through a common effector mechanism. *The Journal of biological chemistry* **273**, 14484 (Jun 05, 1998).
17. D. H. Kim *et al.*, mTOR interacts with raptor to form a nutrient-sensitive complex that signals to the cell growth machinery. *Cell* **110**, 163 (Jul 26, 2002).
18. L. Bar-Peled *et al.*, A Tumor suppressor complex with GAP activity for the Rag GTPases that signal amino acid sufficiency to mTORC1. *Science* **340**, 1100 (May 31, 2013).
19. C. C. Thoreen *et al.*, An ATP-competitive mammalian target of rapamycin inhibitor reveals rapamycin-resistant functions of mTORC1. *The Journal of biological chemistry* **284**, 8023 (Mar 20, 2009).
20. S. Udenfriend, J. R. Cooper, The enzymatic conversion of phenylalanine to tyrosine. *The Journal of biological chemistry* **194**, 503 (Feb, 1952).
21. C. M. Chresta *et al.*, AZD8055 is a potent, selective, and orally bioavailable ATP-competitive mammalian target of rapamycin kinase inhibitor with in vitro and in vivo antitumor activity. *Cancer research* **70**, 288 (Jan 01, 2010).
22. K. Yu *et al.*, Beyond rapalog therapy: preclinical pharmacology and antitumor activity of WYE-125132, an ATP-competitive and specific inhibitor of mTORC1 and mTORC2. *Cancer research* **70**, 621 (Jan 15, 2010).

23. D. D. Sarbassov, D. A. Guertin, S. M. Ali, D. M. Sabatini, Phosphorylation and regulation of Akt/PKB by the rictor-mTOR complex. *Science* **307**, 1098 (Feb 18, 2005).

24. I. G. Ganley *et al.*, ULK1.ATG13.FIP200 complex mediates mTOR signaling and is essential for autophagy. *The Journal of biological chemistry* **284**, 12297 (May 01, 2009).

25. N. Hosokawa *et al.*, Nutrient-dependent mTORC1 association with the ULK1-Atg13-FIP200 complex required for autophagy. *Molecular biology of the cell* **20**, 1981 (Apr, 2009).

26. C. H. Jung *et al.*, ULK-Atg13-FIP200 complexes mediate mTOR signaling to the autophagy machinery. *Molecular biology of the cell* **20**, 1992 (Apr, 2009).

27. J. Kim, M. Kundu, B. Viollet, K. L. Guan, AMPK and mTOR regulate autophagy through direct phosphorylation of Ulk1. *Nature cell biology* **13**, 132 (Feb, 2011).

28. R. Amaravadi, A. C. Kimmelman, E. White, Recent insights into the function of autophagy in cancer. *Genes & development* **30**, 1913 (Sep 01, 2016).

29. M. Komatsu *et al.*, Impairment of starvation-induced and constitutive autophagy in Atg7-deficient mice. *The Journal of cell biology* **169**, 425 (May 09, 2005).

30. J. Zhao, B. Zhai, S. P. Gygi, A. L. Goldberg, mTOR inhibition activates overall protein degradation by the ubiquitin proteasome system as well as by autophagy. *Proceedings of the National Academy of Sciences of the United States of America* **112**, 15790 (Dec 29, 2015).

31. J. Adams *et al.*, Proteasome inhibitors: a novel class of potent and effective antitumor agents. *Cancer research* **59**, 2615 (Jun 01, 1999).

32. X. M. Ma, J. Blenis, Molecular mechanisms of mTOR-mediated translational control. *Nature reviews. Molecular cell biology* **10**, 307 (May, 2009).

33. L. Yu *et al.*, Termination of autophagy and reformation of lysosomes regulated by mTOR. *Nature* **465**, 942 (Jun 17, 2010).

34. J. Zhao, A. L. Goldberg, Coordinate regulation of autophagy and the ubiquitin proteasome system by MTOR. *Autophagy* **12**, 1967 (Oct 02, 2016).

35. S. A. Kang *et al.*, mTORC1 phosphorylation sites encode their sensitivity to starvation and rapamycin. *Science* **341**, 1236566 (Jul 26, 2013).

36. A. Y. Choo, S. O. Yoon, S. G. Kim, P. P. Roux, J. Blenis, Rapamycin differentially inhibits S6Ks and 4E-BP1 to mediate cell-type-specific repression of mRNA translation. *Proceedings of the National Academy of Sciences of the United States of America* **105**, 17414 (Nov 11, 2008).

37. M. E. Feldman *et al.*, Active-site inhibitors of mTOR target rapamycin-resistant outputs of mTORC1 and mTORC2. *PLoS biology* **7**, e38 (Feb 10, 2009).

38. Y. Sancak *et al.*, The Rag GTPases bind raptor and mediate amino acid signaling to mTORC1. *Science* **320**, 1496 (Jun 13, 2008).

39. S. Wang *et al.*, Metabolism. Lysosomal amino acid transporter SLC38A9 signals arginine sufficiency to mTORC1. *Science* **347**, 188 (Jan 09, 2015).

40. J. Jung, H. M. Genau, C. Behrends, Amino Acid-Dependent mTORC1 Regulation by the Lysosomal Membrane Protein SLC38A9. *Molecular and cellular biology* **35**, 2479 (Jul, 2015).

41. M. Rebsamen *et al.*, SLC38A9 is a component of the lysosomal amino acid sensing machinery that controls mTORC1. *Nature* **519**, 477 (Mar 26, 2015).

42. R. L. Wolfson *et al.*, Sestrin2 is a leucine sensor for the mTORC1 pathway. *Science* **351**, 43 (Jan 01, 2016).

43. R. L. Pisoni, J. G. Thoene, R. M. Lemons, H. N. Christensen, Important differences in cationic amino acid transport by lysosomal system c and system y+ of the human fibroblast. *The Journal of biological chemistry* **262**, 15011 (Nov 05, 1987).

44. J. Xia, D. S. Wishart, Using MetaboAnalyst 3.0 for Comprehensive Metabolomics Data Analysis. *Current protocols in bioinformatics* **55**, 14 10 1 (Sep 07, 2016).

45. A. J. Saldanha, Java Treeview--extensible visualization of microarray data. *Bioinformatics* **20**, 3246 (Nov 22, 2004).

Acknowledgments

We thank all members of the Sabatini Laboratory for helpful insights, particularly J.R. Cantor, W.W. Chen, and J.M. Orozco; C.A. Lewis and T. Kunchok from the Whitehead Institute Metabolite Profiling Core Facility; and N.S. Gray (DFCI) for Torin1. This work was supported by grants from the NIH (R01 CA103866, R01 CA129105, and R37 AI47389) and Department of Defense (W81XWH-15-1-0230) to D.M.S., from Department of Defense (W81XWH-15-1-0337) to E.F., from the EMBO Long-Term Fellowship to M.A.-R, Saudi Aramco Ibn Khaldun Fellowship for Saudi Women to N.N.L., and a fellowship support from the National Defense

Science & Engineering Graduate Fellowship (NDSEG) Program to G.A.W. D.M.S. is an investigator of the Howard Hughes Medical Institute.

Figure 1

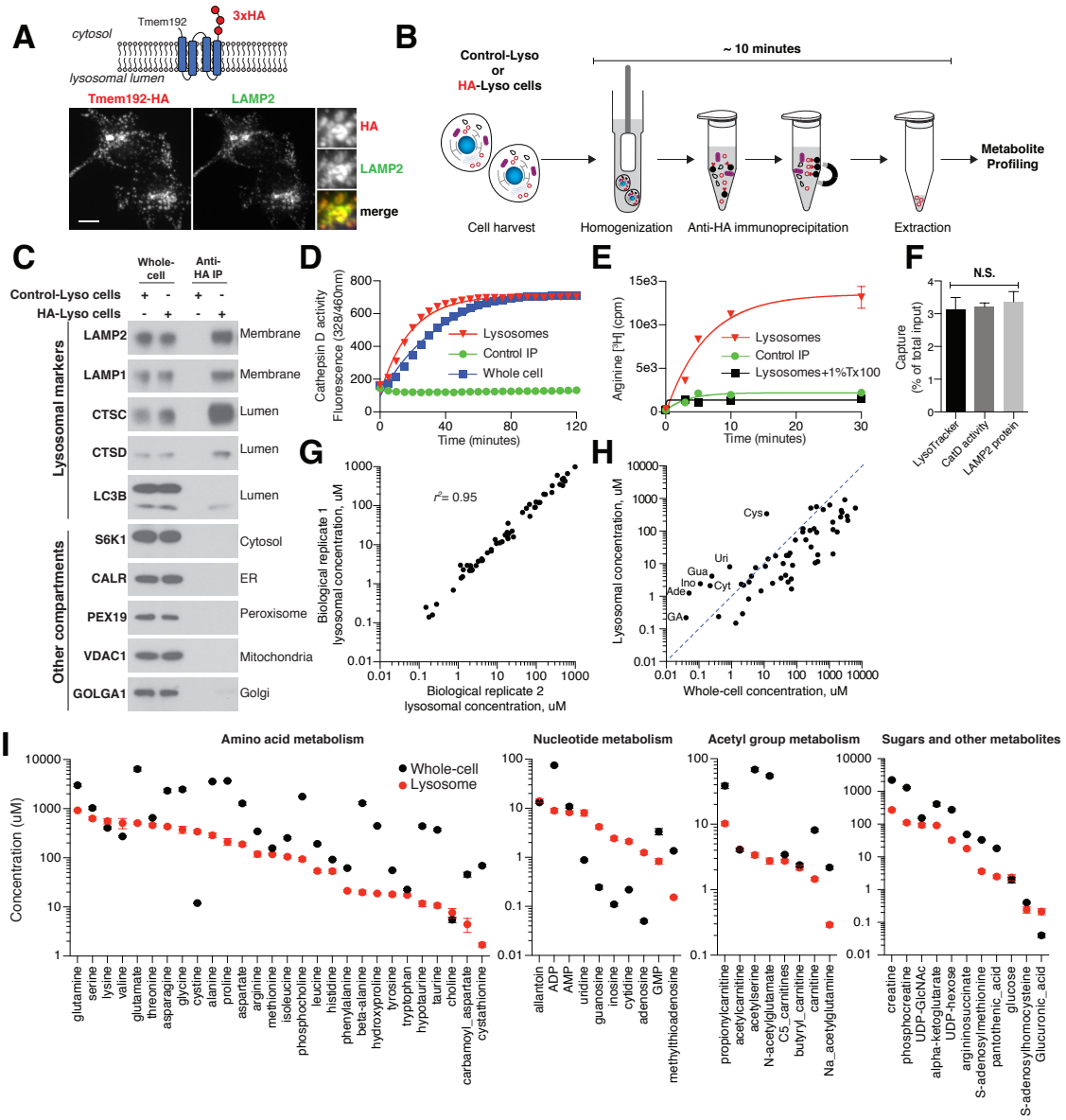
A
cytosol
lysosomal lumen
Tmem192
3xHA
Tmem192-HA
LAMP2
HA
LAMP2
merge
B
Control-Lyso or HA-Lyso cells
~ 10 minutes
Cell harvest
Homogenization
Anti-HA immunoprecipitation
Extraction
Metabolite Profiling
C
Whole-cell
Anti-HA IP
Control-Lyso cells
HA-Lyso cells
Lysosomal markers
Other compartments
LAMP2 Membrane
LAMP1 Membrane
CTSC Lumen
CTSD Lumen
LC3B Lumen
S6K1 Cytosol
CALR ER
PEX19 Peroxisome
VDAC1 Mitochondria
GOLGA1 Golgi
D
Cathepsin D activity Fluorescence (328/460nm)
Lysosomes
Control IP
Whole cell
Time (minutes)
E
Arginine [3H] (cpm)
Lysosomes
Control IP
Lysosomes+1%Tx100
Time (minutes)
F
N.S.
Capture (% of total input)
LysoTracker
CatD activity
LAMP2 protein
G
r2= 0.95
Biological replicate 1 lysosomal concentration, uM
Biological replicate 2 lysosomal concentration, uM
H
Lysosomal concentration, uM
Whole-cell concentration, uM
Cys
Uri
Gua
Ino
Ade
Cyt
GA
I
Amino acid metabolism
Nucleotide metabolism
Acetyl group metabolism
Sugars and other metabolites
Whole-cell
Lysosome
Concentration (uM)
glutamine
serine
lysine
valine
glutamate
threonine
asparagine
glycine
cystine
alanine
proline
aspartate
arginine
methionine
isoleucine
phosphocholine
leucine
histidine
phenylalanine
beta-alanine
hydroxyproline
tyrosine
tryptophan
hypotaurine
taurine
choline
carbamoyl_aspartate
cystathionine
allantoin
ADP
AMP
uridine
guanosine
inosine
cytidine
adenosine
GMP
methylthioadenosine
propionylcarnitine
acetylcarnitine
acetylserine
N-acetylglutamate
C5_carnitines
butyryl_carnitine
carnitine
Na_acetylglutamine
creatine
phosphocreatine
UDP-GlcNAc
alpha-ketoglutarate
UDP-hexose
argininosuccinate
S-adenosylmethionine
pantothenic_acid
glucose
S-adenosylhomocysteine
Glucuronic_acid

Figure legends

Fig. 1: LysoIP method for rapid immunoisolation of intact lysosomes for absolute quantification of their metabolite content

A) Localization of Tmem192-3xHA fusion protein to lysosomes. Tmem192-3xHA and lysosomes were detected by immunofluorescence with antibodies to the HA epitope tag and the lysosomal marker LAMP2, respectively. Scale bars, 10 μm. Insets represent selected fields that were magnified 3.24X.

B) Schematic of the workflow for the LysoIP method. Control-Lyso and HA-Lyso cells refer to cells stably expressing 2xFlag-tagged TMEM192 or 3xHA-tagged Tmem192, respectively.

C) The LysoIP method isolates pure lysosomes. Immunoblotting for protein markers of various subcellular compartments in whole cell (whole-cell) lysates, purified lysosomes, or control immunoprecipitates. Lysates were prepared from cells expressing the 2xFlag-tagged TMEM192 (Control-Lyso cells) or 3xHA-tagged Tmem192 (HA-Lyso cells). ER, endoplasmic reticulum.

D, E and F) Purified lysosomes are intact and retain their contents. (D) Cathepsin D activity was measured in whole-cell lysates and lysosomes, and immunoprecipitates from Control-Lyso cells served as a negative control (Control IP) (mean ± SEM, n=3). (E) Purified lysosomes take up radiolabeled arginine (Arginine [^{3}H]). Lysosomes treated with a detergent were used as a control (mean ± SEM, n=3). (F) Calculations of the amounts of captured lysosomes (mean ± SEM, n=6, $p > 0.05$, N.S., not significant, ANOVA) were similar whether determined by tracking a membrane protein (LAMP2), the activity of the lysosomal

protease cathepsin D (CatD), or a lysosome-specific small molecule (LysoTracker). Data are presented as the fraction of the material in the initial cell lysate.

G) Absolute quantification of lysosomal metabolites. Comparison of concentrations of lysosomal metabolites across two biological replicates, with R-squared value shown.

H) Metabolite concentrations in lysosomes and whole cells. Metabolites above the dotted blue line are enriched in lysosomes. Cys, cystine; Uri, uridine; Gua, guanosine; Ade, adenosine; Cyt, cytidine; Ino, inosine; GA, glucuronic acid.

I) Whole-cell and lysosomal concentrations of 57 metabolites in HEK-293T cells (mean ± SEM, n=5). n indicates the number of independent biological replicates.

Figure 2

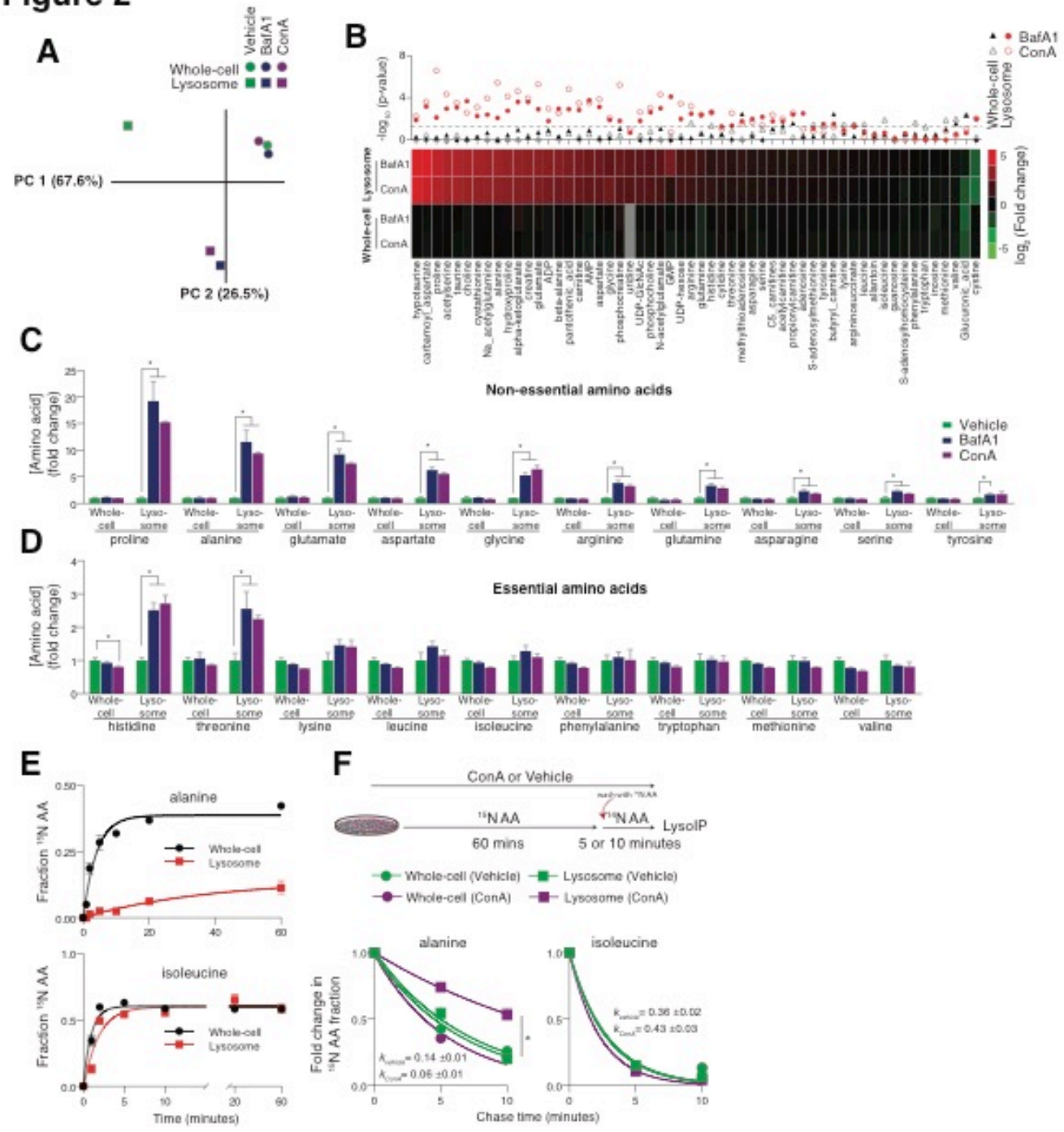
A
Vehicle
BafA1
ConA
Whole-cell
Lysosome
PC 1 (67.6%)
PC 2 (26.5%)
B
BafA1
ConA
Whole-cell
Lysosome
-log10 (p-value)
Lysosome
Whole-cell
log2 (Fold change)
hypotaurine
carbamoyl_aspartate
proline
acetylserine
taurine
choline
cystathionine
Na_acetylglutamine
alanine
hydroxyproline
alpha-ketoglutarate
creatine
glutamate
ADP
beta-alanine
pantothenic_acid
carnitine
AMP
aspartate
glycine
phosphocreatine
uridine
UDP-GlcNAc
phosphocholine
N-acetylglutamate
GMP
UDP-hexose
arginine
glutamine
histidine
cytidine
threonine
methylthioadenosine
asparagine
serine
C5_carnitines
acetylcarnitine
propionylcarnitine
adenosine
S-adenosylmethionine
tyrosine
butyryl_carnitine
lysine
argininosuccinate
leucine
allantoin
isoleucine
guanosine
S-adenosylhomocysteine
phenylalanine
tryptophan
inosine
methionine
xanthine
valine
Glucuronic_acid
cystine
C
Non-essential amino acids
[Amino acid] (fold change)
Vehicle
BafA1
ConA
Whole-cell
Lyso-some
proline
alanine
glutamate
aspartate
glycine
arginine
glutamine
asparagine
serine
tyrosine
D
Essential amino acids
[Amino acid] (fold change)
histidine
threonine
lysine
leucine
isoleucine
phenylalanine
tryptophan
methionine
valine
E
alanine
isoleucine
Fraction 15N AA
Whole-cell
Lysosome
Time (minutes)
F
ConA or Vehicle
15N AA
60 mins
15N AA
5 or 10 minutes
LysoIP
Whole-cell (Vehicle)
Lysosome (Vehicle)
Whole-cell (ConA)
Lysosome (ConA)
alanine
isoleucine
Fold change in 15N AA fraction
Chase time (minutes)

Fig. 2: The efflux from lysosomes of most non-essential, but not essential, amino acids requires the proton gradient

A) Changes in metabolite concentrations in whole-cells and lysosomes upon V-ATPase inhibition. Principal component analyses of changes in metabolite concentrations in whole-cells (circle) or lysosomes (square) after treatment for 1 hour with 200 nM Bafilomycin A1 (BafA1, blue) or Concanamycin A (ConA, purple). DMSO vehicle-treated cells were used as control (vehicle, green).

B) Most metabolites accumulate in lysosomes upon V-ATPase inhibition while their levels in whole-cells are not affected. P-values are for comparisons between metabolite concentrations in whole-cell (triangle) or lysosome (circle) samples shown in (A) (n=3 for each treatment; dotted line represents p-value = 0.05). Lower panel, heat map of fold changes (log_2) in metabolite concentrations after V-ATPase inhibition relative to vehicle-treatment. Gray boxes indicate undetected metabolites.

C and D) Accumulation of most non-essential, but not essential, amino acids in lysosomes upon V-ATPase inhibition. Fold changes in whole-cell and lysosomal concentrations of amino acids in BafA1- or ConA-treated cells relative to vehicle-treated cells (mean ± SEM, n=3, *p<0.05).

E) Tracing of exogenously added alanine and isoleucine in live cells. Cells were incubated in medium containing ^{15}N-labeled alanine and isoleucine for the indicated time points and then subjected to LysoIP. Data are presented as the fraction of the total pool of the amino acid that is ^{15}N-labeled in whole-cells (black) or lysosomes (red) (mean ± SEM, n=3 in each time point).

F) Dependence of lysosomal efflux of alanine but not that of isoleucine on the proton-gradient. Cells treated with or without ConA were incubated in medium containing ^{15}N-labeled alanine and isoleucine for 1 hour (pulse period), which was then replaced with medium containing the natural ^{14}N-containing isotope for the indicated time points (chase period). The fold change in the fraction of ^{15}N-labeled amino acid remaining in the whole cells (circle) or lysosomes (square) was measured (mean ± SEM, n=3; *k* (in min^{-1}) is the rate constant for the decay of the ^{15}N-labeled amino acid from the lysosome and * indicates non-overlapping 95% confidence intervals of the calculated *k* values between the treatments). Two-tailed t tests were used for comparisons between groups.

Figure 3

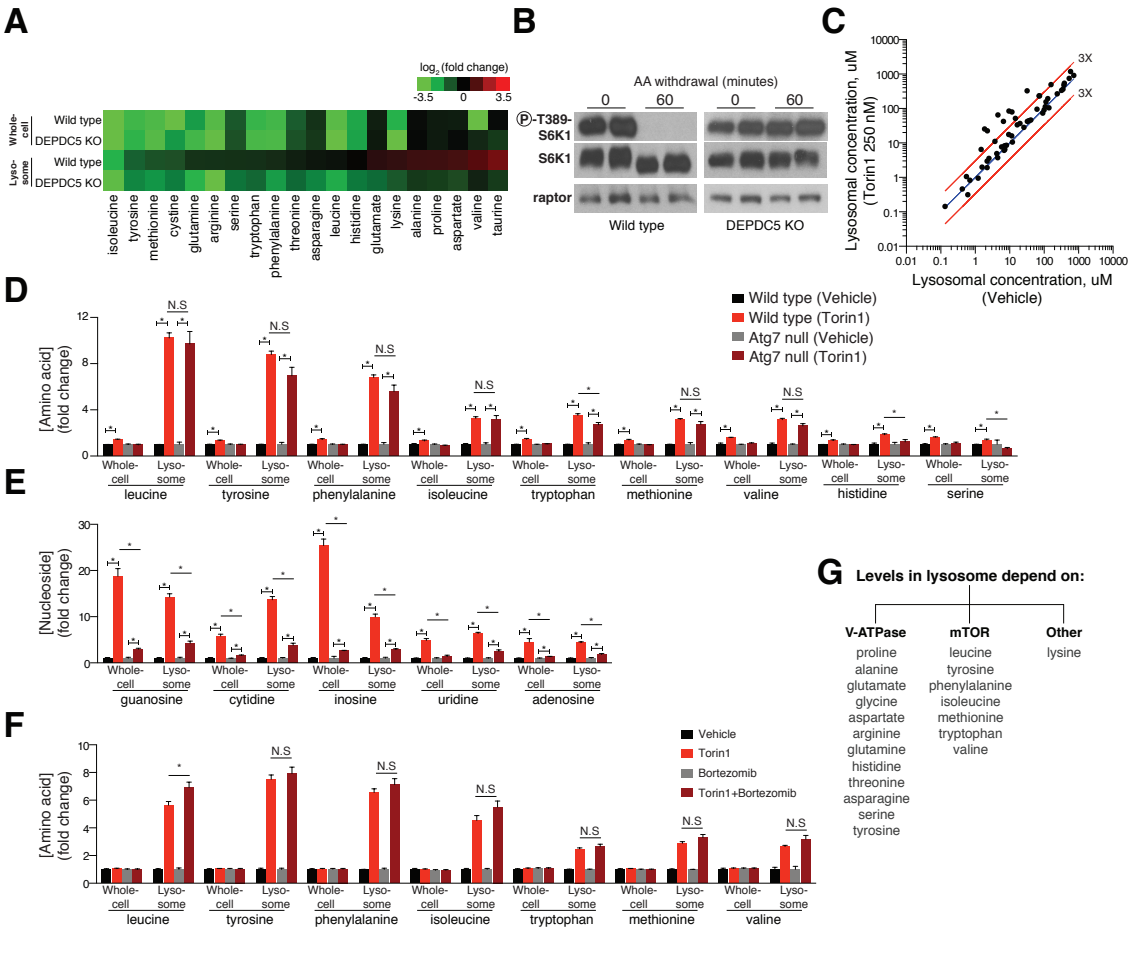
A
log2 (fold change)
-3.5 0 3.5
Whole-cell
Wild type
DEPDC5 KO
Lyso-some
Wild type
DEPDC5 KO
isoleucine
tyrosine
methionine
cystine
glutamine
arginine
serine
tryptophan
phenylalanine
threonine
asparagine
leucine
histidine
glutamate
lysine
alanine
proline
aspartate
valine
taurine
B
AA withdrawal (minutes)
0
60
0
60
Ⓟ-T389-S6K1
S6K1
raptor
Wild type
DEPDC5 KO
C
Lysosomal concentration, uM (Torin1 250 nM)
Lysosomal concentration, uM (Vehicle)
3X
3X
D
[Amino acid] (fold change)
Wild type (Vehicle)
Wild type (Torin1)
Atg7 null (Vehicle)
Atg7 null (Torin1)
N.S
Whole-cell
Lyso-some
leucine
tyrosine
phenylalanine
isoleucine
tryptophan
methionine
valine
histidine
serine
E
[Nucleoside] (fold change)
guanosine
cytidine
inosine
uridine
adenosine
F
[Amino acid] (fold change)
Vehicle
Torin1
Bortezomib
Torin1+Bortezomib
N.S
leucine
tyrosine
phenylalanine
isoleucine
tryptophan
methionine
valine
G
Levels in lysosome depend on:
V-ATPase
proline
alanine
glutamate
glycine
aspartate
arginine
glutamine
histidine
threonine
asparagine
serine
tyrosine
mTOR
leucine
tyrosine
phenylalanine
isoleucine
methionine
tryptophan
valine
Other
lysine

Fig. 3: mTOR regulates the lysosomal levels of essential non-polar amino acids in an autophagy-independent manner

A) mTORC1 regulates the abundance of amino acids in lysosomes upon amino acid starvation. A heat map shows fold changes (log_2) in amino acid (AA) concentrations in whole cell samples or lysosomes of wild-type and DEPDC KO cells after amino acid starvation for 60 minutes relative to cells cultured in medium with all amino acids (n=2 for each time point).

B) Amino acid starvation inhibits mTORC1 signaling. Immunoblotting was used to monitor the levels and phosphorylation state of S6 kinase (S6K1) in the same samples as in (A). Raptor served as a loading control.

C) Pharmacological inhibition of mTOR leads to the accumulation of many metabolites in lysosomes. Cells were treated with 250 nM Torin1 or DMSO (vehicle) for 1 hour and the lysosomal metabolite concentrations were determined and compared (n=3). Red lines indicate three-fold change in lysosomal concentration in Torin1- relative to vehicle-treated cells.

D) Lysosomal accumulation of non-polar essential amino acids and tyrosine in an autophagy-independent manner after mTOR inhibition. Fold changes in the whole-cell and lysosomal concentrations of amino acids in wild-type and *Atg7*-null cells treated with Torin1 relative to vehicle-treated cells (mean ± SEM, n=3, *p<0.05; N.S, non significant). Histidine and serine served as examples of autophagy-dependent amino acids.

E) Upon mTOR inhibition, nucleosides accumulate in lysosomes in a mostly autophagy-dependent manner. Fold changes in whole-cell and lysosomal

concentrations of nucleosides in the same cells as in (D) (mean ± SEM, n=3, *p<0.05).

F) Proteasome activity is dispensable for the lysosomal accumulation of amino acids upon mTOR inhibition. Fold changes in the whole-cell and lysosomal concentrations of amino acids in cells treated with 250 nM Torin1 or Torin1 together with 5 uM Bortezomib relative to DMSO- or Bortezomib-treated cells, respectively (mean ± SEM, n=3, *p<0.05; N.S, non significant).

G) Proteogenic amino acids can be divided into those whose lysosomal levels are regulated by V-ATPase- or mTOR-dependent mechanisms.

Two-tailed t tests were used for comparisons between groups.

Figure 4

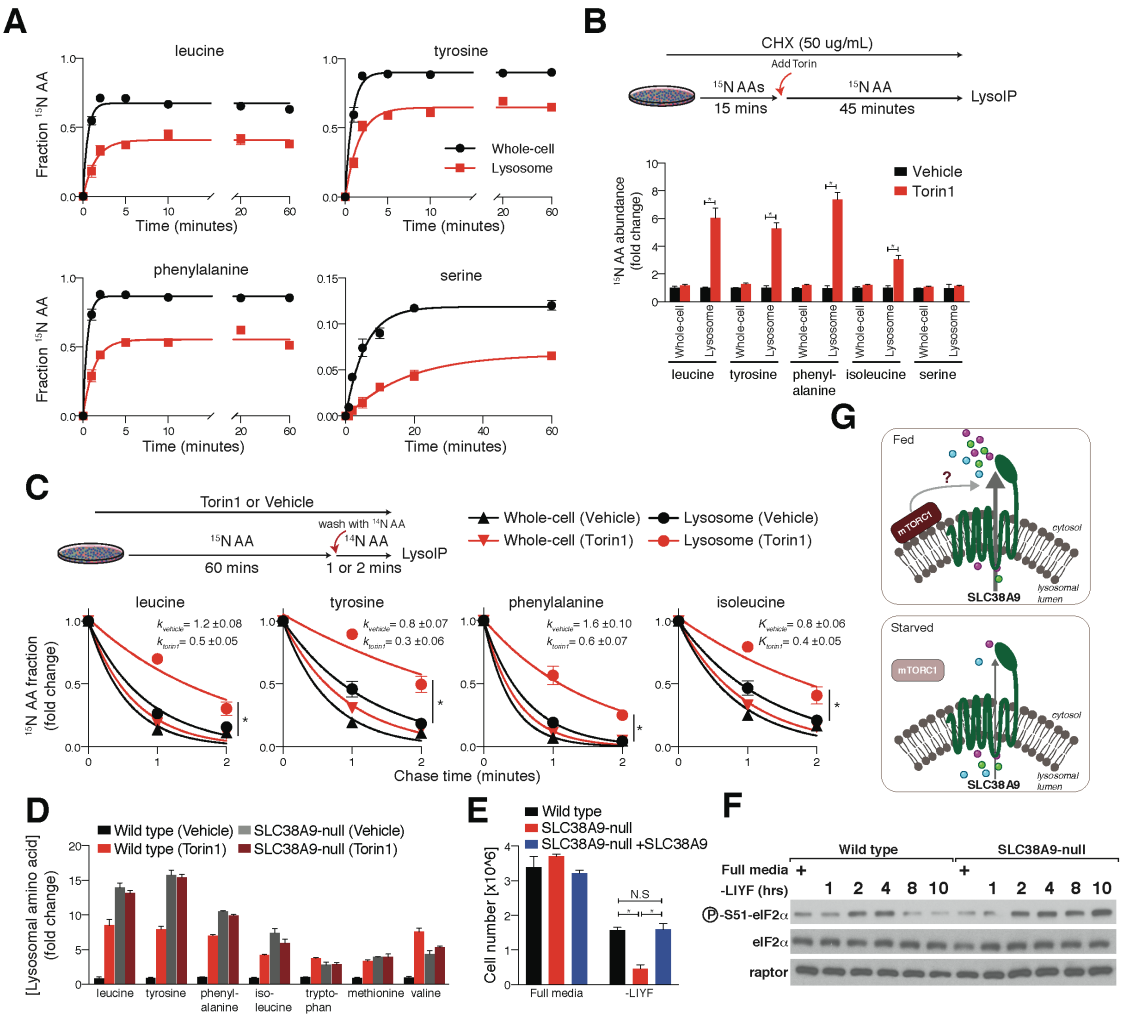
A
leucine
tyrosine
phenylalanine
serine
Fraction ¹⁵N AA
Time (minutes)
Whole-cell
Lysosome
B
CHX (50 ug/mL)
Add Torin
¹⁵N AAs
15 mins
¹⁵N AA
45 minutes
LysoIP
¹⁵N AA abundance (fold change)
Vehicle
Torin1
Whole-cell
Lysosome
leucine
tyrosine
phenyl-alanine
isoleucine
serine
C
Torin1 or Vehicle
¹⁵N AA
60 mins
wash with ¹⁴N AA
¹⁴N AA
1 or 2 mins
LysoIP
Whole-cell (Vehicle)
Lysosome (Vehicle)
Whole-cell (Torin1)
Lysosome (Torin1)
¹⁵N AA fraction (fold change)
Chase time (minutes)
D
Wild type (Vehicle)
SLC38A9-null (Vehicle)
Wild type (Torin1)
SLC38A9-null (Torin1)
[Lysosomal amino acid] (fold change)
leucine
tyrosine
phenyl-alanine
iso-leucine
trypto-phan
methionine
valine
E
Wild type
SLC38A9-null
SLC38A9-null +SLC38A9
Cell number [x10^6]
N.S
Full media
-LIYF
F
Wild type
SLC38A9-null
Full media
-LIYF (hrs)
1 2 4 8 10
Ⓟ-S51-eIF2α
eIF2α
raptor
G
Fed
mTORC1
cytosol
lysosomal lumen
SLC38A9
Starved

Fig. 4: mTOR controls the efflux of non-polar essential amino acids and tyrosine from lysosomes

A) Tracing of exogenously added leucine, tyrosine, phenylalanine, and serine in live cells. Cells were incubated in medium containing the indicated ^{15}N-labeled amino acids for various times and subjected to the LysoIP method. Data are presented as the fraction of the total pool of the amino acid in whole cells (black) or lysosomes (red) that is ^{15}N-labeled (mean ± SEM, n=3 in each time point).

B) Independently of protein synthesis, mTOR inhibition leads to the accumulation in lysosomes of leucine, tyrosine, phenylalanine, and isoleucine, but not serine. Data are presented as the fold change in the whole-cell (black) and lysosomal (red) abundance of the indicated ^{15}N-labeled amino acid after Torin1-treatment relative to the DMSO vehicle treatment. The experiment was performed as indicated in the figure in the presence of 50 ug/mL cycloheximide (CHX) (mean ± SEM, n=3, $p<0.005$). This experiment was performed using *Atg7*-null cells.

C) mTOR controls the lysosomal efflux of non-polar essential amino acids as well as tyrosine. Cells treated with 250 nM Torin1 or DMSO (vehicle) were incubated in medium containing the indicated ^{15}N-labeled amino acids for 1 hour (pulse period). This medium was then replaced with media containing the natural ^{14}N-isotope of the amino acid for the indicated time points (chase period). Data are presented as the fold change in the fraction of ^{15}N-labeled amino acid remaining in whole cells (triangle) or lysosomes (circle) at each time point (mean ± SEM, n≥3; k (in min^{-1}) is the rate constant for the decay of the ^{15}N-labeled amino acid from lysosomes and * indicates non-overlapping 95% confidence intervals of the calculated k between the treatments). This experiment was performed using *Atg7*-null cells.

D) mTORC1 regulates the lysosomal abundance of essential non-polar amino acids and tyrosine in an SLC38A9-dependent manner. Fold changes in the lysosomal concentrations of indicated amino acids in wild-type and SLC38A9-null cells treated with Torin1 relative to vehicle-treated wild-type cells (mean ± SEM, n=3).

E) Loss of SLC38A9 impairs the fitness of cells under starvation conditions. Wild-type, SLC38A9-null, and SLC38A9-null addback (SLC38A9-null+SLC38A9) cells were seeded in medium containing all amino acids (full media) or lacking leucine, isoleucine, tyrosine, and phenylalanine (-LIYF) for 3 days at which point cell numbers were measured (mean ± SD, n=3, *p<0.001).

F) SLC38A9 is required for inhibiting the GCN2 pathway after a prolonged amino acid starvation period. Immunoblotting was used to monitor the levels and phosphorylation state of eIF2α. Raptor served as a loading control. LIYF indicates leucine, isoleucine, tyrosine, and phenylalanine.

G) A model proposing a role for mTORC1 in regulating the efflux of amino acids from lysosomes.

Two-tailed t tests were used for comparisons between two groups.

Material and Methods

Reagents were obtained from the following sources: antibodies to LAMP2 and CTSC, and HRP- and fluorophore-labeled anti-mouse and anti-rabbit secondary antibodies, and Bortezomib from Santa Cruz Biotechnology; antibodies to LAMP1, VDAC1, LC3B, ATG7, GOLGA1, CALR, CTSD, c-Myc, phospho-T389 S6K1, S6K1, phospho-S757 ULK1, ULK1, phospho-S65 4E-BP1, 4E-BP1, phospho-S473 AKT1, AKT1, RICTOR, phospho-S51 eIF2alpha, eIF2alpha and

HA epitope from Cell Signaling Technology; antibody to PEX19 from Abcam; antibody to raptor from Millipore; LysoTracker Red DND-99, anti-HA magnetic beads, and ECL western blotting substrate from Thermo Fisher Scientific; Cathepsin D activity assay kit from Abcam; DMEM from SAFC Biosciences; amino acid-free RPMI from US Biologicals; amino acids, Cycloheximide, and Chloroquine from Sigma Aldrich; [^{3}H]-labeled arginine from American Radiolabeled Chemicals; 15N-labeled amino acid isotopes from Cambridge Isotope Laboratories; XtremeGene9 and Complete Protease Inhibitor Cocktail from Roche; inactivated fetal calf serum (IFS) from Invitrogen; and AZD8055, Rapamycin and WYE-125132 (WYE-132) from Selleck Chemicals. Torin1 was generously provided by Dr. Nathanael Gray (DFCI).

Cell culture

HeLa, PA-TU-8988T and HEK-293T cells and their derivatives were cultured in DMEM base media with 10% inactivated fetal calf serum supplemented with 2 mM glutamine, penicillin, and streptomycin. All cell lines were maintained at 37°C and 5% CO2. For all experiments using HEK-293T lines, cells were cultured in RPMI base media supplemented with the relevant small molecule inhibitors for one hour before processing. Experiments with both HeLa and PA-TU-8988T cell lines were performed in full media containing 10% dialyzed inactivated fetal calf serum. All cell lines were authenticated by STR profiling.

Cell lysate preparation and immunoblotting

Cell lysates were prepared in ice-cold lysis buffer (40 mM HEPES pH 7.4,1%

Triton X-100, 10 mM β-glycerol phosphate, 10 mM pyrophosphate, 2.5 mM MgCl2 and Complete EDTA-free Protease Inhibitor Cocktail (Roche)). The soluble fractions from lysates were collected by centrifugation at 17,000 x g for 10 min in a cold centrifuge. Similar protocol was used to prepare protein lysates from immunopurified lysosomes and control immunoprecipitates. Lysates were then resolved by 12% SDS-PAGE at 120 V. Resolved proteins were transferred for 2 hours at 40 V to ethanol-pretreated PVDF membranes to be further analyzed by immunoblotting. Membranes were blocked with 5% nonfat dry milk prepared in TBST (Tris-buffered saline with Tween 20) for 1 hour, then incubated overnight with primary antibodies in 5% bovine serum albumin (BSA) in TBST at 4°C. All primary antibodies were used at (1:1000) dilution except for CTSC, which was used at (1:250). Following incubation, membranes were washed with TBST three times and each wash lasted 5 min and then incubated with the appropriate secondary antibodies diluted 1:3000 in 5% milk for 1 hour at room temperature. Membranes were then washed three times with TBST before being visualized using ECL western blotting substrate.

Immunofluorescence assays and lysosome volume quantification

~250,000 cells were seeded on fibronectin-coated glass coverslips in 6-well tissue culture plates. After 24 hours, the coverslips were fixed with 4% paraformaldehyde (PFA) in Phosphate Buffered Saline (PBS) for 15 min at room temperature (RT) and rinsed three times with PBS. Fixed cells were incubated with Blocking Buffer (5% normal donkey serum with 0.3% Triton X-100 in PBS) for 1 hour and then incubated overnight with primary antibodies against LAMP2 and HA (1:200 in antibody dilution buffer (1X PBS/1% BSA/0.3% Triton™ X-100)) at 4°C. Cells were then washed three times with PBS for 5 min each and incubated with the corresponding fluorophore-labeled secondary antibodies (1:400) for 1 hour at room temperature in the dark. Coverslips were rinsed three times with PBS for 5 min each, incubated with the Hoechst dye to visualize nuclei (1:10,000) for 10 seconds, and then mounted on glass slides using Vectashield mounting media. Z-Stacks, or cell images in the XY plane stacked along the Z-axis, were captured with a 63x objective mounted on a spinning-disk confocal microscope (Perkin Elmer). For volume quantification, z-stacks of more than 100 cells visualized at 63X magnification from multiple biological replicates for each experimental condition were analyzed using Imaris Bitplane Software. The

channel depicted the HA-tagged lysosomes was used as the source channel for creating 3D projections representing lysosomal surfaces. To ensure consistency when creating the 3D surfaces, the minimum and maximum intensity values of were set to 109 and 2587, respectively, and the threshold setting for background subtraction was set to automatic determination by the software for all fields of cells. The average lysosomal volume per cell was calculated using the volume of enclosed surfaces, generated by the software, divided by the number of cells counted per each field of cells. Lysosomes occupied 3.1% of the volume of HEK-293T cells under basal conditions and in cells treated with Torin1 for 1 hour.

However, in cells treated with Concanamycin A (ConA) or Bafilomycin A1 (BafA1) this fraction was reduced to 2.6% and 2.3%, respectively. These volume changes were taken into account when calculating the concentrations of metabolites under these conditions.

Cell volume calculations

In each experiment, cells were counted and their average volume determined using a Beckman Coulter machine.

Plasmid construction

For production of cell lines stably expressing Tmem192-3xHA, Tmem192-2xFlag, LAMP1-RFP-3xHA, or LAMP1-RFP-2xFlag at moderate levels, constructs were cloned into the pLJC5 lentiviral vector containing the UBC promoter (*1*). To produce pLJC5-Tmem192-3xHA and pLJC5-Tmem192-2xFlag, the Tmem192 sequence was amplified using cDNA prepared from HEK-293T cells using a common forward primer and Tmem192-HA-R or

Tmem192-Flag-R reverse primers containing the corresponding epitope sequence, respectively.

Forward:

TMEM192-F: CCACCGGTACCATGGCGGCGGGGGGCAGGATGGAGGAC

Reverse:

TMEM192-HA-R:

CCGGAATTCTTAGCCGCTCCCTCCAGCATAATCAGGCACATCATAAGGGTA
TCCGGCGCTGCCAGCGTAGTCAGGCACATCATAGGGGTAGGATCCTGTGC
CGGCGTAATCAGGCACGTCATAGGGATAACTACCTCCACCTCCCGTTCTAC
TTGGCTGACAGCCCA

TMEM192-Flag-R:

CCGGAATTCTTACTTGTCGTCATCGTCTTTGTAGTCCTTGTCGTCATCGTCTT
TGTAGTCACTACCTCCACCTCCCGTTCTACTTGGCTGACAGCCCA

To produce pLJC5-LAMP1-RFP-3xHA and pLJC5-LAMP1-RFP-2xFlag, LAMP1 and RFP (red fluorescent protein) sequences were amplified from previously reported LAMP1-mRFP-FLAG plasmid (*2*) using a common forward primer and LAMP1-HA-R or LAMP1-Flag-R reverse primers, respectively.

Forward:

LAMP1-F**:** CCACCGGTACCATGGCGGCCCCGGGCGCCCG

Reverse:

LAMP1-HA-R:

CCGGAATTCTTAGCCGCTCCCTCCAGCATAATCAGGCACATCATAAGGGTA
TCCGGCGCTGCCAGCGTAGTCAGGCACATCATAGGGGTAGGATCCTGTGC

CGGCGTAATCAGGCACGTCATAGGGATAGGCGCCGGTGGAGTGGCGGCC
CT

LAMP1-Flag-R: CCGGAATTCTCACTTGTCGTCATCGTCTTTG

To generate autophagy-defective HEK-293T cells, the following sense (S) and antisense (AS) oligonucleotides encoding the guide RNA against the *Atg7* gene were cloned into the pX330 vector.

sgAtg7_S: caccgATAGCTGGGCAGCAACGGGC

sgAtg7_AS: aaaacGCCCGTTGCTGCCCAGCTAT

To generate *Rictor*-null cells, the following oligonucleotides for a guide RNA against the *Rictor* gene were cloned into the lentiCRISPR-v1 vector.

sgRictor_S: caccgCATTGGTCTTGCTCTCCCGG

sgRictor_AS: aaaacCCGGGAGAGCAAGACCAATG

A non-targeting control was previously described (*3*).

Lentivirus production and viral transduction

Lentiviruses were produced by transfecting HEK-293T with pLJC5-Tmem192-3xHA, pLJC5-Tmem192-2xFlag, pLJC5-LAMP1-RFP-3xHA or pLJC5-LAMP1-RFP-2xFlag constructs in combination with VSV-G and CMV- ΔVPR packaging plasmids. Sixteen hours later, the media was changed to DMEM with 30% IFS. Fifty hours after transfection, the virus containing supernatant was collected, centrifuged at 1,000 x g to remove cells and then frozen at -80°C. To establish stably expressing cell lines, 500,000 HEK-293T, HeLa or PA-TU-8988T cells were plated in 6-well plates in DMEM with 10% IFS and 8 μg/mL polybrene and infected with 250 μL of virus-containing media. Sixteen hours later, the media was

refreshed and puromycin was added for selection. Stable cell lines were tested for the proper localization of the lysosomal tag using immunofluorescence as previously described.

LC/MS-based metabolite profiling

Analytical methodologies for metabolite profiling

LC/MS was used to profile and quantify the polar metabolite content of both whole cell and IP samples as described previously (*4*). LC/MS-based analyses were conducted on a QExactive benchtop orbitrap mass spectrometer equipped with an Ion Max source and HESI II probe, which was coupled to a Dionex UltiMate 3000 ultra-high performance liquid chromatography system (Thermo Fisher Scientific, San Jose, CA). External mass calibration was performed using the standard calibration mixture every 7 days. Acetonitrile was LC/MS HyperGrade from EMD Millipore. All other solvents were LC/MS Optima grade from Thermo Fisher Scientific. The metabolite extraction mix (stored at -20°C) was made of 80:20 (v/v) methanol:water, supplemented with a mixture of 17 isotope-labeled amino acids at 500nM each as internal extraction standards (Cambridge Isotope Laboratories, MSK-A2-1.2).

For chromatographic separation, 2.5µL of each whole cell or lysosomal IP sample was injected onto a SeQuant ZIC-pHILIC Polymeric column (2.1 x 150 mm) connected with a guard column (2.1 x 20 mm). Both analytical and guard columns are of 5 µm particle size purchased from EMD Millipore. Flow rate was set to 0.150 mL per minute, the column compartment was set to 25°C, and the autosampler sample tray to 4 °C. Mobile Phase A consisted of 20 mM

ammonium carbonate, 0.1% ammonium hydroxide. Mobile Phase B was 100% acetonitrile. The chromatographic gradient was as follows: (1) 0-20 min: linear gradient from 80% to 20% B; (2) 20-20.5 min: linear gradient from 20% to 80% B; (3) 20.5-28min: hold at 80% B. The mass spectrometer was operated in full scan, polarity switching mode with the spray voltage set to 3.0 kV, the heated capillary held at 275°C, and the HESI probe held at 350°C. The sheath gas flow rate was set to 40 units, the auxiliary gas flow was set to 15 units, and the sweep gas flow was set to 1 unit. The MS data acquisition was performed in a range of 70-1000 m/z, with the resolution set to 70,000, the AGC target at 10^6, and the maximum injection time at 20 msec.

To detect LysoTracker DND-99 and nucleosides with higher sensitivity, additional tSIM (targeted selected ion monitoring) scans were performed, with resolution set to 70,000, the AGC target at 10^5, and the maximum injection time at 250 msec. The inclusion mass list for tSIM scan in positive mode was as follows: 400.2115 (corresponding to Lysotracker DND-99); 268.1040 (corresponding to adenosine); 284.0989 (corresponding to guanosine); 269.0880 (corresponding to inosine); 244.0928 (corresponding to cytidine). The inclusion mass for tSIM scan in negative mode was 243.0623 (corresponding to uridine). The isolation window around each target mass was set to 1.0 m/z.

Metabolomics data processing and analyses

Metabolite identification and quantification were performed using XCalibur v4.0 software (Thermo Fisher Scientific) by matching accurate mass with a 5 ppm

mass tolerance, and retention times of authentic standards within 0.5 min retention time window. For relative quantification, the raw peak area for each metabolite was divided by the raw peak area of the relevant isotope-labeled internal standard to calculate the relative abundance. The amino acids were normalized with their isotope-labeled counterparts, while for every other metabolite, the internal standard with the closest retention time was used. For absolute quantification, a set of external standards with nine final concentrations (10 nM, 30 nM, 100 nM, 300 nM, 1 μM, 3 μM, 10 μM, 30 μM, and 100 μM) were used to generate a calibration curve. The relative abundances obtained from the calibration curve samples were fitted to a quadratic log-log equation, typically with $r^2 > 0.99$, which was then used to calculate the concentration of the metabolite in each metabolite extract. The molar quantity of a metabolite in a given whole cell or IP sample was then calculated from the sample concentration and the corresponding sample volume. For the 57 metabolites that were quantified in whole cell and lysosome samples, chemical standards were obtained from commercial sources, except that C4- and C5-carnitines were a kind gift of R. Pragani and M. Boxer (NCATS, NIH, Rockville, MD) and were synthesized via a published procedure (Goel, Om P., SSV Therapeutics, Inc., USA; U.S. Patent Number 7777071, B2; Aug. 17, 2010). All standards were validated via LC/MS to confirm that they produced a robust peak at the expected m/z ratio, and were then grouped into five pools as in Chen et al (*4*).

Rapid method for the immunopurification of lysosomes (LysoIP)

~35 million cells in 15 cm plates were used for each LysoIP. Each sample was

processed separately to ensure rapid isolation of lysosomes using equipment and buffers (all prepared in Optima LC/MS water) that were pre-chilled on ice. Control-Lyso cells expressing TMEM192-2xFlag were processed in every experiment to subtract background signal. Cells were quickly rinsed twice with PBS and then scraped in one mL of KPBS (136 mM KCl, 10 mM KH_2PO_4, pH 7.25 was adjusted with KOH, as previously described (*4*)) and centrifuged at 1000 x g for 2 min at 4°C. Pelleted cells were resuspended in 950 µL, and 25 µL (equivalent to 2.5% of the total cells) was reserved for further processing of the whole-cell fraction. The remaining cells were gently homogenized with 20 strokes of a 2 ml homogenizer. The homogenate was then centrifuged at 1000 x g for 2 min at 4°C and the supernatant containing the cellular organelles including lysosomes was incubated with 150 µL (similar results are obtained using 100-200 µL beads) of KPBS prewashed anti-HA magnetic beads on a gentle rotator shaker for 3 min. We noticed that extending incubation time to 15 minutes does increase capturing efficiency without affecting the molar concentration of stable metabolites like amino acids. However, we prefer a 3 minute incubation time to minimize undesirable effects on potentially labile metabolites. Immunoprecipitates were then gently washed three times with KPBS on a DynaMag Spin Magnet. For metabolite extraction from lysosomes, beads with bound lysosomes were resuspended in 50 µL ice-chilled metabolite extraction buffer (80% methanol, 20% water containing internal standards), incubated for 5 min on ice and then the beads were removed with the magnet. The metabolite extract (liquid fraction) was then centrifuged at 1000 x g for 2 min at 4°C. The supernatant was collected and analyzed by LC/MS to determine the total moles

of each metabolite. For the whole-cell sample, a 10X volume (225 µL) of metabolite extraction buffer was added to it, which was followed by a brief vortexing to extract cellular metabolites. After an incubation for 5 min, the metabolite extract was centrifuged at 1000 x g for 2 min at 4°C and the supernatant was then collected and analyzed by LC/MS to determine the total moles of each metabolite. The background-corrected molar values were obtained by subtracting the moles present in the Control-lyso IP from those present in the HA-Lyso IP. The lysosomal concentration of each metabolite was calculated by taking into consideration the total volume of captured lysosomes as derived from the total volume of initially processed cells multiplied by the capturing efficiency in each experiment and the fraction of lysosomal volume in the same cell line as was previously determined using Imaris. Capturing efficiency was calculated using LysoTracker abundance as measured by LC/MS. For V-ATPase inhibitor experiments the average capturing efficiency in control samples were used since drug treatments affect lysoTracker accumulation in lysosome but not the capturing efficiency. The whole-cell concentration for each metabolite was directly calculated using the total volume of cells used as 2.5% input sample and the molar concentration derived from the LC/MS analysis.

Arginine uptake assay

The arginine uptake assay was adapted from Pisoni et al (*5*). Lysosomes were isolated from ~35 million HEK-293T cells as described above. Immunopurified lysosomes were incubated with 20 µM [^{3}H] L-arginine in 700 µL KPBS-based

buffer consisting of 0.125 M sucrose, 2 mM $MgCl_2$, and 2 mM ATP at 4^{o}C. Lysosomes were then transferred to a 37°C warm bath and fractions were collected at the designated time points. Collected lysosomes were washed three times with ice-cold KPBS on the magnet and then resuspended in 100 µL KPBS and mixed with standard scintillation counting fluid. Control-Lyso IP and lysosomes lysed in 1% TritionX-100 were used as controls.

Statistical analyses and heat map generation

All replicates in the manuscript are biological replicates. Entire experiments were performed multiple times to ensure reproducibility. The two-tailed *t* test was used for comparisons between two groups unless indicated. All comparisons were two-sided, and P values are indicated in figure legends. Principal component analysis was performed using MetaboAnalyst v3.0 online software (*6*). Heat maps were generated using Java TreeView (*7*).

References

1. R. L. Wolfson *et al.*, Sestrin2 is a leucine sensor for the mTORC1 pathway.
   Science **351**, 43 (Jan 01, 2016).
2. R. Zoncu *et al.*, mTORC1 senses lysosomal amino acids through an inside-out mechanism that requires the vacuolar H(+)-ATPase.
   Science **334**, 678 (Nov 04, 2011).

3. S. Wang *et al.*, Metabolism. Lysosomal amino acid transporter SLC38A9 signals arginine sufficiency to mTORC1. *Science* **347**, 188 (Jan 09, 2015). W. W. Chen, E. Freinkman, T. Wang, K. Birsoy, D. M. Sabatini, Absolute Quantification of Matrix Metabolites Reveals the Dynamics of Mitochondrial Metabolism. *Cell* **166**, 1324 (Aug 25, 2016).
4. R. L. Pisoni, J. G. Thoene, R. M. Lemons, H. N. Christensen, Important differences in cationic amino acid transport by lysosomal system c and system y+ of the human fibroblast. *The Journal of biological chemistry* **262**, 15011 (Nov 05, 1987).
5. J. Xia, D. S. Wishart, Using MetaboAnalyst 3.0 for Comprehensive Metabolomics Data Analysis. *Current protocols in bioinformatics* **55**, 14 10 1 (Sep 07, 2016).
6. A. J. Saldanha, Java Treeview--extensible visualization of microarray data. *Bioinformatics* **20**, 3246 (Nov 22, 2004).

Author Contributions

M.A-R., G.A.W. and D.M.S. initiated the project and designed the research plan. M.A-R. performed the experiments and analyzed the data with help from G.A.W, C.K., N.L., and M.A.. E.F. played a critical role in establishing the LC/MS platform and assembling the library of metabolite standards and operating the LC/MS equipment. S.H.C., helped with LC/MS data analysis. M.A-R. wrote the manuscript and D.M.S. edited it.

Supplementary figure legends

Supplementary Figure 1

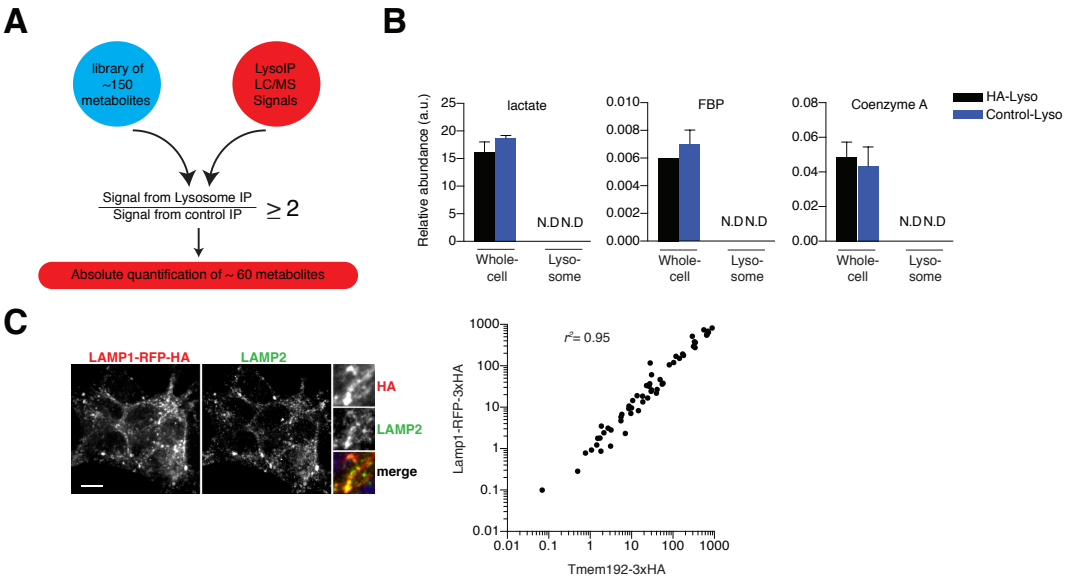

Figure S1

A) Schematic diagram depicting the approach for determining which metabolites are present in lysosomes.

B) Relative abundance of the indicated metabolites compared to internal standards in whole cell or immunoprecipitates samples prepared from cells expressing TMEM192-3xHA (HA-Lyso) or Tmem-2xFlag (Control-Lyso) (n=5 and 2, respectively). FPB, fructose 1,6-bisphosphate; N.D, not detected.

Left panel; immunofluorescence detection of LAMP1-RFP-3xHA and lysosomes with antibodies to the HA epitope tag and the lysosomal marker LAMP2, respectively. Scale bars, 10 μm. Insets represent selected fields that were magnified 3.24X. In the right panel, comparison of lysosomal concentrations of metabolites generated using LAMP1-RFP-3xHA or Tmem192- 3xHA as the lysosomal handle. The R square value shows a high correlation.

Supplementary Figure 2

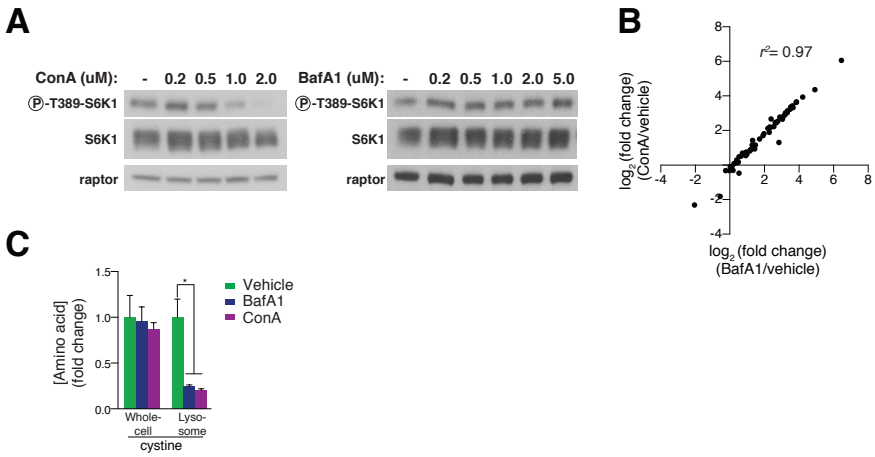

Figure S2

A) Immunoblot analyses of the levels and phosphorylation state of S6K1 in cells treated with increasing doses of Concanamycin A (ConA) or Bafilomycin A1 (BafA1). Raptor was used as loading control.

B) Comparison of fold changes (log_2) in lysosomal metabolite concentrations upon V-ATPase inhibition using 200 nM Bafilomycin A1 (BafA1) or Concanamycin A (ConA) relative to DMSO-treated cells (vehicle) (n=3). R square value shows a high correlation.

C) Fold changes in whole-cell and lysosomal concentrations of cystine in BafA1- or ConA-treated cells relative to vehicle-treated cells (mean ± SEM, n=3, *$p<0.05$).

Two-tailed t tests were used for comparisons between groups.

Supplementary Figure 3

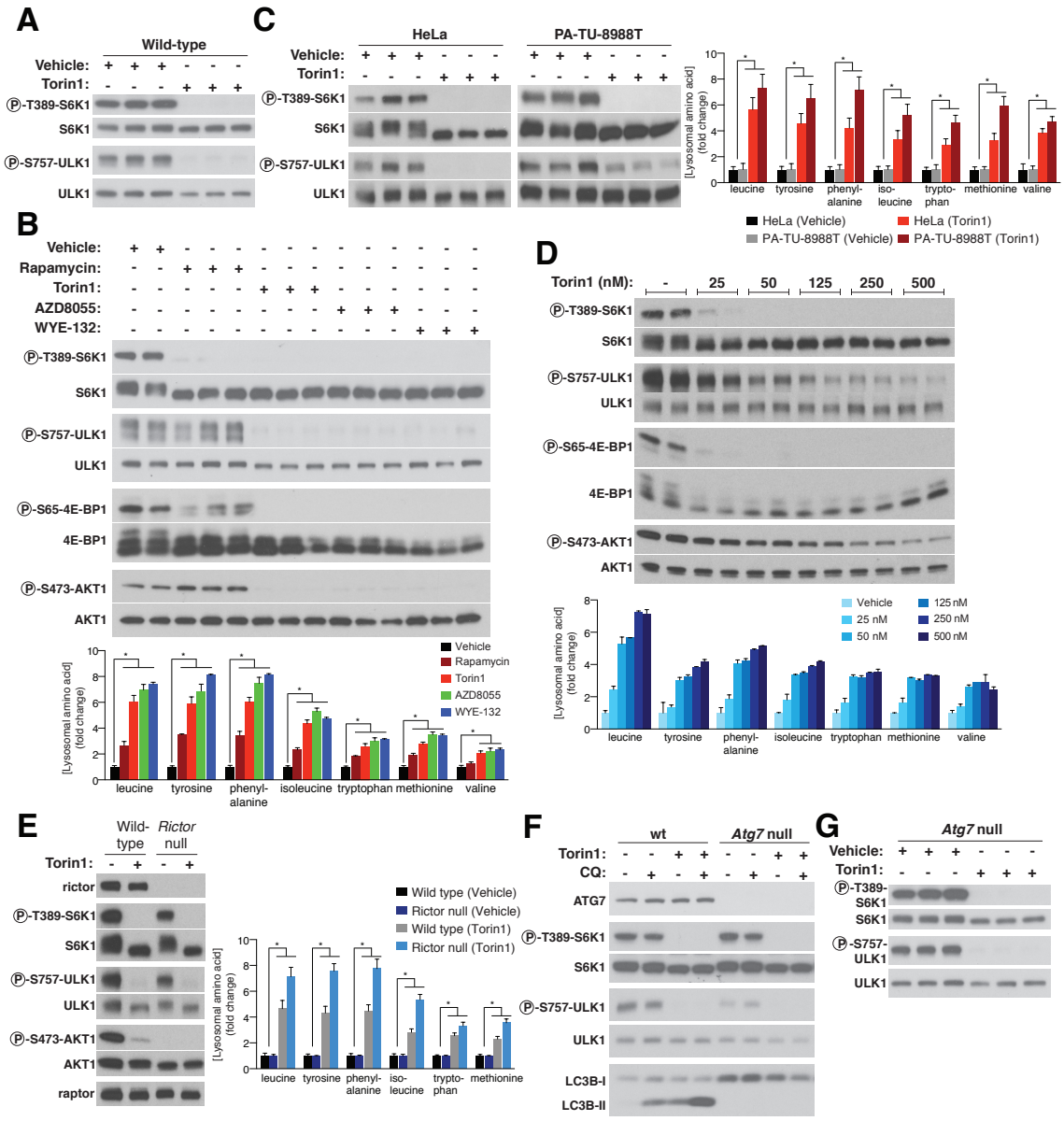

Supplementary Figure 3 (continued)

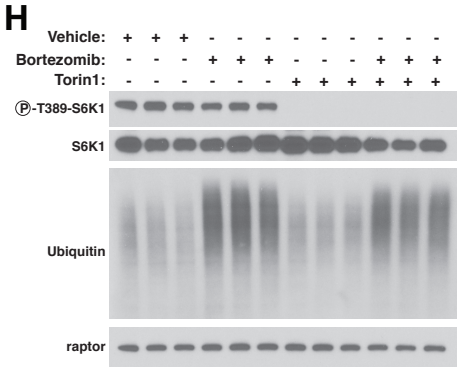

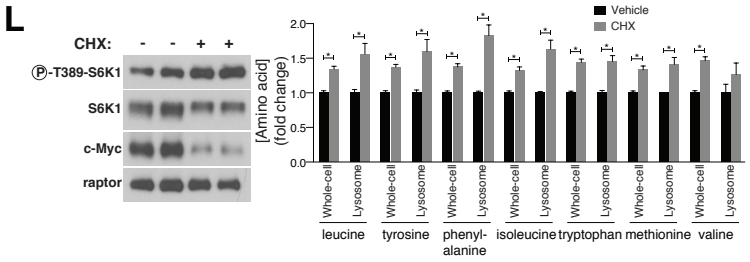

Figure S3

A) Immunoblot analyses for the levels and phosphorylation states of S6 kinase (S6K1) and ULK1 in the wild type cells analyzed in Figure 3C-E.

B) Immunoblot analyses for the levels and phosphorylation states of the indicated proteins in cells treated with DMSO (vehicle), 250 nM Torin1, or 500 nM of Rapamycin, AZD8055, or WYE-132 (top). In the bottom panel, fold changes in the lysosomal concentrations of the indicated amino acids in cells treated with the indicated inhibitors relative to vehicle-treated cells (mean ± SEM, n=3, *p<0.05).

C) Immunoblot analyses of the levels and phosphorylation states of the indicated proteins in HeLa and PA-TU-8988T cells treated with 250 nM Torin1 or DMSO (vehicle) (left). In the right panel, fold changes in the lysosomal concentrations of the indicated amino acids in cells treated with Torin1 relative to vehicle-treated cells (mean ± SEM, n=3, *p<0.05).

D) Immunoblot analyses for the levels and phosphorylation states of the indicated proteins in cells treated with vehicle (DMSO) or escalating doses of Torin1 (top). In the bottom panel, fold changes in lysosomal concentration of the indicated amino acids in cells treated with the indicated Torin1 doses relative to vehicle-treated cells (mean ± SD, n=2 in each dose).

E) Immunoblot analyses for the levels and phosphorylation states of the indicated proteins in wild-type cells expressing control sgRNA and *Rictor*-null HEK-293T cells. In the right panel, fold changes in the lysosomal concentrations of the indicated amino acids in cells treated with 250 nM Torin1 relative to vehicle-treated cells of the same genotype (mean ± SEM, n=3, *p<0.01). In these

experiments the data for valine were unreliable so are not included.

F) Characterization of the *Atg7*-null cells. Cells were treated with 250 nM Torin1 and/or 100 uM Chloroquine (CQ) for 1 hour followed by immunoblot analyses for the levels and phosphorylation states of S6K1 and ULK1, as well as the levels of ATG7, LC3B-I and the lipidated form of LC3B (LC3-B-II).

G) Immunoblot analyses of the levels and phosphorylation states of S6K1 and ULK1 in the *Atg7*-null cells used in figure 3D-E.

H) Immunoblot analyses of the levels and phosphorylation states of S6K1 and ULK1 as well as the levels of total protein ubiquitination in samples used in figure 3F. Raptor was used as loading control.

L) Representative immunoblot analysis of the levels and phosphorylation states of S6K1 and ULK1 as well as the levels of c-Myc (a short-lived protein) in cells treated with 50 ug/ul Cycloheximide or ethanol (vehicle). Raptor was used as loading control. On the right, fold changes in whole-cell and lysosomal concentrations of the indicated amino acids in cells with the same treatments (mean ± SEM, n=3, *$p<0.05$).

Two-tailed t tests were used for comparisons between groups.

Supplementary Figure 4

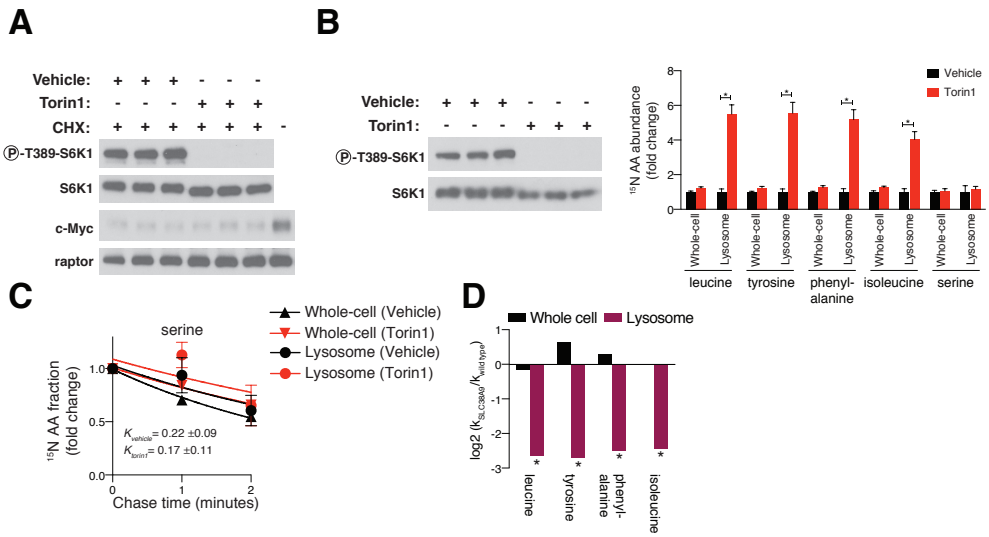

Figure S4

Immunoblot analyses of the levels and phosphorylation states of S6K1 and ULK1 as well as the levels of c-Myc in samples used in figure 4B. Samples not treated with Cycloheximide (CHX) were used as a control for translation inhibition. Raptor was used as loading control.

A) Immunoblot analyses for the levels and phosphorylation states of S6K1 and ULK1 in cells treated with 250 nM Torin1 or DMSO (vehicle). On the right, fold changes in whole-cell and lysosomal abundances of ^{15}N-labeled isotope of the indicated amino acids in cells with the same treatments (mean ± SEM, n=3, *p<0.005). Treatments were as in figure 4B.

B) Fold changes in the fraction of ^{15}N-labeled serine remaining in whole cells (triangle) or lysosomes (circle) as in figure 4C (mean ± SEM, n≥3). Experiment was performed using *Atg7*-null cells.

C) Fold changes ($\log_2$) in rate constants (k) for the decay of the ^{15}N-labeled amino acid from lysosomes in SLC38A9 cells relative to wild-type cells as determined in experiments similar to those in figure 4C. * indicates non-overlapping 95% confidence intervals of the calculated k values between the two genotypes.

Two-tailed t tests were used for comparisons between groups.

CHAPTER 3

Reprinted from Cell press

mTORC1 activator SLC38A9 is required to efflux essential amino acids from lysosomes and use protein as a nutrient

Gregory A. Wyant[1,2,3,4,7], Monther Abu-Remaileh[1,2,3,4,7], Rachel L. Wolfson[1,2,3,4,5], Walter W. Chen[1,2,3,4,5], Elizaveta Freinkman[1,†], Laura V. Danai[3], Matthew G. Vander Heiden[3,4,6], and David M. Sabatini[1,2,3,4,8*]

[1]Whitehead Institute for Biomedical Research and Massachusetts Institute of Technology, Department of Biology, 9 Cambridge Center, Cambridge, Massachusetts 02142, USA. [2]Howard Hughes Medical Institute, Department of Biology, Massachusetts Institute of Technology, Cambridge, Massachusetts 02139, USA. [3]Koch Institute for Integrative Cancer Research and Massachusetts Institute of Technology, Department of Biology, 77 Massachusetts Avenue, Cambridge, Massachusetts 02139, USA. [4]Broad Institute of Harvard and Massachusetts Institute of Technology, 7 Cambridge Center, Cambridge, Massachusetts 02142, USA. [5]Harvard Medical School M.D.-Ph.D. Program, Daniel C. Tosteson Medical Education Center, 260 Longwood Avenue, Boston, MA 02115, USA, [6]Dana-Farber Cancer Institute, Boston, Massachusetts 02115, USA. [†]Current address: Metabolon, Inc., Research Triangle Park, NC 27709, USA. [7]These authors contributed equally to this work. [8]Lead contact.
*Correspondence: sabatini@wi.mit.edu

Experiments in Figure 1 were performed by GAW
Experiments in Figure 2 were performed by GAW with technical assistance from EF
Experiments in Figure 3 were performed by GAW with technical assistance from EF
Experiments in Figure 4 were performed by GAW
Experiments in Figure 5 were performed by GAW with technical assistance from EF
Experiments in Figure 6 were performed by GAW with technical assistance from EF
Experiments in Figure 7 were performed by GAW and RLW with assistance from LVD
Experiments in Figure S1 were performed by GAW
Experiments in Figure S2 were performed by GAW with technical assistance from EF

Experiments in Figure S3 were performed by GAW with technical assistance from EF
Experiments in Figure S4 were performed by GAW
Experiments in Figure S5 were performed by GAW and MAR with technical assistance from EF
Experiments in Figure S6 were performed by GAW
Experiments in Figure S7 were performed by GAW with technical assistance from LVD
Manuscript was written by GAW and DMS with input from MAR

Summary

The mTORC1 kinase is a master growth regulator that senses many environmental cues, including amino acids. Activation of mTORC1 by arginine requires SLC38A9, a poorly understood lysosomal membrane protein with homology to amino acid transporters. Here, we validate that SLC38A9 is an arginine sensor for the mTORC1 pathway, and uncover an unexpectedly central role for SLC38A9 in amino acid homeostasis. SLC38A9 mediates the transport, in an arginine-regulated fashion, of many essential amino acids out of lysosomes, including leucine, which mTORC1 senses through the cytosolic Sestrin proteins. SLC38A9 is necessary for leucine generated via lysosomal proteolysis to exit lysosomes and activate mTORC1. Pancreatic cancer cells, which use macropinocytosed protein as a nutrient source, require SLC38A9 to form tumors. Thus, through SLC38A9, arginine serves as a lysosomal messenger that couples mTORC1 activation to the release from lysosomes of the essential amino acids needed to drive cell growth.

Introduction

The mTORC1 protein kinase controls growth by balancing anabolic processes, such as protein, lipid, and nucleotide synthesis, with catabolic ones like autophagy and proteasomal activity. mTORC1 is deregulated in many diseases, including cancer and epilepsy, and modulates the aging process in multiple model organisms. Diverse environmental cues regulate mTORC1, including growth factors, nutrients, and stress, presenting the challenge of understanding how mTORC1 senses and integrates these various inputs to coordinate a coherent growth program (reviewed in (*15*)).

Amino acids promote the interaction of mTORC1 with the Rag GTPases, which function as heterodimers of RagA or RagB bound to RagC or RagD and localize to the lysosomal surface (*49, 51, 156*). In response to amino acids, the Rag GTPases recruit mTORC1 to the lysosome, where Rheb, a distinct GTPase that directly stimulates the kinase activity of mTORC1, also resides. Growth factors activate Rheb by inducing its inhibitor, the TSC tumor suppressor, to leave the lysosomal surface (*41*). Thus, the Rheb and Rag GTPases form two arms of a co-incidence detector that ensures that mTORC1 activation occurs only when nutrients and growth factors are both present (*49, 51, 157*).

The amino acid sensing pathway is complicated, with several multi-protein complexes regulating the Rag GTPases, each likely serving as the effector of a distinct sensing branch of the pathway. Two such complexes are GATOR1, which is a GTPase activating protein (GAP) for Rag A/B and inhibits the

mTORC1 pathway, and GATOR2, a positive component of the pathway of unknown molecular function that acts upstream of or in parallel to GATOR1 (*55*). The best-characterized amino acid sensors, the Sestrin and CASTOR families of proteins bind cytosolic leucine and arginine, respectively, and interact with and suppress GATOR2 in the absence of their cognate amino acids (*56-62*). A third is the FLCN-FNIP complex, a GAP for Rag C/D, which translocates to the lysosomal surface in the absence of amino acids, but for which the amino acid sensing mechanism is unknown (*64, 158*). Lastly, a fourth is Ragulator, which anchors the Rag GTPase heterodimer to the lysosomal surface and also regulates its nucleotide state (*50*). SLC38A9, a lysosomal 11-transmembrane segment protein with homology to amino acid transporters, binds the Rag GTPase-Ragulator complex and is necessary for the full activation of mTORC1 (*53, 154, 155*).

Here, we validate our previous proposal that SLC38A9 is an arginine sensor for the mTORC1 pathway (*53*), and also uncover, using lysosomal metabolite profiling, a surprisingly important role for SLC38A9 in amino acid homeostasis. SLC38A9 is needed to transport, in an arginine-regulated fashion, most essential amino acids out of lysosomes, including leucine, which mTORC1 senses through the Sestrin1 and Sestrin2 proteins in the cytosol (*56, 57*). In vitro, arginine promotes the leucine transport capacity of SLC38A9 as well as its interaction with the Rag GTPase-Ragulator complex. The transport function of SLC38A9 is required for leucine produced by lysosomal proteolysis to exit lysosomes and activate mTORC1, and for the growth of pancreatic tumors that obtain amino

acids from macropinocytosed extracellular protein. Thus, arginine stimulates SLC38A9 to activate mTORC1 and efflux essential amino acids from lysosomes to the cytosol, where they serve as the building blocks of mass.

Results

A mutant of SLC38A9 that does not interact with arginine cannot signal arginine sufficiency to mTORC1

Two main findings led us to propose that SLC38A9 is a lysosomal arginine sensor for the mTORC1 pathway: the activation of mTORC1 by arginine requires SLC38A9, and SLC38A9 can transport and thus interact with arginine (*53*). To further support this possibility, two predictions should be met: (1) the capacity of SLC38A9 to bind arginine should be necessary for the mTORC1 pathway to sense arginine, and (2) the arginine concentration in lysosomes should be sufficient for SLC38A9 to interact with arginine.

To test the first prediction it was necessary to identify a mutant of SLC38A9 that cannot interact with arginine. SLC38A9 has two distinct regions: an 11-transmembrane segment domain that likely mediates amino acid transport, and an ~110 amino acid cytosolic N-terminal domain that is necessary and sufficient to interact with the Rag GTPase-Ragulator complex (Rag-Ragulator, for short) (*53, 154, 155*). We sought to identify a mutant that does not transport arginine *in vitro* because at the time it was the only known measure of the arginine-SLC38A9 interaction we had. Mutations in residues conserved amongst members of the SLC38 family of transporters did not strongly affect transport by SLC38A9, so we searched for sequence elements in SLC38A9 shared with other

classes of transporters. We noted that a GTS amino acid sequence in transmembrane segment 1 of SLC38A9 aligns with the GSG motif in members of the APC superfamily of Na^+-coupled symporters (e.g., AdiC, CadB, and PotE), which is known to be critical for binding amino acids (Figure 1A) (*159, 160*). Mutation of the threonine in the GTS to tryptophan (T133W) eliminated *in vitro* arginine transport by SLC38A9 without interfering with its capacity to traffic to lysosomes or associate with Ragulator (as detected by its p14 and p18 components) or RagA or RagC in cells (Figure 1B, 1C, and S1). In contrast, the previously identified I68A mutant that does not bind Rag-Ragulator (*53*) transported arginine similarly to wild-type SLC38A9 (Figure 1B and 1C).

To test the capacity of these mutants to activate mTORC1, we took advantage of HEK-293T cells engineered to lack SLC38A9. In these cells activation of mTORC1 in response to arginine, but not leucine, is suppressed, as detected by the phosphorylation of its substrate S6K1 (Figure 1D). In contrast to wild-type SLC38A9, re-constitution of the null cells with either the I68A or T133W mutant did not rescue the arginine-sensing defect (Figure 1E). Thus, to transmit arginine sufficiency to mTORC1, SLC38A9 must interact with Rag-Ragulator as well as arginine, fulfilling the first prediction set forth above.

Arginine, at concentrations found in lysosomes, promotes the interaction of SLC38A9 with Rag-Ragulator

To test the second prediction we measured the lysosomal concentration of arginine using a method we recently developed to rapidly purify lysosomes and

profile their metabolites (Figure 2A). In HEK-293T cells starved of arginine for 50 minutes, lysosomal arginine drops to ~50 uM, and rises to ~250 uM after a 10 minute restimulation with arginine (Figure 2A). Across multiple cell lines, the concentration of arginine in lysosomes ranges from 150-535 uM under nutrient replete conditions (Figure 2A and S2A). These values are much less than the Michaelis constant (K_m) of ~39 mM for arginine in the SLC38A9 transport assay (*53*), suggesting that at the concentrations present in lysosomes arginine does not trigger the transport cycle of SLC38A9, but rather communicates with it through a different mechanism. Indeed, using purified proteins we found that arginine strongly promotes the interaction of full-length SLC38A9 with Rag-Ragulator at a half-maximal concentration of 100-200 uM, which encompasses the arginine concentrations in lysosomes (Figure 2B). At concentrations of 1 mM, no other amino acid besides lysine mimicked the effect of arginine on the interaction of SLC38A9 with Rag-Ragulator (Figure 2C). Consistent with arginine acting directly on SLC38A9, arginine did not promote the interaction of the T133W mutant of SLC38A9 with Rag-Ragulator (Figure 2D). Lastly, the soluble N-terminal domain of SLC38A9 interacted well with Rag-Ragulator (Figure S2C), suggesting that the transmembrane domain of SLC38A9 normally suppresses this interaction in the absence of arginine.

Thus, the arginine-sensitive interaction of SLC38A9 with Rag-Ragulator reveals that SLC38A9 has an affinity for arginine that is compatible with lysosomal arginine concentrations and much better than that indicated by the transport assay. This finding, along with previous data, supports the conclusion

that SLC38A9 can serve as a direct sensor of lysosomal arginine levels for the mTORC1 pathway, and suggests that arginine transport is not required for arginine sensing. That a small molecule binds and regulates a transporter, but is not transported well, is an established concept in transporter biology, perhaps best exemplified by certain ligands of the GAP1 amino acid transporter (*161-164*). Future work, likely requiring high-resolution structures, will be needed to understand how arginine promotes the binding of SLC38A9 to Rag-Ragulator and how this interaction impacts Rag-Ragulator activity.

While lysine also promoted the interaction of SLC38A9 with Rag-Ragulator (Figure 2C), it did so less potently than arginine, acting at a half maximal concentration of 600-700 uM (Figure S2D), which is higher than that of lysine in lysosomes (Figure S2B). Lysine starvation did not appreciably change lysosomal lysine levels but did moderately inhibit mTORC1 signaling and loss of SLC38A9 partially suppressed its re-activation by lysine re-addition (Figure S2B and S2E). These data suggest that lysine is a less physiologically relevant ligand for SLC38A9 than arginine but that SLC38A9 does contribute to the sensing of lysine by the mTORC1 pathway.

Many essential amino acids accumulate in lysosomes lacking SLC38A9

Given its homology to amino acid transporters, it seemed reasonable that, in addition to signaling to mTORC1, SLC38A9 might also regulate lysosomal amino acid levels. To explore this possibility, we measured amino acid concentrations in lysosomes of wild-type and SLC38A9-null HEK-293T cells

(Figure 3A). While loss of SLC38A9 had no effect on whole-cell amino acid levels, it strongly boosted the lysosomal concentrations of several amino acids, including leucine, while having minor effects on arginine levels (Figure 3B). Over-expression of wild-type SLC38A9, but not a control protein, had the opposite effect, reducing the lysosomal concentrations of many of the same amino acids that most increased in lysosomes lacking SLC38A9 (Figure 3C). In subsequent experiments we focused on the set of amino acids affected in both the loss and gain of function experiments, which includes most non-polar, essential amino acids (phenylalanine, leucine, isoleucine, tryptophan, and methionine) as well as tyrosine.

To rule out that SLC38A9 loss increased the lysosomal levels of these amino acids by partially inhibiting mTORC1, we expressed the I68A mutant of SLC38A9 or a variant lacking the N-terminal domain (D110) in the SLC38A9-null cells. Neither binds Rag-Ragulator or rescues mTORC1 signaling (Figure 1C, 1E, S3C, and S3D), but both reversed the increase in lysosomal amino acid concentrations to the same degree as wild-type SLC38A9 (3D and S3B). In contrast, expression of the transport mutant of SLC38A9 (T133W) or just the soluble N-terminal Rag-Ragulator-binding domain of SLC38A9, did not decrease the high concentrations of the amino acid in the lysosomes lacking SLC38A9 (Figure 3D and S3E). Thus, SLC38A9 controls the lysosomal concentrations of most non-polar essential amino acids independently of its effects on mTORC1 signaling.

SLC38A9 is a high affinity transporter for leucine

The simplest explanation for why loss of SLC38A9 causes leucine and the other amino acids to accumulate in lysosomes is that SLC38A9 normally transports them out of lysosomes. In previous work we were unable to assess the capacity of SLC38A9 to transport leucine because the radiolabelled leucine bound non-specifically to the SLC38A9-containing liposomes used in the *in vitro* transport assay (*53*). Using a different lipid composition for the liposomes and a purer preparation of SLC38A9 we developed an improved transport assay for SLC38A9 (see methods). In this new assay the K_m for arginine is ~4 mM, which is substantially lower than the ~39 mM we obtained previously, but still much higher than the ~100-200 uM arginine concentration in lysosomes (Figure 4A and 2A). In contrast, the K_m for leucine in the transport assay is only ~90 uM, which is much lower than that for arginine and compatible with the lysosomal leucine concentrations of 60-80 uM (Figure 4B, 2A, and S4A). The T133W mutant of SLC38A9, which we originally identified because of its inability to transport arginine, was also unable to transport leucine in vitro (Figure S4B), indicating that it is generally defective in amino acid transport. SLC38A9 also transported leucine when the assay was run in the efflux format by placing leucine inside the proteoliposomes (Figure S4C). Lastly, tyrosine, along with isoleucine, valine, and phenylalanine, competed well with the transport of leucine, and tyrosine itself was transported by SLC38A9 as detected using a radiolabelled version (Figure S4D and S4E).

These findings—in intact cells and with purified SLC38A9—suggest that

SLC38A9 is a major lysosomal effluxer for leucine, and likely other amino acids such as tyrosine. In contrast, SLC38A9 loss had only minor effects on lysosomal arginine concentrations, suggesting that SLC38A9 is less important for transporting arginine out of lysosomes. This conclusion is consistent with the high K_m of SLC38A9 for arginine and with previous work identifying a different transporter, PQLC2, as the major effluxer of arginine from lysosomes (*165*). Interestingly, while it has been appreciated that a lysosomal protein must exist for leucine efflux (*166, 167*), no such transporter had been identified. Recent work identified SLC38A7 as an effluxer of glutamine from lysosomes (*168*).

Arginine regulates the lysosomal concentrations of many essential amino acids via SLC38A9

Because arginine regulates the interaction of SLC38A9 with Rag-Ragulator, we asked if it also impacts the capacity of SLC38A9 to transport leucine. Indeed, the addition of 200 uM unlabeled arginine, but not glycine, to the transport assay boosted leucine transport by SLC38A9, increasing its V_{max} for leucine from ~220 to ~470 pmol min^{-1} without significantly affecting its K_m (Figure 4C). Thus, at a concentration that is much below its transport K_m, arginine has two effects on SLC38A9: it stimulates its capacity to transport leucine and to interact with Rag-Ragulator. In the same assay, 200 uM lysine had no effect and it only mildly boosted leucine transport when added at a higher concentration (Figure S4F).

To understand if arginine regulates the transport function of SLC38A9 in cells, we deprived cells of arginine, which lowered its levels in whole cells and in

lysosomes and measured the concentrations of the amino acids that were most affected by loss and gain of SLC38A9 (Figure 5A and S5A). As a control, we starved cells for leucine, which suppressed mTORC1 signaling and induced autophagy (as assessed by LC3B lipidation) to similar extents as arginine deprivation (Figure 5B). Arginine, but not leucine, deprivation increased the lysosomal concentrations of the SLC38A9-regulated amino acids, and 15 minutes of arginine re-addition restored them to normal levels (Figure 5C). Consistent with arginine deprivation not acting through the modulation of mTORC1, it still increased lysosomal amino acid levels in cells lacking GATOR1, which have amino acid-insensitive mTORC1 signaling (Figure S5B and S5C). In contrast, arginine deprivation did not further boost the already high lysosomal levels of the amino acids in cells lacking SLC38A9 or expressing the transport-defective T133W mutant, indicating that arginine acts through the transport function of SLC38A9 (Figure 5D).

As arginine starvation might have effects in intact cells that are hard to control for, we sought to validate the effects of arginine on lysosomal amino acid transport in a cell-free system. We purified lysosomes from wild-type and SLC38A9-null cells and loaded them in vitro with radiolabeled leucine. Stimulation of the lysosomes with arginine, but not several other amino acids, caused the release of ~60% of the radiolabelled leucine in the lysosomes in a fashion that completely depended on SLC38A9 and its transport capacity (Figure 5E and 5F). Stimulation of lysosomes with lysine also promoted the release of radiolabeled leucine, but it did so less potently than arginine (Figure S5D).

Collectively, these data reveal that arginine regulates SLC38A9-mediated transport at the level of the purified protein, in a cell free system, and in intact cells. Thus, arginine signals through SLC38A9 to link two processes: the activation of mTORC1 and the efflux of many essential amino acids from lysosomes. Consistent with arginine being a "lysosomal messenger," in arginine-stimulated cells arginine accumulates in lysosomes before the SLC38A9-regulated amino acids drop in concentration (Figure 5C). Furthermore, arginine is well-established to readily enter lysosomes (*169, 170*), which we verified in intact cells using ^{15}N-arginine and in purified lysosomes using ^{3}H-arginine (Figure S5E). Loss of SLC38A9 does not affect arginine entry into lysosomes (Figure S5F).

SLC38A9 is required for leucine produced via autophagy to activate mTORC1

Because SLC38A9 is important for many essential amino acids to exit lysosomes, we asked if it has a special role in cells that obtain amino acids by degrading proteins in lysosomes, such as cells deprived of free amino acids. Leucine starvation acutely inhibits mTORC1 signaling, but with time the pathway reactivates because cells release endogenous leucine by activating autophagy to increase protein degradation in lysosomes (*150*). In HEK-293T cells, the removal of leucine from the media acutely inhibited mTORC1 signaling, but within 8 hours the pathway reactivated in a fashion that depended on the key autophagy component ATG7 (Figure 6A). Importantly, in the ATG7-null cells, the

addition of free leucine to the cell medium reactivated mTORC1 signaling even after the 8 hours of leucine starvation, indicating that the leucine sensing mechanism remains functional even after long-term leucine deprivation (Figure S6A). Remarkably, loss of SLC38A9, or just its transport activity or ability to interact with Rag-Ragulator, mimicked that of ATG7 loss, and prevented the reactivation of mTORC1 that normally occurs after 8 hours of leucine starvation in the wild-type cells (Figure 6B, 6C, and S6B). As in cells defective for autophagy, free leucine reactivated mTORC1 in the SLC38A9-null cells starved of leucine for 8 hours, showing that the leucine sensing mechanism is also intact in these cells. Importantly, the SLC38A9-null cells do not have a defect in autophagy activation, as assessed by LC3B lipidation (Figure S6C).

An explanation for these findings is that in cells lacking SLC38A9 the leucine produced by lysosomal proteolysis remains trapped in lysosomes. Indeed, while in wild-type cells long-term leucine starvation depletes leucine in whole cells and lysosomes, in cells without SLC38A9, lysosomal leucine levels do not drop despite its significant depletion in whole cells (Figure 6D). Collectively, these results indicate that under long-term leucine starvation, SLC38A9 transports the leucine generated through lysosomal proteolysis into the cytosol, where it reactivates mTORC1 through cytosolic mechanisms.

SLC38A9 is required for macropinocytosed albumin to activate mTORC1 and support cell proliferation and for tumor growth

A faster way than autophagy induction to reactivate mTORC1 in leucine-

starved cells is to feed them extracellular proteins, such as albumin, which are engulfed via macropinocytosis and degraded into amino acids in lysosomes for use in growth-promoting processes (*171, 172*). In leucine-starved HEK-293T cells, which do not have high levels of macropinocytosis (*173*), the addition of 3% albumin to the medium took about 4 hours to moderately restore mTORC1 signaling, an effect that depended on SLC38A9 (Figure S7A).

Because oncogenic Kras signaling activates macropinocytosis, particularly in pancreatic cancer cells (*86, 171, 174, 175*), we undertook similar experiments in murine pancreatic $KRAS^{G12D/+}P53^{-/-}$ tumor cells, and found that albumin fully reactivates mTORC1 in 4 hours in these cells (Figure 7A). As in HEK-293T cells, loss of SLC38A9 suppressed the arginine-induced activation of mTORC1 and prevented albumin from reactivating mTORC1 in leucine deprived cells, an effect that was fully rescued by expression of wild-type SLC38A9, but not the T133W mutant (Figure 7A, 7B, S7B).

Cells with activated Ras can proliferate using albumin as the sole extracellular source of leucine, albeit at a slower rate than cells cultured in media with free leucine (*86, 171*). While the murine pancreatic cancer cells lacking SLC38A9 proliferated normally when cultured in traditional media, they proliferated much more slowly than control cells in media containing albumin as the leucine source (Figure 7C and S7C). We obtained very similar results in two human pancreatic cancer cell lines that also carry oncogenic KRAS (Figure S7D and S7E). In vivo, loss of SLC38A9 or its transport function, strongly inhibited tumor formation by the murine $KRAS^{G12D/+}P53^{-/-}$ cells in an orthotopic allograft

model of pancreatic cancer (Figure 7D and S7F). Immunohistochemical detection of phospho-S6 in tumor sections showed decreased mTORC1 signaling in the absence of SLC38A9 or its transport function (Figure 7E). Thus, under conditions in which cells must obtain amino acids by degrading proteins delivered to lysosomes by macropinocytosis, SLC38A9 plays a key role in the activation of mTORC1 and in cell proliferation and tumor formation.

Discussion

Amino acid sensing by mTORC1 is complicated, with both cytosolic and lysosomal signaling branches transmitting amino acid sufficiency to the Rag GTPases. Here, we used similar criteria as we have for the Sestrin2 and CASTOR1 sensors of cytosolic leucine and arginine, respectively, to establish the lysosomal membrane protein SLC38A9 as a sensor of arginine. While SLC38A9 almost certainly binds arginine in its transmembrane domain, it is very difficult to determine if the sensed arginine comes from the luminal or cytosolic side of the lysosomal membrane and likely both are possible. We favor that the primary function of SLC38A9 is to sense luminal arginine produced in lysosomes through the digestion of proteins, but it is clear that arginine itself can freely enter lysosomes through a transporter (*169, 170*) or via macropinocytosis (see model in Figure 7F). In our previous work, we found that SLC38A9 and the cytosolic sensor CASTOR1 both contribute to arginine sensing by mTORC1 (*53, 61*), and we hypothesize that different cell types use these sensing branches to varying extents, depending on whether they obtain amino acids mostly in the free form or

through the digestion of proteins. Recent work shows that SLC38A9 also has an important role in cholesterol sensing upstream of mTORC1 (*176*).

In addition to its role as an arginine sensor in the mTORC1 pathway, we used a new method for lysosomal metabolomics to make the surprising finding that SLC38A9 is also a major effluxer from lysosomes of leucine and most likely several other non-polar, essential amino acids, as well as tyrosine. Mutants in SLC38A9 can decouple the signaling and amino acid efflux functions of SLC38A9, but normally they are linked and stimulated by arginine. Thus, at the same time that arginine triggers mTORC1 activation it also stimulates the efflux of most essential amino acids from lysosomes, where mTORC1-driven processes, such as protein synthesis, can consume them. Why arginine but not other amino acids would have a “lysosomal messenger” function is unclear. Perhaps it reflects that many of the proteins degraded in lysosomes are ribosomal proteins, which are highly basic because of their RNA binding capacity (*109, 110, 115, 177-179*). In this regard it is interesting that lysine, albeit less potently, also promoted the interaction of SLC38A9 with the Rag-Ragulator complex, and we find that SLC38A9 has a role in signaling lysine levels to mTORC1. Also, perhaps the sensing of arginine at the lysosome evolved from the capacity of its guanidinium group to serve as a storage form of nitrogen in the vacuoles of lower organisms. SLC38A9 loss has minor effects on the concentration of arginine in lysosomes and considering its low affinity for arginine transport, it is unlikely that SLC38A9 has a major role in controlling lysosomal arginine levels, at least in the HEK-293T cells we have studied the most.

The fact that arginine promotes the transport of leucine by SLC38A9 raises the question of how many amino acid binding sites SLC38A9 may have. Previous work suggests that the LeuT, SERT, NET, and DAT transporters, to which SLC38A9 is distantly related, have two small molecule binding sites, one for the transported metabolite and another for a molecule that allosterically regulates transport (*180-185*). Our in vitro data suggest that arginine increases the V_{max} of SLC38A9 for leucine transport without affecting its K_m for leucine. The T133W mutant eliminates the capacity of SLC38A9 to transport leucine *in vitro* and of arginine to induce the conformational change that promotes its interaction with Rag-Ragulator. Thus, this mutant does not have a selective effect on the arginine- or leucine-binding site, suggesting that these sites are either close to each other so that the mutation disrupts both or that the mutation puts SLC38A9 into a "frozen" unresponsive state. To distinguish between these and other possibilities it will be necessary to solve the structure of SLC38A9 in its various conformations. Our attempts to measure the direct binding of amino acids to purified SLC38A9 (rather than using transport into liposomes as a surrogate) have been unsuccessful, likely because its affinity for amino acids is relatively poor compared to that of transporters like LeuT, which has nanomolar affinity for its transport substrates (*181, 186*). It is also important to keep in mind that because we produce SLC38A9 in human cells, it is always possible that proteins that might co-purify with it can impact the activities we measure in vitro.

Pharmacologic inhibitors of mTORC1 have a variety of clinical uses, particularly in diseases with clear hyperactivation of the pathway (reviewed in

(*15*)). Because SLC38A9 has an amino acid binding pocket(s), it may be possible to develop small molecule inhibitors that specifically target the lysosomal amino acid sensing arm of the mTORC1 pathway. These may be of particular value in Ras-driven pancreatic cancers, which depend heavily on macropinocytosis to sustain their amino acid levels, and for cell survival and proliferation (*86, 175*) and which we find require SLC38A9 to form tumors in vivo. In this regard, it is remarkable that SLC38A9 is as necessary as autophagy for protein-derived amino acids to activate mTORC1, revealing SLC38A9 as a key node between lysosomal amino acids and growth control.

Author Contributions

G.A.W. and D.M.S. initiated the project and designed the research plan. G.A.W. performed the experiments and analyzed the data with input from M.A.-R, E.F., and W.W.C. R.L.W. assisted in experimental design and immunohistochemical analyses with G.A.W. E.F. operated the LC/MS equipment. L.V.D. and M.V.G.H. performed the pancreatic cancer cell orthotopic injections. G.A.W and D.M.S. wrote the manuscript and all authors edited it.

Acknowledgments

We thank all members of the Sabatini Laboratory for helpful insights, particularly William Comb, Shuyu Wang, and Jose M. Orozco. We also thank Caroline A. Lewis, Sze Ham Chan, and Tenzin Kunchok from the Whitehead Institute Metabolite Profiling Core Facility. This work was supported by grants from the

NIH (R01 CA103866, R01 CA129105, and R37 AI47389) and Department of Defense (W81XWH-15-1-0230) to D.M.S., from the Department of Defense (W81XWH-15-1-0337) to E.F. Fellowship support was provided by the EMBO Long-Term Fellowship to M.A.-R, NIH to R.L.W. (T32 GM007753 and F30 CA189333), an NIH postdoctoral fellowship (F32CA210421) to L.V.D., and the National Defense Science & Engineering Graduate Fellowship (NDSEG) Program to G.A.W. M.V.G.H. acknowledges support from the Lustgarten Foundation, SU2C, the NCI (R01 CA168653, P30CA1405141), and a Faculty Scholars Award from HHMI. D.M.S. is an investigator of the Howard Hughes Medical Institute.

References

1. R. T. Abraham, G. J. Wiederrecht, Immunopharmacology of rapamycin. *Annual review of immunology* **14**, 483-510 (1996)10.1146/annurev.immunol.14.1.483).
2. C. P. Eng, S. N. Sehgal, C. Vezina, Activity of rapamycin (AY-22,989) against transplanted tumors. *The Journal of antibiotics* **37**, 1231-1237 (1984); published online EpubOct (
3. J. Heitman, N. R. Movva, M. N. Hall, Targets for cell cycle arrest by the immunosuppressant rapamycin in yeast. *Science* **253**, 905-909 (1991); published online EpubAug 23 (
4. Y. Koltin, L. Faucette, D. J. Bergsma, M. A. Levy, R. Cafferkey, P. L. Koser, R. K. Johnson, G. P. Livi, Rapamycin sensitivity in Saccharomyces cerevisiae is mediated by a peptidyl-prolyl cis-trans isomerase related to human FK506-binding protein. *Molecular and cellular biology* **11**, 1718-1723 (1991); published online EpubMar (
5. S. B. Helliwell, P. Wagner, J. Kunz, M. Deuter-Reinhard, R. Henriquez, M. N. Hall, TOR1 and TOR2 are structurally and functionally similar but not identical phosphatidylinositol kinase homologues in yeast. *Molecular biology of the cell* **5**, 105-118 (1994); published online EpubJan (
6. D. M. Sabatini, H. Erdjument-Bromage, M. Lui, P. Tempst, S. H. Snyder, RAFT1: a mammalian protein that binds to FKBP12 in a rapamycin-dependent fashion and is homologous to yeast TORs. *Cell* **78**, 35-43 (1994); published online EpubJul 15 (

7. E. J. Brown, M. W. Albers, T. B. Shin, K. Ichikawa, C. T. Keith, W. S. Lane, S. L. Schreiber, A mammalian protein targeted by G1-arresting rapamycin-receptor complex. *Nature* **369**, 756-758 (1994); published online EpubJun 30 (10.1038/369756a0).
8. C. J. Sabers, M. M. Martin, G. J. Brunn, J. M. Williams, F. J. Dumont, G. Wiederrecht, R. T. Abraham, Isolation of a protein target of the FKBP12-rapamycin complex in mammalian cells. *The Journal of biological chemistry* **270**, 815-822 (1995); published online EpubJan 13 (
9. S. Sengupta, T. R. Peterson, D. M. Sabatini, Regulation of the mTOR complex 1 pathway by nutrients, growth factors, and stress. *Molecular cell* **40**, 310-322 (2010); published online EpubOct 22 (10.1016/j.molcel.2010.09.026).
10. P. Liu, W. Gan, Y. R. Chin, K. Ogura, J. Guo, J. Zhang, B. Wang, J. Blenis, L. C. Cantley, A. Toker, B. Su, W. Wei, PtdIns(3,4,5)P3-Dependent Activation of the mTORC2 Kinase Complex. *Cancer discovery* **5**, 1194-1209 (2015); published online EpubNov (10.1158/2159-8290.CD-15-0460).
11. Y. Sancak, C. C. Thoreen, T. R. Peterson, R. A. Lindquist, S. A. Kang, E. Spooner, S. A. Carr, D. M. Sabatini, PRAS40 is an insulin-regulated inhibitor of the mTORC1 protein kinase. *Molecular cell* **25**, 903-915 (2007); published online EpubMar 23 (10.1016/j.molcel.2007.03.003).
12. D. H. Kim, D. D. Sarbassov, S. M. Ali, J. E. King, R. R. Latek, H. Erdjument-Bromage, P. Tempst, D. M. Sabatini, mTOR interacts with raptor to form a nutrient-sensitive complex that signals to the cell growth machinery. *Cell* **110**, 163-175 (2002); published online EpubJul 26 (
13. D. A. Guertin, D. M. Stevens, C. C. Thoreen, A. A. Burds, N. Y. Kalaany, J. Moffat, M. Brown, K. J. Fitzgerald, D. M. Sabatini, Ablation in mice of the mTORC components raptor, rictor, or mLST8 reveals that mTORC2 is required for signaling to Akt-FOXO and PKCalpha, but not S6K1. *Developmental cell* **11**, 859-871 (2006); published online EpubDec (10.1016/j.devcel.2006.10.007).
14. T. R. Peterson, M. Laplante, C. C. Thoreen, Y. Sancak, S. A. Kang, W. M. Kuehl, N. S. Gray, D. M. Sabatini, DEPTOR is an mTOR inhibitor frequently overexpressed in multiple myeloma cells and required for their survival. *Cell* **137**, 873-886 (2009); published online EpubMay 29 (10.1016/j.cell.2009.03.046).
15. R. A. Saxton, D. M. Sabatini, mTOR Signaling in Growth, Metabolism, and Disease. *Cell* **168**, 960-976 (2017); published online EpubMar 09 (10.1016/j.cell.2017.02.004).
16. C. C. Thoreen, L. Chantranupong, H. R. Keys, T. Wang, N. S. Gray, D. M. Sabatini, A unifying model for mTORC1-mediated regulation of mRNA translation. *Nature* **485**, 109-113 (2012); published online EpubMay 2 (10.1038/nature11083).
17. C. J. Kuo, J. Chung, D. F. Fiorentino, W. M. Flanagan, J. Blenis, G. R. Crabtree, Rapamycin selectively inhibits interleukin-2 activation of p70 S6 kinase. *Nature* **358**, 70-73 (1992); published online EpubJul 2 (10.1038/358070a0).
18. J. Chung, C. J. Kuo, G. R. Crabtree, J. Blenis, Rapamycin-FKBP specifically blocks growth-dependent activation of and signaling by the 70 kd S6 protein kinases. *Cell* **69**, 1227-1236 (1992); published online EpubJun 26 (
19. L. Beretta, A. C. Gingras, Y. V. Svitkin, M. N. Hall, N. Sonenberg, Rapamycin blocks the phosphorylation of 4E-BP1 and inhibits cap-dependent initiation of translation. *The EMBO journal* **15**, 658-664 (1996); published online EpubFeb 1 (

20. B. Magnuson, B. Ekim, D. C. Fingar, Regulation and function of ribosomal protein S6 kinase (S6K) within mTOR signalling networks. *The Biochemical journal* **441**, 1-21 (2012); published online EpubJan 1 (10.1042/BJ20110892).
21. M. Pende, S. H. Um, V. Mieulet, M. Sticker, V. L. Goss, J. Mestan, M. Mueller, S. Fumagalli, S. C. Kozma, G. Thomas, S6K1(-/-)/S6K2(-/-) mice exhibit perinatal lethality and rapamycin-sensitive 5'-terminal oligopyrimidine mRNA translation and reveal a mitogen-activated protein kinase-dependent S6 kinase pathway. *Molecular and cellular biology* **24**, 3112-3124 (2004); published online EpubApr (
22. M. K. Holz, B. A. Ballif, S. P. Gygi, J. Blenis, mTOR and S6K1 mediate assembly of the translation preinitiation complex through dynamic protein interchange and ordered phosphorylation events. *Cell* **123**, 569-580 (2005); published online EpubNov 18 (10.1016/j.cell.2005.10.024).
23. X. M. Ma, J. Blenis, Molecular mechanisms of mTOR-mediated translational control. *Nature reviews. Molecular cell biology* **10**, 307-318 (2009); published online EpubMay (10.1038/nrm2672).
24. C. Mayer, J. Zhao, X. Yuan, I. Grummt, mTOR-dependent activation of the transcription factor TIF-IA links rRNA synthesis to nutrient availability. *Genes & development* **18**, 423-434 (2004); published online EpubFeb 15 (10.1101/gad.285504).
25. B. Shor, J. Wu, Q. Shakey, L. Toral-Barza, C. Shi, M. Follettie, K. Yu, Requirement of the mTOR kinase for the regulation of Maf1 phosphorylation and control of RNA polymerase III-dependent transcription in cancer cells. *The Journal of biological chemistry* **285**, 15380-15392 (2010); published online EpubMay 14 (10.1074/jbc.M109.071639).
26. K. Duvel, J. L. Yecies, S. Menon, P. Raman, A. I. Lipovsky, A. L. Souza, E. Triantafellow, Q. Ma, R. Gorski, S. Cleaver, M. G. Vander Heiden, J. P. MacKeigan, P. M. Finan, C. B. Clish, L. O. Murphy, B. D. Manning, Activation of a metabolic gene regulatory network downstream of mTOR complex 1. *Molecular cell* **39**, 171-183 (2010); published online EpubJul 30 (10.1016/j.molcel.2010.06.022).
27. S. Li, M. S. Brown, J. L. Goldstein, Bifurcation of insulin signaling pathway in rat liver: mTORC1 required for stimulation of lipogenesis, but not inhibition of gluconeogenesis. *Proceedings of the National Academy of Sciences of the United States of America* **107**, 3441-3446 (2010); published online EpubFeb 23 (10.1073/pnas.0914798107).
28. T. Porstmann, C. R. Santos, B. Griffiths, M. Cully, M. Wu, S. Leevers, J. R. Griffiths, Y. L. Chung, A. Schulze, SREBP activity is regulated by mTORC1 and contributes to Akt-dependent cell growth. *Cell metabolism* **8**, 224-236 (2008); published online EpubSep (10.1016/j.cmet.2008.07.007).
29. T. R. Peterson, S. S. Sengupta, T. E. Harris, A. E. Carmack, S. A. Kang, E. Balderas, D. A. Guertin, K. L. Madden, A. E. Carpenter, B. N. Finck, D. M. Sabatini, mTOR complex 1 regulates lipin 1 localization to control the SREBP pathway. *Cell* **146**, 408-420 (2011); published online EpubAug 5 (10.1016/j.cell.2011.06.034).
30. I. Ben-Sahra, G. Hoxhaj, S. J. H. Ricoult, J. M. Asara, B. D. Manning, mTORC1 induces purine synthesis through control of the mitochondrial tetrahydrofolate cycle. *Science* **351**, 728-733 (2016); published online EpubFeb 12 (10.1126/science.aad0489).

31. S. J. Ricoult, J. L. Yecies, I. Ben-Sahra, B. D. Manning, Oncogenic PI3K and K-Ras stimulate de novo lipid synthesis through mTORC1 and SREBP. *Oncogene* **35**, 1250-1260 (2016); published online EpubMar 10 (10.1038/onc.2015.179).
32. A. M. Robitaille, S. Christen, M. Shimobayashi, M. Cornu, L. L. Fava, S. Moes, C. Prescianotto-Baschong, U. Sauer, P. Jenoe, M. N. Hall, Quantitative phosphoproteomics reveal mTORC1 activates de novo pyrimidine synthesis. *Science* **339**, 1320-1323 (2013); published online EpubMar 15 (10.1126/science.1228771).
33. N. Mizushima, M. Komatsu, Autophagy: renovation of cells and tissues. *Cell* **147**, 728-741 (2011); published online EpubNov 11 (10.1016/j.cell.2011.10.026).
34. I. G. Ganley, H. Lam du, J. Wang, X. Ding, S. Chen, X. Jiang, ULK1.ATG13.FIP200 complex mediates mTOR signaling and is essential for autophagy. *The Journal of biological chemistry* **284**, 12297-12305 (2009); published online EpubMay 01 (10.1074/jbc.M900573200).
35. C. H. Jung, C. B. Jun, S. H. Ro, Y. M. Kim, N. M. Otto, J. Cao, M. Kundu, D. H. Kim, ULK-Atg13-FIP200 complexes mediate mTOR signaling to the autophagy machinery. *Molecular biology of the cell* **20**, 1992-2003 (2009); published online EpubApr (10.1091/mbc.E08-12-1249).
36. J. Zhao, A. L. Goldberg, Coordinate regulation of autophagy and the ubiquitin proteasome system by MTOR. *Autophagy* **12**, 1967-1970 (2016); published online EpubOct 02 (10.1080/15548627.2016.1205770).
37. A. A. Alfaiz, L. Micale, B. Mandriani, B. Augello, M. T. Pellico, J. Chrast, I. Xenarios, L. Zelante, G. Merla, A. Reymond, TBC1D7 mutations are associated with intellectual disability, macrocrania, patellar dislocation, and celiac disease. *Human mutation* **35**, 447-451 (2014); published online EpubApr (10.1002/humu.22529).
38. S. M. Goorden, M. Hoogeveen-Westerveld, C. Cheng, G. M. van Woerden, M. Mozaffari, L. Post, H. J. Duckers, M. Nellist, Y. Elgersma, Rheb is essential for murine development. *Molecular and cellular biology* **31**, 1672-1678 (2011); published online EpubApr (10.1128/MCB.00985-10).
39. K. Inoki, Y. Li, T. Xu, K. L. Guan, Rheb GTPase is a direct target of TSC2 GAP activity and regulates mTOR signaling. *Genes & development* **17**, 1829-1834 (2003); published online EpubAug 1 (10.1101/gad.1110003).
40. K. Inoki, T. Zhu, K. L. Guan, TSC2 mediates cellular energy response to control cell growth and survival. *Cell* **115**, 577-590 (2003); published online EpubNov 26 (
41. S. Menon, C. C. Dibble, G. Talbott, G. Hoxhaj, A. J. Valvezan, H. Takahashi, L. C. Cantley, B. D. Manning, Spatial control of the TSC complex integrates insulin and nutrient regulation of mTORC1 at the lysosome. *Cell* **156**, 771-785 (2014); published online EpubFeb 13 (10.1016/j.cell.2013.11.049).
42. K. Inoki, Y. Li, T. Zhu, J. Wu, K. L. Guan, TSC2 is phosphorylated and inhibited by Akt and suppresses mTOR signalling. *Nature cell biology* **4**, 648-657 (2002); published online EpubSep (10.1038/ncb839).
43. D. D. Sarbassov, D. A. Guertin, S. M. Ali, D. M. Sabatini, Phosphorylation and regulation of Akt/PKB by the rictor-mTOR complex. *Science* **307**, 1098-1101 (2005); published online EpubFeb 18 (10.1126/science.1106148).
44. R. J. Shaw, L. C. Cantley, Ras, PI(3)K and mTOR signalling controls tumour cell growth. *Nature* **441**, 424-430 (2006); published online EpubMay 25 (10.1038/nature04869).

45. D. M. Gwinn, D. B. Shackelford, D. F. Egan, M. M. Mihaylova, A. Mery, D. S. Vasquez, B. E. Turk, R. J. Shaw, AMPK phosphorylation of raptor mediates a metabolic checkpoint. *Molecular cell* **30**, 214-226 (2008); published online EpubApr 25 (10.1016/j.molcel.2008.03.003).
46. A. Efeyan, R. Zoncu, S. Chang, I. Gumper, H. Snitkin, R. L. Wolfson, O. Kirak, D. D. Sabatini, D. M. Sabatini, Regulation of mTORC1 by the Rag GTPases is necessary for neonatal autophagy and survival. *Nature* **493**, 679-683 (2013); published online EpubJan 31 (10.1038/nature11745).
47. J. Brugarolas, K. Lei, R. L. Hurley, B. D. Manning, J. H. Reiling, E. Hafen, L. A. Witters, L. W. Ellisen, W. G. Kaelin, Jr., Regulation of mTOR function in response to hypoxia by REDD1 and the TSC1/TSC2 tumor suppressor complex. *Genes & development* **18**, 2893-2904 (2004); published online EpubDec 1 (10.1101/gad.1256804).
48. C. H. Lee, K. Inoki, M. Karbowniczek, E. Petroulakis, N. Sonenberg, E. P. Henske, K. L. Guan, Constitutive mTOR activation in TSC mutants sensitizes cells to energy starvation and genomic damage via p53. *The EMBO journal* **26**, 4812-4823 (2007); published online EpubNov 28 (10.1038/sj.emboj.7601900).
49. Y. Sancak, T. R. Peterson, Y. D. Shaul, R. A. Lindquist, C. C. Thoreen, L. Bar-Peled, D. M. Sabatini, The Rag GTPases bind raptor and mediate amino acid signaling to mTORC1. *Science* **320**, 1496-1501 (2008); published online EpubJun 13 (10.1126/science.1157535).
50. L. Bar-Peled, L. D. Schweitzer, R. Zoncu, D. M. Sabatini, Ragulator is a GEF for the rag GTPases that signal amino acid levels to mTORC1. *Cell* **150**, 1196-1208 (2012); published online EpubSep 14 (10.1016/j.cell.2012.07.032).
51. Y. Sancak, L. Bar-Peled, R. Zoncu, A. L. Markhard, S. Nada, D. M. Sabatini, Ragulator-Rag complex targets mTORC1 to the lysosomal surface and is necessary for its activation by amino acids. *Cell* **141**, 290-303 (2010); published online EpubApr 16 (10.1016/j.cell.2010.02.024).
52. R. Zoncu, L. Bar-Peled, A. Efeyan, S. Wang, Y. Sancak, D. M. Sabatini, mTORC1 senses lysosomal amino acids through an inside-out mechanism that requires the vacuolar H(+)-ATPase. *Science* **334**, 678-683 (2011); published online EpubNov 04 (10.1126/science.1207056).
53. S. Wang, Z. Y. Tsun, R. L. Wolfson, K. Shen, G. A. Wyant, M. E. Plovanich, E. D. Yuan, T. D. Jones, L. Chantranupong, W. Comb, T. Wang, L. Bar-Peled, R. Zoncu, C. Straub, C. Kim, J. Park, B. L. Sabatini, D. M. Sabatini, Metabolism. Lysosomal amino acid transporter SLC38A9 signals arginine sufficiency to mTORC1. *Science* **347**, 188-194 (2015); published online EpubJan 09 (10.1126/science.1257132).
54. R. L. Wolfson, L. Chantranupong, G. A. Wyant, X. Gu, J. M. Orozco, K. Shen, K. J. Condon, S. Petri, J. Kedir, S. M. Scaria, M. Abu-Remaileh, W. N. Frankel, D. M. Sabatini, KICSTOR recruits GATOR1 to the lysosome and is necessary for nutrients to regulate mTORC1. *Nature* **543**, 438-442 (2017); published online EpubMar 16 (10.1038/nature21423).
55. L. Bar-Peled, L. Chantranupong, A. D. Cherniack, W. W. Chen, K. A. Ottina, B. C. Grabiner, E. D. Spear, S. L. Carter, M. Meyerson, D. M. Sabatini, A Tumor suppressor complex with GAP activity for the Rag GTPases that signal amino acid sufficiency to mTORC1. *Science* **340**, 1100-1106 (2013); published online EpubMay 31 (10.1126/science.1232044).

56. R. L. Wolfson, L. Chantranupong, R. A. Saxton, K. Shen, S. M. Scaria, J. R. Cantor, D. M. Sabatini, Sestrin2 is a leucine sensor for the mTORC1 pathway. *Science* **351**, 43-48 (2016); published online EpubJan 01 (10.1126/science.aab2674).
57. R. A. Saxton, K. E. Knockenhauer, R. L. Wolfson, L. Chantranupong, M. E. Pacold, T. Wang, T. U. Schwartz, D. M. Sabatini, Structural basis for leucine sensing by the Sestrin2-mTORC1 pathway. *Science* **351**, 53-58 (2016); published online EpubJan 01 (10.1126/science.aad2087).
58. J. S. Kim, S. H. Ro, M. Kim, H. W. Park, I. A. Semple, H. Park, U. S. Cho, W. Wang, K. L. Guan, M. Karin, J. H. Lee, Sestrin2 inhibits mTORC1 through modulation of GATOR complexes. *Scientific reports* **5**, 9502 (2015); published online EpubMar 30 (10.1038/srep09502).
59. A. Parmigiani, A. Nourbakhsh, B. Ding, W. Wang, Y. C. Kim, K. Akopiants, K. L. Guan, M. Karin, A. V. Budanov, Sestrins inhibit mTORC1 kinase activation through the GATOR complex. *Cell reports* **9**, 1281-1291 (2014); published online EpubNov 20 (10.1016/j.celrep.2014.10.019).
60. L. Chantranupong, R. L. Wolfson, J. M. Orozco, R. A. Saxton, S. M. Scaria, L. Bar-Peled, E. Spooner, M. Isasa, S. P. Gygi, D. M. Sabatini, The Sestrins interact with GATOR2 to negatively regulate the amino-acid-sensing pathway upstream of mTORC1. *Cell reports* **9**, 1-8 (2014); published online EpubOct 09 (10.1016/j.celrep.2014.09.014).
61. L. Chantranupong, S. M. Scaria, R. A. Saxton, M. P. Gygi, K. Shen, G. A. Wyant, T. Wang, J. W. Harper, S. P. Gygi, D. M. Sabatini, The CASTOR Proteins Are Arginine Sensors for the mTORC1 Pathway. *Cell* **165**, 153-164 (2016); published online EpubMar 24 (10.1016/j.cell.2016.02.035).
62. R. A. Saxton, L. Chantranupong, K. E. Knockenhauer, T. U. Schwartz, D. M. Sabatini, Mechanism of arginine sensing by CASTOR1 upstream of mTORC1. *Nature* **536**, 229-233 (2016); published online EpubAug 11 (10.1038/nature19079).
63. X. Gu, J. M. Orozco, R. A. Saxton, K. J. Condon, G. Y. Liu, P. A. Krawczyk, S. M. Scaria, J. W. Harper, S. P. Gygi, D. M. Sabatini, SAMTOR is an S-adenosylmethionine sensor for the mTORC1 pathway. *Science* **358**, 813-818 (2017); published online EpubNov 10 (10.1126/science.aao3265).
64. Z. Y. Tsun, L. Bar-Peled, L. Chantranupong, R. Zoncu, T. Wang, C. Kim, E. Spooner, D. M. Sabatini, The folliculin tumor suppressor is a GAP for the RagC/D GTPases that signal amino acid levels to mTORC1. *Molecular cell* **52**, 495-505 (2013); published online EpubNov 21 (10.1016/j.molcel.2013.09.016).
65. J. L. Jewell, Y. C. Kim, R. C. Russell, F. X. Yu, H. W. Park, S. W. Plouffe, V. S. Tagliabracci, K. L. Guan, Metabolism. Differential regulation of mTORC1 by leucine and glutamine. *Science* **347**, 194-198 (2015); published online EpubJan 9 (10.1126/science.1259472).
66. Q. Venot, T. Blanc, S. H. Rabia, L. Berteloot, S. Ladraa, J. P. Duong, E. Blanc, S. C. Johnson, C. Hoguin, O. Boccara, S. Sarnacki, N. Boddaert, S. Pannier, F. Martinez, S. Magassa, J. Yamaguchi, B. Knebelmann, P. Merville, N. Grenier, D. Joly, V. Cormier-Daire, C. Michot, C. Bole-Feysot, A. Picard, V. Soupre, S. Lyonnet, J. Sadoine, L. Slimani, C. Chaussain, C. Laroche-Raynaud, L. Guibaud, C. Broissand, J. Amiel, C. Legendre, F. Terzi, G. Canaud, Targeted therapy in patients with PIK3CA-related overgrowth syndrome. *Nature* **558**, 540-546 (2018); published online EpubJun (10.1038/s41586-018-0217-9).

67. D. J. Kwiatkowski, B. D. Manning, Molecular basis of giant cells in tuberous sclerosis complex. *The New England journal of medicine* **371**, 778-780 (2014); published online EpubAug 21 (10.1056/NEJMcibr1406613).
68. N. Wagle, B. C. Grabiner, E. M. Van Allen, E. Hodis, S. Jacobus, J. G. Supko, M. Stewart, T. K. Choueiri, L. Gandhi, J. M. Cleary, A. A. Elfiky, M. E. Taplin, E. C. Stack, S. Signoretti, M. Loda, G. I. Shapiro, D. M. Sabatini, E. S. Lander, S. B. Gabriel, P. W. Kantoff, L. A. Garraway, J. E. Rosenberg, Activating mTOR mutations in a patient with an extraordinary response on a phase I trial of everolimus and pazopanib. *Cancer discovery* **4**, 546-553 (2014); published online EpubMay (10.1158/2159-8290.CD-13-0353).
69. B. C. Grabiner, V. Nardi, K. Birsoy, R. Possemato, K. Shen, S. Sinha, A. Jordan, A. H. Beck, D. M. Sabatini, A diverse array of cancer-associated MTOR mutations are hyperactivating and can predict rapamycin sensitivity. *Cancer discovery* **4**, 554-563 (2014); published online EpubMay (10.1158/2159-8290.CD-13-0929).
70. N. Wagle, B. C. Grabiner, E. M. Van Allen, A. Amin-Mansour, A. Taylor-Weiner, M. Rosenberg, N. Gray, J. A. Barletta, Y. Guo, S. J. Swanson, D. T. Ruan, G. J. Hanna, R. I. Haddad, G. Getz, D. J. Kwiatkowski, S. L. Carter, D. M. Sabatini, P. A. Janne, L. A. Garraway, J. H. Lorch, Response and acquired resistance to everolimus in anaplastic thyroid cancer. *The New England journal of medicine* **371**, 1426-1433 (2014); published online EpubOct 9 (10.1056/NEJMoa1403352).
71. J. Okosun, R. L. Wolfson, J. Wang, S. Araf, L. Wilkins, B. M. Castellano, L. Escudero-Ibarz, A. F. Al Seraihi, J. Richter, S. H. Bernhart, A. Efeyan, S. Iqbal, J. Matthews, A. Clear, J. A. Guerra-Assuncao, C. Bodor, H. Quentmeier, C. Mansbridge, P. Johnson, A. Davies, J. C. Strefford, G. Packham, S. Barrans, A. Jack, M. Q. Du, M. Calaminici, T. A. Lister, R. Auer, S. Montoto, J. G. Gribben, R. Siebert, C. Chelala, R. Zoncu, D. M. Sabatini, J. Fitzgibbon, Recurrent mTORC1-activating RRAGC mutations in follicular lymphoma. *Nature genetics* **48**, 183-188 (2016); published online EpubFeb (10.1038/ng.3473).
72. P. B. Crino, K. L. Nathanson, E. P. Henske, The tuberous sclerosis complex. *The New England journal of medicine* **355**, 1345-1356 (2006); published online EpubSep 28 (10.1056/NEJMra055323).
73. J. J. Bissler, J. C. Kingswood, E. Radzikowska, B. A. Zonnenberg, M. Frost, E. Belousova, M. Sauter, N. Nonomura, S. Brakemeier, P. J. de Vries, V. H. Whittemore, D. Chen, T. Sahmoud, G. Shah, J. Lincy, D. Lebwohl, K. Budde, Everolimus for angiomyolipoma associated with tuberous sclerosis complex or sporadic lymphangioleiomyomatosis (EXIST-2): a multicentre, randomised, double-blind, placebo-controlled trial. *Lancet* **381**, 817-824 (2013); published online EpubMar 9 (10.1016/S0140-6736(12)61767-X).
74. K. E. O'Reilly, F. Rojo, Q. B. She, D. Solit, G. B. Mills, D. Smith, H. Lane, F. Hofmann, D. J. Hicklin, D. L. Ludwig, J. Baselga, N. Rosen, mTOR inhibition induces upstream receptor tyrosine kinase signaling and activates Akt. *Cancer research* **66**, 1500-1508 (2006); published online EpubFeb 1 (10.1158/0008-5472.CAN-05-2925).
75. C. C. Thoreen, S. A. Kang, J. W. Chang, Q. Liu, J. Zhang, Y. Gao, L. J. Reichling, T. Sim, D. M. Sabatini, N. S. Gray, An ATP-competitive mammalian target of rapamycin inhibitor reveals rapamycin-resistant functions of mTORC1. *The Journal of biological chemistry* **284**, 8023-8032 (2009); published online EpubMar 20 (10.1074/jbc.M900301200).

76. D. W. Lamming, L. Ye, P. Katajisto, M. D. Goncalves, M. Saitoh, D. M. Stevens, J. G. Davis, A. B. Salmon, A. Richardson, R. S. Ahima, D. A. Guertin, D. M. Sabatini, J. A. Baur, Rapamycin-induced insulin resistance is mediated by mTORC2 loss and uncoupled from longevity. *Science* **335**, 1638-1643 (2012); published online EpubMar 30 (10.1126/science.1215135).
77. R. M. Perera, R. Zoncu, The Lysosome as a Regulatory Hub. *Annual review of cell and developmental biology* **32**, 223-253 (2016); published online EpubOct 6 (10.1146/annurev-cellbio-111315-125125).
78. C. De Duve, R. Wattiaux, Functions of lysosomes. *Annual review of physiology* **28**, 435-492 (1966)10.1146/annurev.ph.28.030166.002251).
79. J. A. Mindell, Lysosomal acidification mechanisms. *Annual review of physiology* **74**, 69-86 (2012)10.1146/annurev-physiol-012110-142317).
80. P. Saftig, J. Klumperman, Lysosome biogenesis and lysosomal membrane proteins: trafficking meets function. *Nature reviews. Molecular cell biology* **10**, 623-635 (2009); published online EpubSep (10.1038/nrm2745).
81. F. M. Platt, B. Boland, A. C. van der Spoel, The cell biology of disease: lysosomal storage disorders: the cellular impact of lysosomal dysfunction. *The Journal of cell biology* **199**, 723-734 (2012); published online EpubNov 26 (10.1083/jcb.201208152).
82. E. D. Carstea, J. A. Morris, K. G. Coleman, S. K. Loftus, D. Zhang, C. Cummings, J. Gu, M. A. Rosenfeld, W. J. Pavan, D. B. Krizman, J. Nagle, M. H. Polymeropoulos, S. L. Sturley, Y. A. Ioannou, M. E. Higgins, M. Comly, A. Cooney, A. Brown, C. R. Kaneski, E. J. Blanchette-Mackie, N. K. Dwyer, E. B. Neufeld, T. Y. Chang, L. Liscum, J. F. Strauss, 3rd, K. Ohno, M. Zeigler, R. Carmi, J. Sokol, D. Markie, R. R. O'Neill, O. P. van Diggelen, M. Elleder, M. C. Patterson, R. O. Brady, M. T. Vanier, P. G. Pentchev, D. A. Tagle, Niemann-Pick C1 disease gene: homology to mediators of cholesterol homeostasis. *Science* **277**, 228-231 (1997); published online EpubJul 11 (
83. G. Bultron, K. Kacena, D. Pearson, M. Boxer, R. Yang, S. Sathe, G. Pastores, P. K. Mistry, The risk of Parkinson's disease in type 1 Gaucher disease. *Journal of inherited metabolic disease* **33**, 167-173 (2010); published online EpubApr (10.1007/s10545-010-9055-0).
84. J. Aharon-Peretz, H. Rosenbaum, R. Gershoni-Baruch, Mutations in the glucocerebrosidase gene and Parkinson's disease in Ashkenazi Jews. *The New England journal of medicine* **351**, 1972-1977 (2004); published online EpubNov 4 (10.1056/NEJMoa033277).
85. T. Hara, K. Nakamura, M. Matsui, A. Yamamoto, Y. Nakahara, R. Suzuki-Migishima, M. Yokoyama, K. Mishima, I. Saito, H. Okano, N. Mizushima, Suppression of basal autophagy in neural cells causes neurodegenerative disease in mice. *Nature* **441**, 885-889 (2006); published online EpubJun 15 (10.1038/nature04724).
86. C. Commisso, S. M. Davidson, R. G. Soydaner-Azeloglu, S. J. Parker, J. J. Kamphorst, S. Hackett, E. Grabocka, M. Nofal, J. A. Drebin, C. B. Thompson, J. D. Rabinowitz, C. M. Metallo, M. G. Vander Heiden, D. Bar-Sagi, Macropinocytosis of protein is an amino acid supply route in Ras-transformed cells. *Nature* **497**, 633-637 (2013); published online EpubMay 30 (10.1038/nature12138).

87. N. N. Pavlova, C. B. Thompson, The Emerging Hallmarks of Cancer Metabolism. *Cell metabolism* **23**, 27-47 (2016); published online EpubJan 12 (10.1016/j.cmet.2015.12.006).
88. R. M. Perera, S. Stoykova, B. N. Nicolay, K. N. Ross, J. Fitamant, M. Boukhali, J. Lengrand, V. Deshpande, M. K. Selig, C. R. Ferrone, J. Settleman, G. Stephanopoulos, N. J. Dyson, R. Zoncu, S. Ramaswamy, W. Haas, N. Bardeesy, Transcriptional control of autophagy-lysosome function drives pancreatic cancer metabolism. *Nature* **524**, 361-365 (2015); published online EpubAug 20 (10.1038/nature14587).
89. L. Chantranupong, R. L. Wolfson, D. M. Sabatini, Nutrient-sensing mechanisms across evolution. *Cell* **161**, 67-83 (2015); published online EpubMar 26 (10.1016/j.cell.2015.02.041).
90. F. Dubouloz, O. Deloche, V. Wanke, E. Cameroni, C. De Virgilio, The TOR and EGO protein complexes orchestrate microautophagy in yeast. *Molecular cell* **19**, 15-26 (2005); published online EpubJul 1 (10.1016/j.molcel.2005.05.020).
91. C. Settembre, C. Di Malta, V. A. Polito, M. Garcia Arencibia, F. Vetrini, S. Erdin, S. U. Erdin, T. Huynh, D. Medina, P. Colella, M. Sardiello, D. C. Rubinsztein, A. Ballabio, TFEB links autophagy to lysosomal biogenesis. *Science* **332**, 1429-1433 (2011); published online EpubJun 17 (10.1126/science.1204592).
92. C. Settembre, A. Fraldi, D. L. Medina, A. Ballabio, Signals from the lysosome: a control centre for cellular clearance and energy metabolism. *Nature reviews. Molecular cell biology* **14**, 283-296 (2013); published online EpubMay (10.1038/nrm3565).
93. C. Settembre, R. De Cegli, G. Mansueto, P. K. Saha, F. Vetrini, O. Visvikis, T. Huynh, A. Carissimo, D. Palmer, T. J. Klisch, A. C. Wollenberg, D. Di Bernardo, L. Chan, J. E. Irazoqui, A. Ballabio, TFEB controls cellular lipid metabolism through a starvation-induced autoregulatory loop. *Nature cell biology* **15**, 647-658 (2013); published online EpubJun (10.1038/ncb2718).
94. C. Settembre, R. Zoncu, D. L. Medina, F. Vetrini, S. Erdin, S. Erdin, T. Huynh, M. Ferron, G. Karsenty, M. C. Vellard, V. Facchinetti, D. M. Sabatini, A. Ballabio, A lysosome-to-nucleus signalling mechanism senses and regulates the lysosome via mTOR and TFEB. *The EMBO journal* **31**, 1095-1108 (2012); published online EpubMar 07 (10.1038/emboj.2012.32).
95. N. N. Noda, Y. Ohsumi, F. Inagaki, Atg8-family interacting motif crucial for selective autophagy. *FEBS letters* **584**, 1379-1385 (2010); published online EpubApr 02 (10.1016/j.febslet.2010.01.018).
96. A. Kuma, M. Hatano, M. Matsui, A. Yamamoto, H. Nakaya, T. Yoshimori, Y. Ohsumi, T. Tokuhisa, N. Mizushima, The role of autophagy during the early neonatal starvation period. *Nature* **432**, 1032-1036 (2004); published online EpubDec 23 (10.1038/nature03029).
97. D. G. Hardie, F. A. Ross, S. A. Hawley, AMPK: a nutrient and energy sensor that maintains energy homeostasis. *Nature reviews. Molecular cell biology* **13**, 251-262 (2012); published online EpubMar 22 (10.1038/nrm3311).
98. G. Marino, F. Pietrocola, T. Eisenberg, Y. Kong, S. A. Malik, A. Andryushkova, S. Schroeder, T. Pendl, A. Harger, M. Niso-Santano, N. Zamzami, M. Scoazec, S. Durand, D. P. Enot, A. F. Fernandez, I. Martins, O. Kepp, L. Senovilla, C. Bauvy, E. Morselli, E. Vacchelli, M. Bennetzen, C. Magnes, F. Sinner, T. Pieber, C. Lopez-Otin, M. C. Maiuri, P. Codogno, J. S. Andersen, J. A. Hill, F. Madeo, G. Kroemer, Regulation of autophagy by cytosolic acetyl-coenzyme A. *Molecular*

cell **53**, 710-725 (2014); published online EpubMar 6 (10.1016/j.molcel.2014.01.016).
99. J. Ye, M. Kumanova, L. S. Hart, K. Sloane, H. Zhang, D. N. De Panis, E. Bobrovnikova-Marjon, J. A. Diehl, D. Ron, C. Koumenis, The GCN2-ATF4 pathway is critical for tumour cell survival and proliferation in response to nutrient deprivation. *The EMBO journal* **29**, 2082-2096 (2010); published online EpubJun 16 (10.1038/emboj.2010.81).
100. N. Hosokawa, T. Hara, T. Kaizuka, C. Kishi, A. Takamura, Y. Miura, S. Iemura, T. Natsume, K. Takehana, N. Yamada, J. L. Guan, N. Oshiro, N. Mizushima, Nutrient-dependent mTORC1 association with the ULK1-Atg13-FIP200 complex required for autophagy. *Molecular biology of the cell* **20**, 1981-1991 (2009); published online EpubApr (10.1091/mbc.E08-12-1248).
101. J. D. Mancias, X. Wang, S. P. Gygi, J. W. Harper, A. C. Kimmelman, Quantitative proteomics identifies NCOA4 as the cargo receptor mediating ferritinophagy. *Nature* **509**, 105-109 (2014); published online EpubMay 01 (10.1038/nature13148).
102. L. M. Harder, J. Bunkenborg, J. S. Andersen, Inducing autophagy: a comparative phosphoproteomic study of the cellular response to ammonia and rapamycin. *Autophagy* **10**, 339-355 (2014); published online EpubFeb (10.4161/auto.26863).
103. Y. Ogasawara, E. Itakura, N. Kono, N. Mizushima, H. Arai, A. Nara, T. Mizukami, A. Yamamoto, Stearoyl-CoA desaturase 1 activity is required for autophagosome formation. *The Journal of biological chemistry* **289**, 23938-23950 (2014); published online EpubAug 22 (10.1074/jbc.M114.591065).
104. S. A. Khaldoun, M. A. Emond-Boisjoly, D. Chateau, V. Carriere, M. Lacasa, M. Rousset, S. Demignot, E. Morel, Autophagosomes contribute to intracellular lipid distribution in enterocytes. *Molecular biology of the cell* **25**, 118-132 (2014); published online EpubJan (10.1091/mbc.E13-06-0324).
105. A. B. Birgisdottir, T. Lamark, T. Johansen, The LIR motif - crucial for selective autophagy. *Journal of cell science* **126**, 3237-3247 (2013); published online EpubAug 01 (10.1242/jcs.126128).
106. D. J. Klionsky, R. Cueva, D. S. Yaver, Aminopeptidase I of Saccharomyces cerevisiae is localized to the vacuole independent of the secretory pathway. *The Journal of cell biology* **119**, 287-299 (1992); published online EpubOct (
107. P. Verlhac, I. P. Gregoire, O. Azocar, D. S. Petkova, J. Baguet, C. Viret, M. Faure, Autophagy receptor NDP52 regulates pathogen-containing autophagosome maturation. *Cell host & microbe* **17**, 515-525 (2015); published online EpubApr 08 (10.1016/j.chom.2015.02.008).
108. D. A. Tumbarello, P. T. Manna, M. Allen, M. Bycroft, S. D. Arden, J. Kendrick-Jones, F. Buss, The Autophagy Receptor TAX1BP1 and the Molecular Motor Myosin VI Are Required for Clearance of Salmonella Typhimurium by Autophagy. *PLoS pathogens* **11**, e1005174 (2015); published online EpubOct (10.1371/journal.ppat.1005174).
109. H. Huang, T. Kawamata, T. Horie, H. Tsugawa, Y. Nakayama, Y. Ohsumi, E. Fukusaki, Bulk RNA degradation by nitrogen starvation-induced autophagy in yeast. *The EMBO journal* **34**, 154-168 (2015); published online EpubJan 13 (10.15252/embj.201489083).
110. C. Kraft, A. Deplazes, M. Sohrmann, M. Peter, Mature ribosomes are selectively degraded upon starvation by an autophagy pathway requiring the Ubp3p/Bre5p

ubiquitin protease. *Nature cell biology* **10**, 602-610 (2008); published online EpubMay (10.1038/ncb1723).
111. A. D. Mathis, B. C. Naylor, R. H. Carson, E. Evans, J. Harwell, J. Knecht, E. Hexem, F. F. Peelor, 3rd, B. F. Miller, K. L. Hamilton, M. K. Transtrum, B. T. Bikman, J. C. Price, Mechanisms of In Vivo Ribosome Maintenance Change in Response to Nutrient Signals. *Molecular & cellular proteomics : MCP* **16**, 243-254 (2017); published online EpubFeb (10.1074/mcp.M116.063255).
112. G. Zaffagnini, S. Martens, Mechanisms of Selective Autophagy. *Journal of molecular biology* **428**, 1714-1724 (2016); published online EpubMay 08 (10.1016/j.jmb.2016.02.004).
113. E. Deosaran, K. B. Larsen, R. Hua, G. Sargent, Y. Wang, S. Kim, T. Lamark, M. Jauregui, K. Law, J. Lippincott-Schwartz, A. Brech, T. Johansen, P. K. Kim, NBR1 acts as an autophagy receptor for peroxisomes. *Journal of cell science* **126**, 939-952 (2013); published online EpubFeb 15 (10.1242/jcs.114819).
114. G. A. Wyant, M. Abu-Remaileh, E. M. Frenkel, N. N. Laqtom, V. Dharamdasani, C. A. Lewis, S. H. Chan, I. Heinze, A. Ori, D. M. Sabatini, NUFIP1 is a ribosome receptor for starvation-induced ribophagy. *Science* **360**, 751-758 (2018); published online EpubMay 18 (10.1126/science.aar2663).
115. A. R. Kristensen, S. Schandorff, M. Hoyer-Hansen, M. O. Nielsen, M. Jaattela, J. Dengjel, J. S. Andersen, Ordered organelle degradation during starvation-induced autophagy. *Molecular & cellular proteomics : MCP* **7**, 2419-2428 (2008); published online EpubDec (10.1074/mcp.M800184-MCP200).
116. Y. Wei, W. C. Chiang, R. Sumpter, Jr., P. Mishra, B. Levine, Prohibitin 2 Is an Inner Mitochondrial Membrane Mitophagy Receptor. *Cell* **168**, 224-238 e210 (2017); published online EpubJan 12 (10.1016/j.cell.2016.11.042).
117. A. Khaminets, T. Heinrich, M. Mari, P. Grumati, A. K. Huebner, M. Akutsu, L. Liebmann, A. Stolz, S. Nietzsche, N. Koch, M. Mauthe, I. Katona, B. Qualmann, J. Weis, F. Reggiori, I. Kurth, C. A. Hubner, I. Dikic, Regulation of endoplasmic reticulum turnover by selective autophagy. *Nature* **522**, 354-358 (2015); published online EpubJun 18 (10.1038/nature14498).
118. T. L. Thurston, G. Ryzhakov, S. Bloor, N. von Muhlinen, F. Randow, The TBK1 adaptor and autophagy receptor NDP52 restricts the proliferation of ubiquitin-coated bacteria. *Nature immunology* **10**, 1215-1221 (2009); published online EpubNov (10.1038/ni.1800).
119. M. Komatsu, S. Waguri, T. Ueno, J. Iwata, S. Murata, I. Tanida, J. Ezaki, N. Mizushima, Y. Ohsumi, Y. Uchiyama, E. Kominami, K. Tanaka, T. Chiba, Impairment of starvation-induced and constitutive autophagy in Atg7-deficient mice. *The Journal of cell biology* **169**, 425-434 (2005); published online EpubMay 09 (10.1083/jcb.200412022).
120. B. Hartleben, M. Godel, C. Meyer-Schwesinger, S. Liu, T. Ulrich, S. Kobler, T. Wiech, F. Grahammer, S. J. Arnold, M. T. Lindenmeyer, C. D. Cohen, H. Pavenstadt, D. Kerjaschki, N. Mizushima, A. S. Shaw, G. Walz, T. B. Huber, Autophagy influences glomerular disease susceptibility and maintains podocyte homeostasis in aging mice. *The Journal of clinical investigation* **120**, 1084-1096 (2010); published online EpubApr (10.1172/JCI39492).
121. E. Masiero, L. Agatea, C. Mammucari, B. Blaauw, E. Loro, M. Komatsu, D. Metzger, C. Reggiani, S. Schiaffino, M. Sandri, Autophagy is required to maintain muscle mass. *Cell metabolism* **10**, 507-515 (2009); published online EpubDec (10.1016/j.cmet.2009.10.008).

122. M. Taneike, O. Yamaguchi, A. Nakai, S. Hikoso, T. Takeda, I. Mizote, T. Oka, T. Tamai, J. Oyabu, T. Murakawa, K. Nishida, T. Shimizu, M. Hori, I. Komuro, T. S. Takuji Shirasawa, N. Mizushima, K. Otsu, Inhibition of autophagy in the heart induces age-related cardiomyopathy. *Autophagy* **6**, 600-606 (2010); published online EpubJul (10.4161/auto.6.5.11947).
123. J. Hampe, A. Franke, P. Rosenstiel, A. Till, M. Teuber, K. Huse, M. Albrecht, G. Mayr, F. M. De La Vega, J. Briggs, S. Gunther, N. J. Prescott, C. M. Onnie, R. Hasler, B. Sipos, U. R. Folsch, T. Lengauer, M. Platzer, C. G. Mathew, M. Krawczak, S. Schreiber, A genome-wide association scan of nonsynonymous SNPs identifies a susceptibility variant for Crohn disease in ATG16L1. *Nature genetics* **39**, 207-211 (2007); published online EpubFeb (10.1038/ng1954).
124. N. Mizushima, A. Yamamoto, M. Matsui, T. Yoshimori, Y. Ohsumi, In vivo analysis of autophagy in response to nutrient starvation using transgenic mice expressing a fluorescent autophagosome marker. *Molecular biology of the cell* **15**, 1101-1111 (2004); published online EpubMar (10.1091/mbc.e03-09-0704).
125. A. Takamura, M. Komatsu, T. Hara, A. Sakamoto, C. Kishi, S. Waguri, Y. Eishi, O. Hino, K. Tanaka, N. Mizushima, Autophagy-deficient mice develop multiple liver tumors. *Genes & development* **25**, 795-800 (2011); published online EpubApr 15 (10.1101/gad.2016211).
126. K. Degenhardt, R. Mathew, B. Beaudoin, K. Bray, D. Anderson, G. Chen, C. Mukherjee, Y. Shi, C. Gelinas, Y. Fan, D. A. Nelson, S. Jin, E. White, Autophagy promotes tumor cell survival and restricts necrosis, inflammation, and tumorigenesis. *Cancer cell* **10**, 51-64 (2006); published online EpubJul (10.1016/j.ccr.2006.06.001).
127. X. H. Liang, S. Jackson, M. Seaman, K. Brown, B. Kempkes, H. Hibshoosh, B. Levine, Induction of autophagy and inhibition of tumorigenesis by beclin 1. *Nature* **402**, 672-676 (1999); published online EpubDec 9 (10.1038/45257).
128. X. Qu, J. Yu, G. Bhagat, N. Furuya, H. Hibshoosh, A. Troxel, J. Rosen, E. L. Eskelinen, N. Mizushima, Y. Ohsumi, G. Cattoretti, B. Levine, Promotion of tumorigenesis by heterozygous disruption of the beclin 1 autophagy gene. *The Journal of clinical investigation* **112**, 1809-1820 (2003); published online EpubDec (10.1172/JCI20039).
129. J. Y. Guo, X. Teng, S. V. Laddha, S. Ma, S. C. Van Nostrand, Y. Yang, S. Khor, C. S. Chan, J. D. Rabinowitz, E. White, Autophagy provides metabolic substrates to maintain energy charge and nucleotide pools in Ras-driven lung cancer cells. *Genes & development* **30**, 1704-1717 (2016); published online EpubAug 1 (10.1101/gad.283416.116).
130. C. T. Murphy, S. A. McCarroll, C. I. Bargmann, A. Fraser, R. S. Kamath, J. Ahringer, H. Li, C. Kenyon, Genes that act downstream of DAF-16 to influence the lifespan of Caenorhabditis elegans. *Nature* **424**, 277-283 (2003); published online EpubJul 17 (10.1038/nature01789).
131. T. Vellai, K. Takacs-Vellai, Y. Zhang, A. L. Kovacs, L. Orosz, F. Muller, Genetics: influence of TOR kinase on lifespan in C. elegans. *Nature* **426**, 620 (2003); published online EpubDec 11 (10.1038/426620a).
132. A. Ballabio, V. Gieselmann, Lysosomal disorders: from storage to cellular damage. *Biochimica et biophysica acta* **1793**, 684-696 (2009); published online EpubApr (10.1016/j.bbamcr.2008.12.001).
133. S. M. Davidson, M. G. Vander Heiden, Critical Functions of the Lysosome in Cancer Biology. *Annual review of pharmacology and toxicology* **57**, 481-507

(2017); published online EpubJan 06 (10.1146/annurev-pharmtox-010715-103101).
134. W. W. Chen, E. Freinkman, T. Wang, K. Birsoy, D. M. Sabatini, Absolute Quantification of Matrix Metabolites Reveals the Dynamics of Mitochondrial Metabolism. *Cell* **166**, 1324-1337 e1311 (2016); published online EpubAug 25 (10.1016/j.cell.2016.07.040).
135. B. Schroder, C. Wrocklage, A. Hasilik, P. Saftig, Molecular characterisation of 'transmembrane protein 192' (TMEM192), a novel protein of the lysosomal membrane. *Biological chemistry* **391**, 695-704 (2010); published online EpubJun (10.1515/BC.2010.062).
136. G. M. Mancini, C. E. Beerens, P. P. Aula, F. W. Verheijen, Sialic acid storage diseases. A multiple lysosomal transport defect for acidic monosaccharides. *The Journal of clinical investigation* **87**, 1329-1335 (1991); published online EpubApr (10.1172/JCI115136).
137. J. D. Schulman, K. H. Bradley, J. E. Seegmiller, Cystine: compartmentalization within lysosomes in cystinotic leukocytes. *Science* **166**, 1152-1154 (1969); published online EpubNov 28 (
138. E. J. Bowman, A. Siebers, K. Altendorf, Bafilomycins: a class of inhibitors of membrane ATPases from microorganisms, animal cells, and plant cells. *Proceedings of the National Academy of Sciences of the United States of America* **85**, 7972-7976 (1988); published online EpubNov (
139. M. Huss, G. Ingenhorst, S. Konig, M. Gassel, S. Drose, A. Zeeck, K. Altendorf, H. Wieczorek, Concanamycin A, the specific inhibitor of V-ATPases, binds to the V(o) subunit c. *The Journal of biological chemistry* **277**, 40544-40548 (2002); published online EpubOct 25 (10.1074/jbc.M207345200).
140. R. L. Pisoni, T. L. Acker, K. M. Lisowski, R. M. Lemons, J. G. Thoene, A cysteine-specific lysosomal transport system provides a major route for the delivery of thiol to human fibroblast lysosomes: possible role in supporting lysosomal proteolysis. *The Journal of cell biology* **110**, 327-335 (1990); published online EpubFeb (
141. C. Sagne, C. Agulhon, P. Ravassard, M. Darmon, M. Hamon, S. El Mestikawy, B. Gasnier, B. Giros, Identification and characterization of a lysosomal transporter for small neutral amino acids. *Proceedings of the National Academy of Sciences of the United States of America* **98**, 7206-7211 (2001); published online EpubJun 19 (10.1073/pnas.121183498).
142. K. Hara, K. Yonezawa, Q. P. Weng, M. T. Kozlowski, C. Belham, J. Avruch, Amino acid sufficiency and mTOR regulate p70 S6 kinase and eIF-4E BP1 through a common effector mechanism. *The Journal of biological chemistry* **273**, 14484-14494 (1998); published online EpubJun 5 (
143. S. Udenfriend, J. R. Cooper, The enzymatic conversion of phenylalanine to tyrosine. *The Journal of biological chemistry* **194**, 503-511 (1952); published online EpubFeb (
144. C. M. Chresta, B. R. Davies, I. Hickson, T. Harding, S. Cosulich, S. E. Critchlow, J. P. Vincent, R. Ellston, D. Jones, P. Sini, D. James, Z. Howard, P. Dudley, G. Hughes, L. Smith, S. Maguire, M. Hummersone, K. Malagu, K. Menear, R. Jenkins, M. Jacobsen, G. C. Smith, S. Guichard, M. Pass, AZD8055 is a potent, selective, and orally bioavailable ATP-competitive mammalian target of rapamycin kinase inhibitor with in vitro and in vivo antitumor activity. *Cancer*

research **70**, 288-298 (2010); published online EpubJan 01 (10.1158/0008-5472.CAN-09-1751).
145. K. Yu, C. Shi, L. Toral-Barza, J. Lucas, B. Shor, J. E. Kim, W. G. Zhang, R. Mahoney, C. Gaydos, L. Tardio, S. K. Kim, R. Conant, K. Curran, J. Kaplan, J. Verheijen, S. Ayral-Kaloustian, T. S. Mansour, R. T. Abraham, A. Zask, J. J. Gibbons, Beyond rapalog therapy: preclinical pharmacology and antitumor activity of WYE-125132, an ATP-competitive and specific inhibitor of mTORC1 and mTORC2. *Cancer research* **70**, 621-631 (2010); published online EpubJan 15 (10.1158/0008-5472.CAN-09-2340).
146. J. Kim, M. Kundu, B. Viollet, K. L. Guan, AMPK and mTOR regulate autophagy through direct phosphorylation of Ulk1. *Nature cell biology* **13**, 132-141 (2011); published online EpubFeb (10.1038/ncb2152).
147. R. Amaravadi, A. C. Kimmelman, E. White, Recent insights into the function of autophagy in cancer. *Genes & development* **30**, 1913-1930 (2016); published online EpubSep 01 (10.1101/gad.287524.116).
148. J. Zhao, B. Zhai, S. P. Gygi, A. L. Goldberg, mTOR inhibition activates overall protein degradation by the ubiquitin proteasome system as well as by autophagy. *Proceedings of the National Academy of Sciences of the United States of America* **112**, 15790-15797 (2015); published online EpubDec 29 (10.1073/pnas.1521919112).
149. J. Adams, V. J. Palombella, E. A. Sausville, J. Johnson, A. Destree, D. D. Lazarus, J. Maas, C. S. Pien, S. Prakash, P. J. Elliott, Proteasome inhibitors: a novel class of potent and effective antitumor agents. *Cancer research* **59**, 2615-2622 (1999); published online EpubJun 01 (
150. L. Yu, C. K. McPhee, L. Zheng, G. A. Mardones, Y. Rong, J. Peng, N. Mi, Y. Zhao, Z. Liu, F. Wan, D. W. Hailey, V. Oorschot, J. Klumperman, E. H. Baehrecke, M. J. Lenardo, Termination of autophagy and reformation of lysosomes regulated by mTOR. *Nature* **465**, 942-946 (2010); published online EpubJun 17 (10.1038/nature09076).
151. S. A. Kang, M. E. Pacold, C. L. Cervantes, D. Lim, H. J. Lou, K. Ottina, N. S. Gray, B. E. Turk, M. B. Yaffe, D. M. Sabatini, mTORC1 phosphorylation sites encode their sensitivity to starvation and rapamycin. *Science* **341**, 1236566 (2013); published online EpubJul 26 (10.1126/science.1236566).
152. A. Y. Choo, S. O. Yoon, S. G. Kim, P. P. Roux, J. Blenis, Rapamycin differentially inhibits S6Ks and 4E-BP1 to mediate cell-type-specific repression of mRNA translation. *Proceedings of the National Academy of Sciences of the United States of America* **105**, 17414-17419 (2008); published online EpubNov 11 (10.1073/pnas.0809136105).
153. M. E. Feldman, B. Apsel, A. Uotila, R. Loewith, Z. A. Knight, D. Ruggero, K. M. Shokat, Active-site inhibitors of mTOR target rapamycin-resistant outputs of mTORC1 and mTORC2. *PLoS biology* **7**, e38 (2009); published online EpubFeb 10 (10.1371/journal.pbio.1000038).
154. J. Jung, H. M. Genau, C. Behrends, Amino Acid-Dependent mTORC1 Regulation by the Lysosomal Membrane Protein SLC38A9. *Molecular and cellular biology* **35**, 2479-2494 (2015); published online EpubJul (10.1128/MCB.00125-15).
155. M. Rebsamen, L. Pochini, T. Stasyk, M. E. de Araujo, M. Galluccio, R. K. Kandasamy, B. Snijder, A. Fauster, E. L. Rudashevskaya, M. Bruckner, S. Scorzoni, P. A. Filipek, K. V. Huber, J. W. Bigenzahn, L. X. Heinz, C. Kraft, K. L. Bennett, C. Indiveri, L. A. Huber, G. Superti-Furga, SLC38A9 is a component of

the lysosomal amino acid sensing machinery that controls mTORC1. *Nature* **519**, 477-481 (2015); published online EpubMar 26 (10.1038/nature14107).
156. T. Sekiguchi, E. Hirose, N. Nakashima, M. Ii, T. Nishimoto, Novel G proteins, Rag C and Rag D, interact with GTP-binding proteins, Rag A and Rag B. *The Journal of biological chemistry* **276**, 7246-7257 (2001); published online EpubMar 09 (10.1074/jbc.M004389200).
157. E. Kim, P. Goraksha-Hicks, L. Li, T. P. Neufeld, K. L. Guan, Regulation of TORC1 by Rag GTPases in nutrient response. *Nature cell biology* **10**, 935-945 (2008); published online EpubAug (10.1038/ncb1753).
158. C. S. Petit, A. Roczniak-Ferguson, S. M. Ferguson, Recruitment of folliculin to lysosomes supports the amino acid-dependent activation of Rag GTPases. *The Journal of cell biology* **202**, 1107-1122 (2013); published online EpubSep 30 (10.1083/jcb.201307084).
159. D. L. Jack, I. T. Paulsen, M. H. Saier, The amino acid/polyamine/organocation (APC) superfamily of transporters specific for amino acids, polyamines and organocations. *Microbiology* **146 (Pt 8)**, 1797-1814 (2000); published online EpubAug (10.1099/00221287-146-8-1797).
160. X. Gao, F. Lu, L. Zhou, S. Dang, L. Sun, X. Li, J. Wang, Y. Shi, Structure and mechanism of an amino acid antiporter. *Science* **324**, 1565-1568 (2009); published online EpubJun 19 (10.1126/science.1173654).
161. H. S. Hundal, P. M. Taylor, Amino acid transceptors: gate keepers of nutrient exchange and regulators of nutrient signaling. *American journal of physiology. Endocrinology and metabolism* **296**, E603-613 (2009); published online EpubApr (10.1152/ajpendo.91002.2008).
162. Y. Popova, P. Thayumanavan, E. Lonati, M. Agrochao, J. M. Thevelein, Transport and signaling through the phosphate-binding site of the yeast Pho84 phosphate transceptor. *Proceedings of the National Academy of Sciences of the United States of America* **107**, 2890-2895 (2010); published online EpubFeb 16 (10.1073/pnas.0906546107).
163. G. Van Zeebroeck, B. M. Bonini, M. Versele, J. M. Thevelein, Transport and signaling via the amino acid binding site of the yeast Gap1 amino acid transceptor. *Nature chemical biology* **5**, 45-52 (2009); published online EpubJan (10.1038/nchembio.132).
164. G. Van Zeebroeck, M. Rubio-Texeira, J. Schothorst, J. M. Thevelein, Specific analogues uncouple transport, signalling, oligo-ubiquitination and endocytosis in the yeast Gap1 amino acid transceptor. *Molecular microbiology* **93**, 213-233 (2014); published online EpubJul (10.1111/mmi.12654).
165. B. Liu, H. Du, R. Rutkowski, A. Gartner, X. Wang, LAAT-1 is the lysosomal lysine/arginine transporter that maintains amino acid homeostasis. *Science* **337**, 351-354 (2012); published online EpubJul 20 (10.1126/science.1220281).
166. R. Milkereit, A. Persaud, L. Vanoaica, A. Guetg, F. Verrey, D. Rotin, LAPTM4b recruits the LAT1-4F2hc Leu transporter to lysosomes and promotes mTORC1 activation. *Nature communications* **6**, 7250 (2015); published online EpubMay 22 (10.1038/ncomms8250).
167. P. M. Taylor, Role of amino acid transporters in amino acid sensing. *The American journal of clinical nutrition* **99**, 223S-230S (2014); published online EpubJan (10.3945/ajcn.113.070086).
168. Q. Verdon, M. Boonen, C. Ribes, M. Jadot, B. Gasnier, C. Sagne, SNAT7 is the primary lysosomal glutamine exporter required for extracellular protein-

dependent growth of cancer cells. *Proceedings of the National Academy of Sciences of the United States of America* **114**, E3602-E3611 (2017); published online EpubMay 02 (10.1073/pnas.1617066114).
169. R. L. Pisoni, J. G. Thoene, H. N. Christensen, Detection and characterization of carrier-mediated cationic amino acid transport in lysosomes of normal and cystinotic human fibroblasts. Role in therapeutic cystine removal? *The Journal of biological chemistry* **260**, 4791-4798 (1985); published online EpubApr 25 (
170. R. L. Pisoni, J. G. Thoene, R. M. Lemons, H. N. Christensen, Important differences in cationic amino acid transport by lysosomal system c and system y+ of the human fibroblast. *The Journal of biological chemistry* **262**, 15011-15018 (1987); published online EpubNov 05 (
171. W. Palm, Y. Park, K. Wright, N. N. Pavlova, D. A. Tuveson, C. B. Thompson, The Utilization of Extracellular Proteins as Nutrients Is Suppressed by mTORC1. *Cell* **162**, 259-270 (2015); published online EpubJul 16 (10.1016/j.cell.2015.06.017).
172. S. Yoshida, R. Pacitto, Y. Yao, K. Inoki, J. A. Swanson, Growth factor signaling to mTORC1 by amino acid-laden macropinosomes. *The Journal of cell biology* **211**, 159-172 (2015); published online EpubOct 12 (10.1083/jcb.201504097).
173. J. T. Wang, R. D. Teasdale, D. Liebl, Macropinosome quantitation assay. *MethodsX* **1**, 36-41 (2014)10.1016/j.mex.2014.05.002).
174. D. Bar-Sagi, J. R. Feramisco, Induction of membrane ruffling and fluid-phase pinocytosis in quiescent fibroblasts by ras proteins. *Science* **233**, 1061-1068 (1986); published online EpubSep 05 (
175. S. M. Davidson, O. Jonas, M. A. Keibler, H. W. Hou, A. Luengo, J. R. Mayers, J. Wyckoff, A. M. Del Rosario, M. Whitman, C. R. Chin, K. J. Condon, A. Lammers, K. A. Kellersberger, B. K. Stall, G. Stephanopoulos, D. Bar-Sagi, J. Han, J. D. Rabinowitz, M. J. Cima, R. Langer, M. G. Vander Heiden, Direct evidence for cancer-cell-autonomous extracellular protein catabolism in pancreatic tumors. *Nature medicine* **23**, 235-241 (2017); published online EpubFeb (10.1038/nm.4256).
176. B. M. Castellano, A. M. Thelen, O. Moldavski, M. Feltes, R. E. van der Welle, L. Mydock-McGrane, X. Jiang, R. J. van Eijkeren, O. B. Davis, S. M. Louie, R. M. Perera, D. F. Covey, D. K. Nomura, D. S. Ory, R. Zoncu, Lysosomal cholesterol activates mTORC1 via an SLC38A9-Niemann-Pick C1 signaling complex. *Science* **355**, 1306-1311 (2017); published online EpubMar 24 (10.1126/science.aag1417).
177. K. Takeshige, M. Baba, S. Tsuboi, T. Noda, Y. Ohsumi, Autophagy in yeast demonstrated with proteinase-deficient mutants and conditions for its induction. *The Journal of cell biology* **119**, 301-311 (1992); published online EpubOct (
178. T. P. Ashford, K. R. Porter, Cytoplasmic components in hepatic cell lysosomes. *The Journal of cell biology* **12**, 198-202 (1962); published online EpubJan (
179. P. Cohn, Properties of ribosomal proteins from two mammalian sources. *The Biochemical journal* **102**, 735-741 (1967); published online EpubMar (
180. S. K. Singh, A. Yamashita, E. Gouaux, Antidepressant binding site in a bacterial homologue of neurotransmitter transporters. *Nature* **448**, 952-956 (2007); published online EpubAug 23 (10.1038/nature06038).
181. L. Shi, M. Quick, Y. Zhao, H. Weinstein, J. A. Javitch, The mechanism of a neurotransmitter:sodium symporter--inward release of Na+ and substrate is triggered by substrate in a second binding site. *Molecular cell* **30**, 667-677 (2008); published online EpubJun 20 (10.1016/j.molcel.2008.05.008).

182. H. A. Neubauer, C. G. Hansen, O. Wiborg, Dissection of an allosteric mechanism on the serotonin transporter: a cross-species study. *Molecular pharmacology* **69**, 1242-1250 (2006); published online EpubApr (10.1124/mol.105.018507).
183. M. Quick, L. Shi, B. Zehnpfennig, H. Weinstein, J. A. Javitch, Experimental conditions can obscure the second high-affinity site in LeuT. *Nature structural & molecular biology* **19**, 207-211 (2012); published online EpubJan 15 (10.1038/nsmb.2197).
184. Z. Li, A. S. Lee, S. Bracher, H. Jung, A. Paz, J. P. Kumar, J. Abramson, M. Quick, L. Shi, Identification of a second substrate-binding site in solute-sodium symporters. *The Journal of biological chemistry* **290**, 127-141 (2015); published online EpubJan 02 (10.1074/jbc.M114.584383).
185. Z. Zhou, J. Zhen, N. K. Karpowich, R. M. Goetz, C. J. Law, M. E. Reith, D. N. Wang, LeuT-desipramine structure reveals how antidepressants block neurotransmitter reuptake. *Science* **317**, 1390-1393 (2007); published online EpubSep 07 (10.1126/science.1147614).
186. C. L. Piscitelli, H. Krishnamurthy, E. Gouaux, Neurotransmitter/sodium symporter orthologue LeuT has a single high-affinity substrate site. *Nature* **468**, 1129-1132 (2010); published online EpubDec 23 (10.1038/nature09581).
187. O. Boussif, F. Lezoualc'h, M. A. Zanta, M. D. Mergny, D. Scherman, B. Demeneix, J. P. Behr, A versatile vector for gene and oligonucleotide transfer into cells in culture and in vivo: polyethylenimine. *Proceedings of the National Academy of Sciences of the United States of America* **92**, 7297-7301 (1995); published online EpubAug 01 (
188. O. H. Yilmaz, P. Katajisto, D. W. Lamming, Y. Gultekin, K. E. Bauer-Rowe, S. Sengupta, K. Birsoy, A. Dursun, V. O. Yilmaz, M. Selig, G. P. Nielsen, M. Mino-Kenudson, L. R. Zukerberg, A. K. Bhan, V. Deshpande, D. M. Sabatini, mTORC1 in the Paneth cell niche couples intestinal stem-cell function to calorie intake. *Nature* **486**, 490-495 (2012); published online EpubJun 28 (10.1038/nature11163).
189. L. Groth-Pedersen, M. Jaattela, Combating apoptosis and multidrug resistant cancers by targeting lysosomes. *Cancer letters* **332**, 265-274 (2013); published online EpubMay 28 (10.1016/j.canlet.2010.05.021).
190. M. Abu-Remaileh, G. A. Wyant, C. Kim, N. N. Laqtom, M. Abbasi, S. H. Chan, E. Freinkman, D. M. Sabatini, Lysosomal metabolomics reveals V-ATPase- and mTOR-dependent regulation of amino acid efflux from lysosomes. *Science* **358**, 807-813 (2017); published online EpubNov 10 (10.1126/science.aan6298).
191. A. Roczniak-Ferguson, C. S. Petit, F. Froehlich, S. Qian, J. Ky, B. Angarola, T. C. Walther, S. M. Ferguson, The transcription factor TFEB links mTORC1 signaling to transcriptional control of lysosome homeostasis. *Science signaling* **5**, ra42 (2012); published online EpubJun 12 (10.1126/scisignal.2002790).
192. J. A. Martina, H. I. Diab, L. Lishu, A. L. Jeong, S. Patange, N. Raben, R. Puertollano, The nutrient-responsive transcription factor TFE3 promotes autophagy, lysosomal biogenesis, and clearance of cellular debris. *Science signaling* **7**, ra9 (2014); published online EpubJan 21 (10.1126/scisignal.2004754).
193. R. P. Murmu, E. Martin, A. Rastetter, T. Esteves, M. P. Muriel, K. H. El Hachimi, P. S. Denora, A. Dauphin, J. C. Fernandez, C. Duyckaerts, A. Brice, F. Darios, G. Stevanin, Cellular distribution and subcellular localization of spatacsin and spastizin, two proteins involved in hereditary spastic paraplegia. *Molecular and*

cellular neurosciences **47**, 191-202 (2011); published online EpubJul (10.1016/j.mcn.2011.04.004).
194. J. Hirst, G. H. Borner, J. Edgar, M. Y. Hein, M. Mann, F. Buchholz, R. Antrobus, M. S. Robinson, Interaction between AP-5 and the hereditary spastic paraplegia proteins SPG11 and SPG15. *Molecular biology of the cell* **24**, 2558-2569 (2013); published online EpubAug (10.1091/mbc.E13-03-0170).
195. B. Bardoni, R. Willemsen, I. J. Weiler, A. Schenck, L. A. Severijnen, C. Hindelang, E. Lalli, J. L. Mandel, NUFIP1 (nuclear FMRP interacting protein 1) is a nucleocytoplasmic shuttling protein associated with active synaptoneurosomes. *Experimental cell research* **289**, 95-107 (2003); published online EpubSep 10 (
196. M. Quinternet, M. E. Chagot, B. Rothe, D. Tiotiu, B. Charpentier, X. Manival, Structural Features of the Box C/D snoRNP Pre-assembly Process Are Conserved through Species. *Structure* **24**, 1693-1706 (2016); published online EpubOct 04 (10.1016/j.str.2016.07.016).
197. B. Rothe, J. M. Saliou, M. Quinternet, R. Back, D. Tiotiu, C. Jacquemin, C. Loegler, F. Schlotter, V. Pena, K. Eckert, S. Morera, A. V. Dorsselaer, C. Branlant, S. Massenet, S. Sanglier-Cianferani, X. Manival, B. Charpentier, Protein Hit1, a novel box C/D snoRNP assembly factor, controls cellular concentration of the scaffolding protein Rsa1 by direct interaction. *Nucleic acids research* **42**, 10731-10747 (2014)10.1093/nar/gku612).
198. S. Boulon, N. Marmier-Gourrier, B. Pradet-Balade, L. Wurth, C. Verheggen, B. E. Jady, B. Rothe, C. Pescia, M. C. Robert, T. Kiss, B. Bardoni, A. Krol, C. Branlant, C. Allmang, E. Bertrand, B. Charpentier, The Hsp90 chaperone controls the biogenesis of L7Ae RNPs through conserved machinery. *The Journal of cell biology* **180**, 579-595 (2008); published online EpubFeb 11 (10.1083/jcb.200708110).
199. K. S. McKeegan, C. M. Debieux, S. Boulon, E. Bertrand, N. J. Watkins, A dynamic scaffold of pre-snoRNP factors facilitates human box C/D snoRNP assembly. *Molecular and cellular biology* **27**, 6782-6793 (2007); published online EpubOct (10.1128/MCB.01097-07).
200. M. Quinternet, B. Rothe, M. Barbier, C. Bobo, J. M. Saliou, C. Jacquemin, R. Back, M. E. Chagot, S. Cianferani, P. Meyer, C. Branlant, B. Charpentier, X. Manival, Structure/Function Analysis of Protein-Protein Interactions Developed by the Yeast Pih1 Platform Protein and Its Partners in Box C/D snoRNP Assembly. *Journal of molecular biology* **427**, 2816-2839 (2015); published online EpubAug 28 (10.1016/j.jmb.2015.07.012).
201. M. K. Sung, T. R. Porras-Yakushi, J. M. Reitsma, F. M. Huber, M. J. Sweredoski, A. Hoelz, S. Hess, R. J. Deshaies, A conserved quality-control pathway that mediates degradation of unassembled ribosomal proteins. *eLife* **5**, (2016); published online EpubAug 23 (10.7554/eLife.19105).
202. M. K. Sung, J. M. Reitsma, M. J. Sweredoski, S. Hess, R. J. Deshaies, Ribosomal proteins produced in excess are degraded by the ubiquitin-proteasome system. *Molecular biology of the cell* **27**, 2642-2652 (2016); published online EpubSep 01 (10.1091/mbc.E16-05-0290).
203. J. R. Warner, In the absence of ribosomal RNA synthesis, the ribosomal proteins of HeLa cells are synthesized normally and degraded rapidly. *Journal of molecular biology* **115**, 315-333 (1977); published online EpubSep 25 (
204. J. R. Warner, The economics of ribosome biosynthesis in yeast. *Trends in biochemical sciences* **24**, 437-440 (1999); published online EpubNov (

205. D. E. Weinberg, P. Shah, S. W. Eichhorn, J. A. Hussmann, J. B. Plotkin, D. P. Bartel, Improved Ribosome-Footprint and mRNA Measurements Provide Insights into Dynamics and Regulation of Yeast Translation. *Cell reports* **14**, 1787-1799 (2016); published online EpubFeb 23 (10.1016/j.celrep.2016.01.043).
206. J. E. Darnell, Jr., Ribonucleic acids from animal cells. *Bacteriological reviews* **32**, 262-290 (1968); published online EpubSep (
207. E. R. Lindley, R. L. Pisoni, Demonstration of adenosine deaminase activity in human fibroblast lysosomes. *The Biochemical journal* **290 (Pt 2)**, 457-462 (1993); published online EpubMar 1 (
208. G. A. Wyant, M. Abu-Remaileh, R. L. Wolfson, W. W. Chen, E. Freinkman, L. V. Danai, M. G. Vander Heiden, D. M. Sabatini, mTORC1 Activator SLC38A9 Is Required to Efflux Essential Amino Acids from Lysosomes and Use Protein as a Nutrient. *Cell* **171**, 642-654 e612 (2017); published online EpubOct 19 (10.1016/j.cell.2017.09.046).
209. S. Klinge, F. Voigts-Hoffmann, M. Leibundgut, N. Ban, Atomic structures of the eukaryotic ribosome. *Trends in biochemical sciences* **37**, 189-198 (2012); published online EpubMay (10.1016/j.tibs.2012.02.007).
210. Y. C. Wong, E. L. Holzbaur, Optineurin is an autophagy receptor for damaged mitochondria in parkin-mediated mitophagy that is disrupted by an ALS-linked mutation. *Proceedings of the National Academy of Sciences of the United States of America* **111**, E4439-4448 (2014); published online EpubOct 21 (10.1073/pnas.1405752111).
211. H. An, J. W. Harper, Systematic analysis of ribophagy in human cells reveals bystander flux during selective autophagy. *Nature cell biology*, (2017); published online EpubDec 11 (10.1038/s41556-017-0007-x).
212. R. Bruderer, O. M. Bernhardt, T. Gandhi, S. M. Miladinovic, L. Y. Cheng, S. Messner, T. Ehrenberger, V. Zanotelli, Y. Butscheid, C. Escher, O. Vitek, O. Rinner, L. Reiter, Extending the limits of quantitative proteome profiling with data-independent acquisition and application to acetaminophen-treated three-dimensional liver microtissues. *Molecular & cellular proteomics : MCP* **14**, 1400-1410 (2015); published online EpubMay (10.1074/mcp.M114.044305).
213. G. Rosenberger, I. Bludau, U. Schmitt, M. Heusel, C. L. Hunter, Y. Liu, M. J. MacCoss, B. X. MacLean, A. I. Nesvizhskii, P. G. A. Pedrioli, L. Reiter, H. L. Rost, S. Tate, Y. S. Ting, B. C. Collins, R. Aebersold, Statistical control of peptide and protein error rates in large-scale targeted data-independent acquisition analyses. *Nature methods* **14**, 921-927 (2017); published online EpubSep (10.1038/nmeth.4398).
214. J. D. Storey, A direct approach to false discovery rates. *J Roy Stat Soc B* **64**, 479-498 (2002)Unsp 1369-7412/02/64479
Doi 10.1111/1467-9868.00346).

Figure 1

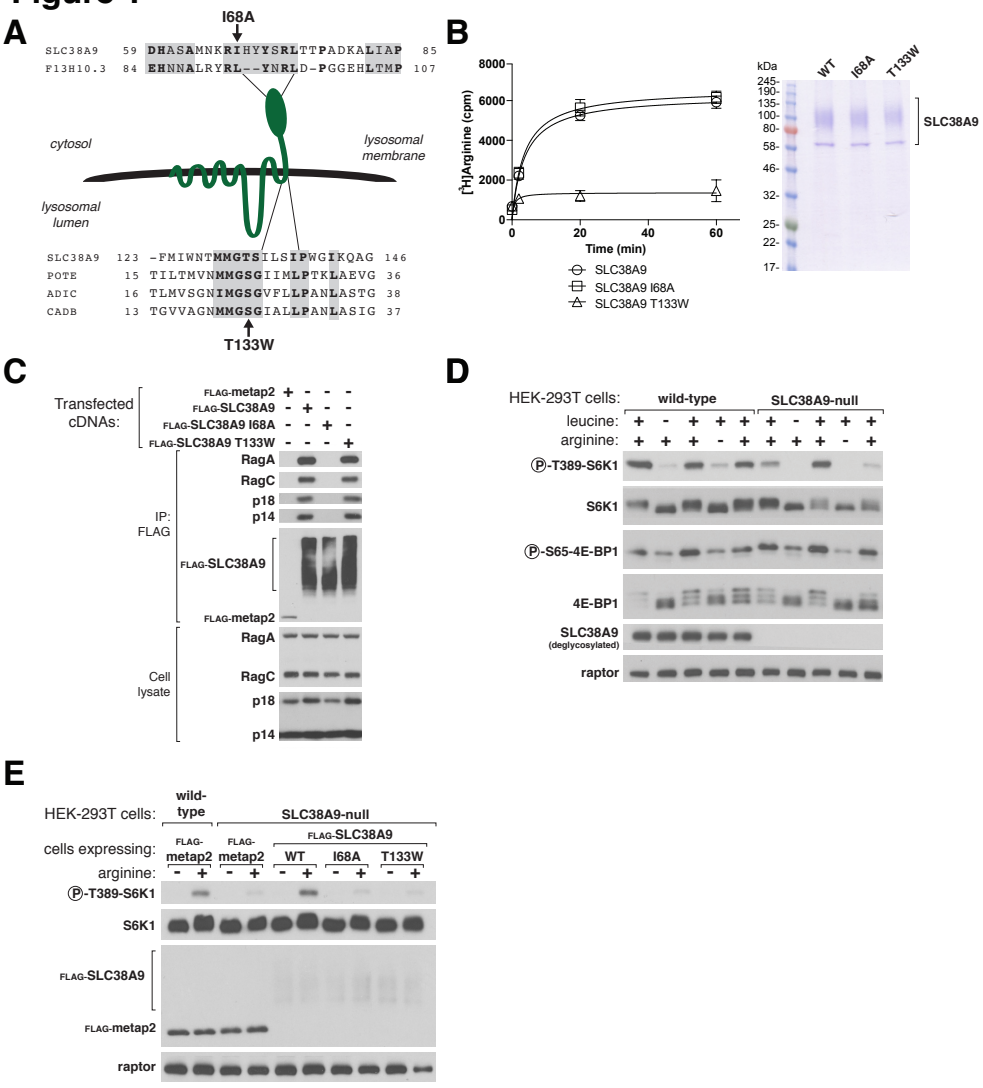
A
I68A
SLC38A9 59 DHASAMNKRIHYYSRLTTPADKALIAP 85
F13H10.3 84 EHNNALRYRL--YNRLD-PGGEHLTMP 107
cytosol
lysosomal membrane
lysosomal lumen
SLC38A9 123 -FMIWNTMMGTSILSIPWGIKQAG 146
POTE 15 TILTMVNMMGSGIIMLPTKLAEVG 36
ADIC 16 TLMVSGNIMGSGVFLLPANLASTG 38
CADB 13 TGVVAGNMMGSGIALLPANLASIG 37
T133W
B
[3H]Arginine (cpm)
Time (min)
SLC38A9
SLC38A9 I68A
SLC38A9 T133W
kDa
WT
I68A
T133W
SLC38A9
C
Transfected cDNAs:
FLAG-metap2
FLAG-SLC38A9
FLAG-SLC38A9 I68A
FLAG-SLC38A9 T133W
IP: FLAG
RagA
RagC
p18
p14
FLAG-SLC38A9
FLAG-metap2
Cell lysate
D
HEK-293T cells:
wild-type
SLC38A9-null
leucine:
arginine:
Ⓟ-T389-S6K1
S6K1
Ⓟ-S65-4E-BP1
4E-BP1
SLC38A9 (deglycosylated)
raptor
E
HEK-293T cells:
wild-type
SLC38A9-null
cells expressing:
FLAG-metap2
FLAG-SLC38A9
WT
I68A
T133W
arginine:
Ⓟ-T389-S6K1
S6K1
FLAG-SLC38A9
FLAG-metap2
raptor

Figure 1, see also Figure S1: A mutant of SLC38A9 that does not interact with arginine cannot signal arginine sufficiency to mTORC1

(A) Schematic depicting domains of SLC38A9 and the location of the I68A and T133W point mutations. Transmembrane segment 1 of SLC38A9 shares sequence similarity with members of the APC superfamily of transporters. F13H10.3 is likely the C. elegans homolog of SLC38A9.

(B) The T133W, but not the I68A, mutant of SLC38A9 is deficient in arginine transport in vitro. SDS-PAGE and Coomassie-blue staining was used to analyze recombinant proteins purified from HEK-293T cells.

(C) Interaction of wild-type SLC38A9 and the T133W mutant, but not the Ragulator-Rag binding mutant I68A or the control protein metap2, with endogenous Ragulator (p18 and p14) and Rag GTPases (RagA and RagC). HEK-293T cells were transfected with the indicated cDNAs and lysates prepared and subjected to anti-FLAG immunoprecipitation and analyzed by immunoblotting.

(D) Loss of SLC38A9 inhibits activation of mTORC1 by arginine, but not leucine. Cells starved of the indicated amino acid for 50 minutes were stimulated for 10 minutes with leucine or arginine and cell lysates analyzed for the specified proteins and phosphorylation states.

(E) For arginine to activate mTORC1 signaling, SLC38A9 must be able to interact with both arginine and Rag-Ragulator. Wild-type and SLC38A9-null cells stably expressing the indicated proteins were analyzed as in (D).

Figure 2

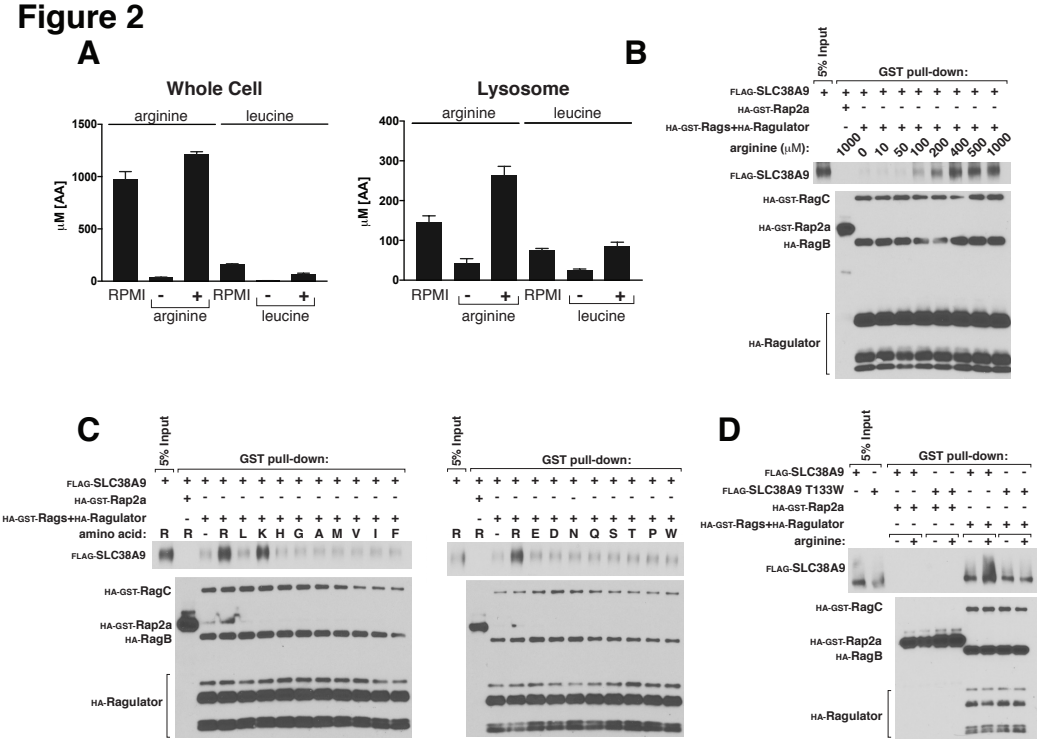
A
Whole Cell
Lysosome
arginine
leucine
μM [AA]
RPMI
arginine
leucine
B
5% Input
GST pull-down:
FLAG-SLC38A9
HA-GST-Rap2a
HA-GST-Rags+HA-Ragulator
arginine (μM):
1000
0
10
50
100
200
400
500
1000
HA-GST-RagC
HA-RagB
HA-Ragulator
C
amino acid:
R R - R L K H G A M V I F
R R - R E D N Q S T P W
D
FLAG-SLC38A9 T133W
arginine:

Figure 2, see also Figure S2: Arginine, at concentrations found in lysosomes, promotes the interaction of SLC38A9 with Rag-Ragulator

(A) Whole-cell and lysosomal arginine and leucine concentrations. HEK-293T cells were starved of the indicated amino acid for 50 minutes and re-stimulated with it for 10 minutes. The RPMI condition represents the non-starved state. Whole-cell and lysosomal arginine and leucine concentrations (mM) were measured using the LysoIP method described in methods. Bar graphs show mean ± SEM (n=3).

(B) In vitro, arginine promotes the interaction of SLC38A9 with the Rag-Ragulator complex in a dose-dependent manner. Purified HA-GST-RagC/HA-RagB and HA-Ragulator were immobilized on glutathione affinity resin and incubated with FLAG-SLC38A9 in the presence of the indicated concentrations of arginine. HA-GST-Rap2A was used as a control. Proteins captured in the glutathione resin pull-down were analyzed by immunoblotting for the indicated proteins using anti-epitope tag antibodies.

(C) Arginine and lysine, but not other amino acids, promote the interaction of SLC38A9 with Rag-Ragulator in vitro. Experiment was performed as in (B), except that all amino acids were at 1 mM.

(D) Arginine does not promote the interaction of SLC38A9 T133W with Rag-Ragulator. The experiment was performed as in (B) except that arginine was used at 500 mM.

Figure 3

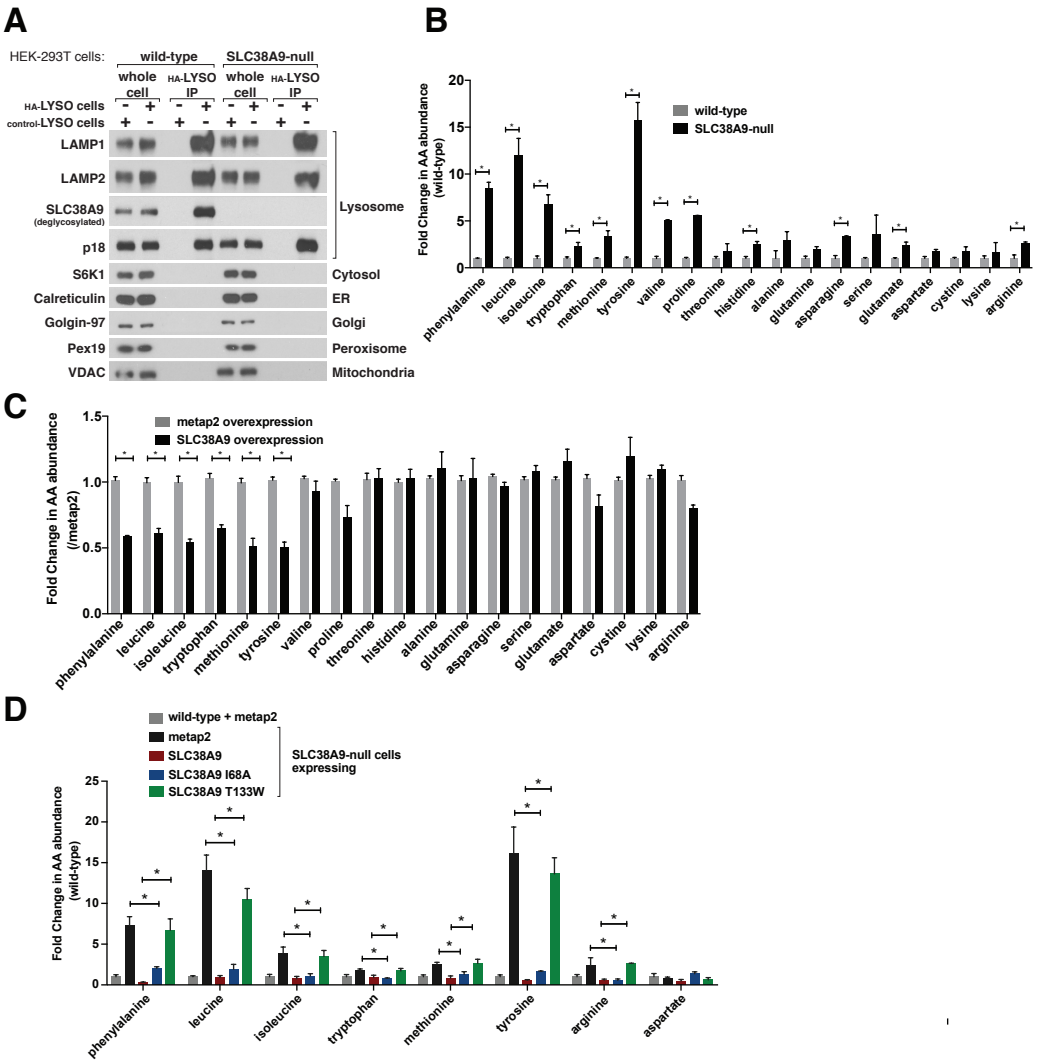
A
HEK-293T cells:
wild-type
SLC38A9-null
whole cell
HA-LYSO IP
HA-LYSO cells
control-LYSO cells
LAMP1
LAMP2
SLC38A9 (deglycosylated)
p18
S6K1
Calreticulin
Golgin-97
Pex19
VDAC
Lysosome
Cytosol
ER
Golgi
Peroxisome
Mitochondria
B
Fold Change in AA abundance (wild-type)
wild-type
SLC38A9-null
phenylalanine
leucine
isoleucine
tryptophan
methionine
tyrosine
valine
proline
threonine
histidine
alanine
glutamine
asparagine
serine
glutamate
aspartate
cystine
lysine
arginine
C
Fold Change in AA abundance (/metap2)
metap2 overexpression
SLC38A9 overexpression
D
Fold Change in AA abundance (wild-type)
wild-type + metap2
metap2
SLC38A9
SLC38A9 I68A
SLC38A9 T133W
SLC38A9-null cells expressing

Figure 3, see also Figure S3: Many essential amino acids accumulate in lysosomes lacking SLC38A9

(A) The rapid immuno-isolation method for lysosomes (LysoIP) yields pure lysosomes from wild-type and SLC38A9-null HEK-293T cells as monitored by immunoblotting for protein markers of various subcellular compartments. Lysates and immunoprecipitates were prepared from HEK-293T cells expressing 2xFLAG-TMEM192 (Control-Lyso cells) or 3XHA-TMEM192 (HA-Lyso cells) as described in the methods.

(B) Many essential amino acids accumulate in the lysosomes of SLC38A9-null HEK-293T cells. Fold changes are relative to concentrations in wild-type HEK-293T cells and bar graphs show mean ± SEM (n=3; *p<0.05).

(C) Overexpression of SLC38A9, but not the control protein metap2, reduces the lysosomal concentrations of most non-polar, essential amino acids (phenylalanine, leucine, isoleucine, tryptophan, and methionine) as well as tyrosine. Fold changes are relative to concentrations in the control metap2-overexpressing HEK-293T cells and bar graphs show mean ± SEM (n= 3; *p<0.05).

(D) Expression of wild-type SLC38A9 or its Rag-Ragulator-binding mutant I68A, but not the transport-deficient T133W mutant, reverses the increase in lysosomal amino acid concentrations caused by loss of SLC38A9. Aspartate was used as a control amino acid as it is unaffected by SLC38A9 loss. Lysosomes were analyzed as in (B) and bar graphs are mean ± SEM (n=3; *p<0.05).

Figure 4

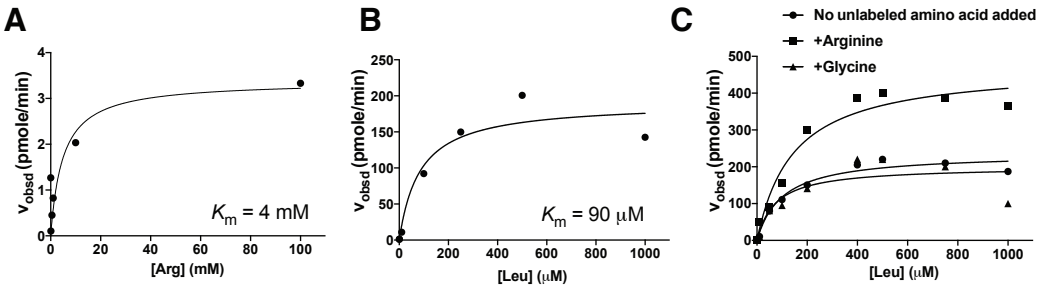
A
B
C
v_{obsd} (pmole/min)
[Arg] (mM)
K_m = 4 mM
[Leu] (μM)
K_m = 90 μM
No unlabeled amino acid added
+Arginine
+Glycine

Figure 4, see also Figure S4: SLC38A9 is an arginine-regulated high affinity transporter for leucine

(A) In vitro SLC38A9 transports arginine with a K_m of ~4 mM in the improved transport assay described in the methods. Experiment was repeated more than three times with similar results, and a representative example is shown.
(B) In vitro SLC38A9 transports leucine with a K_m of ~90 mM. Experiment was repeated more than three times with similar results, and a representative example is shown.
(C) Steady-state kinetic analysis of SLC38A9-mediated leucine transport in the presence of 200 mM arginine, but not glycine, reveals an arginine-induced increase in V_{max} from ~220 to ~470 pmol min^{-1}. Velocity, as shown, was calculated as a function of the leucine concentration. The experiment was repeated three times, with a representative example shown.

Figure 5

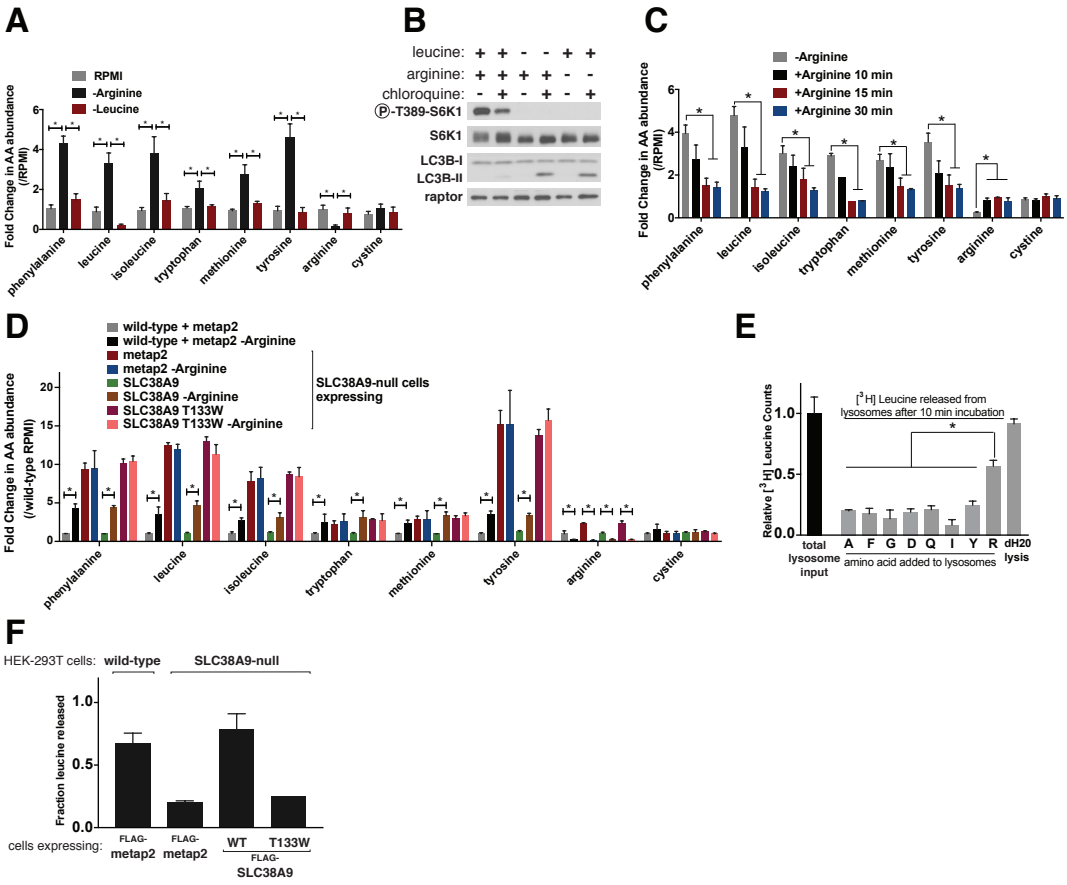
A
RPMI
-Arginine
-Leucine
Fold Change in AA abundance (/RPMI)
phenylalanine
leucine
isoleucine
tryptophan
methionine
tyrosine
arginine
cystine
B
leucine:
arginine:
chloroquine:
Ⓟ-T389-S6K1
S6K1
LC3B-I
LC3B-II
raptor
C
-Arginine
+Arginine 10 min
+Arginine 15 min
+Arginine 30 min
Fold Change in AA abundance (/RPMI)
D
wild-type + metap2
wild-type + metap2 -Arginine
metap2
metap2 -Arginine
SLC38A9
SLC38A9 -Arginine
SLC38A9 T133W
SLC38A9 T133W -Arginine
SLC38A9-null cells expressing
Fold Change in AA abundance (/wild-type RPMI)
E
[3H] Leucine released from lysosomes after 10 min incubation
Relative [3H] Leucine Counts
total lysosome input
A F G D Q I Y R
dH20 lysis
amino acid added to lysosomes
F
HEK-293T cells:
wild-type
SLC38A9-null
Fraction leucine released
cells expressing:
FLAG-metap2
FLAG-metap2
WT
T133W
FLAG-SLC38A9

Figure 5, see also Figure S5: Arginine regulates the lysosomal concentrations of many essential amino acids via SLC38A9

(A) Arginine, but not leucine, deprivation increases the lysosomal concentrations of many of the same amino acids that are affected by loss of SLC38A9. Fold changes are relative to concentrations in cells cultured in RPMI and bar graphs show mean ± SEM (n=3, *p<0.05). HEK-293T cells were incubated in full RPMI media or in RPMI lacking the indicated amino acid for 60 minutes and lysosomes were purified and analyzed as described in methods. Cystine was used as a control metabolite.

(B) Deprivation of arginine or leucine activates autophagy to similar extents. HEK-293T cells were treated as in (A) in the absence or presence of chloroquine and lysates were analyzed for LC3B processing.

(C) Arginine re-addition time-dependently reverses the increase caused by arginine starvation in the lysosomal concentrations of the indicated amino acids. HEK-293T cells deprived of arginine for 50 minutes were re-stimulated with arginine for the indicated times. Fold changes are relative to concentrations in cells cultured in RPMI and bar graphs show mean ± SEM (n=3, *p<0.05). Cystine served as a control metabolite.

(D) In cells lacking SLC38A9 or expressing the transport-deficient T133W mutant, arginine deprivation does not further increase the already high lysosomal concentrations of the SLC38A9-regulated amino acids. Wild-type and SLC38A9-null HEK-293T cells were analyzed as in (A) and fold changes are relative to

cells cultured in RPMI. Bar graphs show mean ± SEM (n=3, *p<0.05). Cystine served as a control metabolite.

(E-F) In vitro, arginine, but not several other amino acids, promotes the release of leucine from lysosomes in a fashion that requires SLC38A9 and its transport function. (E) Purified lysosomes still attached to beads were loaded with [^{3}H]Leucine in vitro for 15 minutes and then stimulated with 500 mM of the indicated amino acid for 10 minutes. The amount of [^{3}H]Leucine released was quantified and normalized to the total amount of [^{3}H]leucine in lysosomes. This amount was obtained in two ways that gave the same value: by measuring the [^{3}H]Leucine in the bead-bound lysosomes not simulated with an amino acid after the 15 minute loading period or in the supernatant of lysosomes lysed with distilled water (dH_20 lysis). (F) Arginine does not induce leucine release in lysosomes lacking SLC38A9 or containing the T133W mutant. The experiment was performed as in (E) using lysosomes from the appropriate cell lines.

Figure 6

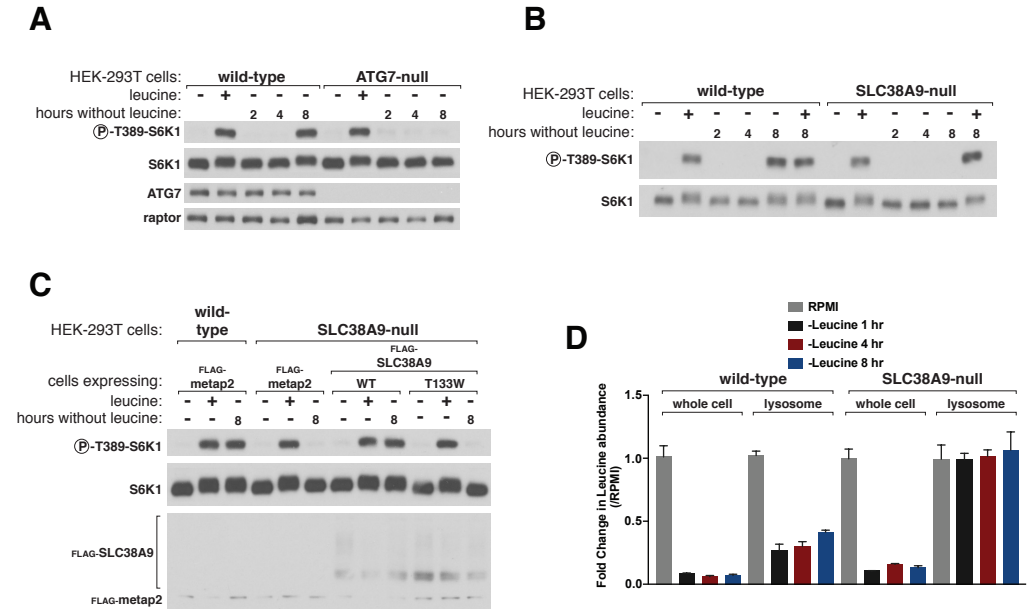
A
HEK-293T cells:
wild-type
ATG7-null
leucine:
hours without leucine:
Ⓟ-T389-S6K1
S6K1
ATG7
raptor
B
HEK-293T cells:
wild-type
SLC38A9-null
leucine:
hours without leucine:
Ⓟ-T389-S6K1
S6K1
C
HEK-293T cells:
wild-type
SLC38A9-null
cells expressing:
FLAG-metap2
FLAG-SLC38A9
WT
T133W
leucine:
hours without leucine:
Ⓟ-T389-S6K1
S6K1
FLAG-SLC38A9
FLAG-metap2
D
RPMI
-Leucine 1 hr
-Leucine 4 hr
-Leucine 8 hr
wild-type
SLC38A9-null
whole cell
lysosome
Fold Change in Leucine abundance (/RPMI)
1.5
1.0
0.5
0.0

Figure 6, see also Figure S6: SLC38A9 is required for amino acids produced via autophagy to activate mTORC1 and to support cell proliferation

(A) Loss of ATG7 prevents the autophagy-mediated reactivation of mTORC1 that occurs after long-term leucine deprivation. Wild-type and ATG7-null HEK-293T cells were deprived of leucine for either 50 minutes or the indicated time points, and where specified, restimulated for 10 minutes with leucine. Cell lysates were analyzed by immunoblotting for the total levels and phosphorylation states of the indicated proteins.

(B) Loss of SLC38A9 prevents the autophagy-mediated reactivation of mTORC1 that occurs after long-term leucine deprivation. Wild-type or SLC38A9-null HEK-293T cells were deprived of leucine for 50 minutes or the indicated time points and, where indicated, re-stimulated with leucine for 10 minutes. Cell lysates were analyzed by immunoblotting for the levels and phosphorylation states of indicated proteins.

(C) mTORC1 signaling does not reactivate after long-term leucine deprivation in cells expressing the T133W SLC38A9 mutant. Wild-type or SLC38A9-null HEK-293T cells stably expressing the indicated proteins were starved for leucine for 50 minutes or 8 hours and, where indicated, re-stimulated with leucine for 10 minutes. Lysates were analyzed as in (A).

(D) In cells lacking SLC38A9, lysosomal leucine concentrations do not drop upon starvation for leucine despite its depletion at the whole-cell level. Metabolite

profiling of lysosomes from wild-type and SLC38A9-null cells deprived of leucine for the indicated times. Fold changes are relative to concentrations of cells in cultured in RPMI. Bar graphs show mean ± SEM (n=3).

Figure 7

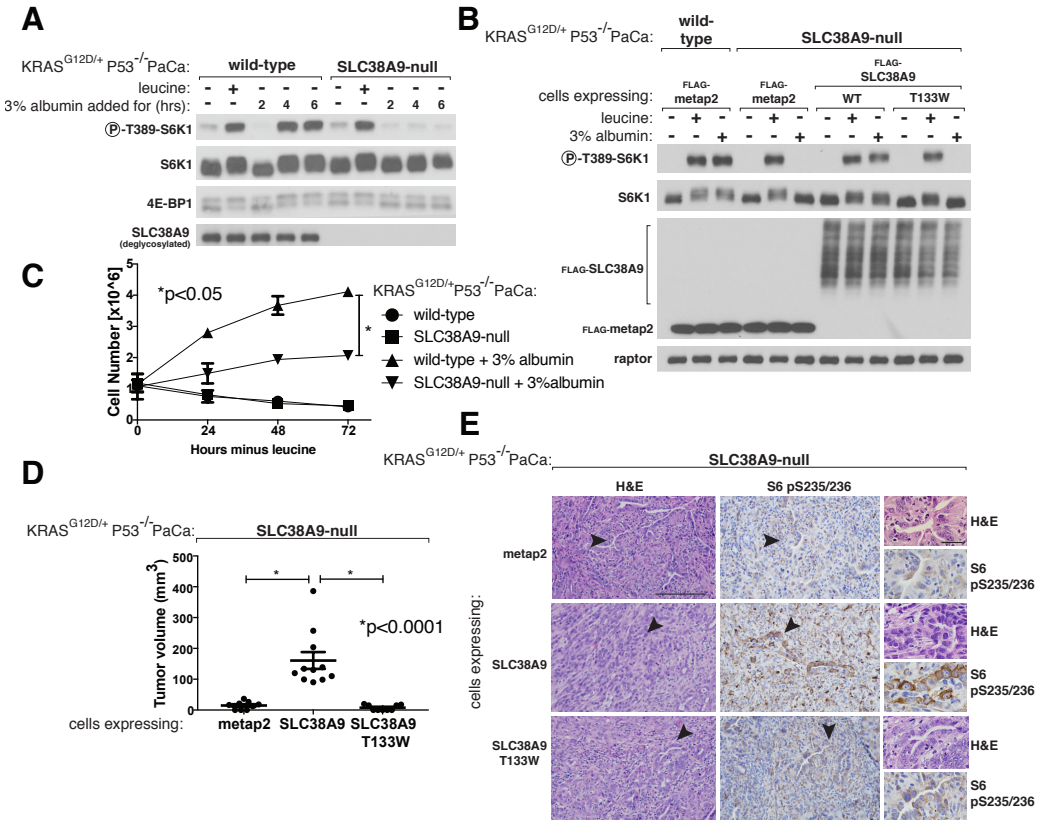
A
KRASG12D/+ P53-/-PaCa:
wild-type
SLC38A9-null
leucine:
3% albumin added for (hrs):
Ⓟ-T389-S6K1
S6K1
4E-BP1
SLC38A9 (deglycosylated)
B
KRASG12D/+ P53-/-PaCa:
wild-type
SLC38A9-null
cells expressing:
FLAG-metap2
FLAG-SLC38A9
WT
T133W
leucine:
3% albumin:
Ⓟ-T389-S6K1
S6K1
FLAG-SLC38A9
FLAG-metap2
raptor
C
*p<0.05
Cell Number [x10^6]
Hours minus leucine
KRASG12D/+P53-/-PaCa:
wild-type
SLC38A9-null
wild-type + 3% albumin
SLC38A9-null + 3%albumin
D
KRASG12D/+ P53-/-PaCa:
SLC38A9-null
Tumor volume (mm3)
*p<0.0001
cells expressing:
metap2
SLC38A9
SLC38A9 T133W
E
KRASG12D/+ P53-/-PaCa:
SLC38A9-null
H&E
S6 pS235/236
cells expressing:
metap2
SLC38A9
SLC38A9 T133W

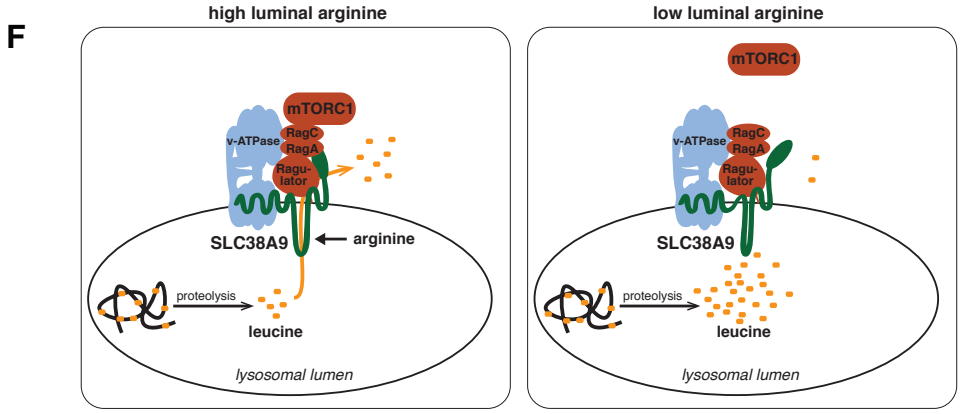
F
high luminal arginine
low luminal arginine
mTORC1
v-ATPase
RagC
RagA
Ragu-lator
SLC38A9
arginine
proteolysis
leucine
lysosomal lumen

Figure 7: SLC38A9 and its transport function are required for albumin to activate mTORC1 and support cell proliferation and for pancreatic tumor growth

(A-B) Loss of SLC38A9 or just its transport capacity prevents the activation of mTORC1 induced by extracellular protein. Murine $KRAS^{G12D/+}P53^{-/-}$ pancreatic cancer cells that are wild-type, null for SLC38A9, or SLC38A9-null and expressing T133W SLC38A9, were deprived of leucine for 50 minutes and re-stimulated with leucine for 10 minutes or 3% albumin for the times indicated. Cell lysates were analyzed by immunoblotting for the levels or phosphorylation states of indicated proteins.

(C) Loss of SLC38A9 inhibits the proliferation of pancreatic cancer cells cultured in 3% albumin as the leucine source. Wild-type and SLC38A9-null murine $KRAS^{G12D/+}P53^{-/-}$ pancreatic cancer cells were cultured for 3 days in media lacking leucine, and supplemented, where indicated, with 3% albumin. Cells were counted every 24 hours and bar graphs show mean ± SD (n=3; *$p<0.05$).

(D) $KRAS^{G12D/+}P53^{-/-}$ pancreatic cancer cells lacking SLC38A9 or expressing its transport deficient T133W mutant have a severe defect in forming tumors in an orthotropic allograft model of pancreatic cancer. SLC38A9-null $KRAS^{G12D/+}P53^{-/-}$ PaCa cells expressing the control protein metap2, SLC38A9, or SLC38A9 T133W were used to generate tumors. Each dot represents the calculated tumor volume (mm^3) of an individual tumor. The mean ± SEM (n= 9-11, *$p<0.0001$) is shown.

(E) Tumors formed by $KRAS^{G12D/+}P53^{-/-}$ pancreatic cancer cells lacking SLC38A9 or expressing its transport deficient T133W mutant have decreased mTORC1 signaling. Tumors were analyzed by immunohistochemistry for S6 pS235/S236 levels and stained with hematoxyline and eosin (H&E) (10X and 40X magnifications are shown, arrow defines pancreatic cancer cells shown in 40X insets). Scale bars represent 100 mM (10X) and 20 mM (40X).

(F) A model depicting how arginine signals through SLC38A9 to promote mTORC1 activation as well as the lysosomal efflux of essential amino acids like leucine.

Supplemental Figure 1

A

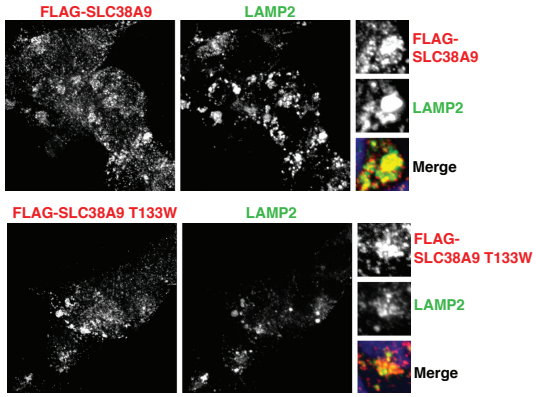

Supplementary Figure 1. The SLC38A9 T133W mutant still localizes to lysosomes, Related to Figure 1

Localization of wild-type and T133W SLC38A9 in HEK-293T cells. The T133W mutation does not affect the lysosomal localization of SLC38A9. HEK-293T cells stably expressing either wild-type or T133W FLAG-SLC38A9 were immunostained for FLAG and LAMP2.

Supplemental Figure 2

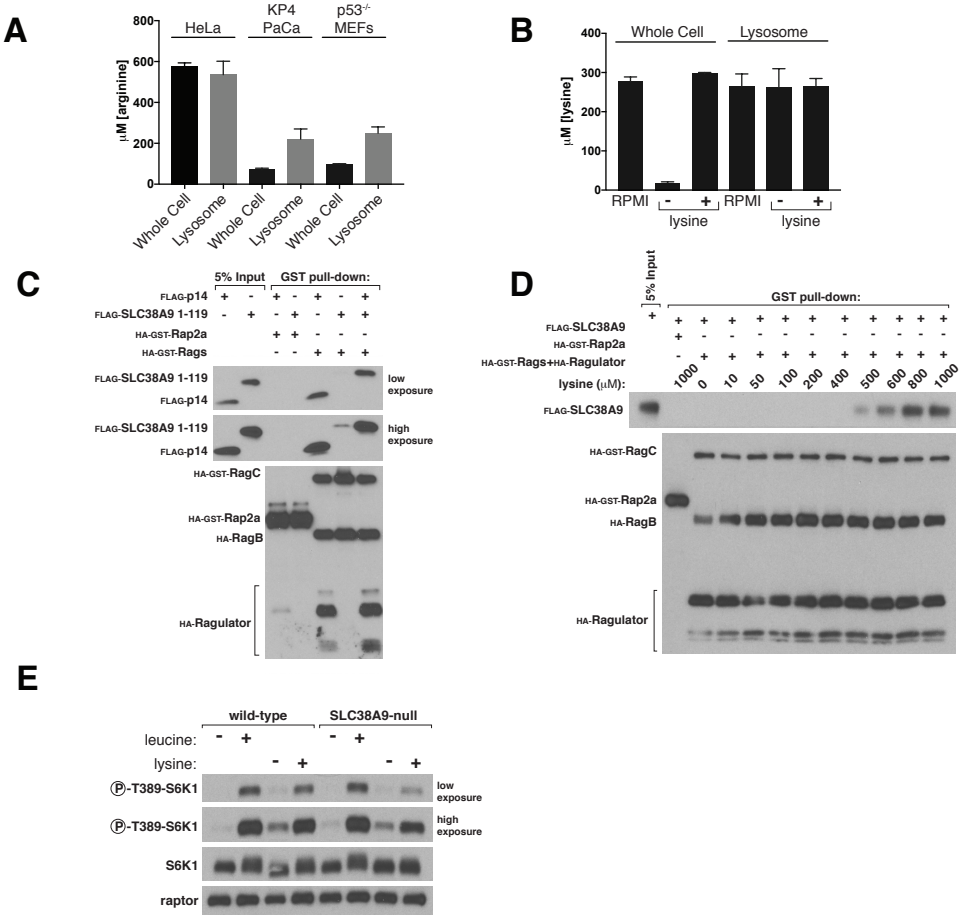

Supplementary Figure 2. At higher concentrations than arginine, lysine promotes the interaction between SLC38A9 and Rag-Ragulator in vitro, , Related to Figure 2

A) Whole-cell and lysosomal arginine concentrations in HeLa, KP4 pancreatic cancer cells, and $P53^{-/-}$ MEFs. Amino acid concentrations (mM) were measured in lysosomes captured using the LysoIP method referenced in the methods. Bar graphs show mean ± SEM (n=3).

B) Whole-cell and lysosomal lysine concentrations. HEK-293T cells were starved of the indicated amino acid for 50 minutes and re-stimulated with it for 10 minutes. The RPMI condition represents the non-starved state. Whole-cell and lysosomal lysine concentrations (mM) were measured using the LysoIP method described in methods. Bar graphs show mean ± SEM (n=3).

C) The soluble N-terminal domain of SLC38A9 interacts with purified Rag-Ragulator in vitro. Purified HA-GST-Rag-Ragulator or HA-GST-RagC-HA-RagB were immobilized on a glutathione affinity resin and incubated with FLAG-SLC38A9 1-119. HA-GST-Rap2A was used as a control. Proteins captured on the glutathione affinity resin were analyzed by immunoblotting for the indicated proteins using anti-epitope tag antibodies.

D) In vitro, lysine promotes the interaction of SLC38A9 with the Rag-Ragulator complex in a dose-dependent manner. Purified HA-GST-RagC/HA-RagB and HA-Ragulator were immobilized on a glutathione

affinity resin and incubated with FLAG-SLC38A9 in the presence of the indicated concentrations of lysine. HA-GST-Rap2A was used as a control. Proteins captured in the glutathione resin pull-down were analyzed by immunoblotting using anti-epitope tag antibodies.

E) Lysine mildly regulates mTORC1 signaling. Cells starved of indicated amino acid for 50 minutes were stimulated for 10 minutes with leucine or lysine and cell lysates analyzed for the specified proteins and phosphorylation states.

Supplemental Figure 3

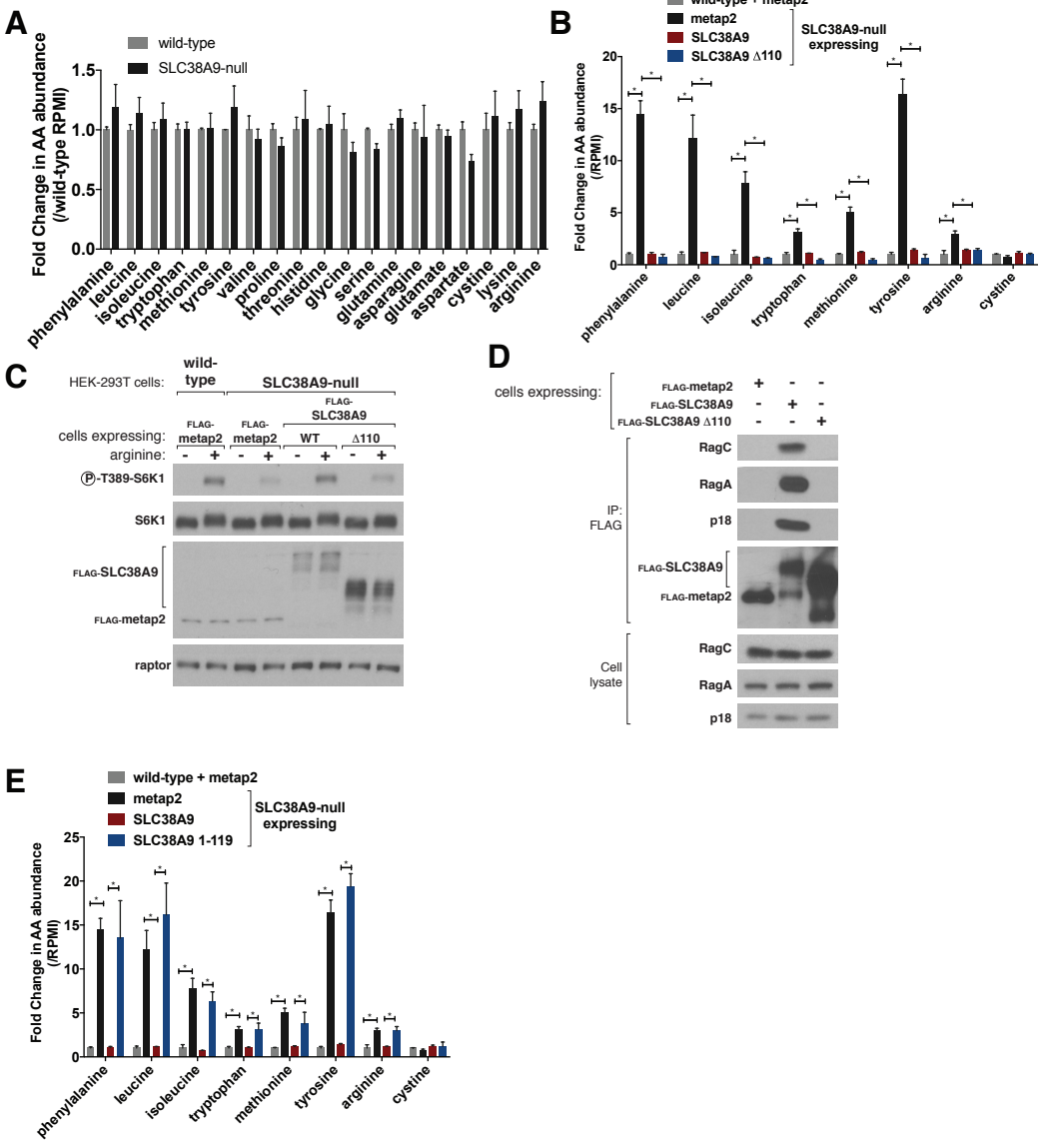

Supplementary Figure 3. Mutants of SLC38A9 that do not interact with Rag-Ragulator are still able to reverse the lysosomal accumulation of essential amino acids caused by loss of SLC38A9, Related to Figure 3

A) Loss of SLC38A9 does not affect whole cell amino acid concentrations in HEK-293T cells. Fold changes are relative to concentrations in wild-type HEK-293T cells. Bar graphs show mean ± SEM (n=3).

B) Expression of wild-type SLC38A9 or a variant lacking the N-terminal domain (D110) in the SLC38A9-null cells reverses the increase in lysosomal amino acid concentrations caused by loss of SLC38A9. Cystine was used as a control metabolite as it is unaffected by SLC38A9 loss. Lysosomes were analyzed as in Figure 3B and bar graphs show mean ± SEM (n=3; *$p<0.05$).

C) Expression of a variant of SLC38A9 lacking the N-terminal domain (D110) in the SLC38A9-null cells does not rescue the arginine-sensing defect. Wild-type or SLC38A9-null cells stably expressing the indicated proteins were deprived of arginine for 50 minutes and were stimulated for 10 minutes with arginine and cell lysates were analyzed for the specified proteins and phosphorylation states.

D) Wild-type SLC38A9, but not a variant lacking the N-terminal domain (D110) or the control protein metap2, interacts with endogenous Ragulator (p18) and the Rag GTPases (RagA and RagC). Lysates prepared from HEK-293T cells stably expressing the indicated proteins were subjected to anti-FLAG immunoprecipitation followed by immunoblotting for the indicated proteins.

E) Expression of wild-type SLC38A9, but not of the soluble N-terminal Rag-Ragulator binding domain of SLC38A9, in SLC38A9-null cells reverses the increase in lysosomal amino acid concentrations caused by loss of SLC38A9. Cystine was used as a control metabolite. Lysosomes were analyzed as in Figure 3B and bar graphs show mean ± SEM (n=3; *p<0.05).

Supplemental Figure 4

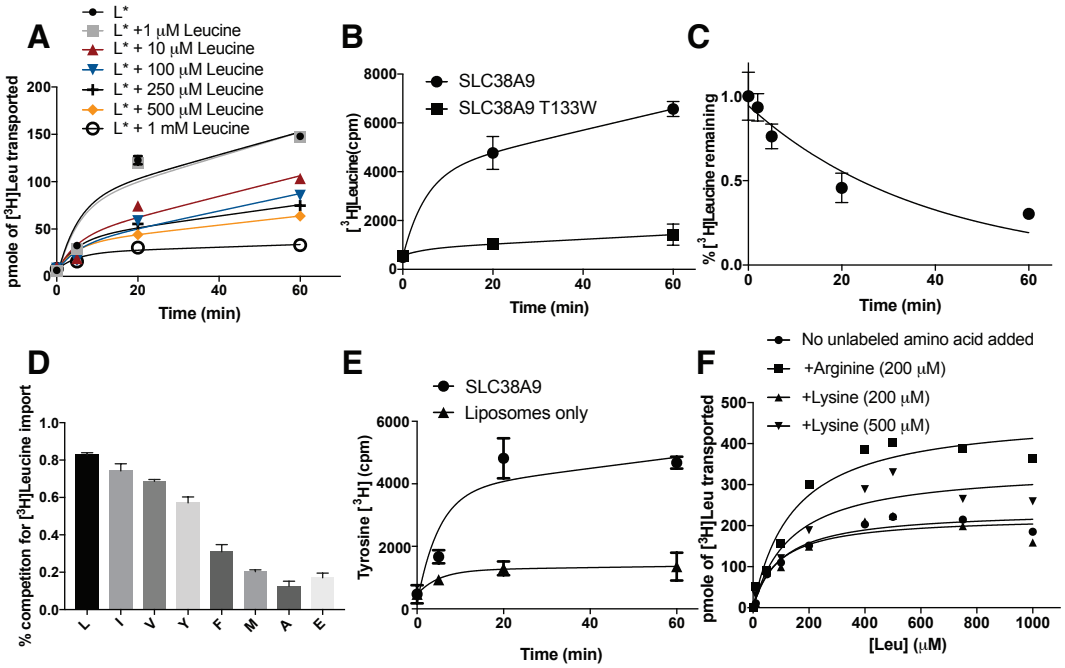

Supplementary Figure 4. Characterization of *in vitro* leucine transport by SLC38A9, Related to Figure 4

A) Steady-state kinetic analyses of SLC38A9 leucine transport reveals a K_m of ~90 mM for leucine. Transport over time of [^{3}H]leucine (0.5 mM) in the presence of increasing concentrations of unlabeled leucine.

B) The T133W mutant of SLC38A9 does not transport leucine in vitro. Each point represents mean ± SD (n=3).

C) Time dependent efflux of leucine from SLC38A9-containing proteoliposomes loaded for 90 minutes with [^{3}H]leucine (0.5 mM). Each point represents mean ± SD (n=3).

D) Competition of SLC38A9-mediated [^{3}H]leucine (0.5 mM) transport by 1 mM of the indicated unlabeled amino acids. Bar graphs show mean ± SD (n=3).

E) SLC38A9 transports [^{3}H]tyrosine (0.5 mM) in vitro. Each point shows mean ± SD (n=3).

F) At concentrations higher than arginine, lysine mildly increases in vitro leucine transport by SLC38A9. Steady-state kinetic analysis of SLC38A9-mediated leucine transport in the presence of 200 or 500 mM lysine.

Supplemental Figure 5

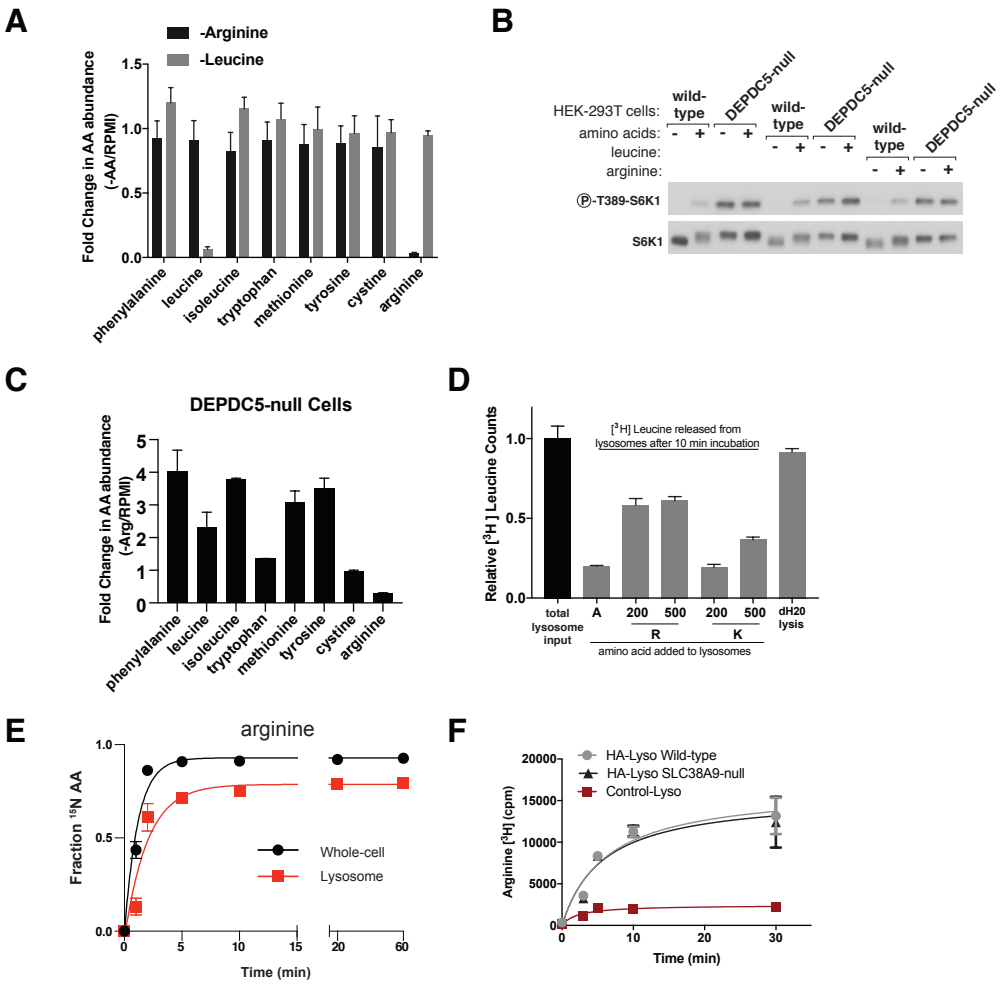

Supplementary Figure 5. The effects of arginine on the lysosomal levels of many essential amino acids is not due to mTORC1 modulation, Related to Figure 5

A) Fold change in whole cell amino acid concentrations in HEK-293T cells incubated in media lacking arginine or leucine relative to those cultured in full RPMI. Bar graphs show mean ± SEM (n=3; *p<0.05).

B) In cells lacking DEPDC5, a component of GATOR1, mTORC1 signaling is insensitive to deprivation of all amino acids, leucine, or arginine as assessed by the phosphorylation of S6K1. Wild-type and DEPDC5-null HEK-293T cells were deprived of all amino acids or the indicated amino acid for 50 minutes and restimulated with all amino acids or indicated amino acid for 10 minutes. Cell lysates were prepared and analyzed by immunoblotting for the total levels and phosphorylation state of S6K1.

C) In DEPDC5-null HEK-293T cells arginine deprivation increases the lysosomal concentrations of many of the same amino acids affected by loss of SLC38A9 in wild type cells. Fold changes are relative to concentrations in full RPMI media.

D) Lysine mildly promotes the release of leucine from lysosomes at higher concentrations than arginine. Purified lysosomes still attached to beads were loaded with [^{3}H]leucine in vitro for 15 minutes and then stimulated with either 200 mM or 500 mM of the indicated amino acids for 10 minutes. Alanine at 500 mM was used as a negative control. The amount of [^{3}H]leucine released

was quantified and normalized to the total amount of [^{3}H]leucine in lysosomes. This amount was obtained in two ways that gave the same value: by measuring the [^{3}H]leucine in the bead-bound lysosomes not simulated with an amino acid after the 15 minute loading period or in the supernatant of lysosomes lysed with distilled water (dH_20 lysis).

E) Exogenously added arginine enters the lysosomes of live cells. Cells incubated in media containing ^{15}N-labeled arginine for various times were subjected to the LysoIP method. Data are presented as the fraction of the total pool of arginine in whole cells (black) or lysosomes (red) that is ^{15}N-labeled (mean ± SEM, n=3 for each time point).

F) Lysosomes lacking SLC38A9 take up [^{3}H]arginine to the same extent as wild-type lysosomes. Purified lysosomes from wild-type or SLC38A9-null cells still attached to beads were loaded with [^{3}H]arginine for indicated time. Control-Lyso cells serve as negative control for background radioactive binding to beads.

Supplemental Figure 6

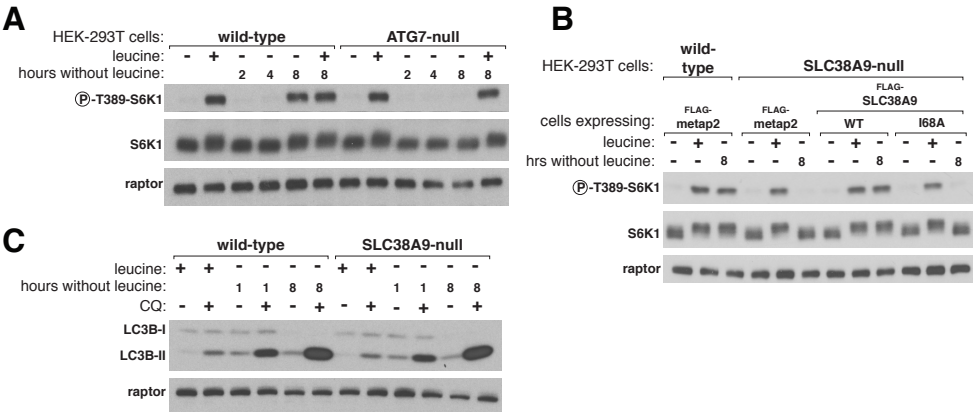

Supplementary Figure 6, Reactivation of mTORC1 following long term leucine deprivation requires ATG7, Related Figure 6

A) Wild-type and ATG7-null HEK-293T cells were deprived of leucine for either 50 minutes or the indicated time points, and where specified, restimulated for 10 minutes with leucine. Cell lysates were analyzed by immunoblotting for the total levels and phosphorylation states of the indicated proteins.

B) mTORC1 signaling does not reactivate after long-term leucine deprivation in cells expressing the I68A SLC38A9 mutant. Wild-type or SLC38A9-null HEK-293T cells stably expressing the indicated proteins were starved for leucine for 50 minutes or 8 hours and, where indicated, re-stimulated with leucine for 10 minutes. Lysates were analyzed as in (A).

C) Loss of SLC38A9 does not affect the activation of autophagy. Wild-type or SLC38A9-null HEK-293T cells were deprived of leucine for the indicated times in the presence or absence of chloroquine (30 mM) to assess LC3B processing. Cell lysates were analyzed by immunoblotting for the indicated proteins.

Supplemental Figure 7

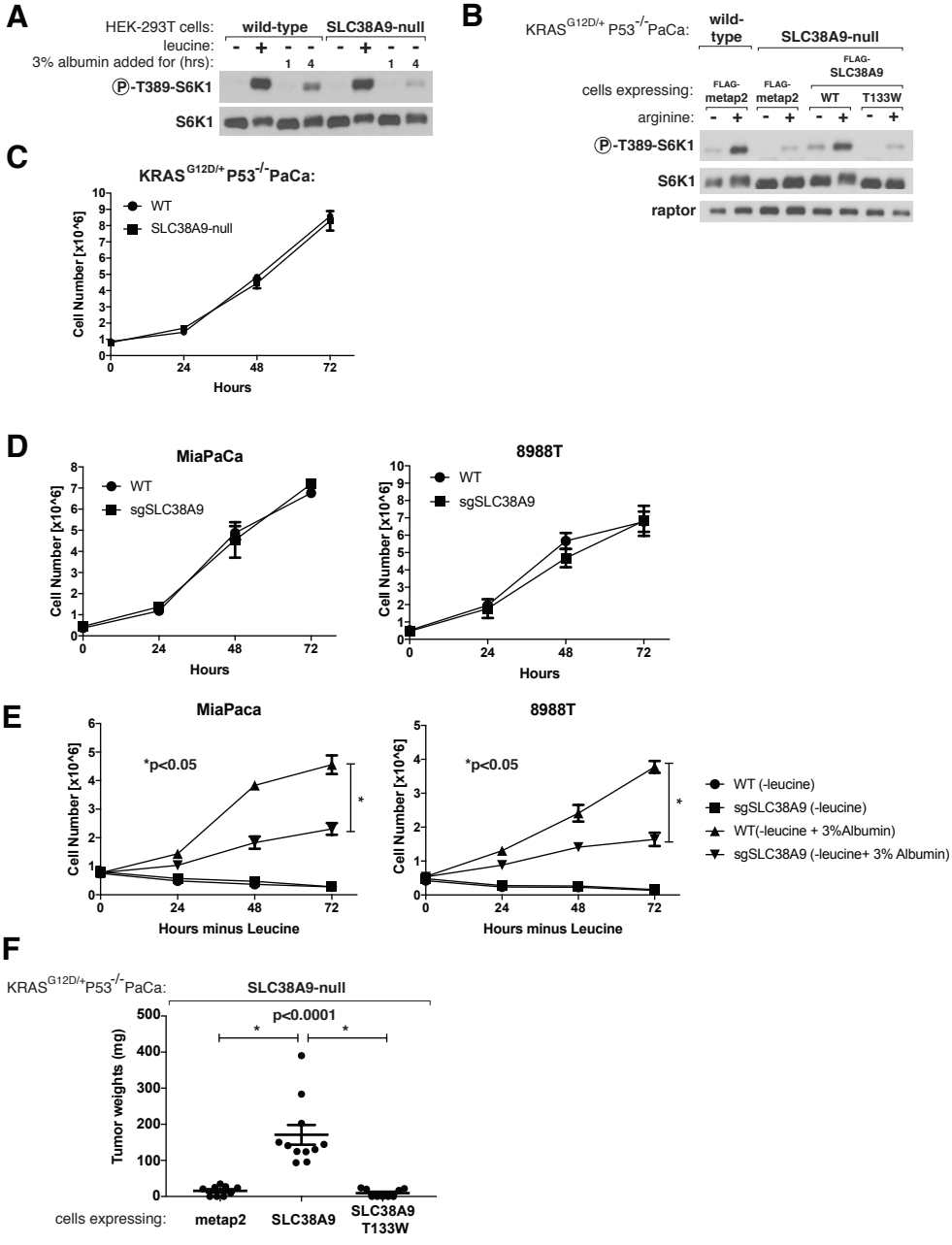

Supplementary Figure 7, SLC38A9 and its transport function are required for albumin to reactivate mTORC1 and support proliferation in culture and tumor formation *in vivo*, Related to Figure 7

A) Loss of SLC38A9 blocks the moderate reactivation of mTORC1 induced by 3% albumin in HEK-293T cells deprived of leucine. Wild-type or SLC38A9-null HEK-293T cells were deprived of leucine for 50 minutes, or the indicated time points, were restimulated with either free leucine for 10 minutes or 3% albumin for 1 or 4 hours. Cell lysates were analyzed by immunoblotting for the total levels and phosphorylation states of the indicated proteins.

B) SLC38A9-null murine $KRAS^{G12D/+}P53^{-/-}$ pancreatic cancer cells do not reactivate mTORC1 in response to arginine. Wild-type or SLC38A9-null cells stably expressing the indicated proteins were analyzed by immunoblotting for the total levels and phosphorylation states of the indicated proteins.

C) Proliferation of wild-type and SLC38A9-null murine $KRAS^{G12D/+}P53^{-/-}$ pancreatic cancer cells cultured in full media (mean ± SD, n=3 for each time point).

D) Proliferation of wild-type and sgSLC38A9 human 8988T and Mia-PaCa pancreatic cancer cells cultured in full media (mean ± SD, n=3 for each time point).

E) Loss of SLC38A9 inhibits the proliferation of human pancreatic cancer cells cultured in 3% albumin as the leucine source. Wild-type and sgSLC38A9 8988T and Mia-PaCa pancreatic cancer cells were cultured for 3 days in

media lacking leucine, which was supplemented, where indicated with 3% albumin. Cells were counted every 24 hours and bar graphs show mean ± SD (n=3, *p<0.05).

F) Estimated weights (mg) of tumors formed by SLC38A9-null $KRAS^{G12D/+}P53^{-/-}$ PaCa cells expressing SLC38A9, SLC38A9 T133W, or a control protein metap2. Data are presented as mean ± SEM (n=9-11, *p<0.05).

Methods

Detailed methods are provided in the online version of this paper and include the following:

Experimental Model and Subject Details

-Cell lines

-Cell Culture Conditions

Method Details

-Cell Lysis, Immunoprecitpitations, and cDNA transfections

-Generation of cells lacking SLC38A9

-Generation of cells stably expressing cDNAs

-Purification of wild-type and mutant FLAG-SLC38A9

-In vitro binding of SLC38A9 to the Rag-Ragulator Complex

-Proteoliposome reconstitution and transport Assay

-Method for rapid purification and metabolite profiling of lysosomes (LysoIP)

-Radiolabeled amino acid uptake by purified lysosomes

-Immunofluorescence assays

- Orthotopic implantation of cells in the mouse pancreas and tumor analyses

Quantification and statistical analyses

Contact for Reagent and Resource Sharing

Further information and requests for resources and reagents should be directed to and will be fulfilled by the Lead Contact, David M. Sabatini (Sabatini@wi.mit.edu)

Experimental Model and Subject detail

Cell Lines

The following cell lines were kindly provided by: Mia-PaCa, KP4, and 8988T, Dr. Rushika Perera (UCSF); Kras G12D/+ P53-/- mouse PaCa cells, Dr. Matt Vander Heiden (MIT). Remaining cell lines (HEK-293T, HeLa) were purchased from the ATCC. Cell lines were verified to be free of mycoplasma contamination and the identities of all were authenticated by STR profiling.

Cell Culture Conditions

HEK-293T, HeLa, MIA-PaCa, 8988T, KP4, $P53^{-/-}$ MEFs, and $KRAS^{G12D/+}$ $P53^{-/-}$ mouse PaCa cells and their derivatives were maintained at 37°C and 5% CO_2 in DMEM supplemented with 10% inactivated fetal calf serum, 2 mM glutamine, penicillin, and streptomycin. For experiments involving amino acid starvation or restimulation, cells were treated as previously described (*53*). For experiments involving amino acid stimulation, wells were incubated in RPMI base media lacking the indicated amino acid for 50 min and then stimulated with indicated amino acid at RPMI concentrations for 10 min. For all experiments involving lysosomal purifications, cells were changed to fresh RPMI base media 1 hr prior to the start of the experiment.

Method Detail

Cell lysis, immunoprecipitations, and cDNA transfections

Cells were first rinsed with chilled PBS and lysed immediately on ice with Triton X-100 lysis buffer (1% Triton, 10 mM B-glycerol phosphate, 10 mM

pyrophosphate, 40 mM HEPES pH 7.4, 2.5 mM $MgCl_2$) supplemented with 1 tablet of EDTA-free protease inhibitor (Roche) per 25 mL buffer. Lysates were kept at 4°C for 15 min and then clarified by centrifugation in a microcentrifuge at 13,000 rpm at 4°C for 10 min. For anti-FLAG immunoprecipitations, the FLAG-M2 affinity gel was washed with 1 mL lysis buffer three times and 30 uL of a 50% slurry of the affinity gel was then added to the clarified lysate and incubated with rotation at 4°C for 90 min.

For transfection-based experiments in HEK-293T cells, 2 million cells were plated in 10 cm culture plates. After twenty-four hours, cells were transfected using the polyethylenimine method using pRK5-based cDNA expression vectors as indicated (*187*). The total amount of transfected plasmid DNA in each transfection was normalized to 5 mg using the empty pRK5 plasmid. After thirty-six hours, cells were lysed and analyzed as described above.

Generation of cells lacking SLC38A9

HEK-293T SLC38A9-null cells are clonal populations generated previously (*53*). sgSLC38A9 8988T and Mia-PaCa cell lines were made using the pLenticrispr system utilizing the same guides as described previously (*53*). For the generation of the SLC38A9-null murine $KRAS^{G12D/+}P53^{-/-}$ PaCa cells, the following guide sequence targeting the first exon of SLC38A9 were designed and cloned into the px459 crispr vector.

Sense: ATGCTATGTGTATAGTCCAT

Antisense: ATGGACTATACACATAGCAT

Generation of cells stably expressing cDNAs

The following lentiviral expression plasmids were used: pLJM1-FLAG-metap2, pLJM60-FLAG-SLC38A9 and subsequent mutants, pLJC5-FLAG-SLC38A9 and subsequent mutants. For lysosomal purifications, pLJC5-3XHA-TMEM192 and pLJC5-2XFLAG-TMEM192 or pLJC6-3XHA-TMEM192 and pLJC6-2XFLAG-TMEM192. Lentiviruses were produced by transfection of HEK-293T cells with plasmids indicated above in combination with the VSV-G and CMV DVPR packaging plasmids. Twelve hours post transfection, the media was changed to DMEM supplemented with 30% IFS. Thirty-six hours later, the virus containing supernatant was collected and frozen at -80°C for 30 min. Cells to be infected were plated in 12-well plates containing DMEM supplemented with 10% IFS with 8 mg ml^{-1} polybrene and infected with the virus containing medium. Twenty-four hours later, the cell culture medium was changed to media containing puromycin or blasticidin for selection.

Purification of wild-type and mutant FLAG-SLC38A9

For isolation of active SLC38A9, it was important to isolate FLAG-SLC38A9 from stably expressing cells rather than from those transiently expressing it. We also developed an optimized purification strategy to enrich for properly folded and membrane inserted SLC38A9. In brief, HEK-293T cells stably expressing FLAG-SLC38A9 were harvested from 15 cm cell culture plates by gentle scraping in Buffer A (20 mM HEPES pH 7.4, 150 mM NaCl, 2 mM DTT) containing protease

inhibitors. Harvested cells were collected and disrupted by douncing 30 times on ice with douncers that were pre-chilled. Unbroken cells and the nuclear fraction were removed by centrifugation at 10,000 g for 20 min. The supernatant from the first centrifugation was then centrifuged at 150,000 g for 90 min to 2 hr to pellet the membrane fraction. The pellet was solubilized using Buffer B (20 mM HEPES pH 7.4, 500 mM NaCl, 2 mM DTT, and 1% DDM) for at least 4 hours to overnight with rotation at 4°C. Following solubilization of the membrane fraction, a supernatant was prepared by centrifuging at 20,000 g to pellet any insoluble material. FLAG-affinity beads (equilibrated in Buffer B) were added to the supernatant followed by a 3 hr immunoprecipitation at 4°C. FLAG-affinity purified SLC38A9 protein was then washed 3 times in Buffer C (20 mM MES, 500 mM NaCl, 2 mM DTT, and 0.1% DDM) and eluted in Buffer C without NaCl containing 1 mg/ml FLAG peptide with rotation at 4°C for 1 hr. The eluted protein was concentrated using Amicon centrifuge filters to ~1 mg/ml, and if necessary, purified SLC38A9 was snap-frozen in Buffer C without NaCl supplemented with glycerol in liquid nitrogen and stored at -80°C.

In vitro binding of SLC38A9 to the Rag-Ragulator Complex

Purifications of GST-tagged Rag GTPases and Ragulator for in vitro binding assays were performed as previously described (*50*) with the following modifications. In brief, 4 million HEK-293T cells were plated in 15 cm culture dishes. For proteins produced via transient expression, after 48 hr cells were transfected with following amounts of cDNAs in the pRK5 expression vector

using the PEI method (*187*): 5 mg HA-GST-Rap2a; or 2 mg HA-GST-RagC, 8 mg of HA-RagB, 8 mg of HA-p18, 8 mg of HA-p14, 8 mg of HA-MP1, 8 mg of HA-HBXIP, and 8 mg of HA-c7orf59. For isolation of Ragulator/Rag GTPase complexes, it was critical to purify them using HA-GST-tagged Rag components rather than HA-GST-tagged Ragulator components. Thirty-six hours post transfection, cells were lysed as indicated above. After clearing of cell lysates, 200 mL of 50% slurry of immobilized glutathione affinity resin equilibrated in lysis buffer was added to lysates expressing GST-tagged proteins. Recombinant proteins were incubated with the affinity resin for 2 hr at 4°C with rotation. Each sample was washed 3 times in binding buffer consisting of 0.1% TX-100, 2.5 mM $MgCl_2$, 20 mM HEPES pH 7.4, and 150 mM NaCl.

The purification of SLC38A9 is described above. For the purification of the FLAG-SLC38A9 1-119 fragment, HEK-293T cells were prepared as above and transfected with 10 mg of FLAG-SLC38A9 1-119 in the pRK5 expression vector. Following cell lysis as described above and clearing of the lysate, 100 mL of a 50% slurry of immobilized FLAG affinity resin equilibrated in lysis buffer was added and the immunoprecipitation proceeded for 2 hr at 4°C with rotation. The immunoprecipitated protein was washed 3 times in binding buffer and eluted in same buffer containing 1 mg/ml FLAG peptide by rotation at 4°C for 1 hr.

For in vitro protein-protein interaction studies, GST-purified complexes were first resuspended in 160 mL binding buffer and 20 mL of this resuspension was incubated with 5 mg of FLAG-SLC38A9 or FLAG-SLC38A9 1-119 and supplemented with 2 mM DTT and 1 mg/mL BSA in a final volume of 50 mL for 2

hours at 4°C with rotation. When required, arginine or specified amino acids was added to the binding reactions at the indicated concentrations. To terminate the binding reactions, samples were washed three times in 1 mL of chilled binding buffer followed by the addition of 50 mL of SDS-containing sample buffer.

Proteoliposome reconstitution and transport assay

The reconstitution and transport assay was previously described in (*53*) and used here with the following modifications. Chloroform-dissolved phosphatidylcholine or E. coli lipids (PC or EC, 50 mg) were evaporated dry under nitrogen in a round bottom flask and desiccated at least 2 hr to overnight under vacuum. Lipids were hydrated in inside buffer (20 mM MES pH 5, 90 mM KCl, and 10 mM NaCl) at 50 mg/ml with light sonication in a chilled water bath. Clarified lipids were aliquoted into 100 mL aliquots in Eppendorf tubes and then extruded through a 100 nm membrane with 15-20 passes (Avanti 6100).

Because the [^{3}H]labeled leucine bound non-specifically to the PC proteoliposomes we used previously, E.coli lipids were utilized for transport assays utilizing [^{3}H]labeled leucine or tyrosine as they achieve low background binding, while [^{3}H]labeled arginine transport assays were performed using PC lipids. In brief, the reconstitution reaction was set up containing 15 mg FLAG-SLC38A9, 80-60:1 ratio of lipid to protein (w/w), 6:1 ratio of detergent (DDM) to lipid, and 1 mM DDT in inside buffer in a volume of 700 mL. The reconstitution was initiated by rotation at 4°C for 60 min. After, in order to remove the detergent, the proteoliposomes were incubated 3 times in succession with bio-

beads. First, bio-beads (50 mg/reaction) were activated by washes of 1 mL once in methanol, 5 times in dH_2O, and twice in inside buffer. After activation, proteoliposome reactions were incubated with 50 mg bio-beads as follows: 1 hr at 4°C with rotation, followed by transfer to fresh bio-beads for overnight incubation, and then once more for 1 hr at 4°C with rotation the following morning. In all transport assay experiments, a liposome only control was also prepared where glycerol-supplemented inside buffer was used in lieu of SLC38A9 and the background binding to these liposomes was subtracted from those containing SLC38A9. All transport experiments were preformed using a pH gradient across the proteoliposome membrane to mimic the pH gradient across the lysosomal membrane. The lumen of the proteoliposome was buffered to pH 5.0 and the external buffer was at pH 7.4.

Method for the rapid purification (LysoIP) and metabolite profiling of lysosomes

The method is described in Abu-Remaileh et al. (In press). LysoIP is a method for the immunoprecipitation-based isolation of TMEM192-3XHA expressing lysosomes, which we developed using insights from the recently reported method for the rapid isolation of mitochondria (*134*). The LysoIP method utilizes anti-HA magnetic beads to immunopurify lysosomes from HEK-293T cells expressing the transmembrane protein 192 (TMEM192) fused to 3XHA epitopes. Starting from live cells, isolation of intact lysosomes takes ~10 min and results in highly pure and intact lysosomes. The method uses buffers compatible with metabolite

profiling and metabolites are extracted at the end of the procedure and analyzed via LC/MS.

On average, ~35 million HEK-293T cells are used for each LysoIP with each sample processed individually in order to ensure rapid isolation. Cells are initially washed with chilled PBS and then scraped in 1 mL of KPBS (136 mM KCl, 10 mM KH_2PO_4, pH 7.25 was adjusted with KOH) and centrifuged at 1000 x g for 2 min at 4°C. The supernatant is aspirated and the pelleted cells are resuspended in 950 uL and 25 uL of resuspension is saved for processing of whole-cell fraction. The remaining cell suspension is then homogenized with 20 strokes of a 2 mL dounce homogenizer. The homogenized sample is then centrifuged at 1000 x g for 2 mins at 4°C and the supernatant incubated with 100 uL of KPBS prewashed anti-HA magnetic beads on rotation at 4°C for 3 min. Immunocaptured lysosomes are then gently washed three times with 1 mL KPBS with a DynaMag spin magnet. Metabolites are then extracted from captured lysosomes after the third wash; beads were resuspended in 50 uL ice-cold metabolite extraction buffer (80% methanol, 20% water containing internal standards). The metabolite extract is then centrifuged at 1000 x g for 2 min at 4°C. The supernatant is then collected and analyzed by LC/MS to determine the total moles of each metabolite. In order to control for the non-specific background binding of metabolites to the anti-HA magnetic beads, TMEM192-2XFlag expressing HEK-293T cells are processed similarly to those expressing TMEM192-3XHA.

Radiolabeled amino acid uptake by purified lysosomes

The amino acid uptake assay was adapted from previously published work (*169*). Lysosomes were isolated from ~35 million HEK-293T cells using the LysoIP method. Lysosomes were incubated with 20 μM [^{3}H]leucine or [^{3}H]arginine in 700 μL KPBS-based buffer consisting of 0.125 M sucrose, 2 mM $MgCl_2$, and 2 mM ATP at 4^{o}C (Lyso Buffer). Lysosomes were then transferred to a 37°C warm bath for 30 min. Collected lysosomes bound to the magnet were washed three times with ice-cold KPBS and resuspended in 100 μL KPBS and mixed with standard scintillation counting fluid. Control-Lyso IP scintillation counts were subtracted and lysosomes lysed in dH_2O were used to determine the maximal amount of labeled leucine that could be released. Where lysosomes were stimulated with the indicated amino acid, [^{3}H]leucine-loaded lysosomes were washed 3 times in the Lyso buffer and then incubated in Lyso buffer containing the indicated amino acid for 10 min prior to collection of supernatant and scintillation counting.

Immunofluorescence assays

HEK-293T cells were plated on fibronectin-coated glass coverslips in 6-well cell culture dishes at 300,000 cells/well. After 12 hr, the coverslips were washed once in PBS and subsequently fixed and permeabilized in a single step using 1 mL of ice-cold methanol at -20°C for 15 min. The coverslips were then washed twice in 1 mL PBS and then incubated with primary antibody (FLAG CST 1:300 dilution, LAMP2 SCBT 1:400 dilution) in 5% normal donkey serum for 1 hr at room

temperature. After incubation with the primary antibody, the cover slips were rinsed 4 times in PBS and incubated with secondary antibodies (1:400 dilution in 5% normal donkey serum) for 45 min at room temperature in the dark. The coverslips were then washed 4 times with PBS and once in dH_2O. Coverslips were mounted on slides using Vectashield containing DAPI (Vector Laboratories) and imaged on a spinning disc confocal system (Perkin Elmer).

Orthotopic implantation of cells in the mouse pancreas and tumor analyses

Male C57BL/6J mice aged 6-8 weeks at the start of the study were used for all pancreatic tumor studies. Recipient mice were first anesthetized with inhaled 2% isoflurane-oxygen mixture; an incision was then made in the abdomen at the left mid-clavicular line, and 50 mL of PBS containing 50,000 cells was injected into the tail of the pancreas. The tumors were grown for 2 weeks before the mice were sacrificed; the resulting tumors were dissected and measured using a caliper for length, width, and height. Tumor weight (mg) was also measured. Tumor volume was calculated for a modified ellipsoid shaped tumor using the following equation: Tumor volume= $(4/3)p(length/2)(width/2)^2$

Tumors were fixed in formalin and processed for S6 pS235/S236 immunohistochemistry as described (*188*).

Quantification and statistical analyses

A two-tailed t-test was used for comparison between two groups. All comparisons were two-sided, and P values are indicated in figure legends.

CHAPTER 4

Reprinted from Science

NUFIP1 is a ribosome receptor for starvation-induced ribophagy

Gregory A. Wyant[1,2,3,4,6], Monther Abu-Remaileh[1,2,3,4,6], Evgeni M. Frenkel[1,2,3,4], Nouf N. Laqtom[1,2,3,4], Vimisha Dharamdasani[1,2,3,4], Caroline A. Lewis[1], Sze Ham Chan[1], Ivonne Heinze[5], Alessandro Ori[5*], and David M. Sabatini[1,2,3,4*]

[1]Whitehead Institute for Biomedical Research and Massachusetts Institute of Technology, Department of Biology, 455 Main Street, Cambridge, Massachusetts 02142, USA. [2]Howard Hughes Medical Institute, Department of Biology, Massachusetts Institute of Technology, Cambridge, Massachusetts 02139, USA. [3]Koch Institute for Integrative Cancer Research,at the Massachusetts Institute of Technology, 500 Main Street, Cambridge, Massachusetts 02142, USA. [4]Broad Institute of Harvard and Massachusetts Institute of Technology, 415 Main Street, Cambridge, Massachusetts 02142, USA. [5]Leibniz Institute on Aging – Fritz Lipmann Institute, Beutenbergstrasse 11, 07745 Jena, Germany. [6]These authors contributed equally to this work.

*Correspondence: sabatini@wi.mit.edu and alessandro.ori@leibniz-fli.de

Experiments in Figure 1 were performed by GAW and MAR and AO
And EMF
Experiments in Figure 2, 3, 4, 5 were performed by GAW with technical assistance from CAL and SHC
Experiments in Figure S1 were performed by MAR and EMF
Experiments in Figure S2, S3, S4, S5, S6, S7, and S8 were performed by GAW
Manuscript was written by GAW, MAR, and DMS

Abstract

The lysosome degrades and recycles macromolecules, signals to the master growth regulator mTORC1, and is associated with human disease. Here, we performed quantitative proteomic analyses of lysosomes rapidly isolated using the LysoIP method and find that nutrient levels and mTOR dynamically modulate the lysosomal proteome. We focus on NUFIP1, a protein that upon mTORC1 inhibition redistributes from the nucleus to autophagosomes and lysosomes. Upon these conditions, NUFIP1 interacts with ribosomes and delivers them to autophagosomes by directly binding to LC3B. The starvation-induced degradation of ribosomes via autophagy (ribophagy) depends on the capacity of NUFIP1 to bind LC3B and promotes cell survival. We propose that NUFIP1 is a receptor for the selective autophagy of ribosomes.

The capacity of lysosomes to degrade macromolecules is necessary for cells to clear damaged components and to recycle nutrients for maintaining homeostasis upon starvation. In the context of disease, lysosomes are best known for their dysfunction in the rare lysosomal storage diseases, but also play roles in neurodegeneration and cancer as well as the aging process (reviewed in (*81, 132, 189*)). Over the last decade it has become apparent that mTOR Complex 1 (mTORC1), the major nutrient-sensitive regulator of growth (mass accumulation), has an intimate relationship with lysosomes (reviewed in (*15*)). Most components of the nutrient sensing machinery upstream of mTORC1 localize to the lysosomal surface, and nutrients generated by lysosomes regulate mTORC1 by promoting its translocation there, a key step in its activation. In turn, mTORC1 regulates the flux of macromolecules destined for lysosomal degradation by controlling autophagosome formation as well as lysosomal biogenesis through the TFEB transcription factor (*15*).

Using our recently developed LysoIP method to rapidly isolate highly pure lysosomes (*190*) we profiled the dynamics of the lysosomal proteome under conditions that inhibit mTORC1 signaling. We identify NUFIP1, a protein not previously associated with lysosomes, as necessary for the starvation-induced degradation of ribosomes and show that it fulfills multiple criteria for being an autophagy receptor for ribosomes.

mTORC1 and nutrients regulate the lysosomal proteome

To define the mTORC1-regulated lysosomal proteome, we used high-resolution quantitative proteomics to analyze lysosomes isolated from HEK-293T cells cultured in nutrient-replete media (full media), starved of nutrients (amino acids and glucose), or treated with the mTOR inhibitor Torin1 for one hour (Fig. 1A and S1A). Nutrient starvation and Torin1 both inhibit mTORC1 signaling (Fig. S1A) but will have distinct effects because Torin1 inhibits mTORC1 more strongly than nutrient deprivation and there are mTORC1-independent mechanisms for sensing nutrients. Nutrient starvation and Torin1 did not impact the abundance of most proteins associated with the purified lysosomes, but even a cursory view of the datasets revealed many proteins affected by one or both treatments (Fig. 1B). Gratifyingly, these included proteins with established nutrient- and Torin1-sensitive associations with lysosomes (*49, 64, 94, 158, 191, 192*), including components of mTORC1 (mTOR, Raptor, and mLST8) and the Folliculin complex (FLCN, FNIP1, and FNIP2) (Fig. 1B and C) as well as the TFEB, MITF, and TFE3 transcription factors (Fig. 1B). Proteins previously connected to lysosomes but not known to have regulated associations with them were also identified. For example, Torin1 decreased and amino acid starvation increased the lysosomal abundance of SPG11 and ZFYVE26 (Fig. 1B and 1C and Table S1), which are associated with Hereditary Spastic Paraplegia and interact with each other as well as the Adaptor-5 complex (*193, 194*), whose components (AP5B1, AP5M1, AP5S1 and AP5Z1) behaved similarly in the datasets (Table S1) (*194*).

Although these examples hinted at the utility of the proteomics data for discovery, we needed a way to a priori designate a protein as associated with lysosomes upon mTOR inhibition and/or nutrient deprivation as the set of such proteins has not been previously defined. To do so we generated a control dataset of proteins that bind non-specifically to magnetic beads coated with antibody to hemagglutinin (HA), used in the immune-isolation of the lysosomes. We defined as "lysosomal" any protein that was more abundant in purified lysosomes than on the control beads by a factor of at least 1.5 (at a significance value of $q<0.1$; Fig. 1A and 1D). We arrived at this value using a sliding-window method to identify a relative change that captured a protein set significantly enriched for those annotated as lysosomal in the UniProt database (Fig. S1B). This approach yielded a total of 828 unique proteins as associated with lysosomes in any of the three experimental conditions (Fig. 1D), with 343 proteins designated as lysosomal under all conditions (Fig. 1D and Table S2).

NUFIP1-ZNHIT3 accumulates on autophagosomes and lysosomes upon mTORC1 inhibition

Of the many proteins whose lysosomal abundance increased upon Torin1 treatment (Tables S1), Nuclear fragile X mental retardation-interacting protein 1 (NUFIP1) piqued our interest because previous work indicates that while NUFIP1 is largely a nuclear protein it has also been observed in the cytoplasm of some cell types (*195*). NUFIP1 forms a heterodimer with a smaller protein, Zinc finger HIT domain-containing protein 3 (ZNHIT3) (*196, 197*), whose lysosomal

abundance also increased upon Torin1 treatment (Tables S1 and S2), albeit to a lesser extent. Similar to the behavior of many constitutively interacting proteins, CRISPR-Cas9-mediated loss of NUFIP1 caused the concomitant loss of ZNHIT3 (Fig. S2A).

Previous work implicates NUFIP1-ZNHIT3 in the assembly of the box C/D snoRNP (*198-200*). Consistent with such a role, NUFIP1 co-immunoprecipitated ZNHIT3 but also snoRNP core components such as Fibrillarin (FBL), NOP58, SNU13/15.5K, and NOP17/PIH1D1 (Fig. S2B). In addition, its loss caused modest reductions in the interaction of FBL with NOP58, and SNU13/15.5K as well as the expression of small nucleolar RNAs (snoRNAs) of the box C/D (U3 and U14), but not H/ACA (U19) or U4, class (Fig. S2, C and D). Although these results confirm a role for NUFIP1 in the function of the box C/D snoRNP, it was intriguing that none of its core components were in our proteomics data, suggesting that NUFIP1-ZNHIT3 might have a previously unappreciated role involving lysosomes.

Acute inhibition of mTORC1 in HEK-293T cells, by either via Torin1 treatment or amino acid starvation, strongly increased the lysosomal abundance of NUFIP1 and ZNHIT3 (Fig. 2A). mTORC1 inhibition did not change the total cellular amount of NUFIP1 or ZNHIT3, so we reasoned that it must affect their subcellular localization. Indeed, upon Torin1 treatment and amino acid starvation NUFIP1-ZNHIT3, but not SNU13/15.5K, redistributed from the nuclear fraction to the post-nuclear supernatant (PNS) that contains lysosomes (Fig. 2B). Imaging studies using HEK-293T cells stably expressing FLAG-NUFIP1 confirmed that

Torin1 caused NUFIP1 to translocate from the nucleus to LAMP2-positive lysosomes (Fig. 2C). Consistent with this shift in localization, Torin1 reduced the amount of NUFIP1-ZNHIT3 that co-immunuprecipitated with FBL, a C/D snoRNP component, without impacting the FBL-SNU13/15.5K interaction (Fig. S2E). Thus, mTOR inhibition promotes the lysosomal accumulation of NUFIP1-ZNHIT3 at the expense of its interaction with the nuclear C/D snoRNP.

Because mTORC1 inhibition strongly induces autophagy, we hypothesized that NUFIP1-ZNHIT3 may travel to lysosomes through an association with incipient autophagosomes. Indeed, NUFIP1 and ZNHIT3 were absent from lysosomes isolated from cells lacking the ATG7 protein (Fig. 2D), which is necessary for the formation of autophagosomes (*119*), and in Torin1 treated cells FLAG-NUFIP1 co-localized with LC3B-positive autophagosomes (Fig. 2E).

NUFIP1-ZNHIT3 interacts with LC3B

Sequence analyses predict that NUFIP1, but not ZNHIT3, has four potential LC3B-interacting regions (LIR) (Fig.2F). LIRs are found in autophagy receptors that physically link their cargo to the autophagosomal membrane through an LC3B/ATG8-binding domain that contains the Trp/Phe-X-X-Leu/Ile/Val sequence motif (reviewed in (*105*)). Consistent with the presence of LIRs in NUFIP1, endogenous LC3B co-immunoprecipitated endogenous NUFIP1 and ZNHIT3 from detergent lysates of HEK-293T cells cultured in full media and, to a much greater extent, in cells treated with Torin1 or starved of amino acids

(Fig. 2G). Even when overexpressed, ZNHIT3 did not co-immunoprecipitate with LC3B in cells lacking NUFIP1 (Fig. S3A). In vitro, purified NUFIP1-ZNHIT3 bound to purified LC3B but not to GABARAP, another autophagosome-associated protein, or to the Rap2A control protein (Fig. 2H).

We sought a NUFIP1 mutant that dissociates its function in the nuclear C/D snoRNP from its capacity to bind LC3B. We generated NUFIP1 mutants with point mutations in each of the four potential LIRs and identified one, W40A NUFIP1, which no longer interacts with LC3B (Fig. 2I). When expressed in NUFIP1-null cells, neither NUFIP1 W40A nor ZNHIT3 associated with lysosomes, whether or not mTORC1 was inhibited (Fig. S3B). The W40A NUFIP1 mutant was indistinguishable from the wild-type protein in its capacity to co-immunoprecipitate FBL and reverse the modest reductions in U3 and U14 snoRNA expression caused by NUFIP1 loss (Fig. S3,C-D). Thus, NUFIP1 interacts with LC3B and the W40A mutant distinguishes between the role of NUFIP1 in C/D snoRNP function and its capacity to bind LC3B and localize to lysosomes.

NUFIP1-ZNHIT3 associates with ribosomes in a nutrient-dependent manner

Because NUFIP1 binds to LC3B we hypothesized that it might serve as a selective autophagy receptor for an unknown cargo in the cytoplasm. Given its role in modifying ribosomal RNA and its reported co-localization with ribosomes in some cell types (*195*), we considered the possibility that NUFIP1-ZNHIT3 can associate with ribosomes. We began by fractionating cell lysates to determine

the amount of NUFIP1-ZNHIT3 that co-migrates with ribosomes pelleted through a 50% sucrose cushion. In lysates from control cells, NUFIP1-ZNHIT3 did not enter the sucrose cushion, but in those from cells treated with Torin1 or deprived of amino acids both proteins shifted markedly to the ribosome-containing pellet (Fig. 3A and Fig. S4A). Consistent with this finding, amino acid starvation increased the amount of ribosomes, as monitored via small (40S) and large (60S) ribosomal subunit proteins, that co-immunoprecipitated with NUFIP1 (Fig. 3B). To probe which ribosomal subunit NUFIP1-ZNHIT3 might associate with, we took advantage of the capacity of EDTA to dissociate ribosomes into their 40S and 60S subunits. When lysates of amino acid starved cells were fractionated through a 10 to 45% sucrose gradient, endogenous NUFIP1 and ZNHIT3 co-migrated with monosomes (80S) and polysomes. The addition of EDTA to the same lysates increased the amount of NUFIP1-ZNHIT3 that migrated with the large ribosomal subunits (Fig. S4B). Collectively, these results suggest that upon mTORC1 inhibition NUFIP1 binds to LC3B and associates with the ribosome, likely through its large subunit.

Given that mTORC1 inhibition increases the interaction of NUFIP1-ZNHIT3 with ribosomes, we considered the possibility that an mTORC1-dependent modification of either NUFIP1-ZNHIT3 or ribosomes regulates the interaction. To test this, we purified ribosomes or NUFIP1-ZNHIT3 from cells cultured in full media or treated with Torin1 and examined their capacity to interact with each other in vitro. Interestingly, only ribosomes from Torin1-treated cells bound strongly to NUFIP1-ZNHIT3, while the source of NUFIP1-ZNHIT3 did

not impact the strength of the interaction (Fig. 3,C and D). These results suggest that mTOR inhibition leads to a stable alteration of ribosomes that promotes their interaction with NUFIP1-ZNHIT3. In contrast, the in vitro interaction of NUFIP1-ZNHIT3 with LC3B was unaffected by the source of either (i.e., control or Torin1-treated cells) (Fig. S4C). Taken together, these data suggest that the loss of nuclear NUFIP1 and the increase in the LC3B-NUFIP1 interaction caused by mTORC1 inhibition results from the binding and trapping of NUFIP1 by modified ribosomes in the cytoplasm. We cannot exclude the possibility that an mTORC1-dependent modification of NUFIP1 also regulates its nuclear entry or exit, but we have failed to identify mTORC1-regulated phosphorylation sites on NUFIP1.

NUFIP1 is required for ribosomal degradation induced by nutrient starvation

While it is known that the proteasome degrades ribosomal proteins that do not incorporate into ribosomal subunits, which we verified (Fig. S5, A to C), how intact ribosomes are degraded is less understood, particularly in mammalian cells (*111, 115, 201-203*). Upon amino acid deprivation or Torin1 treatment, ribosomal proteins decreased in a time-dependent manner in a fashion that depended on ATG7 and a low lysosomal pH (Fig. 4A and S6, A and B), in accord with previous work in yeast showing that intact ribosomes are degraded via autophagy (*110*). In GATOR1 mutant (DEPDC5 KO) cells that have nutrient-insensitive mTORC1 signaling, amino acid starvation did not reduce the

abundance of ribosomal proteins while Torin1 still did (Fig. S6C). Thus, mTORC1 likely mediates the loss of ribosomal proteins caused by mTOR inhibition.

Given that NUFIP1 binds LC3B and also makes an mTORC1-regulated association with ribosomes, we hypothesized that NUFIP1 is required for the degradation of ribosomes via autophagy, a process that has been termed ribophagy in yeast (*110*). Indeed, in multiple cell types, loss of NUFIP1 prevented the depletion of ribosomal proteins caused by nutrient deprivation or Torin1 treatment (Fig. 4B and S6, D to G).

Loss of NUFIP1 had no impact the induction of autophagy, as assessed by LC3B lipidation, nor on the degradation of ferritin, another selective autophagy substrate, whether it was induced by nutrient starvation or iron chelation (Fig. 4B and S6H). NUFIP1 loss also blocked the Torin1-induced depletion of ribosomal RNA (rRNA) (Fig. 4C). Re-expression at levels near that of the endogenous protein of wild-type NUFIP1, but not of the W40A mutant deficient in LC3B binding, restored the capacity of NUFIP1-null HEK-293T and 8988T cells to degrade ribosomes upon nutrient depletion (Fig. 4, D and E and S6I). As assessed by electron microscopy, autophagosomes in HEK-293T cells lacking NUFIP1 or just its LC3B-binding capacity contained many fewer ribosomes than those from control cells (Fig. 4F and S6, J and K). Loss of NUFIP1 did not affect the morphology of the ER, mitochondria, or Golgi (Fig. S6L).

To test the role of the subcellular localization of NUFIP1 in the induction of ribosome degradation, we generated NUFIP1 mutants lacking either a nuclear localization (NLS) or export (NES) signal and expressed them in NUFIP1-null

cells. The NLS mutant localized to the cytoplasm even in cells in full media, but this did not cause ribosome loss. The NLS mutant colocalized to a greater extent with LAMP2 upon Torin1 treatment and restored the capacity of the null cells to degrade ribosomes upon amino acid starvation (Fig. S7, A and B). The NES mutant was constitutively nuclear and did not support ribosome degradation even upon nutrient starvation (Fig. S7, B and C). Loss of ATG7 or LC3B did not affect the nuclear exit of wild-type NUFIP1 (Fig. S7, D and E). Thus, in cells in full media, the presence of NUFIP1 in the cytoplasm is not sufficient to induce ribosome degradation, presumably because mTORC1 inhibition is still needed to promote the interaction of NUFIP1 with ribosomes.

NUFIP1 is important for cells to survive starvation

Because NUFIP1 is required for starvation-induced ribophagy and ribosomes constitute a major fraction of the total cell mass (*204-206*), we asked whether NUFIP1 is important for the cellular response to nutrient deprivation. Indeed, loss of NUFIP1 or just its LC3B-binding ability reduced the capacity of multiple cell types to survive nutrient starvation, as measured in clonogenic survival assays or via direct cell counting (Fig. 5, A and B and Fig. S8, A to C). These results suggest that the NUFIP1-mediated degradation of ribosomes supplies metabolites needed for survival during starvation. Consistent with this possibility, loss of either ATG7 or NUFIP1 suppressed the large increase in nucleoside levels (including inosine, which is generated by the deamination of adenosine in lysosomes (*207*)), caused by mTOR inhibition that we recently

described (*190*), which suggests that most of this increase results from the lysosomal degradation of rRNA (Fig. 5C) (32). The addition of nucleosides to the starvation media rescued the survival defect of the NUFIP1-null cells, and, as previously shown (*129*), of cells lacking the canonical autophagy pathway (Fig. 5D and E and S8D).

Starvation of single amino acids acutely inhibits mTORC1 signaling, but over time it reactivates because of the release of endogenous amino acids by the autophagic degradation of proteins. Analysis of the human proteome annotated in the UniProt database (which includes isoforms) revealed that ribosomal proteins are amongst the most highly enriched for arginine and lysine (Fig. 5F). Because mTORC1 senses lysosomal arginine (and likely lysine) through SLC38A9 (*208*), ribophagy might be important for generating the amino acids necessary for mTORC1 re-activation. Indeed, loss of NUFIP1 severely diminished the reactivation of mTORC1 normally observed after long-term arginine deprivation (Fig. 5G). Thus, NUFIP1-mediated ribophagy contributes significantly to the cellular response to nutrient starvation.

Conclusions

NUFIP1 has several properties suggesting it functions as an autophagy receptor for ribosomes during starvation-induced ribophagy: (i) it is required for nutrient deprivation to degrade ribosomes, (ii) it binds LC3B and ribosomes, and (iii) a NUFIP1 mutant that does not bind LC3B cannot support ribosomal degradation upon autophagy induction. We propose that NUFIP1 cycles in and

out of the nucleus (*195*) (Fig. 2C and S7, A and C), and, upon nutrient starvation, accumulates in the cytoplasm because it binds to ribosomes that acquire an mTORC1-regulated alteration. In the cytoplasm, NUFIP1 transports its ribosome cargo to autophagic vesicles by directly binding LC3B in a fashion that is likely not directly regulated by nutrients and mTORC1. Our NUFIP1 findings suggest that our dataset of lysosomal proteins can serve as a resource for future discoveries.

Many questions remain. Our in vitro data indicate that the ribosome is likely altered upon mTORC1 inhibition in a fashion that strengthens its interaction with NUFIP1-ZNHIT3, but the nature of this alteration—whether a post-translational modification, such as the addition of ubiquitin, or the binding of a protein to the ribosome—is unknown. As NUFIP1-ZNHIT3 most likely interacts with the 60S ribosomal subunit and the atomic structure of the human ribosome is available (*209*), it should be possible to determine where NUFIP1-ZNHIT3 interacts. Note that that NUFIP1-ZNHIT3 may not bind directly to an established ribosomal protein or the rRNA; other currently unknown proteins may be involved in mediating the interaction.

Our identification of NUFIP1 as an autophagy receptor for ribosomes in mammalian cells adds to the growing list of selective autophagy receptors, including for ferritin, mitochondria, peroxisomes, endoplasmic reticulum, and bacteria (*101, 107, 108, 113, 116-118, 210*). We find that ribophagy is an important source of nutrients (particularly nucleosides) upon starvation, and that loss of NUFIP1 decreases the survival of cells under low nutrient conditions. As

RNA-binding proteins, most ribosomal proteins have a high content of basic amino acids, and we find that NUFIP1 is required for the reactivation of mTORC1 that occurs after prolonged arginine starvation. This result suggests that a key role for SLC38A9, which senses lysosomal basic amino acids upstream of mTORC1 (*208*), is to signal the successful degradation of ribosomes in lysosomes to mTORC1.

In the human and mouse cells we have examined, loss of NUFIP1 prevents starvation-induced ribosome degradation but it is possible that other ribosome receptors or mechanisms for ribosome degradation also exist. For example, recent work suggests that ribosomes can be degraded via bulk autophagy at longer starvation times (24 hours) than those we have examined (*211*). In yeast, it has been proposed that the ubiquitin protease Ubp3p/Bre5p is required for the selective degradation of ribosomes, but it is unclear if its homologues play such a role in animals (*110*). As it is estimated that in growing cells ribosomes account for ~50% and ~80% of total cellular protein and RNA (*204-206*), respectively. Our work identifies a key link between starvation and one of the most abundant nutrient sources in cells.

Figure 1

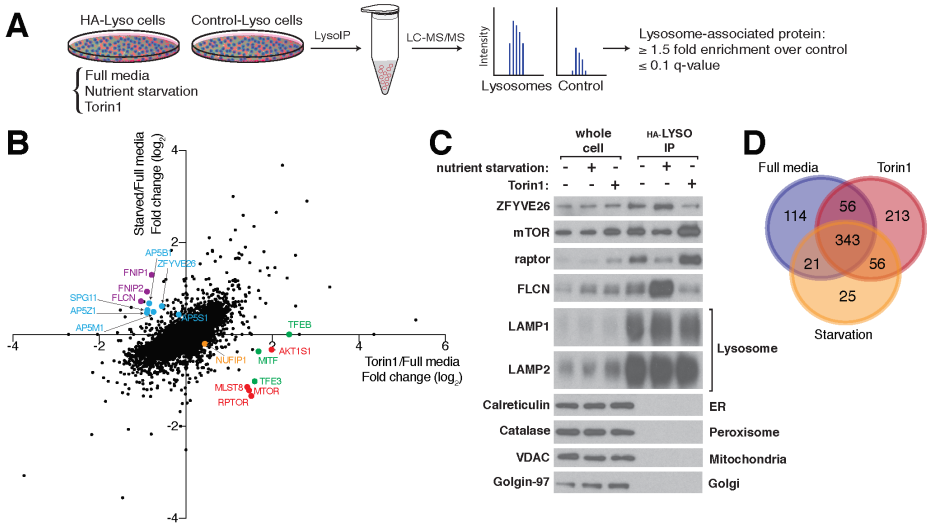
A
HA-Lyso cells
Control-Lyso cells
LysoIP
LC-MS/MS
Intensity
Lysosomes
Control
Lysosome-associated protein:
≥ 1.5 fold enrichment over control
≤ 0.1 q-value
Full media
Nutrient starvation
Torin1
B
Starved/Full media
Fold change (log2)
Torin1/Full media
Fold change (log2)
AP5B1
ZFYVE26
FNIP1
FNIP2
FLCN
SPG11
AP5Z1
AP5M1
MAPKAP1
MPRS1
TFEB
AKT1S1
NUFIP1
MITF
TFE3
MLST8
MTOR
RPTOR
C
whole cell
HA-LYSO IP
nutrient starvation:
Torin1:
ZFYVE26
mTOR
raptor
FLCN
LAMP1
LAMP2
Lysosome
Calreticulin
ER
Catalase
Peroxisome
VDAC
Mitochondria
Golgin-97
Golgi
D
Full media
Torin1
Starvation
114
56
213
343
21
56
25

Fig. 1: Regulation of the lysosomal proteome in response to nutrient starvation and mTOR inhibition

(A) Schematic depicting the workflow for the LysoIP-proteomics method. HA-Lyso and Control-Lyso cells refer to cells stably expressing 3xHA-tagged TMEM192 or 2xFlag-tagged TMEM192, respectively.

(B) Nutrient starvation and mTOR inhibition regulate the lysosomal proteome. The scatter plot shows relative (fold) changes in protein abundances in lysosomes captured from the HA-Lyso cells starved for one hour of nutrients (amino acids and glucose) or treated for one hour with 250 nM Torin1 versus lysosomes from cells cultured in nutrient-replete media (full media). For each condition, three independent isolations were compared. Colors indicate proteins mentioned in the text. The dots denote the 5339 unique proteins detected amongst all the pre-filtered samples. The majority of these are in the immunoprecipitates from both the HA-Lyso and Control-Lyso cells. TFEB was detected only in the Torin1/Full media comparison and assigned an arbitrary $\log_2$ fold change of 0 in the Starved/ Full media comparison.

(C) Validation of changes observed in the lysosomal abundances of the some of the proteins highlighted in Figure 1B. The immunoblot shows analyses for indicated proteins in whole cell lysates or lysosomes purified from HEK-293T cells subjected to the indicated treatments for 1 hour. ER, endoplasmic reticulum.

(D) Venn diagram representation of the number of proteins defined as lysosomal in each of the three conditions. A protein was deemed lysosomal if it had a significant ($q \leq 0.1$) enrichment value of 1.5 fold (> 0.58, $\log_2$). Proteins not detected at all on the control beads were also classified as lysosomal.

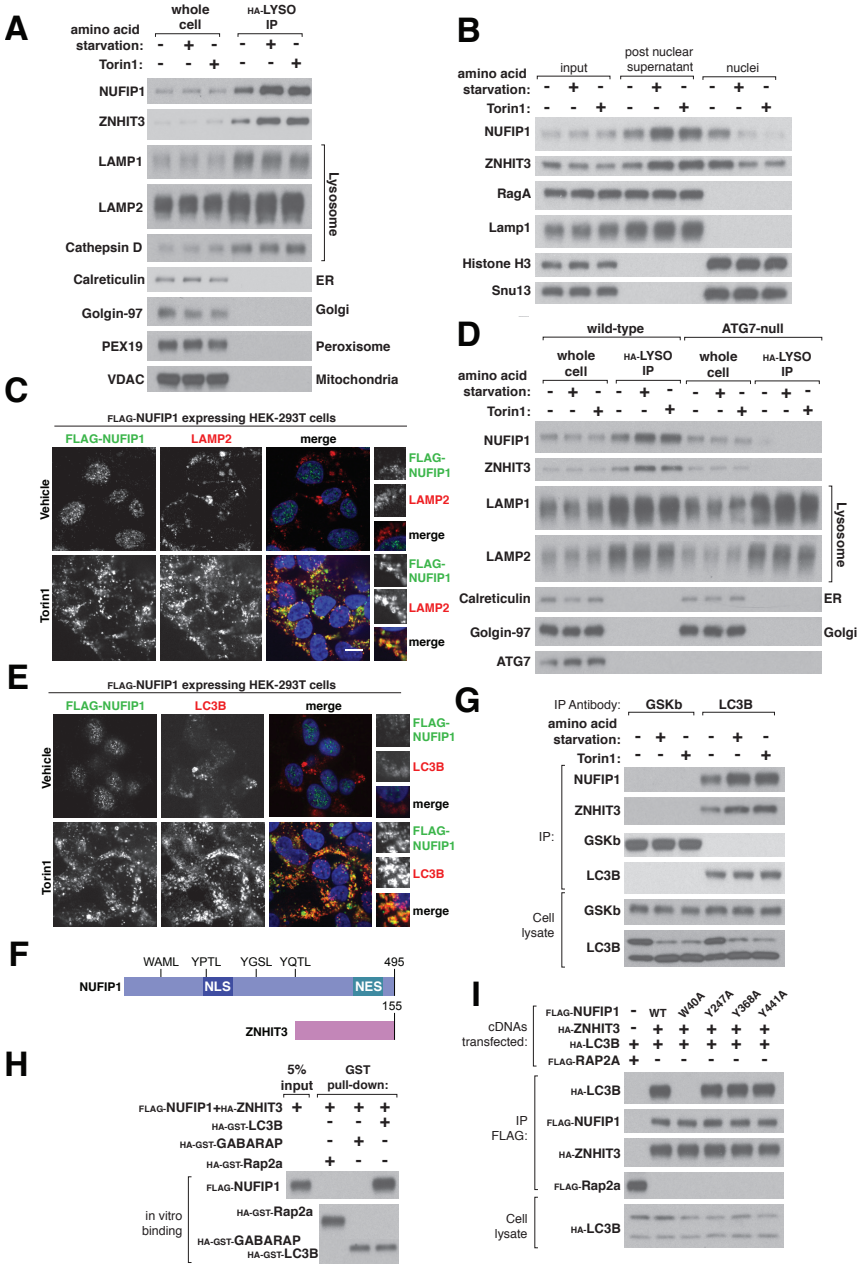
A
amino acid starvation:
Torin1:
whole cell
HA-LYSO IP
NUFIP1
ZNHIT3
LAMP1
LAMP2
Cathepsin D
Lysosome
Calreticulin
ER
Golgin-97
Golgi
PEX19
Peroxisome
VDAC
Mitochondria
B
input
post nuclear supernatant
nuclei
RagA
Lamp1
Histone H3
Snu13
C
FLAG-NUFIP1 expressing HEK-293T cells
FLAG-NUFIP1
LAMP2
merge
Vehicle
Torin1
D
wild-type
ATG7-null
ATG7
E
LC3B
F
WAML
YPTL
YGSL
YQTL
495
NLS
NES
155
G
IP Antibody:
GSKb
LC3B
IP:
Cell lysate
H
5% input
GST pull-down:
FLAG-NUFIP1+HA-ZNHIT3
HA-GST-LC3B
HA-GST-GABARAP
HA-GST-Rap2a
in vitro binding
I
cDNAs transfected:
WT
W40A
Y247A
Y368A
Y441A
FLAG-RAP2A
IP FLAG:

Fig. 2: Upon starvation NUFIP1-ZNHIT3 accumulates at lysosomes in an autophagosome-dependent manner

(A) NUFIP1-ZNHIT3 accumulates at lysosomes upon mTORC1 inhibition. Lysates and immunoprecipitates were prepared from HEK-293T cells cultured in full media, or deprived of amino acids or treated with 250 nM Torin1 for 1 hour as described in the supplementary materials.

(B) Upon mTORC1 inhibition NUFIP1-ZNHIT3 shifts from the nuclear fraction to the post-nuclear supernatant that contains lysosomes. HEK-293T cells were fractionated after being deprived of amino acids or treated with 250 nM Torin1 for 1 hour and the amounts of endogenous NUFIP1 and ZNHIT3 analyzed by immunoblotting. RagA and LAMP1 are lysosome-associated proteins; histone H3 and SNU13 are nuclear.

(C) mTOR inhibition shifts NUFIP1 from the nucleus to LAMP1-positive lysosomes. HEK-293T cells stably expressing FLAG-NUFIP1 were treated with 250 nM Torin1 for 1 hour and analyzed as described in the supplementary materials. Scale bar, 10 mm.

(D) Loss of ATG7 greatly decreases the amount of NUFIP1-ZNHIT3 on lysosomes. Wild-type and ATG7-null HEK-293T cells stably expressing the HA-Lyso tag were deprived of amino acids or treated with 250 nM Torin1 for 1 hour and the amounts of NUFIP1 and ZNHIT3 on lysosomes and in total cell lysates were analyzed as in (A).

(E) mTOR inhibition shifts NUFIP1 from the nucleus to LC3B-positive puncta. HEK-293T cells stably expressing FLAG-NUFIP1 were treated with 250 nM

Torin1 for 1 hour and processed as in (C).

(F) Schematic depicting the localization of the four putative LC3B-binding regions (LIRs) in NUFIP1.

(G) mTORC1 inhibition increases the interaction between endogenous LC3B and NUFIP1-ZNHIT3. Anti-LC3B immunoprecipitates were prepared from HEK-293T cells deprived of amino acids or treated with 250 nM Torin1 for 1 hour and lysates and immunoprecipitates were analyzed for the indicated proteins. Immunoprecipitates prepared with an antibody to GSKb were used as negative controls.

(H) NUFIP1-ZNHIT3 interacts with LC3B in vitro. Purified HA-GST-LC3B immobilized on a glutathione affinity resin was incubated with the purified FLAG-NUFIP1-HA-ZNHIT3 complex. HA-GST-Rap2a and HA-GST-GABARAP were used as negative controls. Proteins captured in the glutathione resin pull-down were analyzed by immunoblotting for the indicated proteins using anti-epitope tag antibodies. GST, glutathione S-transferase.

(I) Identification of a NUFIP1 mutant that does not bind LC3B. Wild-type (WT) FLAG-NUFIP1 or a series of point mutants in its putative LIR motifs were co-expressed with HA-ZNHIT3 and HA-LC3B. HA-Rap2A was used as a negative control. FLAG-immunoprecipitates and lysates were prepared and analyzed by immunoblotting.

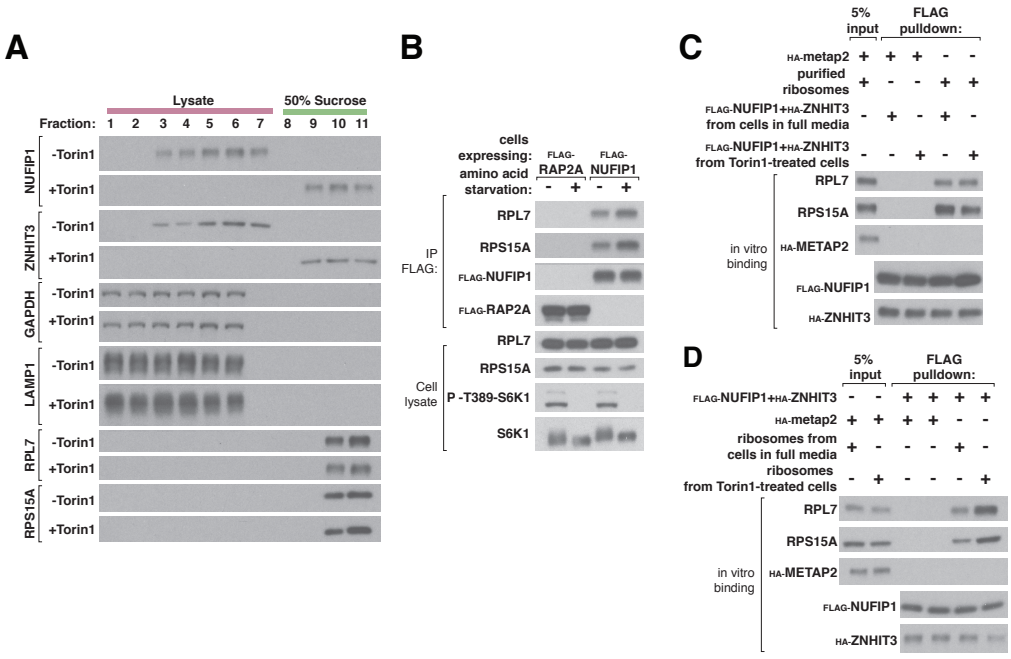
A
Lysate
50% Sucrose
Fraction: 1 2 3 4 5 6 7 8 9 10 11
NUFIP1
ZNHIT3
GAPDH
LAMP1
RPL7
RPS15A
-Torin1
+Torin1
B
cells expressing:
FLAG-RAP2A
FLAG-NUFIP1
amino acid starvation:
IP FLAG:
RPL7
RPS15A
FLAG-NUFIP1
FLAG-RAP2A
Cell lysate
RPL7
RPS15A
P -T389-S6K1
S6K1
C
5% input
FLAG pulldown:
HA-metap2
purified ribosomes
FLAG-NUFIP1+HA-ZNHIT3 from cells in full media
FLAG-NUFIP1+HA-ZNHIT3 from Torin1-treated cells
in vitro binding
RPL7
RPS15A
HA-METAP2
FLAG-NUFIP1
HA-ZNHIT3
D
5% input
FLAG pulldown:
FLAG-NUFIP1+HA-ZNHIT3
HA-metap2
ribosomes from cells in full media
ribosomes from Torin1-treated cells
in vitro binding
RPL7
RPS15A
HA-METAP2
FLAG-NUFIP1
HA-ZNHIT3

Fig. 3: NUFIP1-ZNHIT3 interacts with ribosomes in an mTORC1-dependent fashion

(A) mTOR inhibition increases the amount of NUFIP1-ZNHIT3 that co-migrates with ribosomes. HEK-293T cell lysates prepared from cells in full media or treated with 250 nM Torin1 were fractionated over a 50% sucrose cushion. Fractions were collected and the indicated proteins analyzed by immunoblotting.

(B) Amino acid deprivation increases the amount of ribosomes that co-immunoprecipitates with NUFIP1. HEK-293T cells stably expressing FLAG-NUFIP1 were deprived of amino acid for 1 hour. Lysates and FLAG immunoprecipitates were prepared and analyzed for the indicated proteins by immunoblotting. FLAG-Rap2A was used as a negative control.

(C) In vitro, purified NUFIP1-ZNHIT3 binds to ribosomes and the interaction is not affected by whether or not NUFIP1-ZNHIT3 was obtained from cells with inhibited mTOR. The FLAG-NUFIP1-HA-ZNHIT3 complex was purified from HEK-293T cells in full media or treated with 250 nM Torin1 for 1 hour and immobilized on a FLAG affinity resin. Equal amounts of ribosomes obtained from cells in full media were added to the immobilized FLAG-NUFIP1-HA-ZNHIT3 complex and the proteins captured analyzed by immunoblotting. Ribosomes were purified as described in the supplementary materials. Purified HA-METAP was used as a negative control.

(D) In vitro, ribosomes purified from cells with mTOR inhibition bind better to NUFIP1-ZNHIT3 than those from cells in full media. Ribosomes were purified

from HEK-293T cells in full media conditions or treated with 250 nM Torin1 for 1 hour. The FLAG-NUFIP1-HA-ZNHIT3 complex was immobilized on FLAG affinity beads and equal amounts of ribosomes were added. Proteins captured by the FLAG affinity beads were analyzed by immunoblotting. HA-METAP2 served as a negative control.

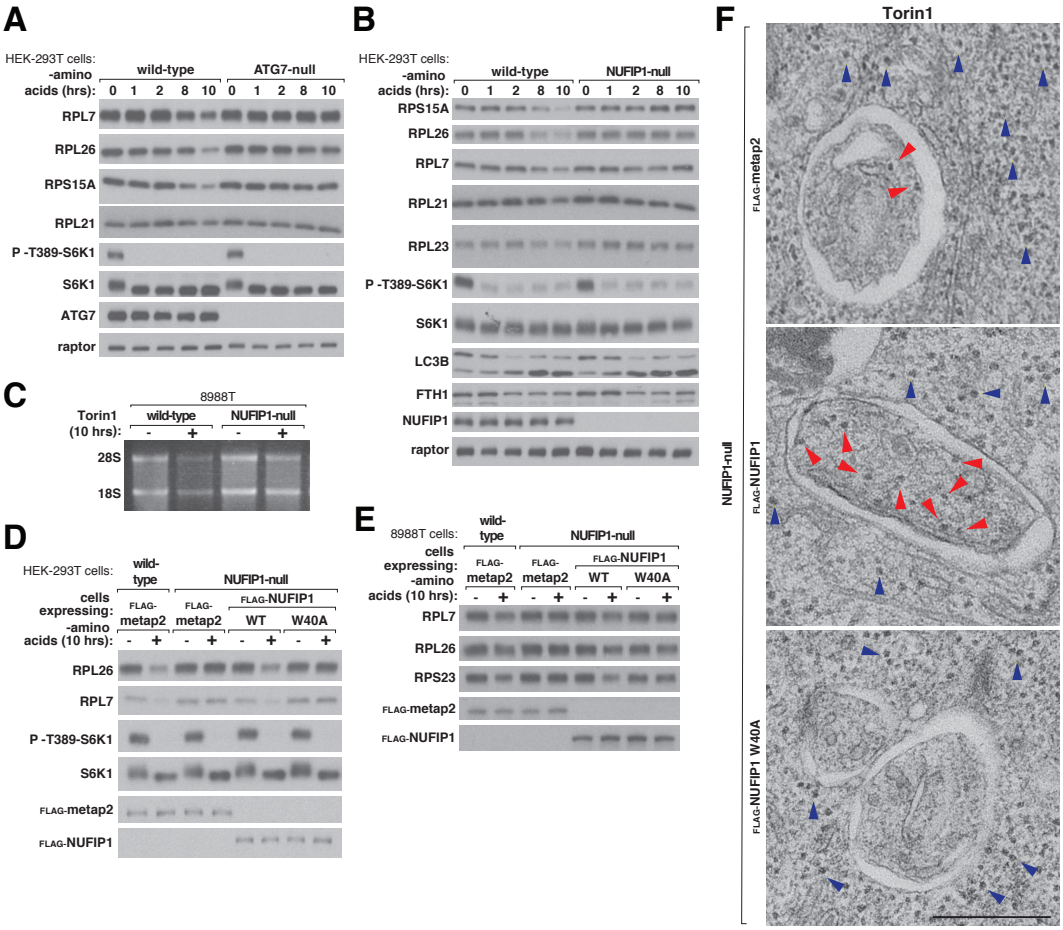
A
HEK-293T cells:
-amino acids (hrs):
wild-type
ATG7-null
0 1 2 8 10 0 1 2 8 10
RPL7
RPL26
RPS15A
RPL21
P -T389-S6K1
S6K1
ATG7
raptor
B
HEK-293T cells:
-amino acids (hrs):
wild-type
NUFIP1-null
0 1 2 8 10 0 1 2 8 10
RPS15A
RPL26
RPL7
RPL21
RPL23
P -T389-S6K1
S6K1
LC3B
FTH1
NUFIP1
raptor
C
8988T
Torin1 (10 hrs):
wild-type
NUFIP1-null
- + - +
28S
18S
D
HEK-293T cells:
wild-type
NUFIP1-null
cells expressing:
FLAG-metap2
FLAG-metap2
FLAG-NUFIP1 WT
FLAG-NUFIP1 W40A
-amino acids (10 hrs):
- + - + - + - +
RPL26
RPL7
P -T389-S6K1
S6K1
FLAG-metap2
FLAG-NUFIP1
E
8988T cells:
wild-type
NUFIP1-null
cells expressing:
FLAG-metap2
FLAG-metap2
FLAG-NUFIP1 WT
FLAG-NUFIP1 W40A
-amino acids (10 hrs):
- + - + - + - +
RPL7
RPL26
RPS23
FLAG-metap2
FLAG-NUFIP1
F
Torin1
NUFIP1-null
FLAG-metap2
FLAG-NUFIP1
FLAG-NUFIP1 W40A

Fig. 4: NUFIP1 is required for ribophagy

(A) ATG7 loss suppresses the degradation of ribosomes caused by amino acid starvation. Wild-type or ATG7-null HEK-293T cells were deprived of amino acids for the indicated time points. Cell lysates were analyzed by immunoblotting for the total levels and phosphorylation states of the indicated proteins.

(B) Loss of NUFIP1 inhibits the degradation of ribosomes caused by amino acid starvation. Wild-type or NUFIP1-null HEK-293T cells were deprived of amino acids for the indicated time points. Cell lysates were analyzed by immunoblotting for the total levels and phosphorylation states of the indicated proteins.

(C) Loss of NUFIP1 inhibits the loss of 28S and 18S rRNA caused by mTOR inhibition. Wild-type and NUFIP1-null 8988T cells were treated with 250 nM Torin1 for 10 hrs and total RNA was extracted and analyzed on a formaldehyde agarose gel. RNA from equal numbers of cells was loaded in each lane.

(D) For amino acid starvation to cause ribosomal degradation, NUFIP1 must be able to interact with LC3B. Wild-type or NUFIP1-null HEK-293T cells stably expressing the indicated proteins were deprived of amino acids for 10 hours and analyzed for the total levels and phosphorylation states of the indicated proteins.

(E) For amino acid starvation to cause ribosomal degradation, NUFIP1 must interact with LC3B. Wild-type or NUFIP1-null 8988T cells stably

expressing the indicated proteins were treated as in (B).

(F) Autophagosomes from HEK-293T cells lacking NUFIP1 or expressing the LC3B-binding W40A mutant contain fewer ribosomes than those from control cells. NUFIP1-null HEK-293T cells expressing the control protein metap2, NUFIP1, or NUFIP1 W40A were treated with Torin1 and ConcanamycinA for 4 hours and analyzed by electron microscopy. Autophagosomes were identified by the presence of a double membrane. Red arrows indicate ribosomes inside an autophagosome. Blue arrows indicate ribosomes present in the cytoplasm. Scale bar, 500 nm

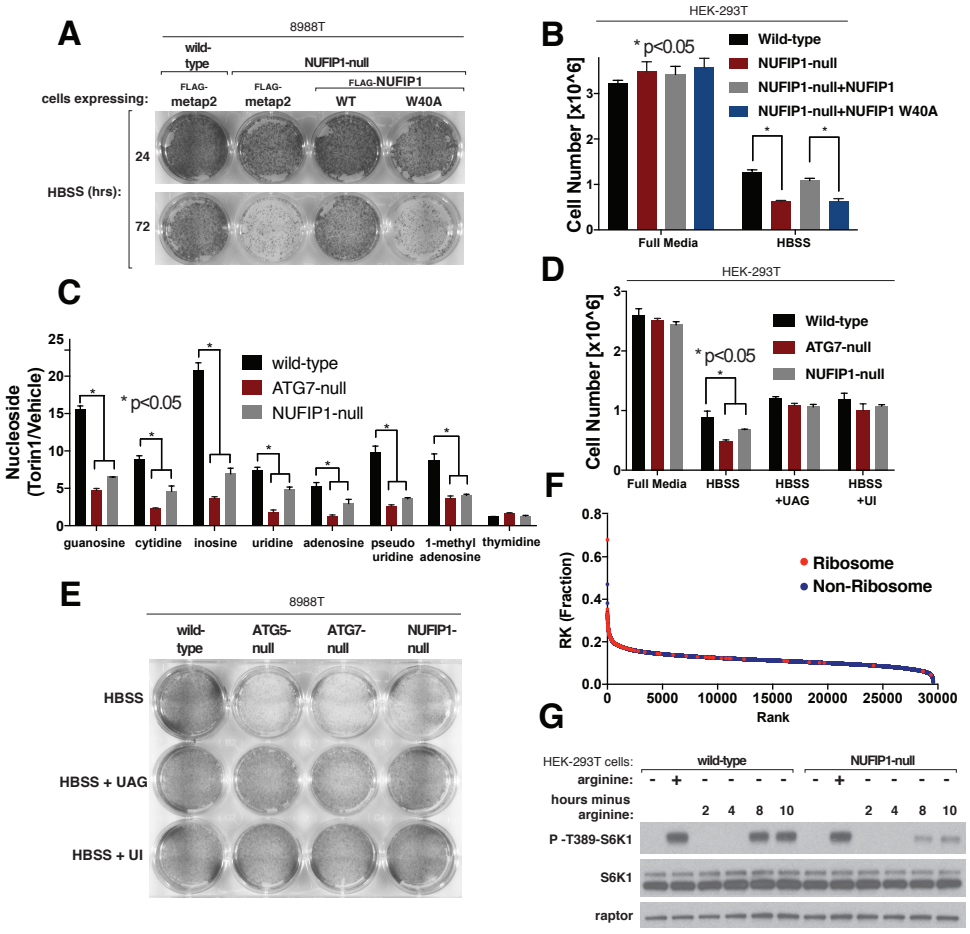
A
8988T
wild-type
NUFIP1-null
cells expressing:
FLAG-metap2
FLAG-metap2
FLAG-NUFIP1 WT
FLAG-NUFIP1 W40A
HBSS (hrs):
24
72
B
HEK-293T
* p<0.05
Wild-type
NUFIP1-null
NUFIP1-null+NUFIP1
NUFIP1-null+NUFIP1 W40A
Cell Number [x10^6]
Full Media
HBSS
C
Nucleoside (Torin1/Vehicle)
* p<0.05
wild-type
ATG7-null
NUFIP1-null
guanosine
cytidine
inosine
uridine
adenosine
pseudo uridine
1-methyl adenosine
thymidine
D
HEK-293T
Cell Number [x10^6]
* p<0.05
Wild-type
ATG7-null
NUFIP1-null
Full Media
HBSS
HBSS +UAG
HBSS +UI
E
8988T
wild-type
ATG5-null
ATG7-null
NUFIP1-null
HBSS
HBSS + UAG
HBSS + UI
F
RK (Fraction)
Ribosome
Non-Ribosome
Rank
G
HEK-293T cells:
wild-type
NUFIP1-null
arginine:
hours minus arginine:
2 4 8 10
2 4 8 10
P -T389-S6K1
S6K1
raptor

Fig. 5: NUFIP1 is important for cells to survive starvation

(A) Loss of NUFIP1 or just its capacity to interact with LC3B impairs cell survival upon nutrient starvation. Wild-type or NUFIP1-null 8988T cells stably expressing the indicated proteins were deprived of nutrients by culturing them in Hank's Balanced Salt Solution (HBSS); after the indicated times the surviving cells were stained and imaged.

(B) Loss of NUFIP1 or just its capacity to interact with LC3B impairs cell survival upon nutrient starvation. Wild-type or NUFIP1-null HEK-293T cells stably expressing the indicated proteins were deprived of nutrients by HBSS, and after 48 hours the number of surviving cells was quantified using cell counting. Values are normalized relative to cell numbers at the start of the starvation period and are mean +/- SD (*P<0.05; n=3).

(C) Loss of NUFIP1 or ATG7 inhibits the increase in nucleosides caused by mTOR inhibition. Data represent relative change in whole-cell concentrations of nucleosides in wild-type, ATG7-null, and NUFIP1-null HEK-293T cells treated with 250 nM Torin1 for 1 hour. Values are mean -/+ SEM (*P<0.05; n=3)

(D) Nucleoside supplementation rescues the survival defects of ATG7-null and NUFIP1-null HEK-293T cells. Indicated cells were deprived of nutrients by culturing in HBSS with or without the indicated nucleosides (2 mM each). After 48 hours, the number of surviving cells was quantified. Values were normalized relative to cell numbers at the start of the starvation period and are mean +/- SD (*P<0.05; n=3).

(E) Nucleoside supplementation rescues survival defect of ATG5-null, ATG7-null, and NUFIP1-null 8988T cells. Wild-type, ATG5-null, ATG7-null, or NUFIP1-null cells were deprived of nutrients by culturing in HBSS with or without the indicated nucleosides (2 mM each). After 48 hours the surviving cells were stained and imaged.

(F) Ribosomes are highly enriched for arginine and lysine. Protein sequences in the UniProt database (including isoforms) were ranked based on their fraction content of arginine and lysine. Ribosomal proteins are shown in red; all other proteins are shown in blue. Mitochondrial ribosomal proteins were not designated as ribosomal in this analysis.

(G) Loss of NUFIP1 suppresses the reactivation of mTORC1 that occurs after long-term arginine deprivation. Wild-type or NUFIP1 HEK-293T cells were deprived of arginine for 50 mins (first lanes of each set) or the indicated times and, where indicated, re-stimulated with arginine for 10 mins. Cell lysates were analyzed by immunoblotting for the levels and phosphorylation states of the indicated proteins.

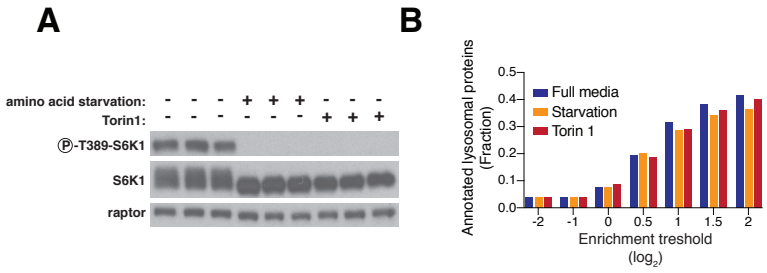
A
B
amino acid starvation: - - - + + + - - -
Torin1: - - - - - - + + +
Ⓟ-T389-S6K1
S6K1
raptor
Annotated lysosomal proteins (Fraction)
0.5
0.4
0.3
0.2
0.1
0.0
Full media
Starvation
Torin 1
-2
-1
0
0.5
1
1.5
2
Enrichment treshold (log2)

Fig. S1.

(A) Immunoblot analyses of the levels and phosphorylation state of S6K1 in cells used to prepare the lysosomal samples for the proteomics analyses described in Figure 1. Raptor was used as the loading control.

(B) A sliding window approach for determining a cut-off value for defining lysosomal proteins. The enrichment score (log_2) of each protein was determined by comparing the intensity of all the peptides unique to the protein in purified lysosomes versus their intensity on the control beads. The UniProt database was used as the source of the lysosomal annotation.

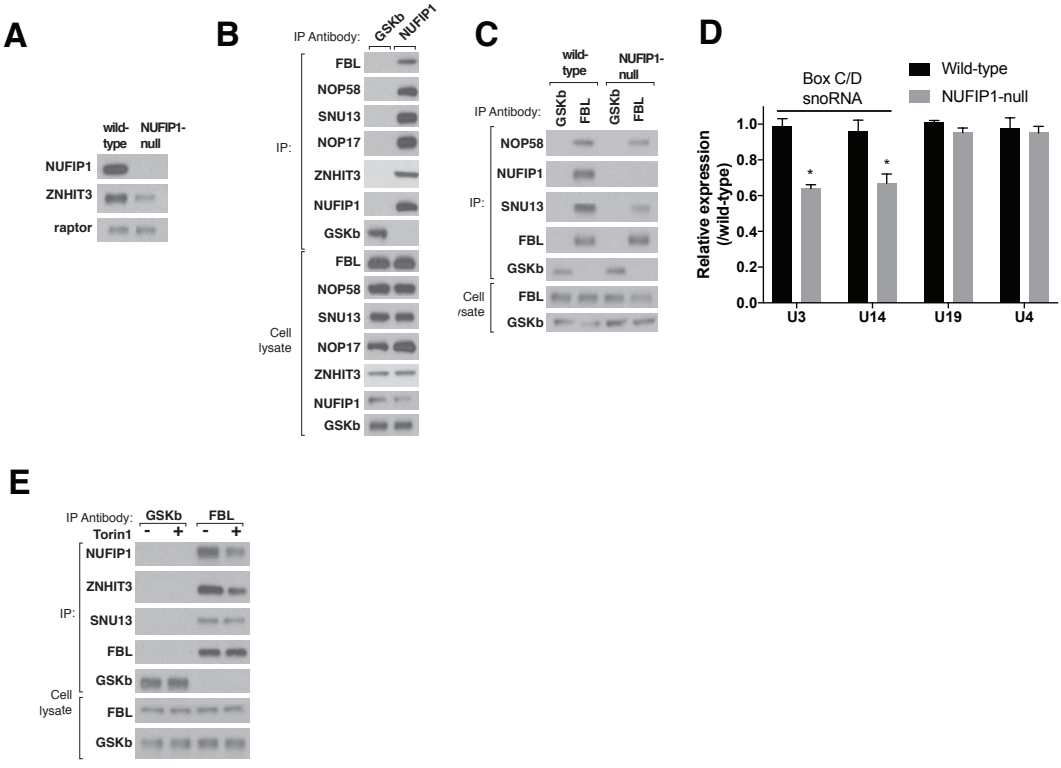
A
wild-type
NUFIP1-null
NUFIP1
ZNHIT3
raptor
B
IP Antibody:
GSKb
NUFIP1
IP:
FBL
NOP58
SNU13
NOP17
ZNHIT3
NUFIP1
GSKb
Cell lysate
FBL
NOP58
SNU13
NOP17
ZNHIT3
NUFIP1
GSKb
C
wild-type
NUFIP1-null
IP Antibody:
GSKb
FBL
GSKb
FBL
IP:
NOP58
NUFIP1
SNU13
FBL
GSKb
Cell lysate
FBL
GSKb
D
Box C/D snoRNA
Wild-type
NUFIP1-null
Relative expression (/wild-type)
1.0
0.8
0.6
0.4
0.2
0.0
*
*
U3
U14
U19
U4
E
IP Antibody:
GSKb
FBL
Torin1
-
+
-
+
IP:
NUFIP1
ZNHIT3
SNU13
FBL
GSKb
Cell lysate
FBL
GSKb

Fig. S2

(A) NUFIP1-loss decreases the expression of ZNHIT3 in HEK-293T cells. Cell lysates were prepared from wild-type and NUFIP1-null HEK-293T cells and total levels of the indicated proteins were analyzed by immunoblotting.

(B) NUFIP1-ZNHIT3 interacts with the core members of the C/D snoRNP complex. Anti-NUFIP1 immunoprecipitates were prepared from HEK-293T cells and lysates and immunoprecipitates were analyzed for the indicated proteins. Anti-GSKb was used as a negative control.

(C) NUFIP1-loss partially disrupts the C/D snoRNP complex. Anti-FBL immunoprecipitates were prepared from wild-type and NUFIP1-null HEK-293T cells and immunoprecipitates and lysates were analyzed for the indicated proteins as in (B). Anti-GSKb was used as a negative control.

(D) NUFIP1-loss reduces the expression of C/D but not H/ACA box or U4 snoRNAs.

(E) mTOR inhibition reduced the amount of NUFIP1-ZNHIT3 associated with FBL. Anti-FBL immunoprecipitates were prepared from HEK-293T cells treated with 250 nM Torin1 for 1 hour and immunoprecipitates and lysates were analyzed for the indicated proteins. mTOR inhibition does not reduce the interaction between core members of the C/D box snoRNP as shown by the SNU13-FBL interaction. Anti-GSKb was used as a negative control.

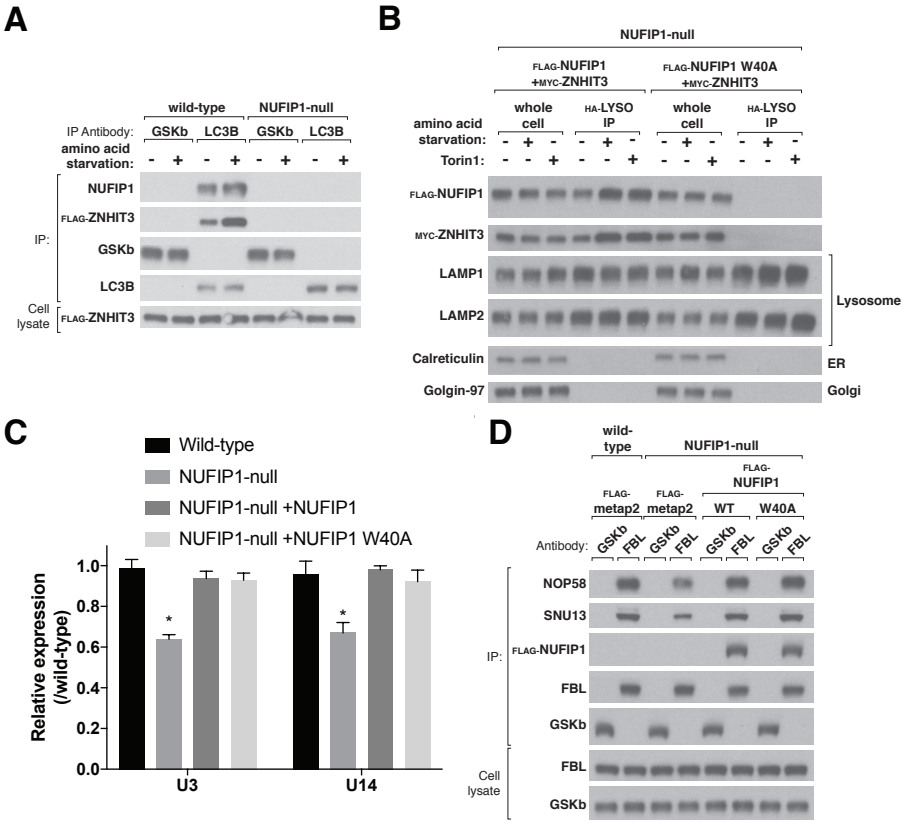
A
wild-type
NUFIP1-null
IP Antibody:
GSKb
LC3B
GSKb
LC3B
amino acid starvation:
- + - + - + - +
IP:
NUFIP1
FLAG-ZNHIT3
GSKb
LC3B
Cell lysate
FLAG-ZNHIT3
B
NUFIP1-null
FLAG-NUFIP1 +MYC-ZNHIT3
FLAG-NUFIP1 W40A +MYC-ZNHIT3
whole cell
HA-LYSO IP
whole cell
HA-LYSO IP
amino acid starvation:
- + - - + - - + - - + -
Torin1:
- - + - - + - - + - - +
FLAG-NUFIP1
MYC-ZNHIT3
LAMP1
LAMP2
Lysosome
Calreticulin
ER
Golgin-97
Golgi
C
Wild-type
NUFIP1-null
NUFIP1-null +NUFIP1
NUFIP1-null +NUFIP1 W40A
Relative expression (/wild-type)
1.0
0.8
0.6
0.4
0.2
0.0
*
*
U3
U14
D
wild-type
NUFIP1-null
FLAG-metap2
FLAG-metap2
FLAG-NUFIP1 WT
FLAG-NUFIP1 W40A
Antibody:
GSKb
FBL
GSKb
FBL
GSKb
FBL
GSKb
FBL
IP:
NOP58
SNU13
FLAG-NUFIP1
FBL
GSKb
Cell lysate
FBL
GSKb

Fig. S3

(A) In the absence of NUFIP1, ZNHIT3 does not interact with endogenous LC3B. Wild-type or NUFIP1-null cells stably expressing FLAG-ZNHIT3 were deprived of amino acids for 1 hour and lysates and anti-LC3B immunoprecipitates were prepared and analyzed for the indicated proteins. As in (B), anti-GSKb immunoprecipitates were used as a negative control.

(B) The NUFIP1 W40A mutant that cannot bind to LC3B can still interact with ZNHIT3, but is not found at lysosomes under any condition, including mTORC1 inhibition. Immunoprecipitates and lysates were prepared from NUFIP1-null HEK-293T cells stably expressing the HA-Lyso tag and transiently expressing the indicated proteins. LAMP1 and LAMP2 are established lysosomal proteins.

(C) In NUFIP1-null expression of the NUFIP1 W40A mutant rescues the modest drop in expression of the C/D box snoRNAs U3 and U14 caused by loss of NUFIP1 loss as well as expression of wild-type NUFIP1.

(D) A NUFIP mutant (W40A) that cannot bind LC3B can still associate with the C/D box snoRNP. Anti-FBL immunoprecipitates were prepared from wild-type or NUFIP1-null HEK-293T cells stably expressing the indicated proteins and analyzed by immunoblotting for the core C/D box snoRNP components SNU13 and NOP58. GSKb was used as a negative control.

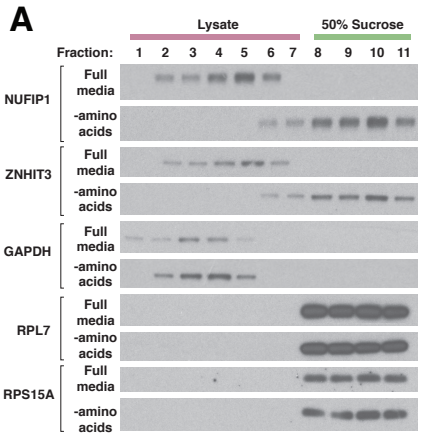
A
Lysate
50% Sucrose
Fraction: 1 2 3 4 5 6 7 8 9 10 11
NUFIP1
ZNHIT3
GAPDH
RPL7
RPS15A
Full media
-amino acids

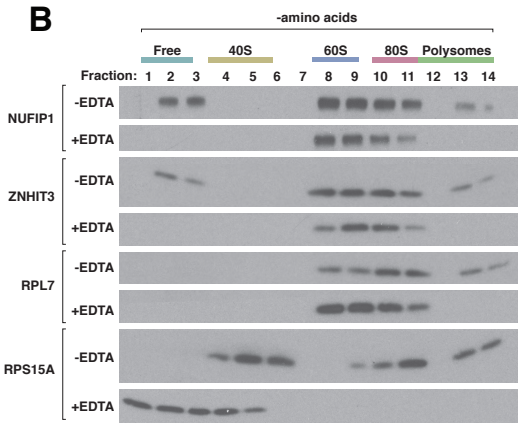
B
-amino acids
Free
40S
60S
80S
Polysomes
Fraction: 1 2 3 4 5 6 7 8 9 10 11 12 13 14
NUFIP1
ZNHIT3
RPL7
RPS15A
-EDTA
+EDTA

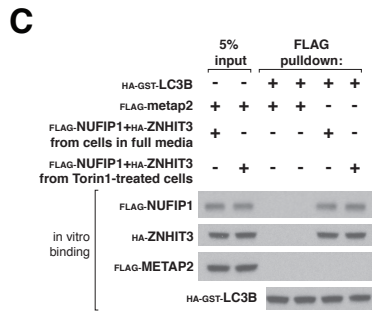
C
5% input
FLAG pulldown:
HA-GST-LC3B - - + + + +
FLAG-metap2 + + + + - -
FLAG-NUFIP1+HA-ZNHIT3 from cells in full media + - - - + -
FLAG-NUFIP1+HA-ZNHIT3 from Torin1-treated cells - + - - - +
in vitro binding
FLAG-NUFIP1
HA-ZNHIT3
FLAG-METAP2
HA-GST-LC3B

Fig. S4

(A) Amino acid deprivation increases the total amount of NUFIP1-ZNHIT3 that co-fractionates with ribosomes. HEK-293T cell lysates prepared from cells in full media or deprived of amino acids for one hour were fractionated over a 50% sucrose cushion. Fractions were collected and the indicated proteins analyzed by immunoblotting.

(B) NUFIP1-ZNHIT3 co-fractionates with the 60S subunit of the ribosome. HEK-293T cells deprived of amino acids for 1 hour were fractionated over a 10-45% sucrose gradient. Lysates were also prepared in the presence of EDTA to dissociate the 40S and 60S subunits and fractions were collected and indicated proteins analyzed by immunoblotting.

(C) The in vitro interaction of LC3B with NUFIP1-ZNHIT3 is unaffected by whether or not the proteins were obtained from cells with mTOR inhibition. Purified HA-GST-LC3B was immobilized on a glutathione affinity resin and incubated with FLAG-NUFIP1-HA-ZNHIT3. NUFIP1-ZNHIT3 was purified either from cells in full media or treated with 250 nM Torin1 for one hour. Proteins captured in the glutathione resin pull-down were analyzed by immunoblotting for the indicated proteins using anti-epitope tag antibodies.

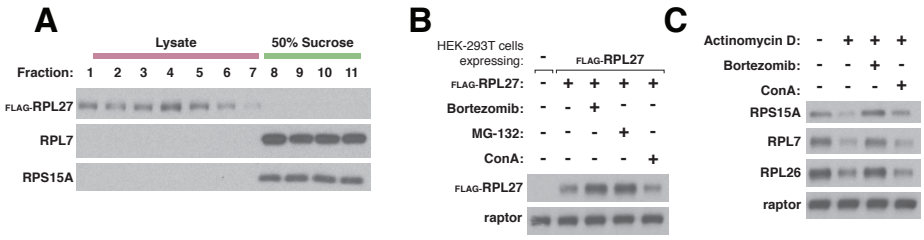
A
Lysate
50% Sucrose
Fraction: 1 2 3 4 5 6 7 8 9 10 11
FLAG-RPL27
RPL7
RPS15A
B
HEK-293T cells expressing: - FLAG-RPL27
FLAG-RPL27: - + + + +
Bortezomib: - - + - -
MG-132: - - - + -
ConA: - - - - +
FLAG-RPL27
raptor
C
Actinomycin D: - + + +
Bortezomib: - - + -
ConA: - - - +
RPS15A
RPL7
RPL26
raptor

Fig. S5

(A) Overexpressed recombinant FLAG-RPL27 does not incorporate into ribosomes. HEK-293T cell lysates stably expressing FLAG-RPL27 were fractionated over a 50% sucrose cushion. Fractions were collected and the indicated proteins were analyzed by immunoblotting.

(B) The degradation of overexpressed recombinant RPL27 requires proteasome activity. HEK-293T cells stably expressing FLAG-RPL27 were treated with Bortezomib (5 mM), MG132 (5 mM), or Concanamycin A (2.5 mM) for 1 hour. Lysates were prepared and the levels of the indicated proteins analyzed by immunoblotting.

(C) Free ribosomal proteins are degraded via the proteasome. Depletion of ribosomal RNA by Actinomycin D treatment leads to the degradation of ribosomal proteins, which requires proteasomal activity but not the acidification of the lysosome. HEK-293T cells were treated overnight with Actinomycin D (10 ng/mL) in the presence of Bortezomib (500 nM) or Concanamycin A (500 nM) and lysates were prepared and total levels of indicated proteins analyzed via immunoblotting.

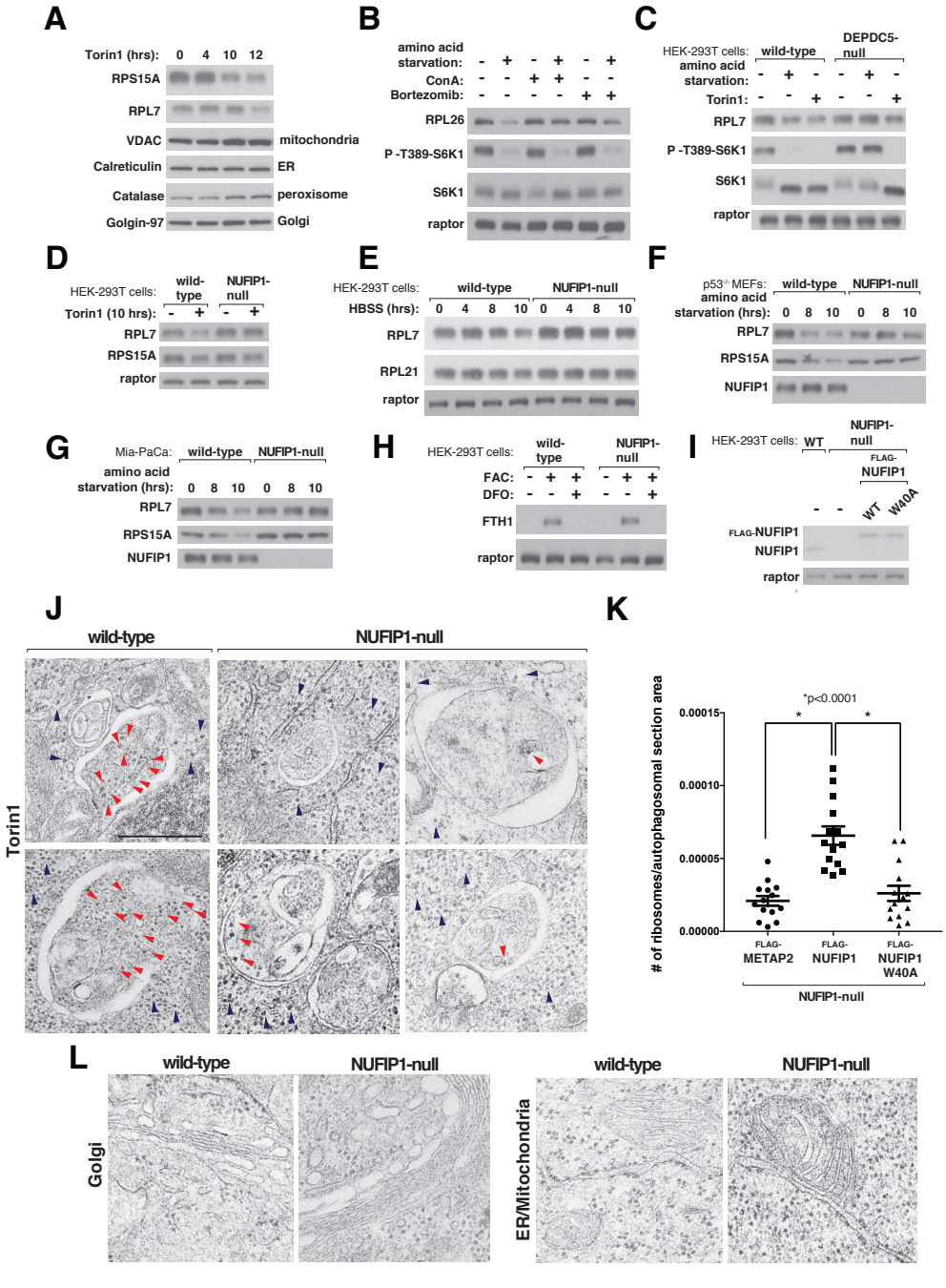
A
Torin1 (hrs): 0 4 10 12
RPS15A
RPL7
VDAC
mitochondria
Calreticulin
ER
Catalase
peroxisome
Golgin-97
Golgi
B
amino acid starvation:
ConA:
Bortezomib:
RPL26
P -T389-S6K1
S6K1
raptor
C
HEK-293T cells:
wild-type
DEPDC5-null
amino acid starvation:
Torin1:
RPL7
P -T389-S6K1
S6K1
raptor
D
HEK-293T cells:
wild-type
NUFIP1-null
Torin1 (10 hrs):
RPL7
RPS15A
raptor
E
HEK-293T cells:
wild-type
NUFIP1-null
HBSS (hrs): 0 4 8 10 0 4 8 10
RPL7
RPL21
raptor
F
p53-/- MEFs:
wild-type
NUFIP1-null
amino acid starvation (hrs): 0 8 10 0 8 10
RPL7
RPS15A
NUFIP1
G
Mia-PaCa:
wild-type
NUFIP1-null
amino acid starvation (hrs): 0 8 10 0 8 10
RPL7
RPS15A
NUFIP1
H
HEK-293T cells:
wild-type
NUFIP1-null
FAC:
DFO:
FTH1
raptor
I
HEK-293T cells:
WT
NUFIP1-null
FLAG-NUFIP1
WT
W40A
FLAG-NUFIP1
NUFIP1
raptor
J
wild-type
NUFIP1-null
Torin1
K
*p<0.0001
# of ribosomes/autophagosomal section area
0.00015
0.00010
0.00005
0.00000
FLAG-METAP2
FLAG-NUFIP1
FLAG-NUFIP1 W40A
NUFIP1-null
L
wild-type
NUFIP1-null
Golgi
wild-type
NUFIP1-null
ER/Mitochondria

Fig. S6

(A) Long term mTOR inhibition leads to the depletion of ribosomal proteins but not proteins that serve as markers of other compartments. HEK-293T cells were treated with 250 nM Torin1 for indicated time points and cell lysates were analyzed by immunoblotting for total levels of the indicated proteins.

(B) Pharmacological inhibition of the lysosomal pH but not the proteasome prevents the degradation of ribosomes caused by amino acid deprivation for 10 hours. HEK-293T cells treated with 1 uM Concanamycin A or 5 uM Bortezomib were deprived of amino acids for 10 hours and cell lysates analyzed by immunoblotting for the total levels and phosphorylation states of the indicated proteins.

(C) mTORC1 regulates ribosomal protein abundance upon nutrient starvation. Wild-type or GATOR1-null (DEPDC5-null) HEK-293T cells were deprived of amino acids or treated with 250 nM Torin1 for 10 hours and cell lysates were prepared and total levels and phosphorylation states of indicated proteins were analyzed by immunoblotting.

(D) NUFIP1-loss suppresses the degradation of ribosomes caused by mTOR inhibition. Wild-type or NUFIP1-null HEK-293T cells were treated with 250 nM Torin1 for 10 hours and cell lysates were prepared and total levels of indicated proteins were analyzed via immunoblotting.

(E) NUFIP1-loss suppresses the degradation of ribosomes induced by total nutrient starvation. Wild-type or NUFIP1-null HEK-293T cells were starved of all nutrients using Hank's Balanced Salt Solution (HBSS) for indicated

time points and cell lysates were prepared and total levels of indicated proteins were analyzed via immunoblotting.

(F) NUFIP1-loss suppresses the degradation of ribosomes induced by nutrient starvation in $P53^{-/-}$ MEFs. $P53^{-/-}$ MEFs stably expressing sgRNAs using the pLentiCrispr system that target the control AAVS1 locus or NUFIP1 were deprived of amino acids for the indicated times and cell lysates were prepared and total protein levels analyzed via immunoblotting.

(G) NUFIP1-loss suppresses the degradation of ribosomes induced by nutrient starvation in human Mia-PaCa cells. Mia-PaCa stably expressing sgRNAs using the pLentiCrispr system that target the control AAVS1 locus or NUFIP1 were deprived of amino acids for the indicated times and cell lysates were prepared and total protein levels analyzed via immunoblotting.

(H) NUFIP1-loss does not impact the degradation of ferritin. Wild-type or NUFIP1-null HEK-293T cells were incubated overnight with FAC to induce Ferritin expression and then treated for 4 hours with iron chelator DFO (*101*). Lysates were prepared and protein levels analyzed via immunoblotting.

(I) In NUFIP1-null HEK-293T cells wild-type NUFIP1 or the W40A mutant is expressed at levels near those of the endogenous protein. Lysates were prepared and protein levels analyzed via immunoblotting.

(J) Autophagosomes from HEK-293T cells lacking NUFIP1 contain fewer

ribosomes. Wild-type or NUFIP1-null HEK-293T cells were treated with Torin1 and ConcanamycinA for 4 hrs and analyzed by electron microscopy. Autophagosomes were identified by the presence of a double membrane and the red arrows indicate ribosomes internalized in autophagosomes. Blue arrows indicate ribosomes present in the cytoplasm but not in autophagosomes. Two representative images are shown for wild-type cells while four representative images are shown for NUFIP1-null HEK-293T cells. Scale bar = 500 nm

(K) Quantification of ribosome numbers in autophagosomes in Torin1-treated HEK-293T cells lacking NUFIP1 or expressing the W40A mutant. Ribosome numbers were determined as described in the methods. Autophagosomal section areas were calculated using ImageJ software. Mean +/- SEM, *P<0.0001, is shown.

(L) NUFIP1-loss does not affect the morphology of several organelles. Wild-type or NUFIP1-null HEK-293T cells were treated with Torin1 and ConcanamycinA for 4 hours and analyzed by electron microscopy. Representative images for the Golgi, ER, and mitochondria are shown.

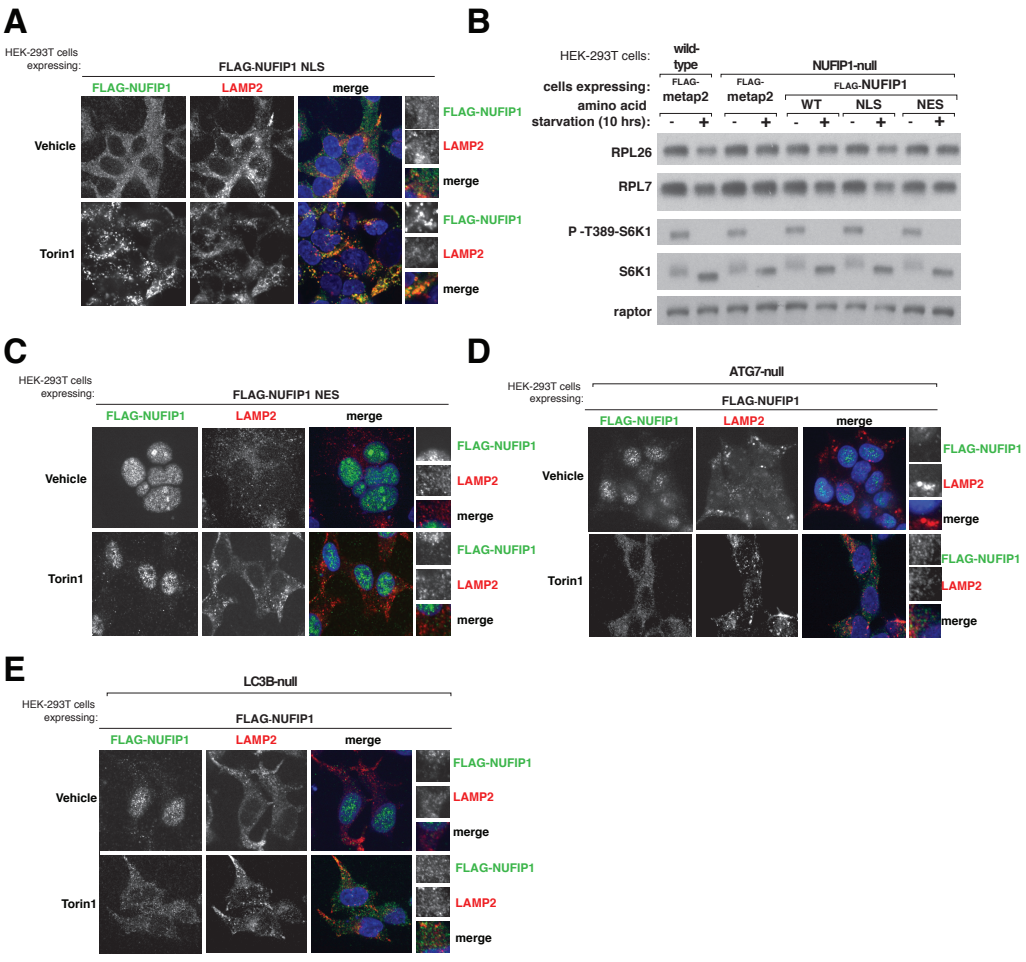
A
HEK-293T cells expressing:
FLAG-NUFIP1 NLS
FLAG-NUFIP1
LAMP2
merge
Vehicle
Torin1
B
HEK-293T cells:
wild-type
NUFIP1-null
cells expressing:
FLAG-metap2
FLAG-NUFIP1
WT
NLS
NES
amino acid starvation (10 hrs):
RPL26
RPL7
P -T389-S6K1
S6K1
raptor
C
HEK-293T cells expressing:
FLAG-NUFIP1 NES
D
ATG7-null
E
LC3B-null

Fig. S7

(A) NUFIP1 lacking its nuclear export sequence does not exit the nucleus upon mTOR inhibition. Imaging study shows that a NUFIP1 NES mutant does not translocate out of the nucleus to LAMP2-positive lysosomes upon Torin1 treatment. HEK-293T cells stably expressing FLAG-NUFIP1 NES were treated with 250 nM Torin1 for 1 hour and analyzed as described in the methods. Scale bar = 10 mm.

(B) For NUFIP1 to degrade ribosomes upon nutrient starvation, NUFIP1 must exit the nucleus. Wild-type or NUFIP1-null HEK-293T cells stably expressing the indicated proteins were deprived of amino acids for 10 hours and cell lysates were prepared and analyzed for phosphorylation states and total levels of indicated proteins.

(C) NUFIP1 lacking its nuclear localization sequence does not enter the nucleus and colocalizes to a greater extent with lysosomes upon mTOR inhibition. In HEK-293T cells stably FLAG-NUFIP1 NLS is constitutively cytoplasmic and upon mTOR inhibition cololocalizes with LAMP2-positive lysosomes. Cells were treated as in (A).

(D) In cells lacking ATG7, NUFIP1 can translocate out of the nucleus but does not localize with lysosomes. ATG7-null HEK-293T cells stably expressing FLAG-NUFIP1 were treated with 250 nM Torin1 for 1 hour and analyzed as in (A).

(E) In cells lacking LC3B, NUFIP1 can exit the nucleus but does not localize with lysosomes. LC3B-null HEK-293T cells stably expressing FLAG-NUFIP1 were

treated with 250 nM Torin1 for 1 hour and analyzed as in (A).

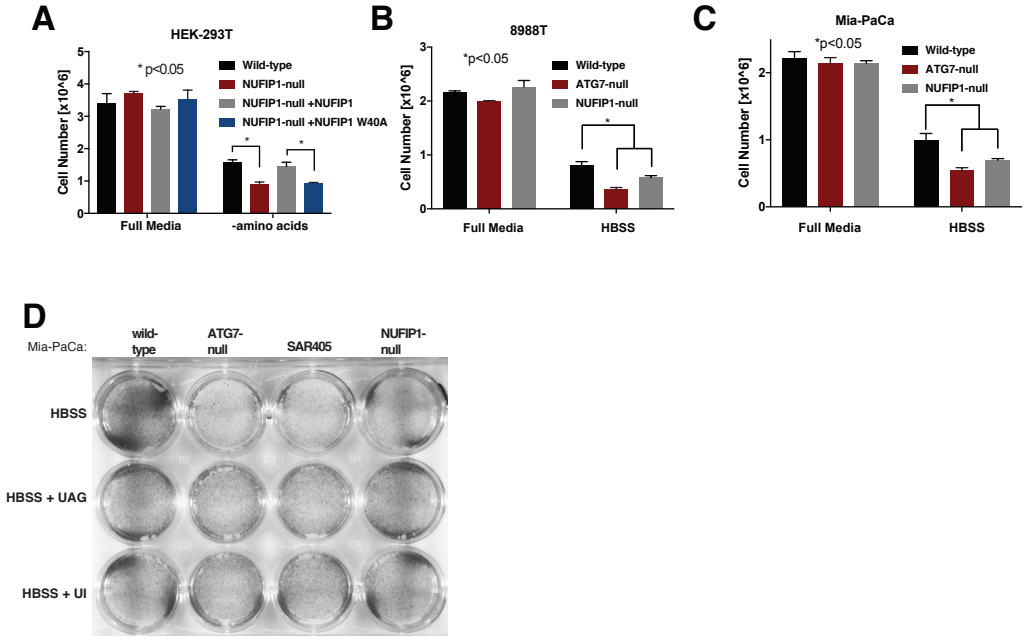
A
HEK-293T
* p<0.05
Wild-type
NUFIP1-null
NUFIP1-null +NUFIP1
NUFIP1-null +NUFIP1 W40A
Cell Number [x10^6]
Full Media
-amino acids
B
8988T
*p<0.05
Wild-type
ATG7-null
NUFIP1-null
Cell Number [x10^6]
Full Media
HBSS
C
Mia-PaCa
*p<0.05
Wild-type
ATG7-null
NUFIP1-null
Cell Number [x10^6]
Full Media
HBSS

D
Mia-PaCa:
wild-type
ATG7-null
SAR405
NUFIP1-null
HBSS
HBSS + UAG
HBSS + UI

Fig. S8

(A) Loss of NUFIP1 or just its capacity to interact with LC3B impairs cell survival upon nutrient starvation. Wild-type or NUFIP1-null HEK-293T cells stably expressing the indicated proteins were deprived of amino acids and after 48 hours the number of surviving cells was quantified. Values are normalized relative to cell numbers at the start of the starvation period and are mean +/- SD (*P<0.05; n=3).

(B) Loss of ATG7 or NUFIP impairs cell survival upon nutrient starvation. Wild-type, ATG7-null, or NUFIP1-null 8988T cells were deprived of nutrients for 48 hours by culturing them in Hank's Balanced Salt Solution (HBSS) and the number of surviving cells was quantified. Values are normalized relative to cell numbers at the start of the starvation period and are mean +/- SD (*P<0.05; n=3).

(C) Loss of ATG7 or NUFIP impairs cell survival upon nutrient starvation. Wild-type, ATG7-null, or NUFIP1-null Mia-PaCa cells were deprived of nutrients by culturing them for 48 hours in Hank's Balanced Salt Solution (HBSS) and the number of surviving cells was quantified. Values are normalized relative to cell numbers at the start of the starvation period and are mean +/- SD (*P<0.05; n=3).

(D) Nucleoside supplementation rescues the survival defect of ATG7-null and NUFIP1-null cells or of wild-type cells treated with VPS34 inhibitor SAR-405 (1 uM). Wild-type, ATG7-null, or NUFIP1-null Mia-PaCa cells, or wild-type Mia-PaCa cells treated with VPS34 inhibitor, were deprived of

nutrients by culturing them in HBSS with or without the indicated nucleosides (2 mM each) and after 48 hours the surviving cells were stained and imaged.

References

1. A. Ballabio, V. Gieselmann, Lysosomal disorders: from storage to cellular damage. *Biochimica et biophysica acta* **1793**, 684-696 (2009); published online EpubApr (10.1016/j.bbamcr.2008.12.001).
2. F. M. Platt, B. Boland, A. C. van der Spoel, The cell biology of disease: lysosomal storage disorders: the cellular impact of lysosomal dysfunction. *The Journal of cell biology* **199**, 723-734 (2012); published online EpubNov 26 (10.1083/jcb.201208152).
3. L. Groth-Pedersen, M. Jaattela, Combating apoptosis and multidrug resistant cancers by targeting lysosomes. *Cancer letters* **332**, 265-274 (2013); published online EpubMay 28 (10.1016/j.canlet.2010.05.021).
4. R. A. Saxton, D. M. Sabatini, mTOR Signaling in Growth, Metabolism, and Disease. *Cell* **168**, 960-976 (2017); published online EpubMar 09 (10.1016/j.cell.2017.02.004).
5. M. Abu-Remaileh, G. A. Wyant, C. Kim, N. N. Laqtom, M. Abbasi, S. H. Chan, E. Freinkman, D. M. Sabatini, Lysosomal metabolomics reveals V-ATPase- and mTOR-dependent regulation of amino acid efflux from lysosomes. *Science* **358**, 807-813 (2017); published online EpubNov 10 (10.1126/science.aan6298).
6. Y. Sancak, T. R. Peterson, Y. D. Shaul, R. A. Lindquist, C. C. Thoreen, L. Bar-Peled, D. M. Sabatini, The Rag GTPases bind raptor and mediate amino acid signaling to mTORC1. *Science* **320**, 1496-1501 (2008); published online EpubJun 13 (10.1126/science.1157535).
7. C. Settembre, R. Zoncu, D. L. Medina, F. Vetrini, S. Erdin, S. Erdin, T. Huynh, M. Ferron, G. Karsenty, M. C. Vellard, V. Facchinetti, D. M. Sabatini, A. Ballabio, A lysosome-to-nucleus signalling mechanism senses and regulates the lysosome via mTOR and TFEB. *The EMBO journal* **31**, 1095-1108 (2012); published online EpubMar 07 (10.1038/emboj.2012.32).
8. A. Roczniak-Ferguson, C. S. Petit, F. Froehlich, S. Qian, J. Ky, B. Angarola, T. C. Walther, S. M. Ferguson, The transcription factor TFEB links mTORC1 signaling to transcriptional control of lysosome homeostasis. *Science signaling* **5**, ra42 (2012); published online EpubJun 12 (10.1126/scisignal.2002790).
9. C. S. Petit, A. Roczniak-Ferguson, S. M. Ferguson, Recruitment of folliculin to lysosomes supports the amino acid-dependent activation of Rag GTPases. *The Journal of cell biology* **202**, 1107-1122 (2013); published online EpubSep 30 (10.1083/jcb.201307084).
10. J. A. Martina, H. I. Diab, L. Lishu, A. L. Jeong, S. Patange, N. Raben, R. Puertollano, The nutrient-responsive transcription factor TFE3 promotes autophagy, lysosomal biogenesis, and clearance of cellular debris. *Science signaling* **7**, ra9 (2014); published online EpubJan 21 (10.1126/scisignal.2004754).
11. Z. Y. Tsun, L. Bar-Peled, L. Chantranupong, R. Zoncu, T. Wang, C. Kim, E. Spooner, D. M. Sabatini, The folliculin tumor suppressor is a GAP for the RagC/D

GTPases that signal amino acid levels to mTORC1. *Molecular cell* **52**, 495-505 (2013); published online EpubNov 21 (10.1016/j.molcel.2013.09.016).
12. R. P. Murmu, E. Martin, A. Rastetter, T. Esteves, M. P. Muriel, K. H. El Hachimi, P. S. Denora, A. Dauphin, J. C. Fernandez, C. Duyckaerts, A. Brice, F. Darios, G. Stevanin, Cellular distribution and subcellular localization of spatacsin and spastizin, two proteins involved in hereditary spastic paraplegia. *Molecular and cellular neurosciences* **47**, 191-202 (2011); published online EpubJul (10.1016/j.mcn.2011.04.004).
13. J. Hirst, G. H. Borner, J. Edgar, M. Y. Hein, M. Mann, F. Buchholz, R. Antrobus, M. S. Robinson, Interaction between AP-5 and the hereditary spastic paraplegia proteins SPG11 and SPG15. *Molecular biology of the cell* **24**, 2558-2569 (2013); published online EpubAug (10.1091/mbc.E13-03-0170).
14. B. Bardoni, R. Willemsen, I. J. Weiler, A. Schenck, L. A. Severijnen, C. Hindelang, E. Lalli, J. L. Mandel, NUFIP1 (nuclear FMRP interacting protein 1) is a nucleocytoplasmic shuttling protein associated with active synaptoneurosomes. *Experimental cell research* **289**, 95-107 (2003); published online EpubSep 10 (
15. M. Quinternet, M. E. Chagot, B. Rothe, D. Tiotiu, B. Charpentier, X. Manival, Structural Features of the Box C/D snoRNP Pre-assembly Process Are Conserved through Species. *Structure* **24**, 1693-1706 (2016); published online EpubOct 04 (10.1016/j.str.2016.07.016).
16. B. Rothe, J. M. Saliou, M. Quinternet, R. Back, D. Tiotiu, C. Jacquemin, C. Loegler, F. Schlotter, V. Pena, K. Eckert, S. Morera, A. V. Dorsselaer, C. Branlant, S. Massenet, S. Sanglier-Cianferani, X. Manival, B. Charpentier, Protein Hit1, a novel box C/D snoRNP assembly factor, controls cellular concentration of the scaffolding protein Rsa1 by direct interaction. *Nucleic acids research* **42**, 10731-10747 (2014)10.1093/nar/gku612).
17. S. Boulon, N. Marmier-Gourrier, B. Pradet-Balade, L. Wurth, C. Verheggen, B. E. Jady, B. Rothe, C. Pescia, M. C. Robert, T. Kiss, B. Bardoni, A. Krol, C. Branlant, C. Allmang, E. Bertrand, B. Charpentier, The Hsp90 chaperone controls the biogenesis of L7Ae RNPs through conserved machinery. *The Journal of cell biology* **180**, 579-595 (2008); published online EpubFeb 11 (10.1083/jcb.200708110).
18. K. S. McKeegan, C. M. Debieux, S. Boulon, E. Bertrand, N. J. Watkins, A dynamic scaffold of pre-snoRNP factors facilitates human box C/D snoRNP assembly. *Molecular and cellular biology* **27**, 6782-6793 (2007); published online EpubOct (10.1128/MCB.01097-07).
19. M. Quinternet, B. Rothe, M. Barbier, C. Bobo, J. M. Saliou, C. Jacquemin, R. Back, M. E. Chagot, S. Cianferani, P. Meyer, C. Branlant, B. Charpentier, X. Manival, Structure/Function Analysis of Protein-Protein Interactions Developed by the Yeast Pih1 Platform Protein and Its Partners in Box C/D snoRNP Assembly. *Journal of molecular biology* **427**, 2816-2839 (2015); published online EpubAug 28 (10.1016/j.jmb.2015.07.012).
20. M. Komatsu, S. Waguri, T. Ueno, J. Iwata, S. Murata, I. Tanida, J. Ezaki, N. Mizushima, Y. Ohsumi, Y. Uchiyama, E. Kominami, K. Tanaka, T. Chiba, Impairment of starvation-induced and constitutive autophagy in Atg7-deficient mice. *The Journal of cell biology* **169**, 425-434 (2005); published online EpubMay 09 (10.1083/jcb.200412022).
21. A. B. Birgisdottir, T. Lamark, T. Johansen, The LIR motif - crucial for selective autophagy. *Journal of cell science* **126**, 3237-3247 (2013); published online EpubAug 01 (10.1242/jcs.126128).

22. M. K. Sung, T. R. Porras-Yakushi, J. M. Reitsma, F. M. Huber, M. J. Sweredoski, A. Hoelz, S. Hess, R. J. Deshaies, A conserved quality-control pathway that mediates degradation of unassembled ribosomal proteins. *eLife* **5**, (2016); published online EpubAug 23 (10.7554/eLife.19105).
23. M. K. Sung, J. M. Reitsma, M. J. Sweredoski, S. Hess, R. J. Deshaies, Ribosomal proteins produced in excess are degraded by the ubiquitin-proteasome system. *Molecular biology of the cell* **27**, 2642-2652 (2016); published online EpubSep 01 (10.1091/mbc.E16-05-0290).
24. J. R. Warner, In the absence of ribosomal RNA synthesis, the ribosomal proteins of HeLa cells are synthesized normally and degraded rapidly. *Journal of molecular biology* **115**, 315-333 (1977); published online EpubSep 25 (
25. A. D. Mathis, B. C. Naylor, R. H. Carson, E. Evans, J. Harwell, J. Knecht, E. Hexem, F. F. Peelor, 3rd, B. F. Miller, K. L. Hamilton, M. K. Transtrum, B. T. Bikman, J. C. Price, Mechanisms of In Vivo Ribosome Maintenance Change in Response to Nutrient Signals. *Molecular & cellular proteomics : MCP* **16**, 243-254 (2017); published online EpubFeb (10.1074/mcp.M116.063255).
26. A. R. Kristensen, S. Schandorff, M. Hoyer-Hansen, M. O. Nielsen, M. Jaattela, J. Dengjel, J. S. Andersen, Ordered organelle degradation during starvation-induced autophagy. *Molecular & cellular proteomics : MCP* **7**, 2419-2428 (2008); published online EpubDec (10.1074/mcp.M800184-MCP200).
27. C. Kraft, A. Deplazes, M. Sohrmann, M. Peter, Mature ribosomes are selectively degraded upon starvation by an autophagy pathway requiring the Ubp3p/Bre5p ubiquitin protease. *Nature cell biology* **10**, 602-610 (2008); published online EpubMay (10.1038/ncb1723).
28. J. R. Warner, The economics of ribosome biosynthesis in yeast. *Trends in biochemical sciences* **24**, 437-440 (1999); published online EpubNov (
29. D. E. Weinberg, P. Shah, S. W. Eichhorn, J. A. Hussmann, J. B. Plotkin, D. P. Bartel, Improved Ribosome-Footprint and mRNA Measurements Provide Insights into Dynamics and Regulation of Yeast Translation. *Cell reports* **14**, 1787-1799 (2016); published online EpubFeb 23 (10.1016/j.celrep.2016.01.043).
30. J. E. Darnell, Jr., Ribonucleic acids from animal cells. *Bacteriological reviews* **32**, 262-290 (1968); published online EpubSep (
31. E. R. Lindley, R. L. Pisoni, Demonstration of adenosine deaminase activity in human fibroblast lysosomes. *The Biochemical journal* **290 (Pt 2)**, 457-462 (1993); published online EpubMar 1 (
32. H. Huang, T. Kawamata, T. Horie, H. Tsugawa, Y. Nakayama, Y. Ohsumi, E. Fukusaki, Bulk RNA degradation by nitrogen starvation-induced autophagy in yeast. *The EMBO journal* **34**, 154-168 (2015); published online EpubJan 13 (10.15252/embj.201489083).
33. J. Y. Guo, X. Teng, S. V. Laddha, S. Ma, S. C. Van Nostrand, Y. Yang, S. Khor, C. S. Chan, J. D. Rabinowitz, E. White, Autophagy provides metabolic substrates to maintain energy charge and nucleotide pools in Ras-driven lung cancer cells. *Genes & development* **30**, 1704-1717 (2016); published online EpubAug 1 (10.1101/gad.283416.116).
34. G. A. Wyant, M. Abu-Remaileh, R. L. Wolfson, W. W. Chen, E. Freinkman, L. V. Danai, M. G. Vander Heiden, D. M. Sabatini, mTORC1 Activator SLC38A9 Is Required to Efflux Essential Amino Acids from Lysosomes and Use Protein as a Nutrient. *Cell* **171**, 642-654 e612 (2017); published online EpubOct 19 (10.1016/j.cell.2017.09.046).

35. S. Klinge, F. Voigts-Hoffmann, M. Leibundgut, N. Ban, Atomic structures of the eukaryotic ribosome. *Trends in biochemical sciences* **37**, 189-198 (2012); published online EpubMay (10.1016/j.tibs.2012.02.007).
36. A. Khaminets, T. Heinrich, M. Mari, P. Grumati, A. K. Huebner, M. Akutsu, L. Liebmann, A. Stolz, S. Nietzsche, N. Koch, M. Mauthe, I. Katona, B. Qualmann, J. Weis, F. Reggiori, I. Kurth, C. A. Hubner, I. Dikic, Regulation of endoplasmic reticulum turnover by selective autophagy. *Nature* **522**, 354-358 (2015); published online EpubJun 18 (10.1038/nature14498).
37. J. D. Mancias, X. Wang, S. P. Gygi, J. W. Harper, A. C. Kimmelman, Quantitative proteomics identifies NCOA4 as the cargo receptor mediating ferritinophagy. *Nature* **509**, 105-109 (2014); published online EpubMay 01 (10.1038/nature13148).
38. Y. Wei, W. C. Chiang, R. Sumpter, Jr., P. Mishra, B. Levine, Prohibitin 2 Is an Inner Mitochondrial Membrane Mitophagy Receptor. *Cell* **168**, 224-238 e210 (2017); published online EpubJan 12 (10.1016/j.cell.2016.11.042).
39. Y. C. Wong, E. L. Holzbaur, Optineurin is an autophagy receptor for damaged mitochondria in parkin-mediated mitophagy that is disrupted by an ALS-linked mutation. *Proceedings of the National Academy of Sciences of the United States of America* **111**, E4439-4448 (2014); published online EpubOct 21 (10.1073/pnas.1405752111).
40. E. Deosaran, K. B. Larsen, R. Hua, G. Sargent, Y. Wang, S. Kim, T. Lamark, M. Jauregui, K. Law, J. Lippincott-Schwartz, A. Brech, T. Johansen, P. K. Kim, NBR1 acts as an autophagy receptor for peroxisomes. *Journal of cell science* **126**, 939-952 (2013); published online EpubFeb 15 (10.1242/jcs.114819).
41. D. A. Tumbarello, P. T. Manna, M. Allen, M. Bycroft, S. D. Arden, J. Kendrick-Jones, F. Buss, The Autophagy Receptor TAX1BP1 and the Molecular Motor Myosin VI Are Required for Clearance of Salmonella Typhimurium by Autophagy. *PLoS pathogens* **11**, e1005174 (2015); published online EpubOct (10.1371/journal.ppat.1005174).
42. P. Verlhac, I. P. Gregoire, O. Azocar, D. S. Petkova, J. Baguet, C. Viret, M. Faure, Autophagy receptor NDP52 regulates pathogen-containing autophagosome maturation. *Cell host & microbe* **17**, 515-525 (2015); published online EpubApr 08 (10.1016/j.chom.2015.02.008).
43. T. L. Thurston, G. Ryzhakov, S. Bloor, N. von Muhlinen, F. Randow, The TBK1 adaptor and autophagy receptor NDP52 restricts the proliferation of ubiquitin-coated bacteria. *Nature immunology* **10**, 1215-1221 (2009); published online EpubNov (10.1038/ni.1800).
44. H. An, J. W. Harper, Systematic analysis of ribophagy in human cells reveals bystander flux during selective autophagy. *Nature cell biology*, (2017); published online EpubDec 11 (10.1038/s41556-017-0007-x).
45. O. Boussif, F. Lezoualc'h, M. A. Zanta, M. D. Mergny, D. Scherman, Demeneix, J. P. Behr, A versatile vector for gene and oligonucleotide transfer into cells in culture and in vivo: polyethylenimine. Proceedings of the National Academy of Sciences of the United States of America 92, 7297-7301 (1995); published online EpubAug 01
46. R. Bruderer, O. M. Bernhardt, T. Gandhi, S. M. Miladinovic, L. Y. Cheng, S. Messner, T. Ehrenberger, V. Zanotelli, Y. Butscheid, C. Escher, O. Vitek, O.Rinner, L. Reiter, Extending the limits of quantitative proteome profiling with data independent acquisition and application to acetaminophen-treated three dimensional liver microtissues. Molecular & cellular proteomics : MCP 14, 1400-1410 (2015); published online EpubMay (10.1074/mcp.M114.044305).

47. G. Rosenberger, I. Bludau, U. Schmitt, M. Heusel, C. L. Hunter, Y. Liu, M. J. MacCoss, B. X. MacLean, A. I. Nesvizhskii, P. G. A. Pedrioli, L. Reiter, H. L.Rost, S. Tate, Y. S. Ting, B. C. Collins, R. Aebersold, Statistical control of peptide and protein error rates in large-scale targeted data-independent acquisition analyses. Nature methods 14, 921-927 (2017); published online EpubSep (10.1038/nmeth.4398).
48. J. D. Storey, A direct approach to false discovery rates. J Roy Stat Soc B 64, 479-498 (2002)Unsp 1369-7412/02/64479 Doi 10.1111/1467-9868.00346).
49. C. Settembre, C. Di Malta, V. A. Polito, M. Garcia Arencibia, F. Vetrini, S. Erdin, S. U. Erdin, T. Huynh, D. Medina, P. Colella, M. Sardiello, D. C. Rubinsztein, A. Ballabio, TFEB links autophagy to lysosomal biogenesis. Science 332, 1429-1433 (2011); published online EpubJun 17 (10.1126/science.1204592)..
50. J. A. Vizcaíno, E. W. Deutsch, R. Wang, A. Csordas, F. Reisinger, D. Ríos, J. A. Dianes, Z. Sun, T. Farrah, N.Bandeira, P.A. Binz, I. Xenarios, M. Eisenacher, G. Mayer, L. Gatto, A. Campos, R. J. Chalkley, H. J. Kraus, J. P. Albar, S. Martinez-Bartolomé, R. Apweiler, G.S. Omenn, L. Martens, A.R. Jones, H. Hermjakob, ProteomeXchange provides globally coordinated proteomics data submission and dissemination. Nat. Biotechnol. **32**, 223-226 (2014). doi:10.1038/nbt.2839pmid:24727771
51.J.A. Vizcaíno, R.G. Côté, A. Csordas,J.A. Dianes, A. Fabregat, J.M. Foster, J. Griss, E. Alpi, M. Birim, J.Contell, G. O'Kelly, A. Schoenegger, D. Ovelleiro, Y. Pérez-Riverol, F. Reisinger, D. Ríos, R. Wang, H.Hermjakob, The PRoteomics IDEntifications (PRIDE) database and associated tools: Status in 2013. Nucleic Acids Res. **41**, D1063–D1069 (2013). doi:10.1093/nar/gks1262pmid:23203882
Acknoldgements: We thank all members of the Sabatini Laboratory for helpful insights, particularly R.L. Wolfson, and the FLI proteomics core facility, in particular J. Kirkpatrick. **Funding:** This work was supported by grants from the NIH (R01 CA103866, R01 CA129105, and R37 AI47389) and Department of Defense (W81XWH-15-1-0230) and the Lustgarten Foundation to D.M.S., from the Department of Defense (W81XWH-15-1-0337) to E.F., as well an EMBO Long-Term Fellowship to M.A.-R, Saudi Aramco Ibn Khaldun Fellowship for Saudi Women to N.N.L., and an MIT School of Science Fellowship in Cancer Research to G.A.W.. A.O. and I.H. acknowledge support from the FLI proteomics core facility. The FLI is a member of the Leibniz Association and is financially supported by the Federal Government of Germany and the State of Thuringia. D.M.S. is an investigator of the Howard Hughes Medical Institute. **Author Contributions:** G.A.W., M.A-R., and D.M.S. initiated the project and designed the research plan. G.A.W and M.A-R. performed the experiments and analyzed the data with help from E.M.F, N.L., and V.D.. A.O. designed the proteomic runs and analyzed the lysosomal proteomic data. C.A.L. and S.Z.H preformed LC/MS runs and quantified metabolites. G.A.W and M.A-R. wrote the manuscript and D.M.S. edited it. All the authors approved and edited the manuscript. **Competing Interests:** D.M.S. is a founding member of the scientific advisory board, a paid consultant, and a shareholder of Navitor Pharmaceuticals, which is targeting for therapeutic benefit the amino acid sensing pathway upstream of mTORC1. **Data and Materials availability:** The mass spectrometry proteomics data have been deposited to the ProteomeXchange Consortium (http://proteomecentral.proteomexchange.org) (50) via the PRIDE partner repository (51) with the dataset identifier PXD009084.
(E)

Materials and Methods

Materials

Reagents were obtained from the following sources. Antibodies to LAMP2, NOP17, and HRP-labeled anti-mouse and anti-rabbit secondary antibodies from Santa Cruz Biotechnology; to PEX19 from Abcam; to NUFIP1 from Protein Tech; to ZNHIT3 from Bethyl Laboratories; to raptor from EMD Millipore; to S6K1 phospho-T389, S6K1, GSKb, LAMP1, LC3B, Histone H3, mTOR, RagA, VDAC, Calreticulin, Golgin-97, GAPDH, ZFYVE26, Catalase and the FLAG and HA epitopes from Cell Signaling Technology (CST); to SPG11 from Proteintech; to SNU13, NOP58, FBL, RPL7, RPS15A, RPL21, RPL23, and RPL26 from Bethyl Laboratories; and to RPS23 from Thermo. SAR405 from Selleck; RPMI and Flag-M2 affinity gel was obtained from Sigma Aldrich. DMEM from SAFC Biosciences; leucine-, arginine-, and lysine-free RPMI from US Biologicals; HBSS without glucose was used to maintain pH and osmotic balance; adenosine, guanosine, uridine, and inosine from Sigma; Giemsa stain from Sigma; XtremeGene9 and Complete Protease Cocktail from Roche; Alexa-488- and -568-conjugated secondary antibodies and inactivated fetal bovine serum (IFS) from Invitrogen; anti-HA magnetic beads, and ECL western blotting substrate from Thermo Fisher Scientific; Protein G Agarose beads from Pierce; and Actinomycin D from Tocris. Torin1 was generously provided by Dr. Nathanael Gray (DFCI).

Cell Culture

HEK-293T, MIA-PaCa, 8988T, and $P53^{-/-}$ MEFs and their derivatives were maintained at 37°C and 5% CO_2 in DMEM supplemented with 10% inactivated fetal calf serum, 2 mM glutamine, penicillin, and streptomycin. For experiments involving amino acid starvation, cells were incubated in RPMI base media lacking the indicated amino acid for 60 min or the indicated time points. For experiments involving analysis of ribosomal protein levels, experiments were preformed at no greater than 50% confluency to ensure active proliferation. As the abundance of ribosomes is extremely high, typically 2 ul of dilute lysate was analyzed via immunoblotting to ensure ribosome protein signal did not saturate and stayed witihin linear range. For all experiments involving lysosomal purifications, the media on the cells was changed to fresh RPMI base media 1 hr prior to the start of the experiment.

Cell lysis, immunoprecipitations, and cDNA transfections

Cells were rinsed with chilled PBS and lysed immediately on ice with a Triton X-100-based lysis buffer (1% Triton, 10 mM B-glycerol phosphate, 10 mM pyrophosphate, 40 mM HEPES pH 7.4, 2.5 mM $MgCl_2$) supplemented with 1 tablet of EDTA-free protease inhibitor (Roche) per 25 mL buffer. Lysates were kept at 4°C for 15 min and then clarified by centrifugation in a microcentrifuge at 13,000 rpm at 4°C for 10 min. For anti-FLAG immunoprecipitations, the FLAG-M2 affinity gel was washed with 1 mL lysis buffer three times and 30 uL of a 50% slurry of the affinity gel was then added to the clarified lysate and incubated with rotation at 4°C for 90 min. In order to reduce non-specific binding of ribosomes in

anti-FLAG immunoprecipitations, low protein binding tubes were used to reduce non-specific binding of ribosomes. Further, the beads were washed for 15 min three times in lysis buffer containing 500 mM NaCl on rotation at 4°C. Immunoprecipitated proteins were denatured by the addition of 50 uL of sample buffer and boiling for 5 min.

For transfection-based experiments in HEK-293T cells, 2 million cells were plated in 10 cm culture plates. After twenty-four hours, cells were transfected using the polyethylenimine method using pRK5-based cDNA expression vectors as indicated (*187*). The total amount of transfected plasmid DNA in each transfection was normalized to 5 mg using the empty pRK5 plasmid. After thirty-six hours, cells were lysed and analyzed as described above.

Clonogenic Survival Assays

Indicated cells were seeded in 12-well plates in normal growth medium (RPMI). The following day, when cells reached ~50% confluence, RPMI was removed and replaced with HBSS or supplemented with 2 mM nucleosides for the indicated time points. Cells were then returned to normal media for 72 hours, fixed with cold methanol for 10 min, and stained with Giemsa.

Lysosome immunopurification (LysoIP)

LysoIP was performed largely as previously described (*190*). Briefly, ~35 million cells were used for each replicate. Cells were rinsed twice with pre-chilled PBS and then scraped in one mL of PBS containing protease and phosphatase

inhibitors and pelleted at 1000 x g for 2 min at 4°C. Cells were then resuspended in 950 µL of the same buffer, and 25 µL (equivalent to 2.5% of the total number cells) was reserved for further processing to generate the whole-cell sample. The remaining cells were gently homogenized with 20 strokes of a 2 ml dounce-type homogenizer. The homogenate was then centrifuged at 1000 x g for 2 min at 4°C to pellet the cell debris and intact cells while cellular organelles including lysosomes remained in the supernatant which was incubated with 150 µL of anti-HA magnetic beads prewashed with PBS on a rotator shaker for 3 min. Immunoprecipitates were then gently washed three times with PBS on a DynaMag Spin Magnet. Beads with bound lysosomes were resuspended in 100 µL ice-chilled 1% Triton X lysis buffer to extract proteins. After 10 min incubation on ice the beads were removed with the magnet. For proteomics experiments all the steps were performed using low protein binding tubes (LoBind, Eppendorf) to minimize variability between samples and maximize the recovery of proteins.

MS data acquisition

Sample preparation for mass spectrometry (MS)

Samples were solubilized by the addition of 20% (w/v) SDS to a final concentration of 2% followed by sonication in a Bioruptor Plus (Diagenode) (5 cycles: 1 min on, 30 sec off, 20°C) at the highest settings. Samples were spun down at 20,800x *g* for 1 min and the supernatant transferred to fresh tubes. Reduction was performed with 2.9 µL DTT (200 mM) for 15 min at 45°C before alkylation with 200 mM IAA (5 µL, 30 minutes, room temperature, in the dark).

Proteins were then precipitated with 4 volumes ice cold acetone to 1 volume sample and left overnight at -20°C. The samples were then centrifuged at 20,800x *g* for 30 min at 4°C. After removal of the supernatant, the precipitates were washed twice with 500 µL 80% (v/v) acetone (ice cold). After each wash step, the samples were vortexed, then centrifuged again for 2 min at 4°C. The pellets were then allowed to air-dry before being dissolved in digestion buffer (50 µL, 3M urea in 0.1 M HEPES, pH 8) containing 0.1 µg of LysC (Wako), and incubated for 4 h at 37°C with shaking at 600 rpm. Then the samples were diluted 1:1 with milliQ water (to reach 1.5 M urea) and incubated with 0.1 µg trypsin (Promega) for 16 h at 37 °C. The digests were then acidified with 10% trifluoroacetic acid and then desalted with Waters Oasis® HLB µElution Plate 30µm in the presence of a slow vacuum. In this process, the columns were conditioned with 3x100 µL solvent B (80% (v/v) acetonitrile; 0.05% (v/v) formic acid) and equilibrated with 3x 100 µL solvent A (0.05% (v/v) formic acid in milliQ water). The samples were loaded, washed 3 times with 100 µL solvent A, and then eluted into PCR tubes with 50 µL solvent B. The samples were then dried in a Speed-Vac and resuspended in 10 µL reconstitution buffer (5% (v/v) acetonitrile, 0.1% (v/v) TFA in water) prior to MS analysis.

Peptides were spiked with retention time HRM kit (Biognosys AG), and analyed using the nanoAcquity UPLC system (Waters) fitted with a trapping (nanoAcquity Symmetry C18, 5 µm, 180 µm x 20 mm) and an analytical column (nanoAcquity BEH C18, 2.5 µm, 75 µm x 250 mm). The outlet of the analytical column was

coupled directly to an Orbitrap Fusion Lumos (Thermo Fisher Scientific) using the Proxeon nanospray source. Solvent A was water, 0.1% (v/v) formic acid and solvent B was acetonitrile, 0.1% (v/v) formic acid. Approx. 1 µg of peptides were loaded for each sample with a constant flow of solvent A at 5 µL/min, onto the trapping column. Trapping time was 6 min. Peptides were eluted via the analytical column at a constant flow of 0.3 µL/min, at 40°C, via a non-linear gradient from 0% to 40% in 90 min. Total runtime was 115 minutes, including clean-up and column re-equilibration. The RF lens was set to 30%. For spectral library generation, 4 pooled samples were generated by mixing equal portions of each sample belonging to a biological condition, and each pool was injected in triplicate (12 runs in total), and measured in Data Dependent Acquisition (DDA) mode. The conditions for DDA data acquisition were as follows: full scan MS spectra with mass range 350-1650 *m/z* were acquired in profile mode in the Orbitrap with resolution of 60000. The filling time was set at maximum of 50 ms with limitation of 2×10^5 ions. The “Top Speed” method was employed to take the maximum number of precursor ions (with an intensity threshold of 5×10^4) from the full scan MS for fragmentation (using HCD collision energy, 30%) and quadrupole isolation (1.4 Da window) and measurement in the Orbitrap (resolution 15000, fixed first mass 120 *m/z*), with a cycle time of 3 seconds. The MIPS (monoisotopic precursor selection) peptide algorithm was employed but with relaxed restrictions when too few precursors meeting the criteria were found. The fragmentation was performed after accumulation of 2×10^5 ions or after filling time of 22 ms for each precursor ion (whichever occurred first). MS/MS data

were acquired in centroid mode. Only multiply charged (2^+ - 7^+) precursor ions were selected for MS/MS. Dynamic exclusion was employed with maximum retention period of 15s and relative mass window of 10 ppm. Isotopes were excluded. For data acquisition and processing of the raw data Xcalibur 4.0 (Thermo Scientific) and Tune version 2.1 were employed.

For the Data Independent Acquisition (DIA) data the same gradient conditions were applied to the LC as for the DDA and the MS conditions were varied as follows: full scan MS spectra with mass range 350-1650 *m/z* were acquired in profile mode in the Orbitrap with resolution of 120000. The filling time was set at maximum of 20ms with limitation of 5×10^5 ions. DIA scans were acquired with 34 mass window segments of differing widths across the MS1 mass range. HCD fragmentation (30% collision energy) was applied and MS/MS spectra were acquired in the Orbitrap with a resolution of 30000 over the mass range 200-2000 *m/z* after accumulation of 2×10^5 ions or after filling time of 70 ms (whichever occurred first). Ions were injected for all available parallelizable time. Data were acquired in profile mode.

MS data analysis

For library creation, the DDA data was searched using the Pulsar search engine (version 1.0.15764.0, Biognosys AG). The data were searched against a human database (Swiss-Prot entries of the Uniprot KB database release 2016_01, 20198 entries). The data were searched with the Biognosys default settings with

the following modifications: Carbamidomethyl (C) and Oxidation (M)/ Acetyl (Protein N-term) (Variable). A maximum of 2 missed cleavages were allowed. The identifications were filtered to satisfy FDR of 1 % on peptide and protein level. The library contained 70796 precursors, corresponding to 5401 protein groups using Spectronaut protein inference. DIA data were then searched against this library. Precursor matching, protein inference and quantification was performed in Spectronaut (version 11) using default settings(*212*). Peptide and protein level FDR for DIA data were controlled to 1% (*213*). Differential protein expression was evaluated using a pairwise t-test performed at the precursor level followed by multiple testing correction according to (*214*). The data (candidate table, Supplementary Tables 1 and 2) was exported from Spectronaut and used for further data analyses.

Generation of cells lacking NUFIP1, ATG7, or ATG5

To generate HEK-293T cells lacking NUFIP1, sgRNAs targeting the first exon of NUFIP1 were designed and cloned into the px459 CRISPR vector using the following olignucleotides.

Sense: AGGGGAGACTGGGCGTCGAA

Antisense: TTCGACGCCCAGTCTCCCCT

To generate HEK-293T cells lacking ATG5, sgRNAs targeting ATG5 were designed and cloned into the px459 CRISPR vector using the following olignucleotides.

Sense: GATCACAAGCAACTCTGGAT

Antisense: ATCCAGAGTTGCTTGTGATC

sgNUFIP1 Mia-PaCa cell lines were made using the pLenticrispr system utilizing the same sgRNAs as described above. sgNUFIP1 P53$^{-/-}$ MEFs were generated using the pLenticrispr system utilizing sgRNA sequences targeting the first exon of murine NUFIP1. HEK-293T cells lacking ATG7 were described previously (*190*).

Generation of cells stably expressing cDNAs

The following lentiviral expression plasmids were used: pLJM1-FLAG-metap2, pLJM60-RAP2A, pLJM60-FLAG-NUFIP1 and subsequent mutants. For lysosomal purifications, pLJC5-3XHA-TMEM192 and pLJC5-2XFLAG-TMEM192 or pLJC6-3XHA-TMEM192 and pLJC6-2XFLAG-TMEM192 were used to tag the lysosome. Lentiviruses were produced by transfecting HEK-293T cells with the plasmids indicated above in combination with the VSV-G and CMV DVPR packaging plasmids. Twelve hours post transfection, the media was changed to DMEM supplemented with 30% IFS. Thirty-six hours later, the virus-containing supernatant was collected and frozen at -80°C for 30 min. Cells to be infected were plated in 12-well plates containing DMEM supplemented with 10% IFS with

8 mg/ml polybrene and infected with the virus containing medium. Twenty-four hours later, the cell culture medium was changed to media containing puromycin or blasticidin for selection.

Immunofluorescence assays

HEK-293T cells were plated on fibronectin-coated glass coverslips in 6-well cell culture dishes at 300,000 cells/well. After 12 hr, the coverslips were washed once in PBS and subsequently fixed and permeabilized in a single step using 1 mL of ice-cold methanol at -20°C for 15 min. The coverslips were washed twice in 1 mL PBS and then incubated with primary antibody (FLAG (CST) 1:300 dilution, LC3B (CST) 1:200 dilution, LAMP2 (SCBT) 1:400 dilution) in 5% normal donkey serum for 1 hr at room temperature. After incubation with the primary antibody, the cover slips were rinsed 4 times in PBS and incubated with secondary antibodies (1:400 dilution in 5% normal donkey serum) for 45 min at room temperature in the dark. The coverslips were then washed 4 times with PBS and once in dH_2O. Coverslips were mounted on slides using Vectashield containing DAPI (Vector Laboratories) and imaged on a spinning disc confocal microscopy system (Perkin Elmer).

In vitro binding of NUFIP1-ZNHIT3 to LC3B

In brief, 4 million HEK-293T cells were plated in 15 cm culture dishes. For proteins produced via transient expression, after 48 hr cells were transfected with following amounts of cDNAs in the pRK5 expression vector using the PEI method

(*187*): 5 mg HA-GST-Rap2a; 10 mg HA-GST-GABARAP; 10 mg HA-GST-LC3B. For isolation of heterodimeric NUFIP1-ZNHIT3: 4 mg FLAG-NUFIP1; 10 mg HA-ZNHIT3.

Thirty-six hours post transfection, cells were lysed as indicated above. After clearing of cell lysates, 200 mL of 50% slurry of immobilized glutathione affinity resin equilibrated in lysis buffer was added to lysates expressing GST-tagged proteins. Recombinant proteins were incubated with the affinity resin for 2 hr at 4°C with rotation. Each sample was washed 3 times in binding buffer consisting of 0.1% TX-100, 2.5 mM $MgCl_2$, 20 mM HEPES pH 7.4, and 150 mM NaCl.

When transiently expressed FLAG-NUFIP1-HA-ZNHIT3 was purified from Torin1 treated HEK-293T cells, cells were first treated with 250 nM Torin1 for 1 hour prior to the purification. For experiments involving in vitro binding to purified ribosomes, low protein binding tubes were used to reduce background signal from ribosomes. Similarly, each sample was washed 3 times for 15 mins each in binding buffer supplemented 500 mM NaCl. In order to reduce non-specific background signal, great care must be taken to wash the walls of the tube.

Cell fractionations

Isolation of nuclear and post-nuclear supernatant fractions was preformed as in (*91*) with the following modifications. Confluent 15 cm plates were deprived of amino acids or treated with 250 nM Torin1 prior to isolation. Cells were lysed in PNS buffer containing 0.01% TritionX-100, 10 mM B-glycerol phosphate, 10 mM

pyrophosphate, 40 mM HEPES pH 7.4, and 2.5 mM $MgCl_2$. After 15 min the lysate was clarified by centrifugation at top speed. The supernatant represented the cytosolic fraction containing lysosomes. The pellet (nuclear fraction) was washed twice in PNS buffer containing 500 mM NaCl and lysed for 1 hour with DNase I.

Isolation of ribosomes using a sucrose cushion

Two 15 cm plates of confluent HEK-293T cells were lysed in freshly prepared lysis buffer as described above with the addition of RNAsin (Promega) and 300mM NaCl in DEPC treated water. After a 30 min lysis at 4° C, the lysate was clarified at maximum speed in a microcentrifuge for 10 min to remove debris, nuclei, and mitochondria. The supernatant was collected and loaded onto a 50% sucrose cushion prepared in Buffer A consisting of 40 mM HEPES pH 7.4, 2.5 mM $MgCl_2$, and 150 mM KCl in DEPC treated water and ultracentrifuged for 16-18 hr at 100,000g to obtain the ribosome-containing pellet. While loading the lysate on top of the cushion, great care must be taken to not disturb the sucrose by the very slow addition of the lysate onto the 50% sucrose. A translucent pellet at the bottom of the ultracentrifuge tube represents the ribosomes. Fractions were collected and homogenized gently using a dounce homogenizer, precipitated, adjusted to 0.5% SDS, and heated in boiling water for 5 min prior to SDS-PAGE followed by immunoblotting.

When HEK-293T cells were first deprived of nutrients or treated with Torin1, two 15 cm plates of HEK-293T cells were deprived of amino acids or

treated with 250 nM Torin1 for 1 hour prior to lysis. For experiments involving in vitro binding of NUFIP1-ZNHIT3 to purified ribosomes, the resulting ribosome pellet is washed once in Buffer A. prior to use.

Ribosome analysis using a sucrose gradient

Prior to lysis, cell were treated with 100 mg/ml cycloheximide for 5 minutes, washed in ice-cold PBS with 100 mg/ml cycloheximide, and then lysed as described above in freshly prepared lysis buffer with the addition of RNAsin (Promega) in DEPC treated water. After a 30 min lysis at 4°C, the lysate was clarified at maximum speed in microcentrifuge for 10 min to remove debris, nuclei, and mitochondria. When EDTA was used, 50 mM EDTA was added during the preparation of the sucrose gradient and to lysis buffer. Lysates were normalized by protein content using the Bradford reagent (Bio-rad) and layered onto an 11 mL 10-45% sucrose gradient made in 40 mM HEPES, 7.5 mM $MgCl_2$, 100 mM KCl, 2 mM DTT, 100 mg/ml cycloheximide, RNAsin. Lysates were ultracentrifuged at 40,000 RPM using a SW-41 Ti rotor at 4°C for 3 hr and 1 mL fractions were collected, precipitated, adjusted to 0.5% SDS, and heated for 5 min in boiling water prior to SDS-PAGE followed by immunoblotting.

LC/MS-based metabolomics and quantification of metabolite abundances

LC/MS-based metabolomics were performed and analyzed as previously described using 500 nM isotope-labeled internal standards(*190*). Briefly, a 80% methanol extraction buffer containing 500 nM isotope-labeled internal standards

was used for whole cell metabolite extractions. Samples were briefly vortexed and dried by vacuum centrifugation. Samples were stored at -80°C until analysis. Upon analysis, samples were resuspended in 100 mL of LC/MS grade water and the insoluble fraction was cleared by centrifugation at 15,000 rpm in a microcentrifuge. The supernatant was then analyzed as previously described by LC/MS (*190*).

Electron Microscopy

In brief, NUFIP1-null HEK-293T cells expressing wild-type NUFIP1 or the W40A mutant were grown to 60% confluency in 10 cm plates and incubated with Torin1 (250 nM) and Concanamycin A (500 nM) for 4 hr. The cells were fixed with 2% gluteraldehyde + 3% paraformaldehyde + 5% sucrose in Sodium Cacodylate (pH 7.4) followed by osmication and uranyl acetate staining, ethanol dehydration, and the samples were then embedded in Epoxy resin. Sections were cut on formvar-coated grids, stained once more with uranyl acetate and lead citrate and imaged with a FEI Tecnai Spirit Transmission Electron Microscope. Autophagosomal sections in which ribosomes could be clearly enumerated were analzyed to determine the number of ribosomes per autophagosome. The number of ribosomes inside autophagosomes were determined by counting and normalized to the area of the autophagosomal section (# of ribosomes/autophagosomal area) as measured using ImageJ.

CHAPTER 5

Future Directions and Discussion

I. Regulation of lysosomal amino acid pools by the mTOR pathway

The development of our LysoIP technique has provided a means to specifically monitor changes in lysosomal metabolite pools under distinct cellular states; measurements that were previously impossible using whole-cell metabolite profiling. And to our surprise, our data show that mTORC1 has a previously unknown role in promoting efflux of essential amino acids from the lysosomal to the cytosol. mTOR inihibition leads to a sequestration of these amino acids in the lysosome by blocking their efflux across the lysosomal membrane, an effect we traced to the lysosomal arginine sensor SLC38A9. Collectively, these results inform our understanding of the regulation of the mTOR pathway during starvation. Specifically, we can imagine that acute nutrient depletion leads to mTOR inhibition that suppresses SLC38A9 function. SLC38A9 inhibition will prevent the release of essential amino acids into the cytoplasm to ensure they are not used for growth promoting processes in a setting when nutrient stores are low. Over time, increased lysosomal proteolysis restores lysosomal amino acid pools thereby reactivating mTORC1 and SLC38A9 promoting the release of essential amino acid into the cytosol so they can be used to execute the necessary processes in order to adapt to starvation. Mechanistically, this creates an interesting model where SLC38A9 acts upstream

of mTORC1 as a positive regulator of the nutrient sensing pathway, while also functioning downstream of mTORC1.

How mTORC1 impacts SLC38A9 function is unknown and it may be either through a direct mechanism or via an unidentified interacting protein. Given that activated mTORC1 resides at the lysosomal surface via its interaction with the Rag GTPases, it is at the correct location to control SLC38A9 function. It is possible that SLC38A9 is a direct mTORC1 kinase substrate and mTORC1-dependent SLC38A9 phosphorylation regulates its transport function, but we have failed to identify any putative phosphorylation sites that affect its transport activity. Similarly, recent evidence shows that SLC38A9 cannot interact with Rag GTPases when they are bound to mTORC1, the state in which mTORC1 is active. This suggests a mutual exclusive binding mode of SLC38A9-Rag and Rag-mTORC1 and detachment of SLC38A9 from the Rag GTPases is an essential step in mTORC1 activation. It remains possible that active mTORC1 regulates an unknown component of the nutrient sensing machinery that thereby impacts SLC38A9 function. It will be necessary to first understand how the interactions of SLC38A9 with the known nutrient sensing components impacts its transport activity, and using our in vitro transport system it will be possible to investigate this.

II. Compartmentalized Metabolism in cellular physiology

A defining characteristic of eukaryotic life is membrane-bound organelles that compartmentalized specialized biochemical pathways within the cell. This unique characteristic allows for the spatial and temporal separation of otherwise

incompatible biochemical processes. Mitochondria, for instance, carry out many essential metabolic processes, such as ATP generation by the respiratory chain, while peroxisomes provide a detoxifying center for hydrogen peroxide. Related to the body of work presented above, the lysosome is critical organelle known for its degradative capacity that requires maintenance of a low pH environment. With the development of our LysoIP method, we have provided a feasible strategy to isolate intact lysosomes suitable for current mass-spectrometry based metabolite profiling techniques and have allowed for the study of the dynamics of lysosomal metabolite pools, a compartment that represents ~2% of cellular volume.

In our study, we have been able to quantify in absolute amounts the concentrations of ~60 metabolites in both whole cell and lysosome samples providing an initial assessment of the lysosomal metabolome. This study is far from exhaustive and is only limited by the availability of pure mass spectrometry standards. With the ever-improving development of untargeted metabolite profiling, it will be possible to not only expand and catalog all lysosomal metabolites across diverse cellular states de novo, but also allows for the possibility to de-orphan lysosomal genes of unknown function that regulate lysosomal metabolism. Our study on SLC38A9 is the first case of the latter, providing an initial example of the power of studying the impact of a lysosomal protein at its physiological environment and whose phenotype would be masked using traditional whole-cell metabolite profiling methods.

Apart from its use in lysosomal metabolites, the development of our method provides a means to study dynamic changes in the lysosome proteome.

Given the rapid nature of our technique, we are able to capture not only core lysosomal proteins but also ones that associate only transiently either with the lysosomal surface or are shuttle to the lysosome with the incipient autophagosome. In our initial studies under conditions of which we inhibit the mTOR pathway, it is clear that the lysosomal proteome is far more dynamic than initially appreciated providing an example that supports studying this organelle under diverse cellular states. We have since begun to move our studies of the lysosomal proteome in vivo with the development of a LysoTag mouse, providing a means to studying intact lysosomes across diverse tissues and cell types.

We believe this method can be adapted for the study of all organellar compartments. Indeed, it has already been shown for mitochondria, from which we gained a lot of insight in our initial development. With the burgeoning excitement in the field of organellar contacts and crosstalk, it will be quite interesting to utilize our method to begin to understand how the function of individual organelles impacts the function of others.

III. Autophagy and lysosome regulation in therapy: Potential strategies and applications

Autophagy is a catabolic pathway that leads to nutrient recycling via the sequestration of cellular proteins and damaged organelles and their ultimate degradation via the lysosome. Alterations to this pathway are both positively and negatively associated with human health and are also causal for multiple human diseases. As an example, many cancers are known to up-regulate flux through autophagy as well as increase expression of many lysosomal genes in order to

increase the benefits of nutrient scavenging to tumors. On the other hand, many potent autophagy inducers, such as mTOR inhibition as well as caloric restriction, are the most consistently shown interventions proven to extend life span across multiple model organisms. Importantly, genetic loss of autophagy blocks the life-span extension seen with mTOR inhibition in worms, suggesting that autophagy-mediated degradation is required for life span extension. Collectively, the need for activators of the autophagy-lysosomal axis as well as inhibitors is potentially an unexplored therapeutic intervention for multiple human diseases.

Currently, there are no known specific autophagy-modifying drugs. mTOR inhibitors, which promote autophagy activation, have been discussed previously for their potential in cancer therapy. Recent pre-clinical studies have shown mTOR inhibition, although growth inhibitory, can also lead to increased lysosomal catabolism of proteins enhancing cellular proliferation during nutrient-depleted conditions. Similarly, autophagy in stromal cells can promote tumor cell metabolism by feeding amino acids (alanine) to neighboring tumor cells. These results suggest mTOR inhibition may actually be pro-tumorigenic in a nutrient-depleted tumor microenvironment and lysosomal inhibition may be a viable treatment strategy to disrupt a critical nutrient source in cancers.

Human trials have focused on the use of chloroquine or hydroxychloroquine as a strategy for autophagy and lysosome inhibition in cancer. However, these have performed to only mixed benefit likely due to their lack of specificity and tolerance as lysosomal function is critical in all cells. The question is then can we identify potential targets in cancer that may provide a

strategy to block autophagy-derived nutrients while leaving normal cells unaffected? Our work on SLC38A9 and NUFIP1 has provided potential therapeutic strategies that fit these criteria. Loss of SLC38A9 or inhibition strictly of its transport function blocks the use of essential amino acids derived from the lysosome as well as inhibits the growth promoting activities of mTORC1. Similarly, NUFIP1 loss disrupts the degradation of likely the cell's most abundant nutrient resource, the ribosome, which provides both an amino acid source to promote protein synthesis as well nucleosides to support DNA and RNA synthesis. SLC38A9 loss severely blocked tumor formation in a pancreatic cancer mouse model. More importantly, SLC38A9 or NUFIP1 loss has no effect on cell growth when nutrients are plentiful, but rather only when cells are required to utilize the lysosomal axis for nutrient stores. These results suggest SLC38A9 or NUFIP1 inhibition may spare normal cells that do not rely as heavily on the lysosome but may only be detrimental to tumor cells residing in a nutrient-depleted environment. Because SLC38A9 has amino acid-binding capabilities, it may be possible to develop small molecule inhibitors that specifically target the lysosomal nutrient axis. However, this will require further structural studies.

Conversely, the interest in autophagy inducers has mainly been associated with longevity and inhibition of age-associated diseases. Currently, most work has been focused on modulators of the mTORC1 pathway (such as pharmacologic inhibitors like rapamycin or caloric restriction) as mTOR inhibition is the most consistent life span inducer across all eukaryotic model organisms. Interestingly, even short-term mTOR inhibition late in life can provide

improvement on age-related disease phenotypes in model organisms. While it is unclear whether autophagy activation is the major mechanism of increased life span upon mTOR inhibition, multiple lines of evidence suggest it plays a major role. For instance, systematically boosting autophagy using a transgenic mouse model that promotes Beclin1 function prolongs lifespan in mammals and almost completely rescues a mouse model of genetic predisposition to premature aging. Also, in mice overexpressing ATG5, enhanced autophagy as well as lifespan extension and improvements in metabolic outcomes such as insulin sensitivity were observed. These results provide further rationale for the development of specific autophagy-inducing compounds.

Concluding Remarks

Over the past decade, we have witnessed exciting advances in our understanding of how cells interpret their nutrient environment and utilize those signals to promote cellular growth. This field has grown to identify the direct nutrient sensors for the mTOR pathway and also emerged with a intimate and functional relationship with the major degradative compartment within the cell. Althought we are far from having a complete understanding of growth control by the mTOR pathway and its impact on cell physiology, future efforts will expand our understanding of lysosome function and will clarify our understanding of growth control and how it becomes deregulated in disease settings.